Proceedings to the 27th Workshop

What Comes Beyond the Standard Models

Bled, July 8–17, 2024

Edited by

Norma Susana Mankoč Borštnik
Holger Bech Nielsen
Maxim Yu. Khlopov
Astri Kleppe

The 27th Workshop *What Comes Beyond the Standard Models*, 8.– 17. July 2024, Bled

Was organized by

Society of Mathematicians, Physicists and Astronomers of Slovenia

And sponsored by

Department of Physics, Faculty of Mathematics and Physics, University of Ljubljana

Society of Mathematicians, Physicists and Astronomers of Slovenia

Beyond Semiconductor (Matjaž Breskvar)

VIA (Virtual Institute of Astroparticle Physics), Paris

MDPI journal "Symmetry", Basel

MDPI journal "Physics", Basel
MDPI journal "Universe"", Basel

Scientific Committee

John Ellis, *King's College London / CERN*

Roman Jackiw, *MIT*

Masao Ninomiya, *Yukawa Institute for Theoretical Physics, Kyoto University*

Organizing Committee

Norma Susana Mankoč Borštnik

Holger Bech Nielsen

Maxim Yu. Khlopov

The Members of the Organizing Committee of the International Workshop "What Comes Beyond the Standard Models", Bled, Slovenia, state that the articles published in the Proceedings to the 27th Workshop "What Comes Beyond the Standard Models", Bled, Slovenia are refereed at the Workshop in intense in-depth discussions.

Workshops organized at Bled

▷ *What Comes Beyond the Standard Models*
  (June 29–July 9, 1998), Vol. **0** (1999) No. 1
  (July 22–31, 1999)
  (July 17–31, 2000)
  (July 16–28, 2001), Vol. **2** (2001) No. 2
  (July 14–25, 2002), Vol. **3** (2002) No. 4
  (July 18–28, 2003) Vol. **4** (2003) Nos. 2-3
  (July 19–31, 2004), Vol. **5** (2004) No. 2
  (July 19–29, 2005) , Vol. **6** (2005) No. 2
  (September 16–26, 2006), Vol. **7** (2006) No. 2
  (July 17–27, 2007), Vol. **8** (2007) No. 2
  (July 15–25, 2008), Vol. **9** (2008) No. 2
  (July 14–24, 2009), Vol. **10** (2009) No. 2
  (July 12–22, 2010), Vol. **11** (2010) No. 2
  (July 11–21, 2011), Vol. **12** (2011) No. 2
  (July 9–19, 2012), Vol. **13** (2012) No. 2
  (July 14–21, 2013), Vol. **14** (2013) No. 2
  (July 20–28, 2014), Vol. **15** (2014) No. 2
  (July 11–19, 2015), Vol. **16** (2015) No. 2
  (July 11–19, 2016), Vol. **17** (2016) No. 2
  (July 9–17, 2017), Vol. **18** (2017) No. 2
  (June 23–July 1, 2018), Vol. **19** (2018) No. 2
  (July 6–14, 2019), Vol. **20** (2019) No. 2
  (July 4–12, 2020), Vol. **21** (2020) No. 1
  (July 4–12, 2020), Vol. **21** (2020) No. 2
  (July 1–12, 2021), Vol. **22** (2021) No. 1
  (July 4–12, 2022), Vol. **23** (2022) No. 1
  (July 10–18, 2023), Vol. **24** (2023) No. 1
  (July 8–17, 2024), Vol. **25** (2024) No. 1
▷ *Hadrons as Solitons* (July 6–17, 1999)
▷ *Few-Quark Problems* (July 8–15, 2000), Vol. **1** (2000) No. 1
▷ *Selected Few-Body Problems in Hadronic and Atomic Physics* (July 7–14, 2001),
    Vol. **2** (2001) No. 1
▷ *Quarks and Hadrons* (July 6–13, 2002), Vol. **3** (2002) No. 3
▷ *Effective Quark-Quark Interaction* (July 7–14, 2003), Vol. **4** (2003) No. 1
▷ *Quark Dynamics* (July 12–19, 2004), Vol. **5** (2004) No. 1
▷ *Exciting Hadrons* (July 11–18, 2005), Vol. **6** (2005) No. 1
▷ *Progress in Quark Models* (July 10–17, 2006), Vol. **7** (2006) No. 1
▷ *Hadron Structure and Lattice QCD* (July 9–16, 2007), Vol. **8** (2007) No. 1
▷ *Few-Quark States and the Continuum* (September 15–22, 2008),
    Vol. **9** (2008) No. 1
▷ *Problems in Multi-Quark States* (June 29–July 6, 2009), Vol. **10** (2009) No. 1
▷ *Dressing Hadrons* (July 4–11, 2010), Vol. **11** (2010) No. 1
▷ *Understanding hadronic spectra* (July 3–10, 2011), Vol. **12** (2011) No. 1
▷ *Hadronic Resonances* (July 1–8, 2012), Vol. **13** (2012) No. 1

IV

Preface in English and Slovenian Language

This year was 27th time that our series of workshops on "What Comes Beyond the Standard Models?" took place. The series started in 1998 with the idea of organising a workshop where participants would spend most of the time in discussions, confronting different approaches and ideas. The picturesque town of Bled by the lake of the same name, surrounded by beautiful mountains and offering pleasant walks, was chosen to stimulate the discussions.

The idea was successful and has developed into an annual workshop, which is taking place every year since 1998. Very open-minded and fruitful discussions have become the trademark of our workshops, producing several published works. It took place in the house of Plemelj, which belongs to the Society of Mathematicians, Physicists and Astronomers of Slovenia.

We discussed in these twenty-seven years a lot of concepts which could help to understand our universe from the level of the second quantized elementary fermion and boson fields up to the level of the born of our universe.

Trying to understand what the elementary constituents of our universe are and what are the laws of nature; physicists suggest theories and look for predictions which need confirmation of experiments and cosmological observations.

What seems to be trustworthy is that the elementary constituents are two kinds of fields: Anti-commuting fermion and commuting boson fields, both assumed to be second quantized fields.

Since experiments require precise predictions to be confirmed by experiments the calculations must be accurate enough and designed for a particular experiment.

Although in these twenty-seventh years the technology of experiments, as well as astronomical observations, have advanced incredibly it is still true that we are only guessing how our universe has started and why it exponentially expanded and then reheated, why do we experience only three space dimensions and one time, why most of matter is almost unobservable in direct measurements, what forces our universe to expand faster than expected; many other open questions remain unanswered.

We improve our knowledge in small steps. But there were also large steps like the special theory of relativity, the general theory of gravity, the quantum theory of groups of constituents (in the first quantization models), the second quantization of bosons and fermions, the electroweak *standard model*, the *cosmological models*.

In trying to understand the born and history of our universe, and the interactions among elementary second quantized fields uniquely, a large step is needed. The strings theories seems promising.

In the Bled workshops, "What comes beyond the standard models" the *spin-charge-family* theory has been discussed and developed, holding the promise that all the fermion and boson second quantized fields can be treated equivalently — the fermion internal spaces can be described as a superposition of an odd products of γ^a, the boson internal spaces can be described as a superposition of an even products of γ^a, what makes unifying all the fermion fields (quarks and leptons and antiquarks and antileptons appearing in families, predicting the fourth family

to the observed three, the fifth stable family describing the dark matter) as well as the boson gauge fields (gravitons, weak bosons, gluons, photons, several scalar fields causing the inflation, the dark energy, the matter anti-matter asymmetry, the electroweak break of symmetry with several Higgs scalar), offering a new large step.

Also, in this year's proceedings, most of the contributions discuss the theoretical concepts of solving the open problems of elementary fermion and boson fields and cosmology, looking for the next step beyond both *standard models*, the electroweak one and the cosmological one.

There is an excellent pioneer project in the direct detection of the dark matter confirming the annual modulation of signals deeply underground in Gran Sasso over many independent annual cycles with various configurations (DAMA/NaI, DAMA/LIBRA–phase1 and DAMA/LIBRA–phase2); the last within the energy scale from less than 1 KeV to 6 KeV. We are all waiting for the other laboratories to confirm their measurements.

There is a proposal for the content of the dark matter, suggesting that it might be formed from the composite Thomson-like atomic dark matter candidates, which might resolve the problem of why no other experiment has not yet succeeded in confirming the Gran Sasso experiment.

There are ideas, discussed in previous Proceedings, suggesting that even the *standard model* offers the contributions to the dark matter.

The *spin-charge-family* theory, which explains the existence of families, suggests (among many other predictions) that to the dark matter the clusters of the stable fifth family quarks may contribute.

There are discussions in this and the previous Proceedings that the dark matter accumulated in the vicinity of the Earth, influence the Earth's ionosphere and stratosphere.

There are ideas in this Proceedings on how to explain the appearance of families within the gauged SU(3) model.

There are two contributions on the *spin-charge-family* theory. The first contribution demonstrates the description of the internal spaces of fermions and bosons with the nilpotents (they are the superpositions of an odd number of operators γ^a) and projectors (they are the superposition of an even number of operators γ^a). The products of an odd number of nilpotents (the rest are projectors) describe the fermion's internal space, appearing in families. The products of an even number of nilpotents (the rest are projectors) describe the boson's internal space. Both have an equal number of internal states. One contribution discusses the *spin-charge-family* theory's latest achievements, with a trial to understand whether the extension to strings or odd-dimensional spaces can lead to a new kind of supersymmetry, offering the renormalizable and anomalies-free theory. The assumption is made that all the fermion and boson fields are active only in d = (3 + 1), while the internal spaces need d = (13 + 1).

There is the contribution explaining the possibility to derive an exact expressions for the renormalization constants using the arguments based on the renormalization group.

There were several suggestions for solving the cosmological hierarchy problem (the smallness of the dark energy).

There are ideas to investigate the behaviour of space-time in the vicinity of the domain walls using an axion-like field. Using the specific models, like it is primordial black hole merging, can help to interpret the results of gravitational wave experiments, and other astronomical observations.

One contribution of micro-quasars in our galaxy offers the explanation for the unexpected and surprising re-collimation of TeV beam jet, by using the well-known high-energy nuclear physics models.

The 'complete' geometric special relativity and its new Lie group in real space is presented.

One contribution demonstrates that the logarithm of the energies of the seriousness of the scale versus the dimension related to number q (pertaining to the dimensions of the scales) behaves as a straight line.

While the *spin-charge-family* theory declares that the description of the internal spaces of fermion and boson fields by the superposition of odd (for fermions) and even (for bosons) products of the operators γ^a not only explains but offers the second quantization of fermion and boson fields, explaining the second quantization postulates, there is the contribution which shows that random dynamics already offers the first step to quantum mechanics.

Maybe next year, we shall report on physically realistic cellular automaton used to offer several illustrations in elementary particle physics. This year, we only received the abstracts.

The workshops at Bled changed after the Covid pandemic: For three years, the workshop became almost virtual and correspondingly less open-minded. The discussions, which asked the speaker to explain and prove each step, can not be done so easily virtually. However, many questions still interrupt the presentations, so the speakers must often continue their talks several times in the following days. Also, this year, the talks were presented virtually.

Many a presented and developed idea in this proceeding might not be in agreement with the others presented in the same proceedings. But yet different ideas, if developed in a consistent way might help to understand the problems in connection with the measurements and observations, which only can confirm what is the status of the laws in our universe.

Looking at the collection of open questions that we set ourselves before starting these Bled workshops and continuously supplementing each workshop, it shows up that we are all the time mostly looking for an answer to the essential questions:

How to explain all the assumptions of both *standard models* in an unique way — with the second quantized fermion and boson fields — enabling to understand the first quantization achievements so far, as well as the classical limits.

Many talks are "unusual" because they seek a new, more trustworthy way of understanding and describing the observed phenomena.

This year, the organisers are again asking the University of Ljubljana for the help in arranging the DOI number.

Although the *Society of Mathematicians, Physicists and Astronomers of Slovenia* remain our organiser, for which we are very grateful, yet the Faculty of Mathematics and Physics starts to be our publisher together with the University of Ljubljana. The technical procedure is now different, and the possibility that the participants send the contributions "the last moment" is less available.

Several participants have not succeeded in sending their contributions in time. We publish only abstracts of those who sent in time at least abstracts. Their contributions will be published next year if they want. The same will also happen with contributions for which even abstracts have not arrived in time. From July to In particular, November is a short time since this period includes vacations.

The organisers are grateful to all the participants for the lively presentations and discussions and an excellent working atmosphere, although most participants appeared virtually, led by Maxim Khlopov.

The reader can find all the talks and soon also the whole Proceedings on the official website of the Workshop: http://bsm.fmf.uni-lj.si/bled2024bsm/presentations.html, and on the Cosmovia Forum https://bit.ly/bled2024bsm ..

Norma Mankoč Borštnik, Holger Bech Nielsen,
Maxim Khlopov, Astri Kleppe   *Ljubljana, December 2024*

1 Predgovor (Preface in Slovenian Language)

Letos je 27. leto, odkar poteka serija delavnic z naslovom "Kako preseči oba standardna modela?". Serija se je začela leta 1998 z idejo o delavnicah, na katerih bi udeleženci večino časa namenili razpravam in soočanju različnih pristopov in idej. Za spodbujanje teh razprav smo izbrali slikovito mesto Bled ob istoimenskem jezeru, obdano s čudovitimi gorami in prijetnimi sprehajalnimi potmi.

Ideja je bila uspešna in se je razvila v vsakoletno delavnico, ki poteka od 1998. leta. Zelo odprte in plodne razprave so postale zaščitni znak naših delavnic in so privedle do številnih objavljenih del. Delavnice potekajo v Plemeljevem domu, ki je v lasti Društva matematikov, fizikov in astronomov Slovenije.

V teh sedemindvajsetih letih smo obravnavali veliko konceptov, ki bi lahko pomagali razumeti naše vesolje, od osnovnih fermionskih in bozononskih polj v drugi kvantizaciji, do začetka našega vesolja.

Pri iskanju razumevanja, kaj so osnovni gradniki našega vesolja in kakšni so zakoni narave, fiziki predlagajo teorije in iščejo napovedi, ki omogočajo potrditev teorij z eksperimenti in kozmološkimi opazovanji.

Zdi se zaupanja vredna predpostavka, da so osnovni gradniki iz dveh vrst polj — iz antikomutativnih fermionskih in komutativnih bozononskih polj v drugi kvantizaciji.

Ker eksperimenti zahtevajo za potrditev natančne modelske napovedi, morajo biti izračuni dovolj natančni in prilagojeni posameznemu eksperimentu.

Čeprav so se v teh sedemindvajsetih letih tehnologije eksperimentov in astronomskih opazovanj neverjetno razvile, še vedno samo ugibamo, kako se je naše vesolje začelo in zakaj se je eksponentno širilo ter nato segrelo. Prav tako ne vemo, zakaj opažamo le tri prostorske razsežnosti in en čas, zakaj je večina snovi skoraj neopažena v neposrednih meritvah, kaj sili naše vesolje, da se širi hitreje, kot pričakujemo; tudi številna druga odprta vprašanja ostajajo brez odgovora.

Znanje izboljšujemo z majhnimi koraki. Vendar so bili v preteklosti tudi veliki preboji, kot so posebna teorija relativnosti, splošna teorija gravitacije, kvantna teorija skupin osnovnih gradnikov (v modelih prve kvantizacije), druga kvantizacija bozonov in fermionov, elektrošibki standardni model in kozmološki modeli.

Da bi si lahko razložili nastanek in zgodovino našega vesolja in hkrati razumeli interakcijo med osnovnimi fermionskimi in bozonskimi polji v drugi kvantizaciji na enoten način, je potreben velik korak. Teorije strun se zde obetavne.

Na Blejskih delavnicah, ki nosijo ime "Kako preseči oba standardna modela", so potekale živahne razprave o teoriji *spin-charge-family*, ki je obetala, da bo vsa fermionska in bozononska polja druge kvantizacije obravnavala ekvivalentno. Teorija opiše zdaj notranje prostore fermionov in bozonov na enoten način: Notranji prostori fermionov so opisani kot superpozicija lihih produktov γ^a, notranji prostori bozonov pa kot superpozicija sodih produktov γ^a. To omogoča enoten opis tudi vseh fermionskih polj (kvarkov, leptonov, antikvarkov in antileptonov in njihovih družin; pri čemer teorija napoveduje četrto družino poleg že opaženih treh ter stabilno peto družino, ki prispeva k temni snovi) ter bozononskih polj

(gravitonov, šibkih bozonov, gluonov, fotonov, skalarnih polj — ki pojasnijo inflacijo, obstoj temne energije, asimetrijo med snovjo in antisnovjo, tudi Higgsove skalarje).

V letošnjem zborniku predstavi večina prispevkov teoretične koncepte za reševanje odprtih problemov osnovnih fermionskih in bozononskih polj ter kozmologije in iščejo naslednji korak za oba standardna modela, elektrošibkega in kozmološkega. Predstavili pa so tudi zadnje izsledke odličnega pionirskega projekta, ki meri letno modulacijo interakcije temne snovi z merilnimi aparaturami globoko pod zemljo v Gran Sassu že vrsto let z neodvisnimi letnimi cikli z različnimi konfiguracijami (DAMA/NaI, DAMA/LIBRA — faza1 in DAMA/LIBRA — faza2), ki potrjujejo letno modulacijo signalov temne snovi. V zadnji konfiguraciji je energijski prag znižan pod 1 KeV. Nestrpno čakamo, da bodo drugi laboratoriji potrdili njihove meritve.

Predlagana hipoteza o vsebini temne snovi nakazuje, da bi temno nov lahko sestavljali skupki, podobni Thomsonovim atomom. To bi utegnilo pojasniti, zakaj nobenemu drugemu eksperimentu doslej še ni uspelo potrditi rezultatov eksperimenta v Gran Sassu.

V prejšnjih zbornikih so bile obravnavane ideje, kako bi lahko pojasnili prisotnost temne snovi tudi s skupki kvarkov in antikvarkov *standardnega modela*.

Teorija *spin-charge-family*, ki pojasnjuje obstoj družin, ocenjuje (med številnimi drugimi napovedmi), da k temni snovi lahko prispevajo nevtralni skupki stabilnih kvarkov pete družine.

V teh in prejšnjih zbornikih potekajo razprave, da temna snov, ki se kopiči v bliĭni Zemlje, vpliva na Zemljino ionosfero in stratosfero.

V tem in prejšnjih zbornikih prispevki razložijo pojav druĭn in njihovih lastnosti z modelom SU(3).

Dva prispevka poročata o napredku teorije *spin-charge-family*. Prvi prispevek predstavi notranje prostore fermionov in bozonov z nilpotentnimi operatorji (ti so superpozicije lihega števila operatorjev γ^a) in projekcijskimi operatorji (ti so superpozicije sodega števila operatorjev γ^a). Produkti lihega števila nilpotentnih operatorjev (preostali so projektorji) opisujejo notranji prostor fermionov, ki se pojavljajo v družinah. Produkti sodega števila nilpotentnih operatorjev (preostali so projektorji) opisujejo notranji prostor bozonov. Obe vrsti imata enako število notranjih stanj.

Drugi prispevek obravnava najnovejše dosežke teorije *spin-charge-family* z namenom raziskati, ali lahko razširitev na strune ali liho-dimenzionalne prostore privede do nove vrste supersimetrije, ki bi omogočila, da bo teorija renormalizabilna in brez anomalij. Predpostavka, da so vsa fermionska in bozononska polja aktivna le v prostoru $d = (3 + 1)$, medtem ko notranji prostori zahtevajo $d = (13 + 1)$, poenostavi opis nastanka vesolja in interakcije med fermionskimi in bozonskimi polji.

Avtor enega od prispevkov predstavi možnost izpeljave točnih izrazov za renormalizacijske konstante s pomočjo argumentov, temelječih na renormalizacijski grupi.

Podanih je bilo nekaj predlogov za reševanje problema kozmične hierarhije (majhnosti temne energije).

Avtorji so predstavili, kako uporabiti polja, podobna aksionom, za raziskavo obnašanja prostor-časa v bližini domennih sten. Uporaba modelov, kot je združevanje primarnih črnih lukenj, pa bi lahko pomagala pri interpretaciji rezultatov eksperimentov z gravitacijskimi valovi in drugih astronomskih opazovanj.

Prispevek o mikro-kvazarjih v naši galaksiji ponuja razlago nepričakovane in presenetljive ponovne kolimacije curka žarkov v območju TeV z uporabo dobro znanih modelov visokoenergijske jedrske fizike.

Ponujen je model "popolne" geometrične slike posebne teorije relativnosti in ustrezne nove Liejeve grupe v realnem prostoru.

V enem od prispevkov je prikazano, da se logaritem energij glede na dimenzijo, povezano s številom q (ki se nanaša na dimenzije skal), obnaša kot premica.

Medtem ko teorija *spin-charge-family* trdi, da opis notranjih prostorov fermionskih in bozononskih polj s superpozicijo lihega (za fermione) oziroma sodega (za bozone) produkta operatorjev γ^a ne le pojasnjuje, temveč tudi ponuja drugo kvantizacijo fermionskih in bozononskih polj ter razlaga postulate druge kvantizacije, pa je prispevek, ki kaže, da naključna dinamika ponuja prvi korak h kvantni mehaniki.

Morda bomo prihodnje leto poročali o realističnem celičnem avtomatu, ki bi ponudil ilustracije delcev na področju fizike osnovnih delcev. Letos smo prejeli le povzetke.

Delavnice na Bledu so se po pandemiji covida spremenile: tri leta so bile skoraj v celoti virtualne in zato manj odprte za nove ideje. Razprave, v katerih so morali govorniki pojasnjevati in dokazovati vsak korak, je v virtualnih soočenjih mnogo težje ponoviti.

Vendar številna vprašanja še vedno prekinjajo predstavitve, zato morajo predavatelji pogosto nadaljevati predavanja v naslednjih dneh.

Tudi letos so bile predstavitve izvedene virtualno.

Mnoge predstavljene in razvite ideje v tem zborniku morda niso skladne z drugimi idejami, predstavljenimi v istem zborniku. Vendar pa lahko različne ideje, če so matematično in idejno korektne in razvite na dosleden način, pomagajo pri razumevanju problemov, povezanih z meritvami in opazovanji, ki lahko edine potrdijo gradnike snovi in stanje zakonov v našem vesolju.

Ko pogledamo zbirko odprtih vprašanj, ki smo si jih zastavili pred začetkom Blejskih delavnic in jih nenehno dopolnjevali na vsaki delavnici, ugotovimo, da ves čas iščemo odgovor na temeljna vprašanja: Kako pojasniti vse predpostavke obeh standardnih modelov na enoten način – s fermionskimi in bozonskimi polji v drugi kvantizaciji – kar bi omogočilo razumevanje dosežkov prve kvantizacije do zdaj, pa tudi klasičnih zakonov.

Mnoga predavanja so "nenavadna", saj iščejo nov, drugačen način kako opisati to kar izmerimo in opazimo.

Letos so se organizatorji ponovno obrnili na Univerzo v Ljubljani za pomoč pri urejanju DOI številke za zbornik.

Čeprav Društvo matematikov, fizikov in astronomov Slovenije ostaja naš organizator, za kar smo zelo hvaležni, je Fakulteta za matematiko in fiziko skupaj z

Univerzo v Ljubljani prevzela vlogo založnika. Tehnični postopek je zdaj drugačen, možnost, da udeleženci pošljejo prispevke "zadnji trenutek", pa je manj dostopna. Kar nekaj udeležencem ni uspelo pravočasno poslati svojih prispevkov. Objavljamo le izvlečke tistih, ki so pravočasno poslali vsaj povzetke. Njihovi prispevki bodo objavljeni prihodnje leto, če bodo to želeli. Enako velja za prispevke, katerih niti povzetki niso prispeli pravočasno. Od julija do novembra je namreč kratko obdobje, saj to obdobje vključuje počitnice.

Organizatorji se zahvaljujejo vsem udeležencem za živahne predstavitve in razprave ter odlično delovno vzdušje, čeprav je večina udeležencev sodelovala virtualno, za kar je poskrbel Maksim Khlopov.

Bralec lahko najde vsa predavanja in kmalu tudi celoten zbornik na uradni spletni strani delavnice

http://bsm.fmf.uni-lj.si/bled2024bsm/presentations.html,

and on the Cosmovia Forum https://bit.ly/bled2024bsm ..

Norma Mankoč Borštnik, Holger Bech Nielsen,
Maxim Khlopov, Astri Kleppe *Ljubljana, december 2024*

Contents

1 Status of DAMA/LIBRA–phase2 and its empowered stage

R. Bernabei**, P. Belli[1], A. Bussolotti[1], V. Caracciolo[1], R. Cerulli[1], A. Leoncini, V. Merlo[1], F. Montecchia[2], F. Cappella[3], A. d'Angelo[3], A. Incicchitti[3], A. Mattei[3], C.J. Dai[4], X.H. Ma[4], X.D. Sheng[4], Z.P. Ye[5]

[1]Dip. Fisica, Università di Roma "Tor Vergata", INFN sezione di Roma, "Tor Vergata", I-00133 Rome, Italy
[2]Dipartimento Ingegneria Civile e Informatica, Università di Roma "Tor Vergata", INFN sezione di Roma, "Tor Vergata", I-00133 Rome, Italy
[3]Dip. Fisica, Università di Roma "La Sapienza", INFN sezione di Roma, I-00185 Rome, Italy
[4]Key Laboratory of Particle Astrophysics, Institute of High Energy Physics, Chinese Academy of Sciences, Beijing 100049, P.R. China
[5]University of Jinggangshan, Ji'an, Jiangxi, P.R. China

Abstract. The model-independent annual modulation effect measured by DAMA deep underground at Gran Sasso National Laboratory with different experimental configurations is summarized; the evidence of a signal that meets all the requirements of the model-independent Dark Matter annual modulation signature at high C.L. has been confirmed over many independent annual cycles with various configurations (DAMA/NaI, DAMA/LIBRA–phase1 and DAMA/LIBRA–phase2; full exposure is 2.86 ton × yr). The DAMA/LIBRA–phase2–empowered configuration has then put in operation with an even lower software energy threshold. As in the plans, the experiment will complete all data takings at fall 2024. The DAMA project has also realized many measurements to investigate various other rare processes.

Povzetek: Avtorji predstavijo dolgoletene meritve letnih modulacij signala, ki ga meri experiment DAMA v laboratoriju Gran Sasso National Laboratory globoko pod zemljo. Da gre za signale letne modulacije temne snovi, ki izpolnjujejo vse zahteve modelno neodvisnih meritev, potrjujejo meritve z različnimi eksperimentalnimi konfiguracijami (DAMA/NaI, DAMA/LIBRA–
faza 1 in DAMA/LIBRA–faza 2; s skupno izpostavljenostjo 2,86 ton × leto). Pri zadnji konfiguraciji, DAMA/LIBRA–faza 2, je bil energetski prag znižan pod 1 KeV. Načrtovano je bilo, da bo eksperiment zaključen jeseni 2024. Projekt DAMA je izvedel številne meritve tudi drugih redkih procesov.

1.1 Introduction

The DAMA project [1] was proposed in 1990 as a pioneer in the field of Dark Matter (DM) direct investigation with the aim to realize large mass set-ups (highly radio-pure NaI(Tl) and liquid Xenon) mainly dedicated to the direct detection of

---

** e-mail: rita.bernabei@roma2.infn.it

DM particles in the galactic halo by exploiting the model-independent DM signature (suggested in the middle of the '80 by Ref. [2, 3]). Many other measurements on various rare processes have also been carried along the DAMA project living time [4]. In particular, the pioneer DAMA/NaI experiment ($\simeq$ 100 kg of highly radiopure NaI(Tl) in a multi-ton multi-component shield) [8] ran deep underground in the Gran Sasso National Laboratory (LNGS) of INFN until 2002 investigating as first the DM signature with suitable exposed mass, sensitivity and control of the running parameters [4, 6, 8]. After several years of new developments, at fall 2002 the experimental site as well as many components of the installation were implemented [7] and the new DAMA/LIBRA(–phase1) experimental set-up (about 250 kg of highly radiopure NaI(Tl)) was installed; all the procedures were performed in high purity (HP) Nitrogen atmosphere, and the detectors have also continuously maintained in such an atmosphere in all the operations since then. That configuration has been upgraded at the end of 2010 in DAMA/LIBRA–phase2 by replacing all the PMTs with new ones having higher quantum efficiency (i.e. lowering the software energy threshold of the experiment). For many experimental details see in Ref. [8, 9]. After a period of commissioning, this set-up began data collection; at the end of 2012 new preamplifiers and special developed trigger modules were installed, and the apparatus was equipped with more compact electronic modules. For our setups the details of the experimental aspects which are always important and specify the difference among experiments claimed similar, can be found in published papers and documents. Many model-independent results and related corollary analyses have been published [4, 10, 11]. More recently, after studies and tests to lower the software energy threshold below 1 keV, all the PMTs have been equipped with new low-background voltage dividers with pre-amps on the same board and new Transient Digitizers (TD) with higher vertical resolution (14 bits). This new configuration, named DAMA/LIBRA–phase2–empowered, is in measurements since December 1, 2021 and data collection is planned to be completed at fall 2024.

It is worthy to remind that the largely model-independent DM annual modulation signature is related to the Earth's motion with respect to the DM particles of the Galactic Dark Halo. In fact, as a consequence of the Earth's revolution around the Sun, which is moving in the Galaxy with respect to the Local Standard of Rest towards the star Vega near the constellation of Hercules, the Earth should be crossed by a larger flux of DM particles around $\simeq$ 2 June and by a smaller one around $\simeq$ 2 December (in the first case the Earth orbital velocity is summed to that of the solar system with respect to the Galaxy, while in the other one the two velocities are subtracted). This DM signature depends on Earth's and DM particles' velocities and, thus, it has different origin and peculiarities than the seasons on the Earth and than effects correlated with seasons (consider the expected value of the phase as well as its other specific requirements) and it also does not depend on the Earth hemisphere where it is measured.

We remind that this signature is very distinctive since the effect induced by DM particles must simultaneously satisfy all the following requirements: the rate must contain a component modulated according to a cosine function (1) with one–year period (2) and a phase that peaks roughly $\simeq$ 2 June (3); this modulation must only

be found in a well-defined low energy range, where DM particle induced events can be present (4); it must apply only to those events in which just one detector of many actually "fires" (*single-hit* events), since the DM particle multi-interaction probability is negligible (5); the modulation amplitude in the region of maximal sensitivity must be 7% of the constant part of the signal for usually adopted halo distributions (6), but it can be larger in case of some proposed scenarios such as e.g. those in Ref. [12–16] (even up to $\simeq$ 30%). This signature with its many peculiarities allows the test of a wide range of parameters in many possible astrophysical, nuclear and particle physics scenarios. It might be mimicked only by systematic effects or side reactions able to account for the whole observed modulation amplitude and to simultaneously satisfy all the requirements given above. Finally, the NaI(Tl) target nuclei and procedures adopted by DAMA provide sensitivity to large and low mass DM candidates inducing nuclear recoils and/or electromagnetic signals.

For completeness, we note that the sensitivity of the DM annual modulation signature depends – apart from the counting rate – on the product: $\epsilon \times \Delta E \times M \times T \times (\alpha - \beta^2)$, thus increasing either the detection efficiency, ϵ, or the measurement time, T, or enlarging the energy interval, ΔE, is in practice equivalent to increase the exposed mass M; $(\alpha - \beta^2) \simeq 0.5$ is the squared cosine averaged over the period where the data taking is active. Therefore, the followed strategy along the DAMA project was to pursue an increasing of the experimental sensitivity.

1.2   Short summary on results on DM annual modulation results

The data released so far by DAMA/NaI, DAMA/LIBRA–phase1 and DAMA/LIBRA–phase2 have been analyzed with many different and independent analysis strategies, obtaining always consistent results. Any possible systematics or side processes able to mimic the exploited signature has been excluded, both because neither quantitatively significant amplitude can be given nor simultaneous satisfaction of all the specific requirements of the signature. Details on the data and the analyses can be found in the wide DAMA literature (see e.g. [4, 10, 11] and refs therein). Here we recall just few points.

As first in Fig. 1.1-top: the $(2 - 6)$ keV residual rates of the *single-hit* scintillation events for the data released so far by the former DAMA/NaI, by DAMA/LIBRA–phase1 and by DAMA/LIBRA–phase2 (total exposure 2.86 ton $\times$ yr) are shown. The function $A \cos \omega(t - t_0)$ was used to fit the data taking into account a period $T = \frac{2\pi}{\omega} = 1$ yr and a phase $t_0 = 152.5$ day (June 2nd) as predicted by the DM annual modulation signature. The obtained χ^2/d.o.f. is 130/155 and the modulation amplitude is $A = (0.00996 \pm 0.00074)$ cpd/kg/keV. Fig. 1.1-bottom shows instead the experimental residual rate of the *single-hit* scintillation events measured by DAMA/LIBRA–phase2 (having lower software energy threshold) in the $(1 - 6)$ keV energy intervals as a function of the time.

A further relevant investigation on the data has been performed by applying the same hardware and software procedures, used to acquire and to analyze the *single-hit* residual rate, to the *multiple-hit* one. Since the probability that a DM particle interacts in more than one detector is negligible, a DM signal can be present just
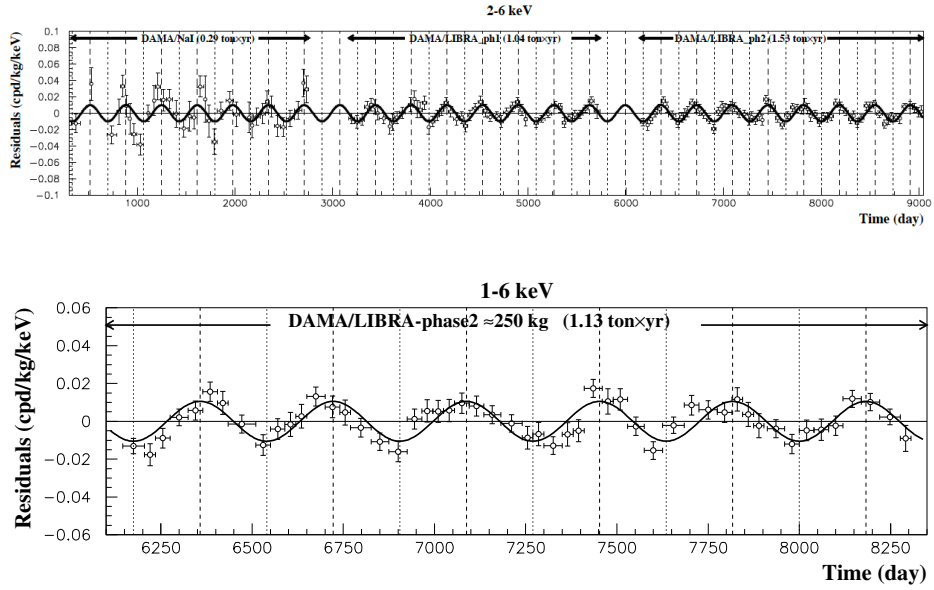
2-6 keV

1-6 keV

Fig. 1.1: *Top:* Experimental residual rate of the *single-hit* scintillation events measured by DAMA/NaI, DAMA/LIBRA–phase1 and DAMA/LIBRA–phase2 (total exposure 2.86 ton × yr) in the (2 − 6) keV energy intervals as a function of the time. The superimposed curve is the cosinusoidal functional forms $A \cos \omega(t - t_0)$ with a period $T = \frac{2\pi}{\omega} = 1$ yr, a phase $t_0 = 152.5$ day (June 2nd) and modulation amplitude, A, equal to the central value obtained by best fit. Vertical dashed lines indicate the expected maximum rate, while the dotted lines represent the expected minimum rate. *Bottom:* Experimental residual rate of *single-hit* scintillation events measured by DAMA/LIBRA–phase2, which operates with a lower software energy threshold, in the (1 − 6) keV energy range, shown as a function of time.

in the *single-hit* residual rate. Thus, the comparison of the results of the *single-hit* events with those of the *multiple-hit* ones corresponds to compare the cases of DM particles beam-on and beam-off. This procedure also allows an additional test of the background behaviour in the same energy interval where the positive effect is observed. A clear modulation, satisfying all the peculiarities of the DM annual modulation signature, is present in the *single-hit* events, while the fitted modulation amplitude for the *multiple-hit* residual rate is well compatible with zero (see e.g. Ref. [17]). Since the same identical hardware and the same identical software procedures have been used to analyze the two classes of events, the obtained result gives an additional support for the presence of a DM particle component in the galactic halo. The *single-hit* residuals have also been investigated by a Fourier analysis (see e.g. Ref. [18]). A clear peak corresponding to a period of 1 year is evident in the low energy intervals; the same analysis in the (6 − 14) keV energy region shows only aliasing peaks instead. Neither other structure at different frequencies has been observed.

The annual modulation present at low energy can also be pointed out by depicting the energy dependence of the modulation amplitude, $S_m(E)$, obtained by maximum likelihood method considering fixed period and phase: T =1 yr and t_0 = 152.5 day. The modulation amplitudes for the whole data sets: DAMA/NaI, DAMA/LIBRA–phase1 and DAMA/LIBRA–phase2 (total exposure 2.86 ton × yr) are plotted in Fig. 1.2; the data below 2 keV refer only to the DAMA/LIBRA–phase2 exposure (1.53 ton × yr). It can be inferred that positive signal is present in the (1 − 6) keV energy interval (a new data point below 1 keV has been added as mentioned in the caption), while S_m values compatible with zero are present just above.
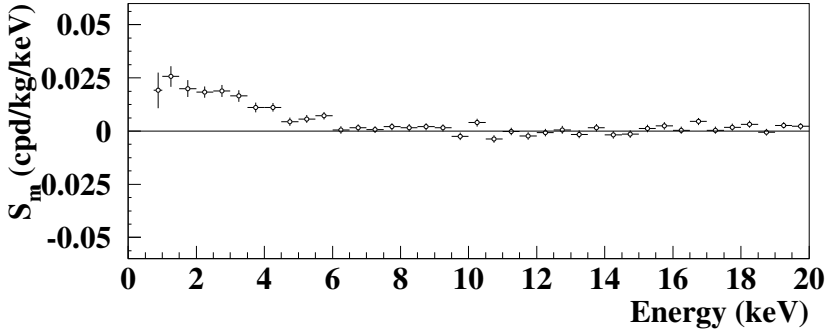
Fig. 1.2: Modulation amplitudes, S_m, as function of the energy for the whole data sets: DAMA/NaI, DAMA/LIBRA–phase1 and DAMA/LIBRA–phase2 (total exposure 2.86 ton×yr) above 2 keV; in the bin (1 − 2) keV only the DAMA/LIBRA-phase2 exposure (1.53 ton × yr) is available and used, while the first lowest energy point has been obtained by a cautious re-analysis with specific dedicated efficiency analysis there. A clear modulation is present in the lowest energy region, while S_m values compatible with zero are present just above.

It has also been verified that the observed annual modulation effect is well distributed in all the 25 detectors.

It is worth noting that in all the analyses, when releasing the period and phase, values consistent with those expectations are obtained.

In particular, in Fig. 1.3 the results obtained with the same exposure of 2.86 ton × yr, when adopting in the maximum likelihood analysis of the *single-hit* events the most general expression for the signal component (i.e. releasing the assumption of a phase value $t_0 = 152.5$ day):

$$S_i(E) = S_0(E) + S_m(E) \cos \omega(t_i - t_0) + Z_m(E) \sin \omega(t_i - t_0) \qquad (1.1)$$
$$= S_0(E) + Y_m(E) \cos \omega(t_i - t^*)$$

are shown.

For signals induced by DM particles, one would have: i) $Z_m \sim 0$ (because of the orthogonality between the cosine and the sine functions); ii) $S_m \simeq Y_m$; iii) $t^* \simeq t_0 = 152.5$ day. In fact, these conditions hold for most of the dark halo models;

however, as mentioned above, slight differences can be expected in case of possible contributions from non-thermalized DM components.
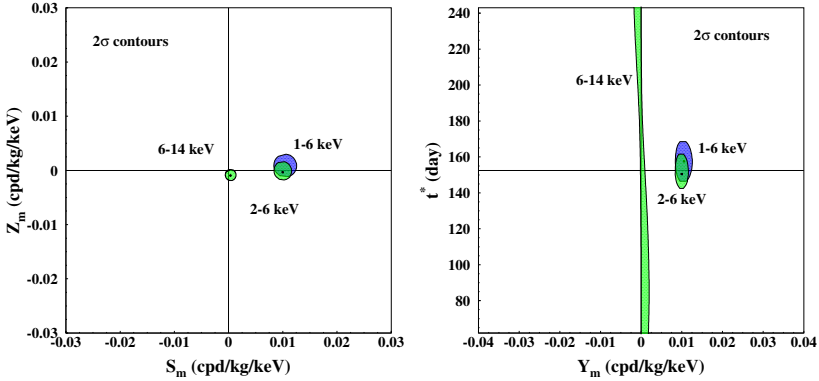
Fig. 1.3: 2σ contours in the plane (S_m, Z_m) (*left*) and in the plane (Y_m, t^*) (*right*) for: i) DAMA/NaI, DAMA/LIBRA–phase1 and DAMA/LIBRA–phase2 in the $(2-6)$ keV and $(6-14)$ keV energy intervals (light areas, green on-line); ii) only DAMA/LIBRA–phase2 in the $(1-6)$ keV energy interval (dark areas, blue on-line). The contours have been obtained by the maximum likelihood method. A modulation amplitude is present in the lower energy intervals and the phase agrees with that expected for DM induced signals.

As shown in Fig. 1.3 a clear modulation is present in the lower energy intervals and the phase agrees with that expected for DM signal while such a modulation is absent just above.

Among further additional analyses the modulation amplitudes separately for the nine inner detectors and the external ones have been studied for DAMA/LIBRA–phase1 and DAMA/LIBRA–phase2, as already done for the other data sets [11, 17–24]. The obtained values are fully in agreement showing that the effect is also well shared between inner and outer detectors. Moreover, to test the hypothesis that the modulation amplitudes calculated for each DAMA/LIBRA–phase1 and DAMA/LIBRA–phase2 annual cycle are compatible and normally fluctuating around their mean values, the χ^2 test and the *run test* have been used; this analysis has confirmed that the data collected in all the annual cycles with DAMA/LIBRA–phase1 and –phase2 are statistically compatible and can be considered together [11].

We invite the reader to see details and other kind of different and independent analyses of the data in the DAMA literature [4] and, in particular, in [10, 11] and Refs. therein.

No systematic or side processes able to mimic the signature, i.e. able to simultaneously satisfy all the many peculiarities of the signature and to account for the whole measured modulation amplitude, has been found or suggested by anyone throughout some decades thus far (for details see e.g. Ref. [6–9, 11, 17–28]). In particular, arguments related to any possible role of some natural periodical

phenomena have been discussed and quantitatively demonstrated to be unable to mimic the signature (see references; e.g. Refs. [26, 27]). Thus, on the basis of the exploited signature, the model independent DAMA results give evidence at 13.7σ C.L. (over 22 independent annual cycles and in various experimental configurations) for the presence of DM particles in the galactic halo.

The DAMA model independent evidence is compatible with a wide set of astrophysical, nuclear and particle physics scenarios for high and low mass candidates inducing nuclear recoil and/or electromagnetic radiation, as also shown in various literature. Moreover, both the negative results and all the possible positive hints, achieved so-far in the field, can be compatible with the DAMA model independent DM annual modulation results in many scenarios considering also the existing experimental and theoretical uncertainties; the same holds for indirect approaches. For a discussion see e.g. Ref. [17, 18] and Refs. therein. Here we just mention the model of Ref. [29] based on the assumption of the existence of a low-energy bound state of dark atoms and nuclei while also considering the self-consistent influence of nuclear attraction and Coulomb repulsion, discussed – at various extent – in this series of Bled conferences.

It is worthy to note that in complete model-dependent corollary analyses, the estimate of the upper limit on the signal component in the measured rate (see e.g. in Ref. [10]) has obviously to be considered as a prior.

1.3   Few arguments about the analysis procedure

As reported several times along the years [11,17–24], the data taking of each annual cycle in DAMA/LIBRA starts before the expected minimum of the DM signal (about 2 December) and ends after its expected maximum (about 2 June). Thus, adopting in the data analysis a constant background evaluated within each annual cycle, any possible decay of long–term–living isotopes cannot mimic a DM positive signal with all its peculiarities. On the contrary, it may only lead to underestimate the DM annual modulation amplitude, depending on the radio-purity of the set-up.

Despite this obvious fact, Refs. [30,31] claim that the DAMA annual modulation result might be mimicked by the adopted analysis procedure. Detailed analyses on this argument have already been reported in Ref. [17], confuting these claims quantitatively, even considering the case of a rate at low energy in DAMA/LIBRA with odd behavior, increasing with time.

More recently, since Ref. [31] claims that an annual modulation in the COSINE–100 data can appear if they use an analysis method somehow similar to DAMA/LIBRA. However, as expected from the rate of COSINE–100 that is very–decreasing with time and from what mentioned above, the authors obtain a modulation with reverse phase [31]; this corresponds, when fixing the phase to $t_0 = 152.5$ day, to *NEGATIVE* modulation amplitudes, as expected by the elementary considerations reported before. This artificial effect has no way to mimic the observed DM signature with its peculiarity.

Thus, while the appearance of modulation with *NEGATIVE* amplitudes is due to the peculiar behavior of the COSINE–100 rate very–decreasing with time, this is

not the case of DAMA/LIBRA. In particular, the DAMA/LIBRA NaI(Tl) detectors are not the "same" as those of COSINE–100, since e.g. they were grown starting from different powders, using different purification, growing procedures and protocols; they have been stored underground since decades, they have different quenching factors for alpha's and nuclear recoils (i.e. nominally equal interval in keV electron equivalent corresponds to different energy interval in keV of nuclear recoil), etc. Thus, they have well different residual contaminations and features[1] as well as different electronics and all other details of the experimental set-up and procedures, the storage underground, etc.

Moreover, the stability with time of the running parameters of each DAMA/LIBRA annual cycle is reported e.g. in Refs. [11, 17–24]. As regards the odd idea that the low-energy rate in DAMA/LIBRA might increase with time due to spill out of noise [31], we just recall two facts that rule out this possibility: 1) the stability with time of noise, reported in several papers [11, 17–24]; 2) the estimate of the remaining noise tail after the noise rejection procedure $\ll 1\%$ [8].

Finally, the arguments of Ref. [17] already showed that any possible effect in DAMA/LIBRA due to either long–term time–varying background or odd behavior of the rate, increasing with time, is negligible. Here we just recall:

- The $(2 - 6)$ keV *single-hit* residual rates have been recalculated considering a possible time–varying background. They provide modulation amplitude, fitted period and phase well compatible with those obtained in the *original* analysis, showing that the effect of long–term time–varying background – if any – is marginal [17].

- Any possible long–term time–varying background would also induce a fake modulation amplitudes (Σ) on the tail of the $\mathcal{S}_{\mathrm{m}}$ distribution above the energy region where the signal has been observed. The analysis in Ref. [17] shows that $\mid \Sigma \mid < 1.5 \times 10^{-3}$ cpd/kg/keV. Thus, taking into account that the observed *single-hit* annual modulation amplitude at low energy is order of 10^{-2} cpd/kg/keV, any possible effect of long–term time–varying background – if any – is marginal [17].

- The maximum likelihood analysis has been repeated including a linear term decreasing with time. The obtained $\mathcal{S}_{\mathrm{m}}$ averaged over the low energy interval are compared with those obtained in the *original* analysis, showing that their differences are well below the statistical errors [17].

- The behaviour of the *multiple-hit* events, where no modulation has been found [11, 17] in the same energy region where the annual modulation is present in the *single-hit* events, strongly disfavours the hypothesis that the counting rate has significant long–term time–varying contributions.

- The last three published years of DAMA/LIBRA–phase2 (in which there was continuity between one year and the next) were analyzed considering the same background (w/ and w/o any slope). This detailed analysis has been reported in this Conference; here we summarize it showing in Fig. 1.4

---

[1] The DAMA/LIBRA set-up had some upgrades – one of them is that from phase1 to phase2 to lower the software energy threshold – also acting to improve the signal/background ratio.

the comparison between the modulation amplitudes, S_m, obtained with the whole data set: DAMA/NaI, DAMA/LIBRA–phase1 and DAMA/LIBRA–phase2 (total exposure 2.86 ton×yr) and with the last three published years of DAMA/LIBRA–phase2 analyzed considering the same background. The modulation amplitudes of the two data sets are compatible, implying that any effect of long–term time–varying background or odd low-energy rate increasing with time is negligible in DAMA/LIBRA, thanks to the radiopurity and long-time underground of the ULB DAMA/LIBRA NaI(Tl). Thus, the original DAMA analyses can be safely adopted.
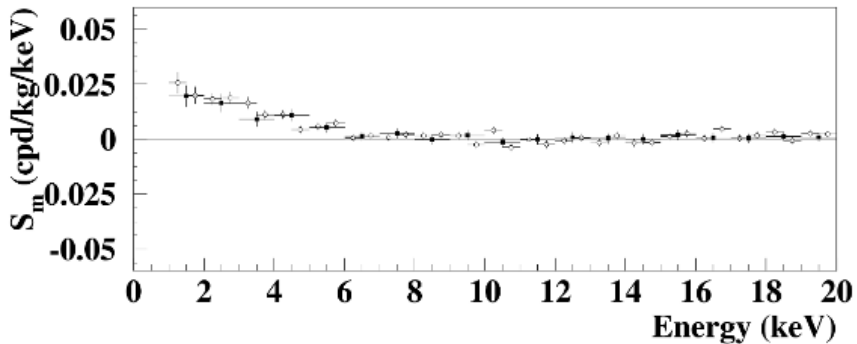
Fig. 1.4: Comparison between the modulation amplitudes, S_m, for the whole data set (open circles): DAMA/NaI, DAMA/LIBRA–phase1 and DAMA/LIBRA–phase2 (total exposure 2.86 ton×yr) and for the data set (black circles) of the last three published years of DAMA/LIBRA–phase2 (in which there was continuity between one year and the next) analyzed considering the same background, see text. The modulation amplitudes of the two data sets are compatible, implying that any effect of long–term time–varying background or odd low-energy rate increasing with time is negligible in DAMA/LIBRA, thanks to the radiopurity and long-time underground of the ULB DAMA/LIBRA NaI(Tl). Thus, the original DAMA analyses can be safely adopted.

Summarizing, the arguments of Ref. [17] and the analysis of the last three published years of DAMA/LIBRA–phase2 already showed that any possible effect in DAMA/ LIBRA due either to long–term time–varying background or to any odd behavior of the rate, increasing with time, is negligible and the *original* analyses, that assume a constant background within each annual cycle, can be safely adopted. Similar conclusions were also reported in Ref. [32].

1.4   Running DAMA/LIBRA–phase2–empowered

In more recent years the DAMA collaboration has worked to further increase the experimental sensitivity, to improve the measurement of the modulation parameters (such as the phase, which brings important information), and to explore the
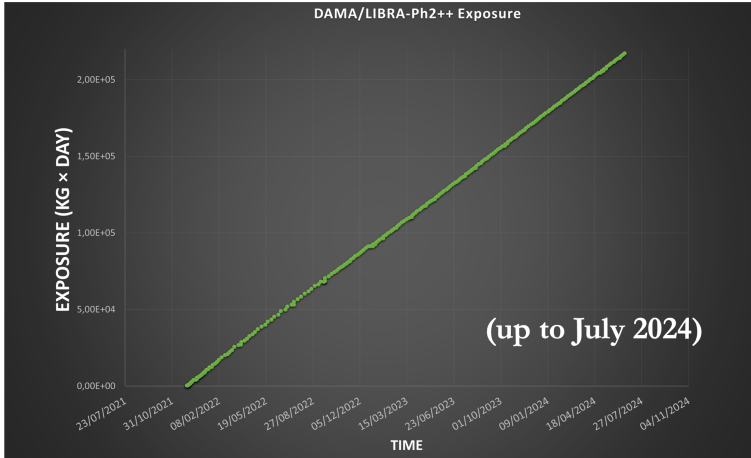
Fig. 1.5: Data taking behaviour of DAMA/LIBRA–phase2–empowered; see text.

DM annual modulation signature at lower software energy threshold with high overall efficiency (also improving the possibility to disentangle among different possible scenarios).

After various R&D's, a safer and cheaper solution has been adopted to improve the signal over noise ratio in the lowest energy bins and, thus, to lower the software energy threshold and to improve related quantities. In particular, new low-background preamplifiers have been developed to realize a single device with high signal/noise ratio, where the voltage divider and the preamplifier with miniaturized selected components are integrated on the same low background board. The main features of this new voltage divider plus preamplifier system are: i) signal/noise: $\simeq 3.0 - 9.0$; ii) discrimination of single photoelectron from electronic noise: 3 – 8; iii) peak to valley ratio: 4.7 – 11.6; iv) residual radioactivity lower than that of single PMT. Further relevant improvements arise from improvements in the electronic chain; in particular, all the Transient Digitizers were substituted with new ones having higher vertical resolution (14 bits).

The DAMA/LIBRA–phase2 set-up was upgraded during fall 2021, and the data taking in this new configuration, identified as DAMA/LIBRA–phase2–empowered, started on Dec, 1 2021. The operational features are very stable; in particular, the baseline fluctuations are more than a factor two lower than those of the previous configuration and the RMS of the baseline distributions is around 150 μV, ranging between 110 and 190 μV. The software Trigger Level (STL) is decreased in the offline analysis. The "noise" events near software energy threshold due to single photoelectron have evident different structures than the scintillation pulses with the same energy, and this feature is used to discriminate them. DAMA/LIBRA–phase2–empowered is planned to continuously run up to fall 2024; for example, up to July 2024 (see Fig. 1.5) about 0.558 ton × yr exposure has been collected with $(\alpha - \beta^2) \simeq 0.501$. In the same period, about 7.75×10^7 events have been collected from sources for energy calibration and about 4.35×10^7 events ($\simeq 1.74 \times 10^6$ events/keV) for determining the acceptance window efficiency for all the crystals.

Just few examples of the quality of the data taking are shown in Fig. 1.6 where the stability of the counting rate and energy scale is given for some detectors (as the other components of the set-up, always kept in High Purity Nitrogen atmosphere and without exposure to neutron sources) in the region where both ^{210}Pb and ^{129}I contribute and are dominant. There the data collected in the period December 2022 to December 2023 are divided in four time-intervals. As evident the energy scale and the counting rate are well stable.
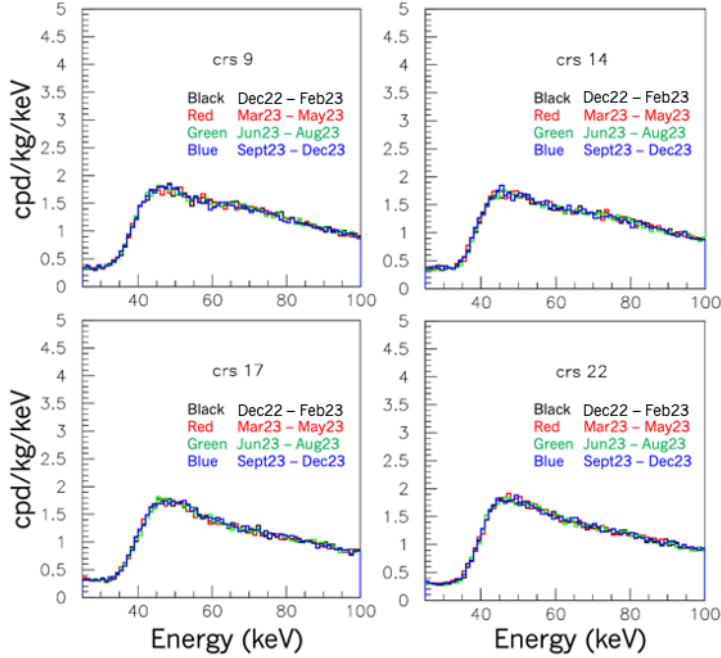
Fig. 1.6: Examples of the stability of the counting rate and energy scale of some detectors in the energy region where both ^{210}Pb and ^{129}I contribute and are dominant (as also the other components of DAMA set-ups, they have been always kept in High Purity Nitrogen atmosphere and without exposure to neutron sources). There the data collected in the period December 2022 to December 2023 are divided in four time-intervals. As evident the energy scale and the counting rate are well stable.

In addition, in Fig. 1.7-Left the distribution of the percentage variations (ϵ_{tdcal}) of each low-energy energy scale factor (td_{cal_k}) with respect to the value measured in the previous calibration ($td_{cal_{k-1}}$) from Dec 1, 2021 to Feb 23, 2023 is shown. The Gaussian behaviour with $\sigma = 0.3\%$ assures that the low energy calibration factor for each detector is known with an uncertainty $<< 1\%$ during the data taking periods implying a maximum relative contribution to annual modulation amplitude $< (1 - -2) \times 10^{-4}$ cpd/kg/keV. Thus, no quantitatively significant

energy scale variation is present: moreover, in every case, that cannot mimic the exploited DM signature also failing some of the requirements.
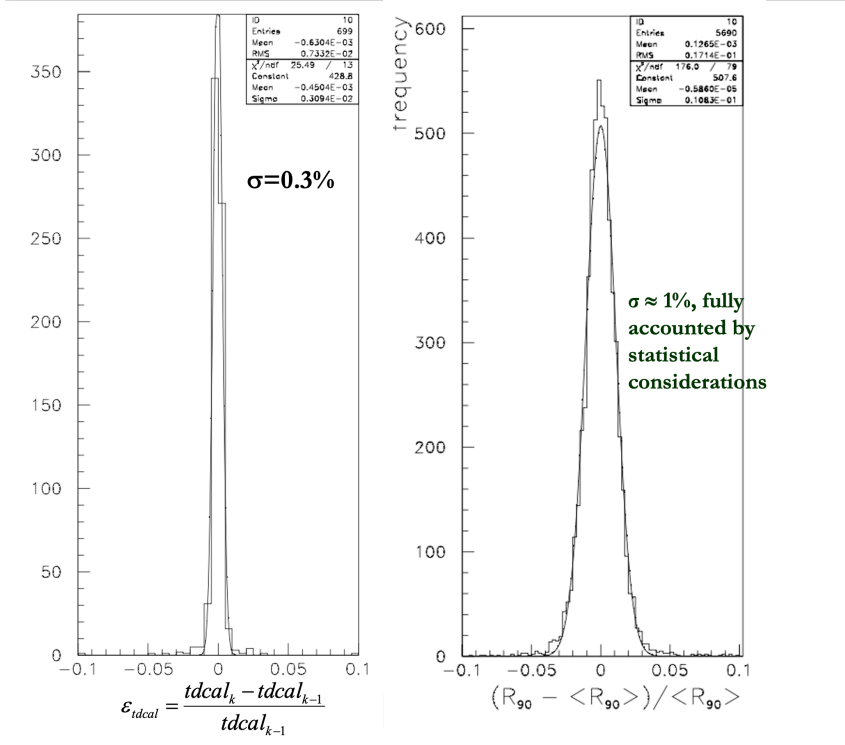
Fig. 1.7: *Left*: Measured distribution of the percentage variations (ϵ_{tdcal}) of each low-energy energy scale factor (td_{cal_k}) with respect to the value measured in the previous calibration ($td_{cal_{k-1}}$) from Dec 1, 2021 to Feb 23, 2023; see text. *Right*: Measured distribution of the percentage variations of the R_{90} integral rate for the data taken from Dec 1, 2021 to Feb 23, 2023; see text.

Finally, in Fig. 1.7-Right the stability of the overall background above 90 keV is shown for the same data by studying the integral rate at higher energy (above 90 keV), R_{90}. In particular, there is shown the R_{90} percentage variations with respect to their mean values for single crystal. Fitting the behaviour with time, adding a term modulated with period and phase as expected for DM particles, an amplitude $A_{mod} = (0.04 \pm 0.11)$ cpd/kg is found, well consistent with zero. Note that, if a modulation would be present in the whole energy spectrum at the level found in the lowest energy region by previous configurations, a R_{90} of tens cpd/kg would be present, i.e about 100 σ far away from the measured value.

1.5   ..and more

For completeness we mention that other complementary strategies already pursued – at some extent – by DAMA are still promising when analysing data corre-

sponding to sensitivities larger than the previously published one. In particular, the investigation of the DM diurnal modulation, already studied with the data of DAMA/LIBRA–phase1 [33]. In fact, a DM diurnal modulation with sidereal time is expected because of Earth rotation; this is a second order effect and thus difficult to point out since very important sensitivity and overall experimental stability are required, much more than e.g. those needed for DM annual modulation investigations. An important aspect is that the ratio R_{dy} of the diurnal over annual modulation amplitude is a model independent constant at a given latitude; at LNGS latitude $R_{dy} \simeq 0.016$, the expected period in sidereal time is 24 h and the phase is 14 h.

Another interesting effect has been preliminarily investigated with the same set of data searching for possible Earth shadowing effect [34]. This effect could be expected for DM candidate particles inducing just nuclear recoils and only for candidates with high cross-section with ordinary matter (i.e. low DM local density). In such a case a variation of the measured DM rate could be expected during the day because of the different Earth thickness crossed by the DM particle to reach the experimental set-up deep underground. Those DM candidate particles lose their energy crossing the Earth and the DM velocity distribution, observed in the laboratory frame, is modified as function of time. In this scenario, suitable analysis strategies can allow to disentangle the DM local density and the cross section as well as to add constraints for those DM candidates.

Moreover, DAMA has suggested in 1992 the use of anisotropic scintillators to investigate the directionality approach to investigate the presence of DM candidates inducing just nuclear recoils by exploiting the non-isotropic nuclear recoil distribution correlated to the Earth motion in the galactic frame. The idea has been subsequently further developed [35,36] focusing more recently the $ZnWO_4$ scintillators as the more suitable one for the purpose [37]. In fact, the light output and the pulse shape of $ZnWO_4$ for highly ionizing particles (as nuclear recoils) depend on the direction with respect to the crystal axes and both anisotropic features can provide two independent ways to exploit this approach. Moreover, no anisotropy is present for electromagnetic signals. Many developments have then been carried out and published since then (see in [4]), including measurements of quenching factors both for α and recoiling nuclei [38]. The anisotropy for nuclear recoils were established for the first time at 5.4 σ [38].

Finally, looking very forward, we remind the suggestion in Ref. [10] to exploit the DM annual modulation on other celestial body and, in particular, on Mars where the expected DM annual modulation would have period $T_M = 668.6$ Sols, phase $\simeq 354$ Sols in the Mars calendar and an amplitude $\simeq 5\%$ (i.e. the S_m/S_0 value) for usually adopted halo distributions (Mars parameters evaluated by Starlink Project).

1.6   Conclusions

DAMA has been a pioneer project in the direct detection of Dark Matter, obtaining the first model-independent evidence for the presence of a particle component of the Dark Matter particles in the galactic halo on the basis of the exploited DM

annual modulation signature with various experimental configurations. Three independent experimental set-ups have confirmed the presence of a peculiar annual modulation of the *single–hit* events in the energy region (2 – 6) keV, that meets all the many requirements of the DM annual modulation signature; the cumulative exposure, considering them all together is 2.86 tons × yr (over 22 independent annual cycles and with different experimental configurations). No systematic or side processes able to account for the observed signal are available. Similar result has also been obtained when lowering the software energy threshold down to 1 keV in DAMA/LIBRA-phase2. Corollary investigations on the nature of the DM particle(s) in given scenarios have been performed by corollary model-dependent analyses. Various models and parameters (experimental and theoretical) are possible, and many hypotheses have to be considered.

For completeness, we remind that preliminarily to DAMA/LIBRA–phase2–empowered, particular efforts for lowering the software energy threshold have been done in the already-published data of DAMA/LIBRA–phase2 by using the same technique as before with dedicated studies on the efficiencies, obtaining modulation amplitude as a function of energy down to 0.75 keV; the peculiar modulation has also been observed below 1 keV [11].

Finally, DAMA/LIBRA–phase2–empowered was realized and put in operation to lower the software energy threshold below 1 keV with suitable acceptance efficiency in order to further increase the experimental sensitivity and to better disentangle some of the many possible astrophysical, nuclear and particle physics scenarios in the investigation on the DM candidate particles. It is planned to collect data until fall 2024.

References

1. P. Belli, R. Bernabei, C. Bacci, A. Incicchitti, R. Marcovaldi, D. Prosperi: DAMA proposal to INFN Scientific Committee II, April 24th, 1990.
2. A.K. Drukier, K. Freese, D.N. Spergel: Detecting cold dark-matter candidate, Phys. Rev. D **33** (1986) 3495.
3. K. Freese, J.A. Frieman, A. Gould: Signal modulation in cold-dark-matter detection, Phys. Rev. D **37** (1988) 3388.
4. see publication list in dama.web.roma2.infn.it
5. R. Bernabei et al.: Performances of the 100 kg NaI(Tl) set-up of the DAMA experiment at Gran Sasso, Il Nuovo Cimento A **112** (1999) 545.
6. R. Bernabei et al.: Dark Matter search, Riv. Nuovo Cimento **26** (2003) 1; R. Bernabei et al.: Dark Matter particles in the galactic halo: results and implications from DAMA/NaI, Int. J. Mod. Phys. D **13** (2004) 2127; references therein.
7. R. Bernabei et al.: The DAMA/LIBRA apparatus, Nucl. Instr. and Meth. A **592** (2008) 297.
8. R. Bernabei et al.: Performances of the new high quantum efficiency PMTs in DAMA/LIBRA, J. Instrum. **7** (2012) P03009
9. P. Belli et al.: The electronics and DAQ system in DAMA/LIBRA, Int. J. Mod. Phys. A **31** (2016) 1642005; dedicated issue to DAMA/LIBRA of Int. J. Mod. Phys. A **31** (2016).
10. R. Bernabei et al.: The DAMA project: achievements, implications and perspectives, Progress in Particle and Nuclear Physics **114** (2020) 103810.

11. R. Bernabei et al.: Further results from DAMA/LIBRA-phase2 and perspectives, Nucl. Phys. At. Energy **22** (2021) 329; refs. therein.
12. D. Smith, N. Weiner: Inelastic dark matter, Phys. Rev. D **64** (2001) 043502.
13. D. Tucker-Smith, N. Weiner: Status of inelastic dark matter, Phys. Rev. D **72** (2005) 063509.
14. D.P. Finkbeiner et al.: Inelastic dark matter and DAMA/LIBRA: An experimentum crucis, Phys. Rev. D **80** (2009) 115008.
15. K. Freese et al.: Detectability of weakly interacting massive particles in the Sagittarius dwarf tidal stream, Phys. Rev. D **71** (2005) 043516.
16. K. Freese et al.: Effects of the Sagittarius dwarf tidal stream on dark matter detectors, Phys. Rev. Lett. **92** (2004) 111301.
17. R. Bernabei et al., The DAMA project: Achievements, implications and perspectives, Prog. Part. Nucl. Phys. **114**, 103810 (2020).
18. R. Bernabei et al., Dark Matter Investigation by DAMA at Gran Sasso, Int. J. of Mod. Phys. A **28** (2013), 1330022.
19. R. Bernabei et al., First results from DAMA/LIBRA and the combined results with DAMA/NaI, Eur. Phys. J. C **56**, 333 (2008).
20. R. Bernabei et al., New results from DAMA/LIBRA, Eur. Phys. J. C **67**, 39 (2010).
21. R. Bernabei et al., Final model independent result of DAMA/LIBRA–phase1, Eur. Phys. J. C **73**, 2648 (2013).
22. R. Bernabei et al., First Model Independent Results from DAMA/LIBRA–phase2, Universe **4**, 116 (2018).
23. R. Bernabei et al., First Model Independent Results from DAMA/LIBRA–phase2, Nucl. Phys. At. Energy **19**, 307 (2018).
24. R. Bernabei, New model independent results from the first six full annual cycles of DAMA/LIBRA–phase2, Bled Workshops in Physics **19** n. 2, 27 (2018).
25. R. Bernabei and A. Incicchitti, Low background techniques in NaI(Tl) setups, Int. J. of Mod. Phys. A **32**, 1743007 (2017).
26. R. Bernabei et al., No role for muons in the DAMA annual modulation results, Eur. Phys. J. C **72**, 2064 (2012).
27. R. Bernabei et al., No role for neutrons, muons and solar neutrinos in the DAMA annual modulation results, Eur. Phys. J. C **74**, 3196 (2014).
28. R. Bernabei et al., Improved Model-Dependent Corollary Analyses after the First Six Annual Cycles of DAMA/LIBRA–phase2, Nucl. Phys. At. Energy **20(4)**, 317 (2019).
29. T. Bikbaev, M. Khlopov and A. Mayorov, Numerical Modeling of the Interaction of Dark Atoms with Nuclei to Solve the Problem of Direct Dark Matter Search, Symmetry **15** (2024) 2182.
30. D. Buttazzo et al., Annual modulations from secular variations: relaxing DAMA?, JHEP **2020**, 137 (2020).
31. G. Adhikari et al., An induced annual modulation signature in COSINE–100 data by DAMA/LIBRA's analysis method, http://arxiv.org/abs/2208.05158.
32. A. Messina et al., Annual modulations from secular variations: not relaxing DAMA?, JCAP **04**, 037 (2020).
33. R. Bernabei et al., Model independent result on possible diurnal effect in DAMA/LIBRA-phase1, Eur. Phys. J. C **74** (2014) 2827.
34. R. Bernabei et al., Investigating Earth shadowing effect with DAMA/LIBRA–phase1, Eur. Phys. J. C **75**, 239 (2015).
35. P. Belli et al., Identifying a dark matter signal by non-isotropic scintillation detectors. N.Cim.C15(1992)475
36. R. Bernabei et al., Anisotropic scintillators for WIMP direct detection: revisited, Eur. Phys. J. C **28** (2003) 203.

37. R. Bernabei et al., Anisotropic scintillators for WIMP direct detection: revisited, Eur. Phys. J. C **73** (2013) 2276.

38. P. Belli et al., Measurements of $ZnWO_4$ anisotropic response to nuclear recoils for the ADAMO project, Eur. Phys. J. A **56** (2020) 83.

BLED WORKSHOPS
IN PHYSICS
VOL. 25, NO. 1

Proceedings of the 27th Workshop
What Comes Beyond . . . *(p. 17)*
Bled, Slovenia, July 8–17, 2024

2   Problems of dark atom cosmology

V. A. Beylin[1†], M. Yu. Khlopov[1,2,3‡], D. O. Sopin[2,3§]

[1] Virtual Institute of Astroparticle physics, 75018 Paris, France
[2] National Research Nuclear University MEPhI, 115409 Moscow, Russia
[3] Research Institute of Physics, Southern Federal University, 344090
Rostov on Don, Russia

Abstract. The dark atoms XHe are the composite Thomson like atomic dark matter candidates. We address two cosmological problems of this model. The excess of new superheavy particles with even negative charge X^{-2n} over the corresponding antiparticles is balanced by sphaleron transitions with baryon asymmetry and the mass range of X particles should be specified at which this excess can provide dominance of dark atoms in the dark matter density. The other problem is possible capture of light nuclei by dark atoms, which can lead to formation of anomalous isotopes. The possibility of formation of multi dark atom systems at the nucleosynthesis stage is also studied. We approach these open questions of dark atom cosmology in the present work.

Povzetek: Temni atomi XHe so kandidati za temno snov v obliki Thomsonovih atomskih struktur. Obravnavamo različne lastnosti tega modela: Presežek supertežkih delcev z enakomernim negativnim nabojem $X - 2n$ glede na ustrezne antidelce uravnotežimo s sfaleronskimi prehodi z barionsko asimetrijo, maso delcev X pa določimo tako, da je XHe v temni snovi dominanten. Če temni atomi ujamejo lahka jedra, pride do nastanka nenavadnih izotopov. Lahko pa se zgodi tudi, da pri nukleosintezi nastanejo skupki večjega števila temnih atomov XHe.

2.1   Introduction

The modern cosmological paradigm involves dark matter (DM). Its existing is confirmed by numerous astrophysical observations: gravitational lensing, anisotropy of the cosmic microwave background and the behavior of galaxies. The theoretical study of cosmological large-scale structures formation also requires to introduce new stable forms of non-relativistic non-baryonic matter.

The nature of DM particles is determined by physics beyond the Standard Model (SM). It was shown that new states could have only even negative electric charge to fulfill the constraints on anomalous isotopes concentration [1]. In that scenario the DM density should be provided by the X-helium dark atoms $X^{-2n}(He^{+2})_n$, which forms in two steps. At first of them the excess of heavy negatively charged

---

particles X^{-2n} over the corresponding antiparticles finally generates in sphaleron transitions. The density of the DM could be balanced with the density of baryonic matter [2–4]. In particular model the constraints on the mass of the new particles can also be found if it is only one source of the DM. The second stage is the formation of a bound state by capturing the light primordial nuclei.

However, the description of both steps should be clarified. The properties of the sphaleron transitions are depends on a model significantly [5, 6]. Therefore calculations with using the SM parameters could be considered only as the first estimation. At the same time, the process of the bound state formation is well described only for small values of charge [7, 8]. The serial capture of light nuclei leads to the significant changes in the inner structure of the dark atom. Moreover, such reactions have not been described yet. Also the possible interaction of two bound states at early stages of Universe evaluation has not been studied. In general case, to solve this problems, it is necessary to use the quantum description of Thompson-like dark atoms, which is absent.

We approach these open questions of dark atom cosmology in the present work. Section 2.2 provides a brief review of papers on the properties of sphaleron(s) in models with heavy particle. The minimal Walking Technicolor (WTC) model is considered as an example. In section 2.3 the dark atom formation at nucleosynthesis stage is discussed. The results are summarized in the Conclusion.

2.2 Sphaleron in WTC model

The static unstable solution of electroweak field equations in pure gauge theory was originally found by Manton in 1983 [9] and called "sphaleron" . It corresponds to the saddle point at the top of the potential barrier separating topologically nonequivalent vacuums in configuration space. Author pointed that sphaleron arises as a consequence of the topology of the $SU(2)$ group. The main properties of the similar solution in the SM were considered in several papers throughout the 90s [10–13]. There were found that

1. Only for non-physical values of the Higgs parameters, the existence of additional branches of sphaleron transitions are possible [10].
2. Sphaleron can be described with high accuracy using the spherically symmetric ansatz [11]. Its physical energy should be $E_{Sph} \approx 9.1 \, \text{TeV}$.

The further study has shown that both these statements can be violated by physics beyond the SM. For instance, the existing of heavy fermions (with mass in order of 1 TeV) leads to a significant change in the sphaleron energy [13]. The additional solution of field equations may arise as a consequence of a deformation of the Higgs potential [6]. Such changes should affect baryosynthesis due to sphaleron freezing out temperature T_* decreases (or increases) [15]. Actually the predicted ratio of DM and baryonic matter densities depends on the ratio $\frac{m_i}{T_*}$, where m is a mass of "i" type particle. It means that the resulting uncertainty in the temperature value is insignificant and can be compensated by tuning unknown masses of heavy species. However, it is also necessary to compare the shifted sphaleron freezing

out temperature T_* with the temperature of electroweak phase transition T_c. The predictions may differ significantly for cases $T_* > T_c$ and $T_* < T_c$ [2–4, 16].

Therefore, the determination of the exact properties of sphaleron transitions is needed to consider models suggesting the existence of dark atoms. This is especially true for the minimal WTC model which assumes both the new heavy fermions and a modified Higgs potential [17–19]. Unfortunately, studying the features of this SM extension involves some technical difficulties. Indeed, among others the low energy effective WTC model predicts 19 new (pseudo)scalar fields, which should be introduced into the system of equations. The problem is not only in the number of additional degrees of freedom, but also in the fact that the effect of spinless fields on the sphaleron solution has not yet been studied. All the same can be said with respect to composite vector fields.

However, it can be expected that this approach will allow to find more precise upper limits on the masses of heavy particles. Indeed, the height of the sphaleron potential barrier significantly decreases if new fermions are too heavy. This contradicts the absence of sphaleron transitions in modern experiments [20]. The influence of additional branches of sphaleron transitions on cosmological evolution is less obvious and requires a particular case study.

2.3   Dark atom formation

The second step of the dark atom formation is serial capturing of light primordial nuclei N^i by negatively charged heavy particles X^{-2n}. The simplest possible scenario assumes $n = 2$. In that case dark atom $X^{--}He^{++}$, which is usually denoted as OHe, can be considered as a Bohr-like bound state with energy

$$E_{OHe}^{Bohr} = 8\alpha^2 m_{He} \approx 1.6\,\text{MeV}. \tag{2.1}$$

It could easily estimated that O-helium is formed almost immediately after the formation of helium during standard nucleosynthesis [7]. It is happens at temperatures $T \sim 1 - 100\,\text{keV}$.

However, in general case $n > 1$ it is necessary to consider the much more complicated scenario. Indeed, there are four types of processes are possible at nucleosynthesis stage

$$N^1 + N^2 \rightarrow N^3 + \gamma/N^4, \tag{2.2}$$

$$X + N \rightarrow XN + \gamma, \tag{2.3}$$

$$XN^1 + N^2 \rightarrow XN^3 + \gamma/N^4, \tag{2.4}$$

$$XN^1 + XN^2 \rightarrow X_2N^3 + \gamma/N^4. \tag{2.5}$$

The first of them (2.2) describes the standard nuclear reactions. There are eleven main processes that produce helium-4 and some heavier nuclei (isotopes of lithium and beryllium) [14]. Reactions (2.3) are similar to the standard recombination. In general case they produce negatively charged bound states (dark ions) $(XN)^{-2n+q_N}$, which are burns in type (2.4) reactions. Unfortunately, this may lead to overproduction of anomalous isotopes and/or primordial metals [8]. The last

type processes (2.5) describes the merging of two dark ions into the molecule-like bound state.

A correct description of nucleosynthesis in the presence of multicharged particles requires to consider each step of the dark atom formation. First of all, it is necessary to find the temperature when the (2.3) type reactions become possible. By analogy with hydrogen recombination for non-relativistic equilibrium concentrations

$$n_i^{now} \left(\frac{T}{T_{now}} \right)^3 = g_i \left(\frac{m_i T^{\frac{3}{2}}}{2\pi} \right) e^{-\frac{m_i}{T}}, \tag{2.6}$$

the Saha equation [14] gives

$$T_{rec} = E_{X-N} \left(\ln \left(\frac{g_X g_N}{g_{XN}} \left(\frac{m_N T_{now}^2}{2\pi E_{X-N}} \right)^{\frac{3}{2}} \frac{1}{n_N^{now}} \right) \right)^{-1}, \tag{2.7}$$

where g_i is the the number of spin degrees of freedom, m_N is the mass of captured light nucleus, n_N^{now} is its present concentration and E_{X-N} is a binding energy for the system "heavy core plus nuclear shell". The last one depends on the inner structure of the dark ion.

For high values of the charge parameter n the ratio of nuclear and X^{-2n} Bohr radii

$$a = \frac{r_N}{r_B} \approx Z_X Z_N \alpha m_N r_0 A_N^{1/3} \tag{2.8}$$

may have values higher than one. This means that composite particle has not a Bohr, but Thomson structure (see Figure 2.1). Table 2.1 shows the results of
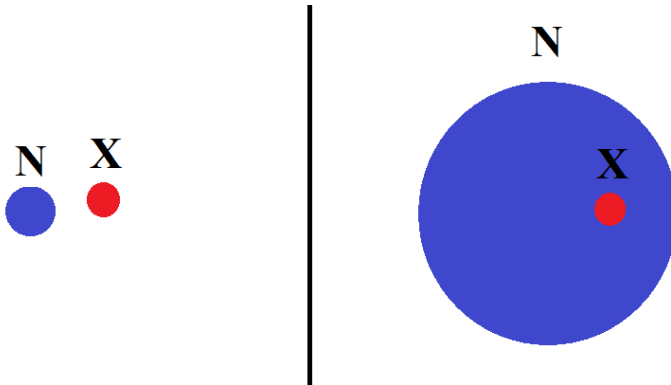
Fig. 2.1: Bohr-like (left) and Thompson-like (right) dark atoms

calculations of some XN bound states:

- B — all isotopes form Bohr-like particles;
- T — all isotopes form Thomson-like particles;

- Number — the mass number of the lightest Thomson-like particle.

There was accepted $r_0 = 1.3 \cdot 5 \, \text{GeV}$. It can be noted that almost all neutral and positively charged states should have a Thomson structure, but hydrogen mostly forms Bohr-type dark ions. This is consistent with the result of solving the two-body Coulomb problem obtained in [8]. The predicted structure of transitional states, which are indicated in the table by numbers, depends on value of r_0. For instance, OHe is Bohr-like dark atom if the values $r_0 \sim (1.1 - 1.2) \cdot 5 \, \text{GeV}$ are accepted.

n	A			
	H	He	Li	Be
1	B	4	3	T
2	4	3	T	T
3	3	T	T	T
4	3	T	T	T
5	2	T	T	T

Table 2.1: The structure of the dark ions XN.

Therefore the Bohr energy

$$E_{X-N}^{Bohr} = 2n^2 Z^2 \alpha^2 m_N = \frac{1}{2 m_N r_B^2}. \tag{2.9}$$

can be used in equation (2.7) only for hydrogen and helium (in case $n = 1$). To find the binding energy of other bound states, the harmonic oscillator approximation is often used in literature [7,21,22]. The Hamiltonian

$$\mathcal{H} = \begin{cases} \dfrac{p^2}{2m_N} - \dfrac{Z_X Z_N \alpha}{2 r_N} \left(3 - \dfrac{r^2}{r_N^2} \right), & r < r_N \\[2mm] \dfrac{p^2}{2m_N} - \dfrac{Z_X Z_N \alpha}{r}, & r > r_N \end{cases} \tag{2.10}$$

leads to the Thompson energy formula

$$E_{X-N}^{Thompson} = \frac{3}{2} \frac{Z_X Z_N \alpha}{r_N} \left(1 - \sqrt{\frac{1}{Z_X Z_N \alpha m_N r_N}} \right) =$$

$$= \frac{3}{2} \frac{Z_X Z_N \alpha}{r_N} \left(1 - \sqrt{\frac{r_B}{r_N}} \right), \tag{2.11}$$

which should be correct at region $2 < a < \infty$. For intermediate values ($1 < a < 2$) it is proposed to find the binding energy variationally. The binding energy value of Bohr-like states is higher than for Thomson-like dark ions. This can be qualitatively explained by the compensation of Coulomb repulsion because of the spherical symmetry of the Hamiltonian (2.10).

Table 2.2 shows approximate values of dark ions recombination temperatures (start of reactions (2.3)) calculated with equations (2.9) and (2.11). For the transitional cases (D and ^{4}He), only the boundary values are presented. The inner structure of the bound states is specified by the corresponding letter in brackets. The result depends weakly on the values of g_X and g_{XN}. Since helium-4 forms at temperature $T \approx 65$ keV [14], there are two possible scenarios are predicted:

- For the $n < 4$, the helium capturing happens earlier than protons and/or deuterium can be captured. Then, the excess of dark ions, $(XHe)^{-2n+2}$, is formed to start reactions (2.4).
- For $n \geq 4$, hydrogen capturing becomes possible before the ^{4}He formation. Therefore, another branch of reactions $(XH + N \rightarrow ...)$ is started. Such processes lead to an additional danger of anomalous isotopes overproduction at later stages of the dark atom formation. This may help to set limits on the maximum charge of a heavy core.

Unfortunately, the temperature T_{rec} for deuterium in case $n = 5$ can not be estimated in this simple approach. Moreover, the drop in the energy value caused by the change of the inner structure can lead to non-trivial consequences.

n	T_{rec}, keV			
	p	D	^{3}He	^{4}He
1	3 (B)	4 (B)	28 (B)	37 (B) / 6 (T)
2	13 (B)	19 (B)	~ 42 (T)	85 (T)
3	29 (B)	44 (B)	~ 116 (T)	180 (T)
4	54 (B)	79 (B)	~ 198 (T)	285 (T)
5	86 (B)	~ 126 (B) / 17 (T)	~ 286 (T)	395 (T)

Table 2.2: Recombination temperatures of the dark atoms

Since the standard reactions of nucleosynthesis and formation of dark atoms occur at the same temperatures, the Saha equation becomes inapplicable. Indeed, it requires that concentrations change only due to the expansion of the Universe, which is not true in considered case. Therefore, to describe processes (2.3)-(2.5) it is necessary to use the system of kinetic equations [23]

$$\frac{dn_i}{dt} + 3Hn_i = \sum_{j,k} n_j n_k \langle \sigma v \rangle_i^{jk} - n_i \sum_j n_j \langle \sigma v \rangle^{ij}, \qquad (2.12)$$

where the energy-averaged cross sections $\langle \sigma v \rangle_i^{jk}$ corresponds to $2 \rightarrow 2$ reactions $j + k \rightarrow i + l$. Also it should be mentioned that produced in such processes ordinary nuclei are not thermalized and should be described by additional equations

$$\frac{\partial \phi_{N_i}}{\partial t} = \sum_{j,k} n_j n_k \frac{d(\sigma v)_{N_i}^{jk}}{dp_{N_i}} - \phi_{N_i} \sum_j n_j (\sigma v)^{N_i j}(p_{N_i}) - \phi_{N_i} \sum_j \int \phi_{N_j} (\sigma v)^{N_i N_j} dp_{N_j},$$

$$(2.13)$$

where it is defined

$$\frac{dn_N}{dp_N} = \phi_N(p_N, t). \tag{2.14}$$

Finally, reactions (2.4) and (2.5) may freeze out before the nucleosynthesis stops. They are possible only if

$$n_{XN} \langle \sigma v \rangle t > 1. \tag{2.15}$$

For a simple estimation, it can be assumed that

$$n_{XN} \approx \frac{\rho_c}{m_{XHe}} \Omega_{DM}^{now} \left(\frac{T}{T_{now}} \right)^3, \tag{2.16}$$

where Ω_{DM}^{now} is the observable energy density of dark matter. Also it should be taken into account that radiation dominates. Therefore

$$t = \frac{3}{4} \frac{m_{Pl}}{T^2} \sqrt{\frac{5}{\pi^3 g_*}}. \tag{2.17}$$

Here m_{Pl} is the Plank mass and g_* is a number of ultrarelativistic degrees of freedom at the considered temperature [14]. For the non-relativistic particles "i" with the average thermal speed $\langle v \rangle = \sqrt{\frac{8T}{\pi m_i}}$ the condition (2.15) can be rewritten as (energy is measured in GeV)

$$n_{XN} \langle \sigma v \rangle t \approx \frac{3}{2\pi^2} \frac{\rho_c \, \Omega_{DM}^{now} \, m_{Pl} \, \sigma}{m_{XHe} T_{now}^3} \sqrt{\frac{10 \, T^3}{g_* \, m_i}} \approx$$

$$\approx 3 \cdot 10^9 \, \frac{\sigma}{m_{XN} \sqrt{m_i}} T^{\frac{3}{2}} > 1. \tag{2.18}$$

If the cross section σ has a typical nuclear value

$$\sigma \sim \pi r_{XN}^2 \approx 10^{-25} \, \text{cm}^2 = 250 \, \text{GeV}^{-2}, \tag{2.19}$$

then equation (2.18) predicts the similar scenario for both types of reactions. This condition is fulfilled at high temperatures $T \sim 50 - 100 \, \text{keV}$, but strongly violated at $T \sim 1 \, \text{keV}$. The rate difference between the reactions of (2.4) and (2.5) types is determined by the ratio of masses m_{XHe}/m_N. The production of dark molecules should stop earlier then capturing of light nuclei. Moreover, if masses of heavy particles is high enough ($m_X \sim 10 \, \text{TeV}$), the formation of molecule-like states X_2N does not start.

The main source of inaccuracy in considered estimation is the value of cross section (2.19). Its exact value is unknown for the most reactions therefore it is impossible to make a correct prediction of the modified nucleosynthesis result.

2.4   Conclusion

The dark atoms XHe are the composite DM candidates. The cosmological consequences of this model are studied pretty well for the simplest case when the

heavy particles X are only doubly charged. However, the description of dark atom formation is still incomplete. On the one hand, the predicted density of DM significantly depends on the properties of sphaleron transitions, which may change in different extensions of the SM. On the other hand, the process of light nuclei serial capturing has not been sufficiently studied.

To solve these two problems of considered model it is necessary to

- find the sphaleron solution of the field equations for the particular extension of the SM and then to estimate the freezing out temperature of sphaleron transitions;
- find the solution of the system of kinetic equations which describes the modified nucleosynthesis.

The computational complexity of such calculations is complemented by the lack of an accurate quantum description of the Thompson-like dark atoms.

Acknowledgements

References

1. K. M. Belotsky, M. Y. Khlopov, K. I. Shibaev: Composite Dark Matter and its Charged Constituents, in: Proceedings Gravitation and Cosmology. Vol. 12., (KPS 06), Moscow, 2006. — e-PrintArchive: astro-ph/0604518.
2. S.B. Gudnason, C. Kouvaris, F.: Sannino: Dark matter from new technicolor theories, Phys. Rev. D **74** (2006) 095008
3. M.Y. Khlopov, C. Kouvaris: Strong interactive massive particles from a strong coupled theory, Phys. Rev. D **77** (2008) 065002
4. V.A. Beylin, M.Y. Khlopov, D.O. Sopin: Asymmetric Dark Matter in Baryon Asymmetrical Universe, Symmetry **16** (2024) 311
5. G. Nolte, J. Kunz: Sphaleron barrier in the presence of fermions, Phys. Rev. D. **48(12)** (1993) 5905–5916
6. M. Spannowsky, C. Tamarit: Sphalerons in composite and nonstandard Higgs models, Phys. Rev. D. **95(1)** (2017) 015006
7. M. Y. Khlopov, A. G. Mayorov, E. Y. Soldatov: Dark Atoms of the Universe: towards OHe nuclear physics, arXiv (2010) 1011.4586
8. E. Akhmedov, M. Pospelov: BBN catalysis by doubly charged particles, JCAP **08** (2024) 028
9. N. S. Manton: Topology in the Weinberg-Salam Theory, Phys. Rev. D. **28** (1983) 2019
10. J. Kunz, Y. Brihaye: New sphalerons in the Weinberg-Salam theory, Phys. Lett. B. **216(3)** (1989) 353–359
11. J. Kunz, B. Kleihaus, Y. Brihaye: Sphalerons at finite mixing angle, Phys. Rev. D. **46(8)** (1992) 3587–3600
12. D. Diakonov [et al.]: Fermion sea along the sphaleron barrier, Phys. Rev. D. **49(12)** (1994) 6864–6882

13. G. Nolte, J. Kunz, B. Kleihaus: Nondegenerate fermions in the background of the sphaleron barrier, Phys. Rev. D. **53(6)** (1996) 3451–3459
14. D. S. Gorbunov, V. A. Rubacov: *INTRODUCTION TO THE THEORY OF THE EARLY UNIVERSE Hot Big Bang Theory*, World Scientific Publishing Co. Pte. Ltd., Singapore, 2011
15. V. A. Kuzmin, V. A. Rubakov, M. E. Shaposhnikov: On the Anomalous Electroweak Baryon Number Nonconservation in the Early Universe, Phys. Lett. B **155** (1985) 36
16. J. A. Harvey, M. S. Turner: Cosmological baryon and lepton number in the presence of electroweak fermion-number violation, Phys. Rev. D **42(10)** (1990) 3344–3349
17. S. B. Gudnason, C. Kouvaris, F. Sannino: Towards working technicolor: Effective theories and dark matter, Phys. Rev. D. **73(11)** (2006)
18. R. Foadi [et al.]: Minimal walking technicolor: Setup for collider physics, Phys. Rev. D. **76(5)** (2007)
19. F. Sannino: Conformal Dynamics for TeV Physics and Cosmology, arXiv (2009) 0911.0931
20. J. Ellis, K. Sakurai, M. Spannowsky: Search for Sphalerons: IceCube vs. LHC, arXiv (2016) 1603.06573
21. R. N. Cahn, S. L Glashow, Chemical Signatures for Superheavy Elementary Particles, Science **213** (1981) 607–611
22. K. Kohri, F. Takayama: Big bang nucleosynthesis with long-lived charged massive particles, Phys. Rev. D **76(6)** (2007)
23. M. Khlopov: *Fundamentals of Cosmic Particle Physics* Cambridge International Science Publishing Ltd, Cambridge, UK, 2012

3 Quantum-mechanical numerical model of interaction between dark atom and nucleus of substance

T.E. Bikbaev[1,*], M.Yu. Khlopov[1,2,3], A.G. Mayorov[1]

[1] National Research Nuclear University MEPhI
115409 Moscow, Russia;
[2] Institute of Physics, Southern Federal University, Stachki 194 Rostov on Don 344090, Russia;
[3] Université de Paris, CNRS, Astroparticule et Cosmologie, F-75013 Paris, France; e-mail: khlopov@apc.univ-paris7.fr (M.K.);
[*] Correspondence: bikbaev.98@bk.ru

Abstract. The hypothesis of composite XHe dark atoms may provide solution to the long-standing problem of direct searches for dark matter particles. The main problem of the XHe dark atom is its ability to strongly interact with the nucleus of substance, arising from the unshielded nuclear attraction between the helium nucleus and the nucleus of matter. It is assumed that in order to prevent the destruction of the bound structure of dark atom, the effective potential of interaction between XHe and the nucleus of substance must have dipole Coulomb barrier that prevents the fusion of dark matter atom particles with the nucleus of substance. The problem in describing the interaction between dark atom and substance nucleus is the three-body problem, for which an exact analytical solution is not available. Consequently, to assess the physical meaning of the proposed scenario, it is essential to develop a numerical approach. Our approach involves consistently developing an accurate quantum mechanical description of this three-body system, comprising bound dark atom and the external nucleus of substance. We incorporate the necessary effects and interactions to enhance the precision of the results, which helps to elucidate the most significant aspects of the proposed dark atom scenario.

Povzetek Hipoteza o skupkih temnih atomov XHe lahko ponudi razlago za dolgoletni problem neposrednega iskanja delcev temne snovi. Ker temni atomi XHe močno interagirajo z jedri običajne snovi, je možnost, da se zlijejo z njimi, velika. Da se to ne zgodi avtorji predpostavijo, da zlitje prepreči dipolna Coulombova pregrada. Gre za problem treh delcev, za katerega ni analitične rešitve. Avtorji so se lotili reševanja tega kvantnomehanskega problema treh delcev numerično. V prispevku poročajo o dosežkih doslej.

Keywords: Dark atoms; composite dark matter; stable charged particles; ipole coulomb barrier; effective interaction potential; XHe; X-helium

3.1   X-helium dark atoms

The non-baryonic essence of dark matter suggests the existence of new stable forms of non-relativistic matter that play the role of stable dark matter particles in the universe. If dark matter is particle-based, it implies the presence of new stable particles beyond the Standard Model. It has been proposed that such particles may include stable, electrically charged particles [1–4]. This article discusses the minimal walking technicolor (WTC) model, which introduces a novel perspective on dark matter as a composite entity [5–7]. The WTC model suggests the existence of heavy fermions associated with new gauge interactions, and within this framework, the Higgs boson is characterized by composite structure derived from single scalar doublet. In the WTC model, the electric charge of stable, multicharged particles remains undefined, yet stringent experimental constraints dictate that these particles can only possess stable, negatively charged state of $-2n$ [8,9], where n is natural number. We denote these particles as X, with the specific case when X has charge of -2 is denoted as O^{--}.

This article focuses on composite dark matter scenario in which hypothetical, stable, heavy X^{-2n} particles with lepton-like characteristics (i.e., without QCD interactions or with highly suppressed QCD interactions) form neutral atom-like states with n ^4He nuclei of primary helium via usual electromagnetic Coulomb binding. Such configurations are called XHe dark atoms, where X^{-2n} particles may exhibit lepton-like properties or represent unique combinations of heavy quark new families, marked by weak interactions with hadrons [10].

The structural features of bound dark atom system are defined by parameter $a \approx Z_\alpha Z_X \alpha A_\alpha m_p R_{nHe}$, with α denoting the fine-structure constant, Z_X and Z_α are the charge numbers of the X particle and nHe nucleus, m_p is the proton mass, A_α is the mass number of nHe, and R_{nHe} is the radius of the nHe nucleus. Here, a signifies the ratio of the Bohr radius of the dark atom to the radius of the n-helium nucleus. When the Bohr radius of the XHe atom is smaller than the radius of n-helium nucleus, the dark atom resembles Thomson-like structure, otherwise, it represents Bohr atom.

For values of a within $0 < a < 1$, the XHe configuration aligns with Bohr atom model, where the helium nucleus, approximated as point particle, orbits the centrally positioned, negatively charged X particle. Conversely, for a values within $1 < a < \infty$, the structure aligns with Thomson's atomic model, where the not-point-like helium nucleus oscillates around the heavier negatively charged X particle, reflecting a more distributed atomic configuration.

The unique characteristics of dark atoms give rise to a "warmer-than-cold dark matter" scenario in the formation of large-scale structures, which, though requiring additional exploration, aligns with data from precision cosmology [10]. The relevance of this article is expressed by the need for further investigation into the nuclear properties of dark atoms and the potential impacts of X-helium on nuclear transformations. Understanding these interactions is crucial for quantifying the role of dark atoms in primary cosmological nucleosynthesis, stellar evolution, and other physical, astrophysical, and cosmological processes in the early universe [11].

The varied results from direct dark matter detection experiments highlight the complexities in interactions between dark matter particles and materials in underground detectors. The X-helium hypothesis suggests that the formation of low-energy bound states between dark atoms and nuclei in detector materials could account for the positive findings of the DAMA/NaI and DAMA/LIBRA experiments, which differ from the negative results observed in XENON100, LUX, and CDMS [10, 12].

Due to the unscreened nuclear charge of dark atoms, the possibility of strong nuclear interactions between XHe atoms and matter nuclei could disrupt the bound state of dark atoms, potentially producing anomalous isotopes, whose environmental abundance is highly constrained by experimental limits [8]. To address this, the XHe hypothesis introduces a shallow potential well and a dipole Coulomb barrier within the effective interaction potential between dark atoms and nuclei, which prevents the fusion of nHe and X particles with ordinary matter nuclei. This is crucial condition for the stability and viability of the X-helium hypothesis.

Modeling the interaction between dark atoms and ordinary nuclei presents three-body problem, lacking an exact analytical solution. Thus, to understand the physical implications of this scenario – defined by a dipole Coulomb barrier and shallow well in the effective interaction potential – precise quantum mechanical numerical model for this three-body system is being developed. The model aims to reconstruct the effective interaction potential, allowing detailed analysis of the properties and dynamics of the interactions between dark atoms, as composite constituents of dark matter, and nuclei of ordinary matter.

3.2   The isolated dark atom system

It is well understood that dark atom, when exposed to an alternating electric field from external nucleus, experiences the Stark effect, causing polarization of the XHe atom. This polarization generates dipole Coulomb repulsion between the dark atom and the nucleus, which, in turn, can lead to the establishment of bound state between the X-helium and the nucleus of substance. This bound state arises due to potential well that precedes the dipole Coulomb barrier in the total effective interaction potential in XHe–nucleus system.

To reconstruct the effective interaction potential in the XHe–nucleus system with accuracy, precise calculation of the Stark potential is crucial. This potential determines the interaction between the polarized dark atom, functioning as XHe dipole, and the charged heavy nucleus. The Stark potential significantly influences both the depth of the potential well, which defines the low-energy bound state between XHe and the nucleus of ordinary matter, and the height of the dipole Coulomb barrier, which repels the dark atom from the nucleus and thus prevents their fusion. To accomplish this, quantum mechanical calculations of the dark atom's dipole moment $\vec{\delta}$ under the influence of an alternating external electric field (via the Stark effect) are essential, as the Stark potential depends directly on the dipole moment $\vec{\delta}$ according to the relation:

$$U_{St} = eZ_{nHe}(\vec{E}_{nuc} \cdot \vec{\delta}), \qquad (3.1)$$

where $\vec{E}_{nuc}$ denotes the strength of the external electric field generated by the heavy charged nucleus of substance, and Z_{nHe} represents the charge number of the nHe nucleus.

In this article, we will examine the special case where the charge of the X particle is -2, such that the X particle is O^{--} particle bound to ^{4}He nucleus of primordial helium, forming neutral OHe dark atom.

For accurate quantum mechanical calculation of the dipole moment of polarized dark atom, it is necessary not only to obtain the helium wave functions in its ground state within the OHe–nucleus system but also to determine the ground-state wave function of helium within an isolated, non-polarized OHe dark atom. Consequently, the initial step involves studying $\hat{H}_0$, the Hamiltonian operator of isolated OHe dark atom, which is free from external influences. Using numerical difference scheme, $\hat{H}_0$ is represented as a matrix, and its eigenvalues are computed numerically. These eigenvalues yield the discrete energy levels of helium, E_{OHe}, within the isolated OHe atom, while the eigenvectors corresponding to these states represent the wave functions, Ψ, of helium in O-helium. This involves solving the following one-dimensional Schrödinger equation:

$$\hat{H}_0 \Psi(\vec{r}) = E_{OHe} \Psi(\vec{r}), \tag{3.2}$$

or by presenting this expression in another form:

$$\Delta_r \Psi(\vec{r}) + \frac{2m_{He}}{\hbar^2} \left(E_{OHe} + \frac{4e^2}{r} \right) \Psi(\vec{r}) = 0, \tag{3.3}$$

where $\vec{r}$ denotes the position vector of the helium nucleus, m_{He} refers to the mass of the helium nucleus, and $\hbar$ is the Planck constant. The coordinate system is centered at the position of the O^{--} particle.

By numerically solving the one-dimensional Schrödinger equation (3.2) using numerical difference scheme, with the helium radius vector range set to $r = |2.5 \times 10^{-12}$ cm$|$ and the number of iterations $N_{iter} = 2000$, the first three eigenvalues of the Hamiltonian operator, $\hat{H}_0$, were determined: $E_{1,2,3_{num}} = -1.585, -0.393, -0.042$ MeV. Theoretical calculations for the first three energy levels of helium in the O-helium dark atom yield $E_{1,2,3_{OHe}} = -1.589, -0.397, -0.177$ MeV [22]. As observed, the first two calculated energy levels are consistent with the theoretical values to the second decimal place. For the purposes of quantum mechanical numerical calculation of the dipole moment of polarized OHe, it is necessary to know only the wave function corresponding to the first, ground energy level of helium within isolated O-helium atom.

3.3 Interaction potential of helium in the three-body OHe-nucleus system

The three-body problem at hand involves three-body interaction within the XHe–nucleus system. We focus on the particular case where the XHe dark atom resembles hydrogen-like Bohr atom, namely O-helium. Here, the coordinate system has its origin at the center of the O^{--} particle, which binds to the point-like helium

nucleus via Coulomb forces, forming bound atomic system of composite dark matter. The OHe dark atom is subjected to an inhomogeneous external electric field generated by a third particle, namely, a nucleus characterized by charge number Z_{nuc}, neutron number N_{nuc}, and mass number A. This nucleus approaches the dark atom gradually, engaging in both electromagnetic and strong nuclear interactions.

The Hamiltonian for the point-like helium nucleus in the OHe – nucleus system can be expressed as:

$$\hat{H} = \hat{H}_0 + \hat{U}, \tag{3.4}$$

where $\hat{H}_0$ represents the Hamiltonian of the isolated OHe dark atom, unaffected by external forces, and $\hat{U}$ corresponds to the interaction potential between helium and the external nucleus of substance.

We define the vectors $\vec{r}$, $\vec{R}_{OA}$, and $\vec{R}_{HeA}$ as follows: $\vec{r}$ represents the relative distance vector between the O^{--} particle and the helium nucleus, $\vec{R}_{OA}$ is the position vector of the external nucleus, and $\vec{R}_{HeA}$ denotes the vector pointing from the center of the helium nucleus to the center of the external nucleus. These vectors are related by the equation:

$$\vec{R}_{HeA} = \vec{R}_{OA} - \vec{r}. \tag{3.5}$$

Next, let's write down $\hat{H}_0$ and $\hat{U}$:

$$\hat{H}_0 = -\frac{\hbar^2}{2m_{He}}\Delta - \frac{4e^2}{r}, \tag{3.6}$$

$$\hat{U} = U_{Coulomb}(|\vec{R}_{OA} - \vec{r}|) + U_{Nuc}(|\vec{R}_{OA} - \vec{r}|) + U_{rot_{(He-Na)}}(|\vec{R}_{OA} - \vec{r}|), \tag{3.7}$$

here $U_{Nuc}(|\vec{R}_{OA} - \vec{r}|)$ signifies the nuclear interaction potential, formulated using the Woods–Saxon potential. $U_{Coulomb}(|\vec{R}_{OA} - \vec{r}|)$ describes the Coulomb potential between the point-like helium nucleus and the not-point-like of the external nucleus. The term $U_{rot_{(He-Na)}}$ accounts for the centrifugal potential arising from the interaction between helium and sodium nuclei.

The nuclear potential is calculated dependent on the spacing between the neutron distribution surfaces of the interacting nuclei. Specifically, $U_{Nuc}(|\vec{R}_{OA} - \vec{r}|)$ is defined by:

$$U_{Nuc}(|\vec{R}_{OA} - \vec{r}|) = -\frac{U_0}{1 + \exp\left(\dfrac{|\vec{R}_{OA} - \vec{r}| - R_{N_{nuc}} - R_{N_{He}}}{p}\right)}, \tag{3.8}$$

where $R_{N_{nuc}}$ and $R_{N_{He}}$ denote the root-mean-square radii of neutron distributions in the heavy nucleus and helium, respectively, U_0 is the depth of the potential well (approximately 43 MeV for sodium), and p is the diffuseness parameter, set to about 0.55 fm.

The radii $R_{N_{nuc}}$ and $R_{N_{He}}$ are computed using the following expressions [14]:

$$R_{N_{nuc,He}} = \sqrt{\frac{3}{5}R_{0N_{nuc,He}}^2 + \frac{7\pi^2}{5}a_{N_{nuc,He}}^2}\sqrt{1 + \frac{5b_{nuc,He}^2}{4\pi}} \text{ fm}, \tag{3.9}$$

where $b_{nuc,He}$ denotes the deformation parameter for both the heavy nucleus of the substance and the helium nucleus. For the sodium nucleus, this deformation parameter is assigned value of $b_{Na} = 0.447$, while the helium nucleus is considered spherically symmetric, giving it deformation parameter of zero. The variable $R_{0N_{nuc,He}}$ represents the half-radius of the neutron distribution for both the heavy nucleus of matter and the helium nucleus. This radius is calculated based on the neutron number N and proton number Z of the respective nucleus using the formula:

$$R_{0N_{nuc,He}} = 0.953N_{nuc,He}^{1/3} + 0.015Z_{nuc,He} + 0.774 \text{ fm}, \tag{3.10}$$

and the parameter $a_{N_{nuc,He}}$ is dimensional constant related to the proton and neutron counts Z and N of respective nucleus, and it is determined according to the following expression:

$$a_{N_{nuc,He}} = 0.446 + 0.072\frac{N_{nuc,He}}{Z_{nuc,He}} \text{ fm}. \tag{3.11}$$

The Coulomb interaction potential, $U_{Coulomb}(|\vec{R}_{OA} - \vec{r}|)$, between the point-like helium nucleus and the nucleus of heavy element, whose radius corresponds to the root-mean-square radius of proton distribution $R_{p_{nuc}}$, is given by:

$$U_{Coulomb}(|\vec{R}_{OA} - \vec{r}|) = \begin{cases} \dfrac{2e^2 Z_{nuc}}{|\vec{R}_{OA} - \vec{r}|} & \text{for } |\vec{R}_{OA} - \vec{r}| > R_{p_{nuc}}, \\ \dfrac{2e^2 Z_{nuc}}{2R_{p_{nuc}}}\left(3 - \dfrac{|\vec{R}_{OA} - \vec{r}|^2}{R_{p_{nuc}}^2}\right) & \text{for } |\vec{R}_{OA} - \vec{r}| <= R_{p_{nuc}}, \end{cases} \tag{3.12}$$

where the radius $R_{p_{nuc}}$ is defined according to the expression [14]:

$$R_{p_{nuc}} = \sqrt{\frac{3}{5}R_{0p_{nuc}}^2 + \frac{7\pi^2}{5}a_{p_{nuc}}^2}\sqrt{1 + \frac{5b_{nuc}^2}{4\pi}} \text{ fm}, \tag{3.13}$$

here, the parameter $R_{0p_{nuc}}$ denotes the half-radius of the proton distribution within the nucleus and is calculated as function of the charge number Z_{nuc} and neutron number N_{nuc} for the heavy nucleus as follows:

$$R_{0p_{nuc}} = 1.322Z_{nuc}^{1/3} + 0.007N_{nuc} + 0.022 \text{ fm}, \tag{3.14}$$

the constant $a_{p_{nuc}}$ is dimensional parameter that also depends on the number of protons and neutrons of the nucleus, expressed by the relation:

$$a_{p_{nuc}} = 0.449 + 0.071\frac{Z_{nuc}}{N_{nuc}} \text{ fm}. \tag{3.15}$$

$U_{rot_{(He-Na)}}(|\vec{R}_{OA} - \vec{r}|)$ is calculated by the formula (refer to formula 27 in [15]):

$$U_{rot_{(He-Na)}}(|\vec{R}_{OA} - \vec{r}|) = \frac{\hbar^2 c^2 J_{(He-Na)}(J_{(He-Na)} + 1)}{2m_{He}c^2|\vec{R}_{OA} - \vec{r}|^2}, \tag{3.16}$$

in this context, $\vec{J}_{(He-Na)}$ represents the total angular momentum of the helium and sodium nuclei in their interaction.

The total angular momentum of the helium-sodium interaction, $\vec{J}_{(He-Na)}$, is equal to the intrinsic angular momentum of the sodium nucleus, $\vec{I}_{Na} = 3/2$. Since the helium nucleus has intrinsic angular momentum of $\vec{I}_{He} = \vec{0}$ and because the impact parameter of the sodium nucleus approaching the helium nucleus is zero, the orbital angular momentum between the helium and sodium nuclei is also zero. Thus, we obtain $\vec{J}_{(He-Na)} = 3/2$.

Accordingly, the Hamiltonian $\hat{H}$ for the helium nucleus within the OHe–nucleus system is determined by the radius vectors $\vec{r}$ and $\vec{R}_{OA}$. However, by setting $\vec{R}_{OA}$ as fixed value and incrementally changing the external nucleus position (i.e., by varying $\vec{R}_{OA}$), set of Schrödinger equations dependent on $\vec{r}$ can be derived, each equation corresponding to certain set position of the external nucleus relative to the dark atom.

Thus, the Schrödinger equation to be solved takes the form:

$$\hat{H}\Psi(\vec{r}) = E\Psi(\vec{r}), \tag{3.17}$$

which, upon expanding $\hat{H}$ and applying relevant transformations, results in the following expression:

$$\Delta\Psi(\vec{r}) + \frac{2m_{He}}{\hbar^2}\left(E + \frac{4e^2}{r} - U_{Coulomb}(|\vec{R}_{OA} - \vec{r}|) - U_N(|\vec{R}_{OA} - \vec{r}|) - \right.$$
$$\left. - U_{rot_{(He-Na)}}(|\vec{R}_{OA} - \vec{r}|)\right)\Psi(\vec{r}) = 0. \tag{3.18}$$

To numerically determine the eigenvalues of the Hamiltonian operator $\hat{H}$, which correspond to the energy levels of helium E within the OHe–nucleus system for each fixed position $\vec{R}_{OA}$ of the external nucleus, we approximate $\hat{H}$ using finite difference operator in matrix form. This approach also allows the calculation of the Hamiltonian's eigenvectors, which represent the helium wave functions Ψ for this system.

To achieve this, in addition to expressing the Laplace operator in matrix form, we must construct the matrix representation of the interaction potential of the helium nucleus within the OHe–nucleus system for each specific fixed value of $\vec{R}_{OA}$:

$$U_{He} = -\frac{4e^2}{r} + U_{Coulomb}(|\vec{R}_{OA} - \vec{r}|) + U_N(|\vec{R}_{OA} - \vec{r}|) + U_{rot_{(He-Na)}}(|\vec{R}_{OA} - \vec{r}|). \tag{3.19}$$

Figure 3.1 presents example of the reconstructed total interaction potential, U_{He}, for helium within the OHe–Na system as function of the helium radius vector $\vec{r}$, while keeping the radius vector $\vec{R}_{OA}$ of the external sodium nucleus fixed.

Figure 3.1 illustrates the Coulomb and nuclear interaction potentials between the helium and sodium nuclei, also the centrifugal potential for helium–sodium interaction at zero impact parameter, $U_{rot_{(He-Na)}}(|\vec{R}_{OA}-\vec{r}|)$. Additionally, it shows the Coulomb interaction potential between helium and the O^{--} particle, alongside the total interaction potential for helium in the OHe–Na system.
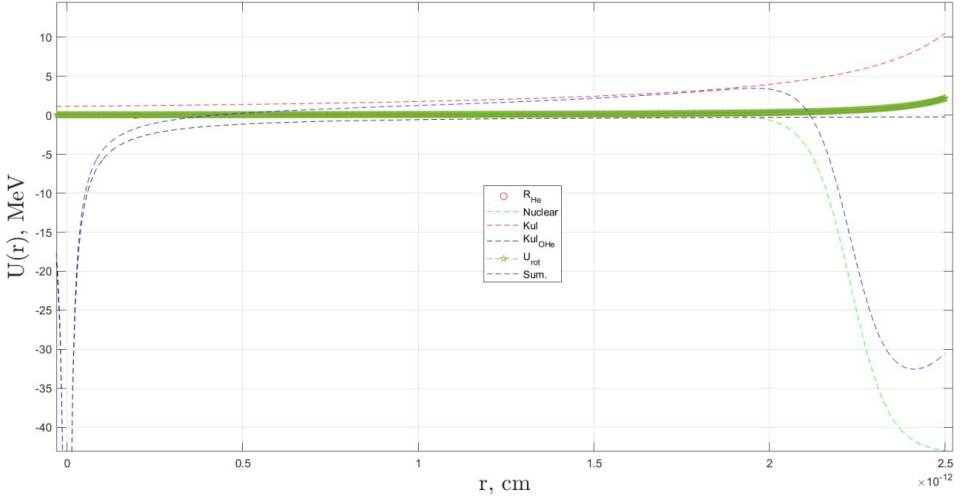
Fig. 3.1: Potentials of Coulomb (red dotted line), nuclear (green dotted line) and centrifugal (green solid line) interaction between helium and the nucleus of Na, the potential of Coulomb interaction between helium and O^{--} particle (black dotted line) and the total interaction potential of the helium nucleus (blue dotted line) in the OHe–Na system at fixed $\vec{R}_{OA}$. The red circle marks the value of the radius of the He nucleus. Original authors' figure taken from [22].

Thus, the quantum mechanical numerical approach to solving the three-body problem in the OHe–nucleus system involves resolving the Schrödinger equation for the helium nucleus within the OHe–nucleus framework for each fixed external nucleus position, $\vec{R}_{OA}$. This requires expressing the Hamiltonian of the helium nucleus in matrix form and performing numerical calculations of its eigenvalues and eigenvectors, which represent the energy levels and wave functions (Ψ-functions) of helium in the OHe–nucleus system, respectively.

3.4 Calculation of the dipole moment values of polarized dark atom

When external nucleus is not present, the dark matter atom remains unpolarized, with the helium energy level in the ground state of OHe around 1.6 MeV. However, as an external nucleus approaches, the varying electric field from this heavy nucleus induces the Stark effect, causing polarization of the dark atom. Consequently, OHe develops non-zero dipole moment and begins to interact with the external nucleus as dipole. This interaction can be described by the Stark potential, as shown in Equation (3.1). According to the dark atom model, dipole barrier is expected to form within the effective interaction potential between OHe and the heavy nucleus of substance, preventing the fusion of dark matter particles with the nucleus. Furthermore, low-energy bound state between the dark atom and the heavy nucleus should also emerge.

In addressing the one-dimensional Schrödinger equation (SE) for the helium nucleus in the OHe–nucleus system (see Equation (3.18)), it is essential to define the range for the helium radius vector $\vec{r}$ with the external nucleus position $\vec{R}_{OA}$ held constant. Here, $\vec{r}$ acts as free parameter that determines the shape of the total interaction potential for helium in the OHe–nucleus system, in which the corresponding SE to be solved for each specified fixed location of the heavy nucleus. To solve this set of SE – SE for each fixed position of the slowly approaching external nucleus – the interval for the radius vector of the heavy nucleus, $\vec{R}_{OA}$, must also be determined.

By overlapping $\vec{r}$ with $\vec{R}_{OA}$, helium would likely reside within the deep potential well created by the heavy nucleus. Given that the helium nucleus is situated within the dark atom – where OHe forms bound quantum mechanical system prior to its interaction with the heavy nucleus begins – the ranges for $\vec{r}$ and $\vec{R}_{OA}$ should be chosen that their boundaries to be close in proximity without overlapping. This configuration ensures that the helium nucleus remains part of the dark atom initially, gradually sensing the influence of the approaching nucleus. As the heavy nucleus draws nearer, the probability of the helium nucleus tunneling through the Coulomb barrier into the nucleus increases. Therefore, for the specified interval of $\vec{r}$, defined by boundary points that are equal in magnitude yet opposite in sign, the interval for $\vec{R}_{OA}$ is set to begin at considerable distance from the dark atom and to end close to the right endpoint of the helium radius vector interval. In this case, the radius vector for helium is represented as $\vec{r} = [-a; a]$, while the radius vector for the external nucleus is expressed as $\vec{R}_{OA} = [c; b]$, where $a, c, b > 0$ and $a \leqslant b < c$. Consequently, the fixed position of the external nucleus, $\vec{R}_{OA}$, will consistently take values within the interval $[c; b]$, progressing from point c to point b. For each point $p^* \in [c; b]$, the distance between the helium nucleus and the matter nucleus, $\vec{R}_{HeA} = \vec{R}_{OA} - \vec{r}$, will vary within the interval $\vec{R}_{HeA} = [p^* + a; p^* - a]$. As the external nucleus approaches the dark matter atom, the polarization of OHe is expected to increase in response to the nucleus's proximity.

As the nucleus of the substance moves closer to dark atom, the ground state of the helium nucleus within O-helium undergoes corresponding shifts. To calculate changes in the dipole moment of the polarized dark atom, it is necessary to calculate the shifts in the energy of the ground state and the corresponding wave functions of the polarized dark atom.

By solving the set of Schrödinger equations for helium in the OHe–Na system for various fixed positions of the heavy nucleus of matter $\vec{R}_{OA}$, we have obtained set of energy values of the ground state of helium corresponding to certain polarization of the OHe atom at certain fixed position of the outer nucleus of matter and the wave functions of helium corresponding to these ground states of the polarized dark atom.

Utilizing the normalized ground-state wave function of helium in unpolarized dark atom, Ψ_{OHe}, obtained by solving the Schrödinger equation for helium in the isolated O-helium dark atom, along with the normalized wave functions of helium in the polarized dark atom for different ground-state energy values, Ψ_{OHeNa}, we determined the spectrum of dipole moment values δ for the polarized OHe. The

dipole moment δ corresponding to each Ψ_{OHeNa} was computed as follows:

$$\delta = \int_r \Psi^*_{OHe} \cdot r \cdot \Psi_{OHeNa} \cdot 4\pi r^2 dr. \qquad (3.20)$$

To accurately evaluate the integral in (3.20), precise determination of its integration limits is required. Since we are calculating the dipole moments of the polarized dark atom, it is crucial to account for the probability distribution of locating the helium nucleus within the dark atom. To define the left and right bounds of integration, we must identify the intersection points between the plot of the squared modulus of the helium wave function and the plot of the total helium potential within the OHe – Na system at fixed value of $\vec{R}_{OA}$. For each fixed position of the external heavy nucleus, this approach allows us to set the integration region within the dark atom, effectively establishing the integration limits. These limits are defined by the intersection points where the graphs of the total helium interaction potential and the squared modulus of the wave function, associated with specific ground-state energy level, meet.

Figure 3.2 illustrates the method for determining these integration limits necessary for calculating the integral in (3.20). In the figure, the blue solid line represents the total interaction potential of helium within the OHe – Na system for specific fixed position of the sodium nucleus, $\vec{R}_{OA}$, while the red solid line shows the squared modulus of the helium ground-state wave function within the polarized dark atom at this fixed $\vec{R}_{OA}$. The black circles mark the intersection points of the two curves, with the first two intersections from left to right indicating the integration bounds for (3.20). In the example shown in Figure 3.2, the dark atom is negatively polarized, as the probability density of locating helium to the left of the origin (or the O^{--} particle) is greater than that on the right. Here, the sodium nucleus is positioned close enough that the helium begins to experience the nuclear potential (visible as potential well forming to the right of the Coulomb barrier), but not so close as to result in significant tunneling of helium through the barrier.

By calculating the spectrum of dipole moment values, δ, for polarized OHe at various positions of the sodium nucleus $\vec{R}_{OA}$, we can illustrate how the dipole moment of the polarized dark atom varies with the radius vector $\vec{R}_{OA}$ (as depicted in Figure 3.3).

In Figure 3.3, red stars indicate the values of the dipole moment for the polarized OHe atom, each corresponding to specific fixed values of $\vec{R}_{OA}$ within the helium radius vector interval $r = |1.1 \times 10^{-12}$ cm$|$. From Figure 3.3, it can be observed that when the sodium nucleus is distant from OHe, the dark atom behaves as isolated system, with dipole moment approaching zero. As the sodium nucleus moves closer to the O-helium atom, OHe becomes more polarized, resulting in progressively larger negative dipole moment. This increase in polarization occurs because the sodium nucleus exerts repulsive Coulomb force on helium, encouraging the helium to shift leftward relative to the O^{--} particle. When the sodium nucleus is in close proximity to the dark atom and $\vec{R}_{OA}$ nears the right boundary of the helium radius vector interval $\vec{r}$, the nuclear force between helium and sodium dominates over the Coulomb interaction, causing δ to approach above zero.
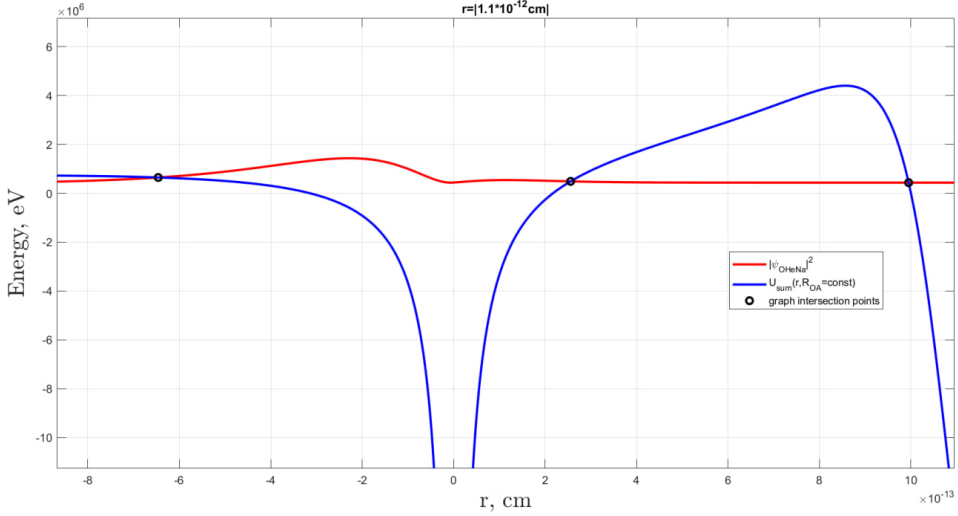
Fig. 3.2: The total potential of helium in the OHe–Na system for fixed position of sodium $\vec{R}_{OA}$ (blue solid line), graph of the squared modulus of the wave function of the ground state of helium in polarized dark atom for fixed $\vec{R}_{OA}$ (red solid line), the intersection points of the graph of the total potential of helium and the graph of the squared modulus of the wave function of the ground state of helium (black circles). Original authors' figure taken from [22].

3.5 Reconstruction the total effective interaction potential of the OHe – Na system

To reconstruct the Stark potential form, as given in Formula (3.1), which describes the electric interaction between the dipole of polarized dark atom and substance nucleus, we employ the dipole moment values calculated through quantum mechanical methods. Additionally, to obtain the total effective interaction potential for the OHe–Na system (the total interaction potential between the sodium nucleus and the dark atom of O-helium), it is necessary also to reconstruct the form of the nuclear interaction potential, this is achieved by using the Woods–Saxon model for helium and sodium nuclei, along with the electric interaction potential, U_{XHe}^{e}, between the unpolarized OHe dark atom and the sodium nucleus. The latter potential, U_{XHe}^{e}, is derived by solving the self-consistent Poisson equation, accounting for the screening effect of the O^{--} particle by the helium nucleus. This screening effect becomes significant only at close distances to the dark atom, as it decays exponentially (see Section 5.1 on the "Approach of Reconstructing of Interaction Potentials in the XHe–nucleus system" in [16]). In addition, in order to reconstruct the shape of the total effective interaction potential of the sodium nucleus with the dark atom, we must also take into account the potential of the centrifugal interaction of the sodium nucleus with the dark atom of O-helium. The centrifugal potential of the interaction of the OHe dark atom with the sodium nucleus, denoted as $U_{rot(OHe-Na)}$, is determined by the total angular momentum
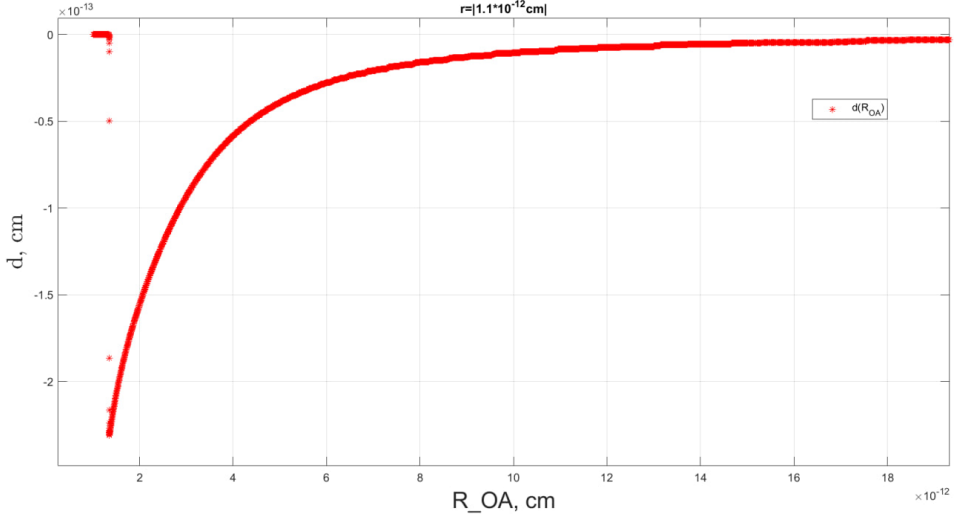
Fig. 3.3: Graph of the dependence of the dipole moment of polarized OHe atom (red stars) on the radius vector of the outer sodium nucleus. Original authors' figure taken from [22].

of the system of interacting particles, $\vec{J}_{(OHe-Na)}$, as well as the distance between the interacting particles, R. Ignoring the moments of inertia of the nuclei, it is defined by the following expression (see formula 27 in [15]):

$$U_{rot_{(OHe-Na)}}(R) = \frac{\hbar^2 c^2 J_{(OHe-Na)}(J_{(OHe-Na)} + 1)}{2\mu c^2 R^2},$$

(3.21)

where μ represents the reduced mass of the interacting particles.

Since the mass of OHe is entirely determined by the mass of the heavy particle O^{--}, taken as 1 TeV, and the sodium nucleus has mass of approximately $m_{Na} \approx 21.4$ GeV, which is significantly smaller in comparison with OHe's mass, the reduced mass of the system can be approximated by the sodium mass, $\mu \approx m_{Na}/c^2$.

The total angular momentum of the interacting particles, $\vec{J}_{(OHe-Na)}$, is given by:

$$\vec{J}_{(OHe-Na)}(\rho) = \vec{l}_{(OHe-Na)}(\rho) + \vec{I}_{Na} + \vec{I}_{OHe},$$

(3.22)

here $\vec{l}_{(OHe-Na)}(\rho)$ denotes the orbital angular momentum, which depends on the impact parameter ρ, $\vec{I}_{Na}$ represents the intrinsic angular momentum of the sodium nucleus, and $\vec{I}_{OHe}$ signifies the spin of the OHe dark atom. The spin $\vec{I}_{OHe}$ is defined as the sum of vectors of the spin of the O^{--} particle, $\vec{I}_{O^{--}}$, and the intrinsic angular momentum of the helium nucleus, $\vec{I}_{He}$.

We consider the case of frontal collision between the sodium nucleus and the OHe dark atom. In this head-on collision, where the sodium nucleus approaches with zero impact parameter, $\rho = 0$, the orbital angular momentum of the interacting particles also becomes zero, $\vec{l}_{(OHe-Na)}(0) = \vec{0}$. The intrinsic angular momentum of the sodium nucleus is $\vec{I}_{Na} = 3/2$.

Thus, for the scenario with an impact parameter $\rho = 0$, the total angular momentum of system of the OHe dark atom and sodium nucleus, $\vec{J}_{(OHe-Na)}$, is expressed as:

$$\vec{J}_{(OHe-Na)} = \frac{\vec{3}}{2} + \vec{I}_{O^{--}}. \tag{3.23}$$

If O^{--} is technibaryon, its spin, $\vec{I}_{O^{--}}$, could be either $\vec{0}$ or $\vec{1}$, and if O^{--} belonged to technilepton particle, its spin would be $\vec{I}_{O^{--}} = 1/2$ [17, 18]. if O^{--} takes the form of $\Delta^{--}_{\bar{u}\bar{u}\bar{u}}$ and includes new quarks from extended families, then $\vec{I}_{O^{--}} = 3/2$ [19].

As a result, summing up the potential of the Woods–Saxon nuclear interaction, U^e_{XHe}, U_{St} and $U_{rot_{(OHe-Na)}}$, we obtain the total effective interaction potential of the O-helium dark atom with the sodium nucleus (see Figure 3.4).

The OHe model suggests that the magnitude of the dipole Coulomb barrier in the total effective interaction potential of the OHe–Na system should be sufficient to prevent direct fusion between the dark atom and the sodium nucleus. Under the conditions of the DAMA experiment, the relative velocity of the sodium nucleus in the OHe–Na system is thermal, corresponding to normal room temperature (around 300 K). This thermal motion corresponds to kinetic energy of roughly $\sim 2.6 \times 10^{-2}$ eV for the sodium nucleus. As result, the height of dipole Coulomb barrier in the effective interaction potential of the OHe–Na system is expected to be higher than this kinetic energy of sodium nucleus.

Finally, we can construct the total effective interaction potential of OHe with the sodium nucleus in the OHe–Na system, for example, for the value of the total angular momentum of the system of interacting particles $\vec{J}_{(OHe-Na)} = \vec{3}$, which corresponds to the value of the spin of the O^{--} particle, $\vec{I}_{O^{--}} = 3/2$, as shown in Figure 3.4. In general case, the shape of this total effective interaction potential strongly depends on the value of the spin of the O^{--} particle, $I_{O^{--}}$, however, in all cases, the shape of the total effective interaction potential between sodium and OHe qualitatively corresponds to theoretical expectations. This allows for extended range of the helium radius vector interval, $\vec{r}$, to get the depth of potential well near ~ 6 keV and positive potential barrier height that exceeds zero as well as greater than the thermal kinetic energy of sodium $\sim 2.6 \times 10^{-2}$ eV. This barrier height and depth of potential well align with theoretical predictions and experimental data. Such positive potential barrier value playing critical role in preventing the fusion of He and/or O^{--} particles with atomic nuclei, thereby preserving the stability of the dark atom. The presence of this barrier in the total effective interaction potential of the OHe–nucleus system, which ensures the impossibility of direct fusion of dark atom with ordinary atomic nuclei of matter, is fundamental requirement for sustaining the viability of the OHe dark atom model.

3.6   Conclusions

The numerical model presented in this article is founded on quantum mechanical numerical approximation to describe three-particle system, where interactions
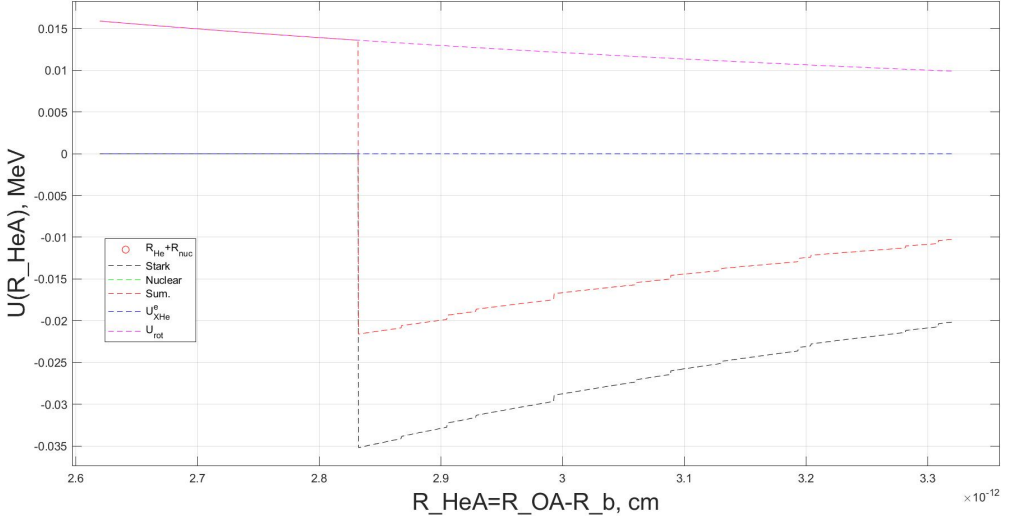
Fig. 3.4: Graphs of Woods–Saxon nuclear potential (green dotted line), U^e_{XHe} (blue dotted line), Stark potential (gray dotted line), centrifugal potential (purple dotted line) and total effective interaction potential of OHe with the nucleus of the sodium (red dotted line) on the distance between the He nucleus, located in the Bohr orbit of the OHe atom, and the Na nucleus for $J_{(OHe-Na)} = 3$. Original authors' figure taken from [22].

occur through electric, centrifugal, and nuclear forces. This method entails solving the Schrödinger equation for helium in the OHe–Na system for each fixed position of the sodium nucleus relative to the O-helium atom. By considering the distinctive features of nuclear and electromagnetic interactions within OHe–Na system, we can precisely determine the polarization of dark matter atom, calculate the dipole moments of polarized OHe atom as function of the distance between the dark atom and the sodium nucleus, and, thereby, accurately reconstruct the Stark potential, which plays crucial role in shaping the effective interaction potential in the OHe–Na system.

Thus, within the framework of the developed numerical model, the helium interaction potential in the OHe–Na system has been reconstructed, allowing for the solution of the Schrödinger equation for the helium nucleus in both isolated, unpolarized dark atom and polarized O-helium within the OHe–Na system. Then, dipole moments of the polarized OHe atom were derived using the helium wave functions for both isolated dark matter atom and polarized dark atom in the OHe–Na system. After that, the Stark potential was computed, enabling the reconstruction of the total effective interaction potential between the sodium nucleus and the OHe dark atom in the OHe–Na system. This total effective potential includes contributions from the Stark potential, nuclear potential, centrifugal potential, and the electric interaction potential of unpolarized OHe dark atom with the sodium nucleus and this total effective potential qualitatively coincides with its theoretically expected form.

To improve the precision of the effective interaction potential reconstruction and achieve more accurate physical model of dark atom interaction with heavy nucleus, as well as to explain the findings of direct dark matter detection experiments, refinements to the quantum mechanical approach to the total effective interaction potential reconstruction are planned. These improvements will involve determining the nuclear and electromagnetic potentials for interaction between X-helium and ordinary matter nucleus, with accounting for the finite sizes of the interacting particles by incorporating electric charge and nucleon distributions within the nuclei. Additionally, the model will incorporate nuclei deformation by modeling the nuclei as spherically asymmetric.

Acknowledgements

References

1. Khlopov, M. Fundamental particle structure in the cosmological dark matter. *International Journal of Modern Physics A* **2013**, *28*, 1330042.
2. Bertone, G.; Hooper, D.; Silk, J. Particle dark matter: evidence, candidates and constraints. *Physics Reports* **2005**, *405*, 279 – 390.
3. Scott, P. Searches for Particle Dark Matter: An Introduction. *arXiv* **2011**, arXiv:1110.2757.
4. Belotsky, K. M.; Khlopov, M.Y.; Shibaev, K. I. Composite Dark Matter and its Charged Constituents. *Grav.Cosmol.* **2006**, *12*, 93-99, arXiv:astro-ph/0604518.
5. Khlopov, M. Yu.; Kouvaris, C. Composite dark matter from a model with composite Higgsboson. *Phys. Rev.* **2008**, *78*, 065040.
6. Fargion, D.; Khlopov, M. Yu. Tera-leptons' shadows over Sinister Universe. *Gravitation Cosmol.* **2013**, *19*, 219.
7. Beylin, V.; Khlopov, M.; Kuksa, V.; Volchanskiy, N. New Physics of Strong Interaction and Dark Universe. *Universe* **2020**, *6*, 196.
8. Cudell, J. R.; Khlopov, M. Y.; Wallemacq, Q. The nuclear physics of OHe. *Bled Workshops in Physics* **2012**, *13*, 10 –27.
9. Bulekov, O. V.; Khlopov, M. Yu.; Romaniouk, A. S.; Smirnov, Yu. S. Search for Double Charged Particles as Direct Test for Dark Atom Constituents. *Bled Workshops in Physics* **2017**, *18*, 11-24.
10. Khlopov, M. What comes after the Standard Model? *Prog. Part. Nucl. Phys.* **2020**, *116*, 103824.
11. Khlopov, M.Y.; Mayorov, A.G.; Soldatov, E.Y. The dark atoms of dark matter. *Prespace J.* **2010**, *1*, 1403–1417.
12. Bernabei, R.; Belli, P.; Bussolotti, A.; Cappella, F.; Caracciolo, V.; Cerulli, R.; Dai, C.J.; d'Angelo, A.; Di Marco, A.; Ferrari, N.; et al. The DAMA project: Achievements, implications and perspectives. *Prog. Part. Nucl. Phys.* **2020**, *114*, 103810.
13. Beylin, V. A.; Bikbaev, T. E.; Khlopov, M. Y.; Mayorov, A. G.; Sopin, D. O. Dark Atoms of Nuclear Interacting Dark Matter. *Universe* **2024**, *10*, 368.
14. Seif, W. Mansour, Hesham. Systematics of nucleon density distributions and neutron skin of nuclei. *Int. J. Mod. Phys. E* **2015**, *24*, 1550083.

15. Adamian, G.G.; Antonenko, N.V.; Jolos, R.V.; Ivanova, S.P.; Melnikova, O.I. Effective nucleus-nucleus potential for calculation of potential energy of a dinuclear system. *Int. J. Mod. Phys. E* **1996** *5*, 191–216.
16. Bikbaev, T.; Khlopov, M.; Mayorov, A. Numerical Modeling of the Interaction of Dark Atoms with Nuclei to Solve the Problem of Direct Dark Matter Search. *Symmetry* **2023**, *15*, 2182.
17. Sannino, F.; Tuominen, K.; Orienfold Theory Dynamics and Symmetry Breaking. *Phys. Rev. D* **2005**, *71*, 051901.
18. Khlopov, M.Y.; Kouvaris, C. Strong interactive massive particles from a strong coupled theory. *Phys. Rev. D* **2008**, *77*, 065002.
19. Belotsky, K.; Khlopov, M.; Shibaev, K. Stable quarks of the 4th family? *arXiv* **2008**, arXiv:0806.1067.

BLED WORKSHOPS
IN PHYSICS
VOL. 25, NO. 1

Proceedings of the 27th Workshop
What Comes Beyond . . . *(p. 42)*
Bled, Slovenia, July 8–17, 2024

4   Advances for QCD and the Standard Model: Color-Confining Light-Front Holography and the Principle of Maximum Conformality

Stanley J. Brodsky

SLAC National Accelerator Laboratory, Stanford University
e-mail: sjbth@slac.stanford.edu

Abstract. I review how the application of superconformal quantum mechanics and light-front holography leads to new insights into the physics of color confinement and the spectroscopy and dynamics of hadrons, as well as surprising supersymmetric relations between the masses of mesons, baryons, and tetraquarks. Spontaneous chiral symmetry breaking is automatically fulfilled by supersymmetric Light-Front Supersymmetric QCD. The light-front holographic approach (HLFQCD) also predicts the behavior of the QCD running coupling and other observables from the nonperturbative color-confining domain to the perturbative domain. I also review how one can determine the QCD running coupling to high precision from the data of just a single experiment over the entire perturbative regime by using the Principle of Maximum Conformality (PMC). The PMC, which generalizes the conventional Gell-Mann-Low method for scale-setting in perturbative QED to non-Abelian QCD, provides a rigorous method for achieving unambiguous scheme-independent, fixed-order Standard Model predictions for observables consistent with the principles of the renormalization group.

Povzetek: Avtor predstavi uporabo superkonformne kvantne mehanike in holografije "light-front" za opis gruč kvarkov v hadronih, kar omogoči nov vpogled v spektroskopijo in dinamiko hadronov, pa tudi v presenetljive supersimetrične relacije med masami mezonov, barionov in tetrakvarkov. Holografija "light-front" ponudi tudi napoved spremembe sklopitvene konstante med kvarki in gluoni in drugih opazljivk od območja barvnega ujetja do območja, kjer je teoria motenj uporabna. Uporaba načela največje skladnosti avtorju omogoči, da lahko z veliko natančnostjo določi spreminjanje sklopitvene konstante med kvarki in gluoni že na podlagi enega samega eksperimenta. To načelo, ki je splošitev perturbativne kvantne elektrodinamike Gell-Mann-Low na neabelsko kvantno kromodinamiko, zagotavlja metodo za neodvisne napovedi Standardnega modela skladno z načeli renormalizacijske grupe.

QCD, Light-Front, Holography, Supersymmetry, Principle of Maximum Conformality

4.1   Color Confinement and Light-Front Holography

A central problem in hadron physics is to obtain a first approximation to QCD, which not only has color confinement, but can also predict the spectroscopy of

hadrons and the light-front wave functions which underly their properties and dynamics. Guy de Téramond, Guenter Dosch, and I [1] have shown that a mass gap and a fundamental color confinement scale can be derived from light-front holography – the duality between five-dimensional anti-de Sitter (AdS) space physical 3+1 spacetime using light-front time. The combination of superconformal quantum mechanics [2,3], light-front quantization [4] and the holographic embedding on a higher dimensional gravity theory [5] (gauge/gravity correspondence) has led to new analytic insights into the structure of hadrons and their dynamics [1,6–10]. This new approach to nonperturbative QCD dynamics, *holographic light-front QCD*, has led to effective semi-classical relativistic bound-state equations for arbitrary spin [13], and it incorporates fundamental properties which are not apparent from the QCD Lagrangian, such as the emergence of a universal hadron mass scale, the prediction of a massless pion in the chiral limit, and remarkable connections between the spectroscopy of mesons, baryons and tetraquarks across the full hadron spectrum [14–17].

4.2 Light-Front Theory and Holographic QCD

Light-Front Hamiltonian theory [4] provides a causal, frame-independent, and ghost-free nonperturbative formalism for analyzing gauge theories such as QCD. Remarkably, LF theory in 3+1 physical space-time is holographically dual to five-dimensional AdS space, if one identifies the LF radial variable ζ with the fifth coordinate z of AdS_5 [1,6–10]. If the metric of the conformal AdS_5 theory is modified by a dilaton of the form $e^{+\kappa^2 z^2}$, one obtains an analytically-solvable Lorentz-invariant color-confining LF Schrödinger equations for hadron physics. The parameter κ of the dilaton becomes the fundamental mass scale of QCD, underlying the color-confining potential of the LF Hamiltonian and the running coupling $\alpha_s(Q^2)$ in the nonperturbative domain. When one introduces superconformal algebra, the result is "Holographic LF QCD" which not only predicts a unified Regge-spectroscopy of mesons, baryons, and tetraquarks, arranged as supersymmetric 4-plets, but also the hadronic LF wavefunctions which underly form factors, structure functions, and other dynamical phenomena. In each case, the quarks and antiquarks cluster in hadrons as 3_C diquarks, so that mesons, baryons and tetraquarks all obey a two-body $3_C - \bar{3}_C$ LF bound-state equation. Thus tetraquarks are compact hadrons, as fundamental as mesons and baryons. "Holographic LF QCD" also leads to novel phenomena such as the color transparency of hadrons produced in hard-exclusive reactions traversing a nuclear medium and asymmetric intrinsic heavy-quark distributions $Q(x) \neq \bar{Q}(x)$, appearing at high x in the non-valence higher Fock states of hadrons [11,12].

The light front holographic approach also incorporates the essential consequence of spontaneous chiral symmetry breaking. All of the typical features of spontaneous chiral symmetry breaking are automatically fulfilled by supersymmetric LFHQCD: There is a mass-less boson (the pion in the chiral limit), and the parity doublets (ρ, A_1) and $(N, N(1535))$ have different masses. A detailed discussion is given in ref. [20]

Phenomenological extensions of the holographic QCD approach have also led to nontrivial connections between the dynamics of form factors and polarized and unpolarized quark distributions with pre-QCD nonperturbative approaches such as Regge theory and the Veneziano model [21–23]. As discussed in the next section, it also predicts the analytic behavior of the QCD coupling $\alpha_s(Q^2)$ in the nonperturbative domain [24, 25].

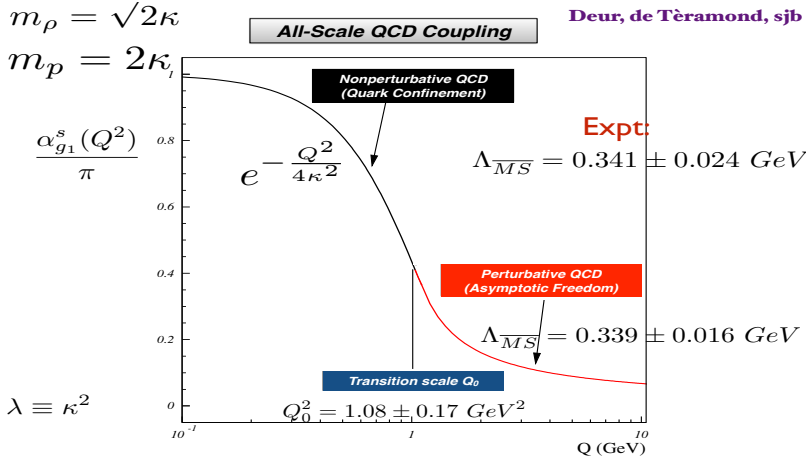## 4.3   The QCD Coupling at All Scales

The QCD running coupling can be defined [26] at all momentum scales from any perturbatively calculable observable, such as the coupling $\alpha_{g_1}^s(Q^2)$ which is defined from measurements of the Bjorken sum rule. At high momentum transfer, such "effective charges" satisfy asymptotic freedom, obey the usual pQCD renormalization group equations, and can be related to each other without scale ambiguity by commensurate scale relations [38]. The dilaton $e^{+\kappa^2 z^2}$ soft-wall modification [27] of the AdS_5 metric, together with LF holography, predicts the functional behavior in the small Q^2 domain [24]: $\alpha_{g_1}^s(Q^2) = \pi e^{-Q^2/4\kappa^2}$. Measurements of $\alpha_{g_1}^s(Q^2)$ are remarkably consistent with this predicted Gaussian form. The predicted coupling is thus finite at $Q^2 = 0$.

The parameter κ, which determines the mass scale of hadrons in the chiral limit, can be connected to the mass scale Λ_s controlling the evolution of the perturbative QCD coupling [24, 25, 28]. This connection can be done for any choice of renormalization scheme, including the $\overline{MS}$ scheme, as seen in Fig. 4.1. The relation between scales is obtained by matching at a scale Q_0^2 the nonperturbative behavior of the effective QCD coupling, as determined from light-front holography, to the perturbative QCD coupling with asymptotic freedom. The result of this perturbative/nonperturbative matching at the analytic inflection point is an effective QCD coupling which is defined at all momenta.

Recently [29], Guy de Teramond, Guenter Dosch, Alexandre Deur, Arpon Paul, Tianbo Liu, Raza Sabbir Sufian and I have used analytic continuation to extend the gauge/gravity duality nonperturbative description of the strong force coupling into the transition, near-perturbative, regime where perturbative effects become important. By excluding the unphysical region in coupling space from the flow of singularities in the complex plane, we have derived a specific relation between the scales relevant at large and short distances; this relation is uniquely fixed by requiring maximal analyticity. The unified effective coupling model gives an accurate description of the data in the nonperturbative and the near-perturbative regions. The analytic determination of $\alpha_s(Q^2)$ over all domains increases the precision and reliability of QCD predictions.

4.4   Superconformal Algebra and Supersymmetric Hadron Spectroscopy

Another advance in LF holography is the application [7,8,30] of *superconformal algebra*, a feature of the underlying conformal symmetry of chiral QCD. The conformal

$m_\rho = \sqrt{2}\kappa$

$m_p = 2\kappa$

All-Scale QCD Coupling

Deur, de Tèramond, sjb

$\dfrac{\alpha_{g_1}^s(Q^2)}{\pi}$

Nonperturbative QCD
(Quark Confinement)

$e^{-\frac{Q^2}{4\kappa^2}}$

Expt:

$\Lambda_{\overline{MS}} = 0.341 \pm 0.024 \; GeV$

Perturbative QCD
(Asymptotic Freedom)

$\Lambda_{\overline{MS}} = 0.339 \pm 0.016 \; GeV$

Transition scale Q_0

$\lambda \equiv \kappa^2$

$Q_0^2 = 1.08 \pm 0.17 \; GeV^2$

Q (GeV)

Running Coupling from Light-Front Holography and AdS/QCD

Analytic, defined at all scales, IR Fixed Point

$\dfrac{\alpha_s(Q)}{\pi}$

$\alpha_s^{AdS}(Q)/\pi = e^{-Q^2/4\kappa^2}$

$\kappa = 0.54 \; GeV$

- ····· Modified AdS
- —— AdS
- α_{g_1}/π (pQCD)
- □ α_{g_1}/π world data
- ····· GDH limit ✳ α_{F3}/π
- ◇ α_τ/π OPAL
- ▲ α_{g_1}/π JLab CLAS
- ■ α_{g_1}/π Hall A/CLAS
- ● Lattice QCD (2004) ▼ (2007)

Q (GeV)

AdS/QCD dilaton captures the higher twist corrections to effective charges for Q < 1 GeV

$e^\varphi = e^{+\kappa^2 z^2}$

Deur, de Teramond, sjb
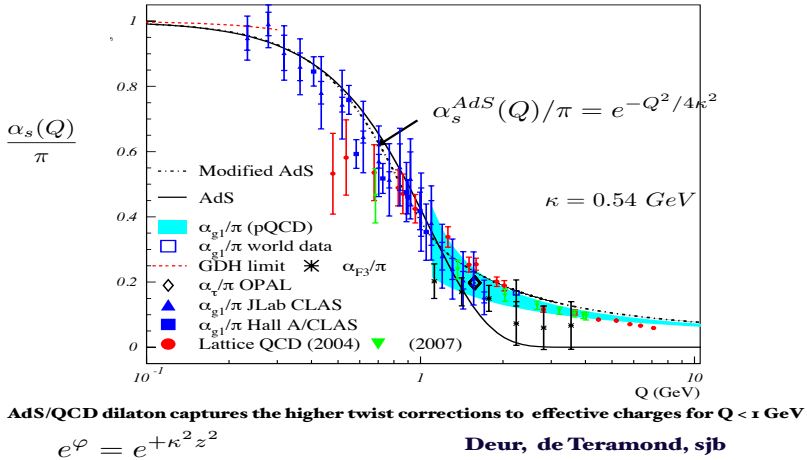
Fig. 4.1: (A). Prediction from LF Holography for the QCD running coupling $\alpha_{g_1}^s(Q^2)$. The magnitude and derivative of the perturbative and nonperturbative coupling are matched at the scale Q_0. This matching connects the perturbative scale $\Lambda_{\overline{MS}}$ to the nonperturbative scale κ which underlies the hadron mass scale. (B). Comparison of the predicted nonperturbative coupling with measurements of the effective charge $\alpha_{g_1}^s(Q^2)$ defined from the Bjorken sum rule. See Ref. [28].
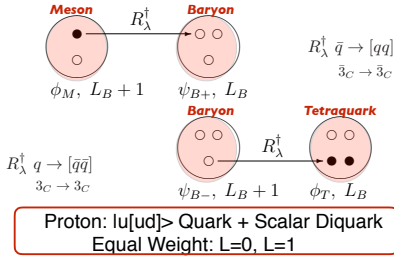
Fig. 4.2: The 4-plet representation of mass-degenerate hadronic states predicted by superconformal algebra [1]. Mesons are $q\bar{q}$ bound states, baryons are quark – antidiquark bound states and tetraquarks are diquark-antidiquark bound states. The supersymmetric ladder operator $R_\lambda^\dagger$ connects quarks and anti-diquark clusters of the same color.
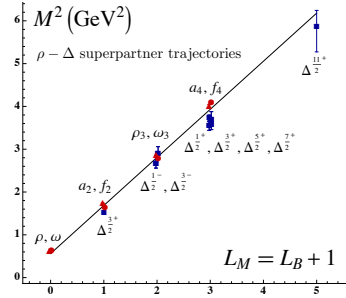
Fig. 4.3: Comparison of the ρ/ω meson Regge trajectory with the $J = 3/2$ Δ baryon trajectory. Superconformal algebra predicts the degeneracy of the meson and baryon trajectories if one identifies a meson with internal orbital angular momentum L_M with its superpartner baryon with $L_M = L_B + 1$. See Refs. [7,8].

group has an elegant 2×2 Pauli matrix representation called *superconformal algebra*, originally discovered by Haag, Lopuszanski, and Sohnius [31]. The conformal Hamiltonian operator and the special conformal operators can be represented as anticommutators of Pauli matrices $H = 1/2[Q, Q^\dagger]$ and $K = 1/2[S, S^\dagger]$. As shown by Fubini and Rabinovici, [3], a nonconformal Hamiltonian with a mass scale and universal confinement can then be obtained by shifting $Q \to Q + \omega K$, the analog of the dAFF procedure. In effect, one has obtained generalized supercharges of the superconformal algebra [3]. This ansatz extends the predictions for the hadron spectrum to a "4-plet" – consisting of mass-degenerate quark-antiquark mesons, quark-diquark baryons, and diquark-antidiquark tetraquarks, as shown in fig. 4.2. The 4-plet contains two entries $\Psi^\pm$ for each baryon, corresponding to internal orbital angular momentum L and L + 1. This property of the baryon LFWFs is the analog of the eigensolution of the Dirac-Coulomb equation which has both an upper component Ψ^+ and a lower component $\Psi^- = \frac{\vec{\sigma}\cdot\vec{p}}{m+E-V}\Psi^+$.

LF Schrödinger Equations for both baryons and mesons can be derived from superconformal algebra [7, 8, 30, 32]. The baryonic eigensolutions correspond to bound states of 3_C quarks to a $\bar{3}_C$ spin-0 or spin-1 qq diquark cluster; the tetraquarks in the 4-plet are bound states of diquarks and anti-diquarks. The quark-diquark baryons have two amplitudes $L_B, L_B + 1$ with equal probability, a feature of "quark chirality invariance". The proton Fock state component ψ^+ (with parallel quark and baryon spins) and ψ^- (with anti-parallel quark and baryon spins) have equal Fock state probability – a feature of "quark chirality invariance". Thus the proton's spin is carried by quark orbital angular momentum in the nonperturbative domain. Predictions for the static properties of the nucleons

are discussed in Ref. [33]. The overlap of the $L = 0$ and $L = 1$ LF wavefunctions in the Drell-Yan-West formula is required to have a non-zero Pauli form factor $F_2(Q^2)$ and anomalous magnetic moment [34]. The existence of both components is also necessary to generate the pseudo-T-odd Sivers single-spin asymmetry in deep inelastic lepton-nucleon scattering [35].

The predicted spectra $M^2(n, L) = 4\kappa^2(n + L)$ for mesons, and $M^2(n, L) = 4\kappa^2(n + L + 1)$ for baryons, is remarkably consistent with observed hadronic spectroscopy. The Regge-slopes in n and L are identical. The predicted meson, baryon and tetraquark masses coincide if one identifies a meson with internal orbital angular momentum L_M with its superpartner baryon or tetraquark with $L_B = L_M - 1$. Superconformal algebra thus predicts that mesons with $L_M = L_B + 1$ have the same mass as the baryons in the supermultiplet. An example of the mass degeneracy of the ρ/ω meson Regge trajectory with the $J = 3/2$ Δ-baryon trajectory is shown in Fig. 4.3. The value of κ can be set by the ρ mass; only ratios of masses are predicted. The combination of light-front holography with superconformal algebra thus leads to the novel prediction that hadron physics has supersymmetric properties in both spectroscopy and dynamics. The excitation spectra of relativistic light-quark meson, baryon and tetraquark bound states all lie on linear Regge trajectories with identical slopes in the radial and orbital quantum numbers. Detailed predictions for the tetraquark spectroscopy and comparisons with the observed hadron spectrum are presented in ref. [16].

4.5   Renormalization Scale Setting

A key problem in making precise perturbative QCD predictions is the uncertainty in determining the renormalization scale μ of the running coupling $\alpha_s(\mu^2)$. The purpose of the running coupling in any gauge theory is to sum all terms involving the β function; in fact, when the renormalization scale is set properly, all non-conformal $\beta \neq 0$ terms in a perturbative expansion arising from renormalization are summed into the running coupling. The remaining terms in the perturbative series are then identical to that of a conformal theory; i.e., the corresponding theory with $\beta = 0$. There is no renormalization scale-setting ambiguity for precision tests of quantum electrodynamics. The scale of the running QED coupling is set to absorb all vacuum polarization diagrams; i.e. the β terms. The coefficients in the perturbative QCD series then matches conformal theory; i.e. the corresponding perturbative series with $\beta = 0$. This is the standard Gell-Mann Low scale-setting procedure for high precision tests of QED, where all vacuum polarization contributions are summed into the QED running coupling. The same scale-setting procedure applies to the $SU(2)_{EW}$ theory of the electroweak interactions. An important analytic property of non-Abelian QCD with N_C colors is that it must agree analytically with Abelian QED in the $N_C \to 0$ limit, at fixed $\hat{\alpha}_s = C_F \alpha_s$ and fixed $\hat{n}_f = T \frac{n_f}{C_F}$ with $C_F = \frac{N_C^2 - 1}{2N_C}$ and $T = 1/2$. This is the "Abelian correspondence principle." Thus the setting of the renormalization scale in QCD must agree with Gell-Mann-Low scale setting for QED in the $N_C \to 0$ limit.

It has become conventional to simply guess the renormalization scale and choose an arbitrary range of uncertainty when making perturbative QCD (pQCD) pre-

dictions. However, this *ad hoc* assignment of the renormalization scale and the estimate of the size of the resulting uncertainty leads to anomalous renormalization scheme-and-scale dependences. In fact, relations between physical observables must be independent of the theorist's choice of the renormalization scheme, and the renormalization scale in any given scheme at any given order of pQCD is not ambiguous. This was the motivation for the BLM (Brodsky-Lepage-Mackenzie) [36] procedure for QCD scale-setting. It was then generalized to all orders as the PMC (the Principle of Maximum Conformality. The *Principle of Maximum Conformality* (PMC) [40, 46], which generalizes the conventional Gell-Mann-Low method for scale-setting in perturbative QED to non-Abelian QCD, provides a rigorous method for achieving unambiguous scheme-independent, fixed-order predictions for observables consistent with the principles of the renormalization group.

The PMC scale-setting procedure sets the renormalization scale $\alpha_s(Q^2_{PMC})$ at every order by absorbing the β terms appearing in the pQCD series. The resulting pQCD series thus matches the corresponding conformal series with all β terms set to 0. The problematic $n!$ "renormalon" divergence of pQCD series associated with the nonconformal terms does not appear in the conformal series and the conformal series is independent of the theorist's choice of renormalization scheme. This also means that relations between any two perturbatively calculable observables are scheme-independent. These relations are called "commensurate scale relations" [38, 46]. The PMC also satisfies the requirement that one must use the same scale-setting procedure in all sectors of a Grand-Unified Theory of QED, the electroweak interactions, and QCD [39]. The renormalization scale of the running coupling depends dynamically on the virtuality of the underlying quark and gluon subprocess and thus the specific kinematics of each event.

The resulting scale-fixed predictions for physical observables using the PMC are also *independent of the choice of renormalization scheme* – a key requirement of renormalization group invariance. The PMC predictions are also independent of the choice of the *initial* renormalization scale μ_0. The PMC sums all of the non-conformal terms associated with the QCD β function, thus providing a rigorous method for eliminating renormalization scale ambiguities in quantum field theory. We have also showed that a single global PMC scale, valid at leading order, can be derived from basic properties of the perturbative QCD cross section. We have given a detailed comparison of these PMC approaches by comparing their predictions for three important quantities R_{e+e}, R_τ and $\Gamma_{H\to b\bar{b}}$ up to four-loop pQCD corrections [40]. The numerical results show that the single-scale PMCs method, which involves a somewhat simpler analysis, can serve as a reliable substitute for the full multi-scale PMCm method, and that it leads to more precise pQCD predictions with less residual scale dependence. The PMC thus greatly improves the reliability and precision of QCD predictions at the LHC and other colliders [40]. As we have demonstrated, the PMC also has the potential to greatly increase the sensitivity of experiments at the LHC to new physics beyond the Standard Model.

Predictions based on PMC scale setting satisfies the self-consistency conditions of the renormalization group, including reflectivity, symmetry and transitivity [41]. The resulting PMC predictions satisfy all of the basic requirements of RGI.

The transition scale between the perturbative and nonperturbative domains can also be determined by using the PMC [25, 42–44], thus providing a procedure for setting the "factorization" scale for pQCD evolution. The running coupling resums all of the $\{\beta_i\}$-terms by using the PMC, which naturally leads to a more convergent and renormalon-free pQCD series.

In more detail: the PMC scales are determined by applying the RGE of the QCD running coupling. By recursively applying the RGE one establishes a perturbative β-pattern at each order in a pQCD expansion. For example, the usual scale-displacement relation for the running couplings at two different scales Q_1 and Q_2 can be deduced from the RGE, which reads

$$
\begin{aligned}
a_{Q_2} = a_{Q_1} &- \beta_0 \ln\left(\frac{Q_2^2}{Q_1^2}\right) a_{Q_1}^2 + \left[\beta_0^2 \ln^2\left(\frac{Q_2^2}{Q_1^2}\right) - \beta_1 \ln\left(\frac{Q_2^2}{Q_1^2}\right)\right] a_{Q_1}^3 \\
&+ \left[-\beta_0^3 \ln^3\left(\frac{Q_2^2}{Q_1^2}\right) + \frac{5}{2}\beta_0\beta_1 \ln^2\left(\frac{Q_2^2}{Q_1^2}\right) - \beta_2 \ln\left(\frac{Q_2^2}{Q_1^2}\right)\right] a_{Q_1}^4 + \left[\beta_0^4 \ln^4\left(\frac{Q_2^2}{Q_1^2}\right)\right. \\
&\left. - \frac{13}{3}\beta_0^2\beta_1 \ln^3\left(\frac{Q_2^2}{Q_1^2}\right) + \frac{3}{2}\beta_1^2 \ln^2\left(\frac{Q_2^2}{Q_1^2}\right) + 3\beta_2\beta_0 \ln^2\left(\frac{Q_2^2}{Q_1^2}\right) - \beta_3 \ln\left(\frac{Q_2^2}{Q_1^2}\right)\right] a_{Q_1}^5 + \cdots
\end{aligned}
\tag{4.1}
$$

where $a_{Q_i} = \alpha_s(Q_i)/\pi$, the functions $\beta_0, \beta_1, \cdots$ are generally scheme dependent, which correspond to the one-loop, two-loop, $\cdots$, contributions to the RGE, respectively. The PMC utilizes this perturbative β-pattern to systematically set the scale of the running coupling at each order in a pQCD expansion.

The coefficients of the $\{\beta_i\}$-terms in the β-pattern can be identified by reconstructing "degeneracy relations" [45, 46] among different orders. The degeneracy relations, which underly the conformal features of the resultant pQCD series by applying the PMC, are general properties of a non-Abelian gauge theory [47]. The PMC prediction achieved in this way resembles a skeleton-like expansion [48, 49]. The resulting PMC scales reflect the virtuality of the amplitudes relevant to each order, which are physical in the sense that they reflect the virtuality of the gluon propagators at a given order, as well as setting the effective number (n_f) of active quark flavors. The momentum flow for the process involving three-gluon vertex can be determined by properly dividing the total amplitude into gauge-invariant amplitudes [50]. Specific values for the PMC scales are computed as a perturbative expansion, so they have small uncertainties which can vary order-by-order. The PMC scales and the resulting fixed-order PMC predictions are to high accuracy independent of the initial choice of renormalization scale, e.g. the residual uncertainties due to unknown higher-order terms are negligibly small because of the combined suppression effect from both the exponential suppression and the α_s-suppression [45, 46].

When one applies the standard PMC procedures, different scales generally appear at each order; this is called the PMC multi-scale approach which often requires considerable theoretical analysis. To make the PMC scale-setting procedure simpler and more easily to be automatized, a single-scale approach (PMC-s), which

achieves many of the same PMC goals, has been suggested in Ref. [60]. This method effectively replaces the individual PMC scale at each order by a single (effective) scale in the sense of a mean value theorem; e.g. it can be regarded as a weighted average of the PMC scales at each order derived under PMC multi-scale approach. The single "PMC-s" scale shows stability and convergence with increasing order in pQCD, as observed by the e^+e^- annihilation cross-section ratio $R_{e^+e^-}$ and the Higgs decay-width $\Gamma(H \rightarrow b\bar{b})$, up to four-loop level. Moreover, its predictions are again explicitly independent of the choice of the initial renormalization scale. Thus the PMC-s approach, which involves a simpler analysis, can be adopted as a reliable substitute for the PMC multi-scale approach, especially when one does not need detailed information at each order.

There are also cases in which additional momentum flows occur, whose scale uncertainties can also be eliminated by applying the PMC. For example, there are two types of log terms, $\ln(\mu/M_Z)$ and $\ln(\mu/M_t)$ [61–64], for the axial singlet r_S^A of the hadronic Z decays. By applying the PMC, one finds the optimal scale is $Q^{AS} \simeq 100$ GeV [65], indicating that the typical momentum flow for r_S^A is closer to M_Z than M_t. The PMC can also be systematically applied to multi-scale problems. The typical momentum flow can be distinct; thus, one should apply the PMC separately in each region. For example, two optimal scales arise at the N^2LO level for the production of massive quark-anti-quark pairs ($Q\bar{Q}$) close to threshold [67], with one being proportional to $\sqrt{\hat{s}}$ and the other to $v\sqrt{\hat{s}}$, where v is the Q and $\bar{Q}$ relative velocity.

The renormalization scale depends on kinematics such as thrust $(1 - T)$ for three jet production via e^+e^- annihilation. A definitive advantage of using the PMC is that since the PMC scale varies with $(1 - T)$, one can extract directly the strong coupling α_s at a wide range of scales using the experimental data at single center-of-mass-energy, $\sqrt{s} = M_Z$. In the case of conventional scale setting, the predictions are scheme-and-scale dependent and do not agree with the precise experimental results; the extracted coupling constants in general deviate from the world average. In contrast, after applying the PMC, we obtain a comprehensive and self-consistent analysis for the thrust variable results including both the differential distributions and the mean values [54]. Using the ALEPH data [56], the extracted α_s are presented in Figure **??**. It shows that in the scale range of 3.5 GeV $< Q < 16$ GeV (corresponding $(1 - T)$ range is $0.05 < (1 - T) < 0.29$), the extracted α_s are in excellent agreement with the world average evaluated from $\alpha_s(M_Z)$.

An essential property of renormalizable SU(N)]/U(1) gauge theories, is "Intrinsic Conformality," [66]. It underlies the scale invariance of physical observables and can be used to resolve the conventional renormalization scale ambiguity *at every order* in pQCD. This reflects the underlying conformal properties displayed by pQCD at NNLO, eliminates the scheme dependence of pQCD predictions and is consistent with the general properties of the PMC. We have also introduced a new method [66] to identify the conformal and β terms which can be applied either to numerical or to theoretical calculations and in some cases allows infinite resummation of the pQCD series, The implementation of the PMC_∞ can significantly improve the precision of pQCD predictions; its implementation in multi-loop analysis also simplifies the calculation of higher orders corrections in a

general renormalizable gauge theory. This method has also been used to improve the NLO pQCD prediction for $t\bar{t}$ pair production and other processes at the LHC, where subtle aspects of the renormalization scale of the three-gluon vertex and multi gluon amplitudes, as well as large radiative corrections to heavy quarks at threshold play a crucial role. The large discrepancy of pQCD predictions with the forward-backward asymmetry measured at the Tevatron is significantly reduced from 3 σ to approximately 1 σ.

The PMC has also been used to precisely determine the QCD running coupling constant $\alpha_s(Q^2)$ over a wide range of Q^2 from event shapes for electron-positron annihilation measured at a single energy $\sqrt{s}$ [68]. The PMC method has been applied to a spectrum of LHC processes including Higgs production, jet shape variables, and final states containing a high p_T photon plus heavy quark jets, all of which, sharpen the precision of the Standard Model predictions. Recently, the PMC has been used to determine the QCD coupling over the entire range of validity of perturbative QCD to high precision from the data of a single experiment: the thrust and C-parameter distributions in e^+e^- annihilation at a single annihilation energy $\sqrt{s} - M^z$ [57]. We have also showed that a single global PMC scale, valid at leading order, can be derived from basic properties of the perturbative QCD cross section. We have given a detailed comparison of these PMC approaches by comparing their predictions for three important quantities R_{e+e}, R_τ and $\Gamma_{H \to b\bar{b}}$ up to four-loop pQCD corrections [40]. The numerical results show that the single-scale PMCs method, which involves a somewhat simpler analysis, can serve as a reliable substitute for the full multi-scale PMCm method, and that it leads to more precise pQCD predictions with less residual scale dependence.

The PMC provides first-principle predictions for QCD; it satisfies renormalization group invariance and eliminates the conventional renormalization scheme-and-scale ambiguities, greatly improving the precision of tests of the Standard Model and the sensitivity of collider experiments to new physics. Since the perturbative coefficients obtained using the PMC are identical to those of a conformal theory, one can derive all-orders commensurate scale relations between physical observables evaluated at specific relative scales. The PMC thus can greatly increase the sensitivity of experiments at the LHC to new physics beyond the Standard Model. A detailed discussion of how the PMC eliminates renormaiization-scale and scheme ambiguities is given in the review [58]. The QCD running coupling and the definition of effective charges are discussed in the article [59].

Acknowledgements

its implications for hadron physics. This work is supported by the Department of Energy, Contract DE–AC02–76SF00515.

References

1. S. J. Brodsky, G. F. de Téramond and H. G. Dosch, "Threefold complementary approach to holographic QCD," http://www.sciencedirect.com/science/article/pii/S0370269313010198Phys. Lett. B **729**, 3 (2014) [http://arxiv.org/abs/arXiv:1302.4105`arXiv:1302.4105 [hep-th]`].
2. V. de Alfaro, S. Fubini and G. Furlan, "Conformal invariance in quantum mechanics," http://link.springer.com/article/10.1007
3. S. Fubini and E. Rabinovici, "Superconformal quantum mechanics," https://www.sciencedirect.com/science/article/abs/pii/055032138490422X?via
4. P. A. M. Dirac, " Forms of relativistic dynamics," http://rmp.aps.org/abstract/RMP/v21/i3/p392₁Rev. Mod. Phys. 21, 392(1949).
5. J. M. Maldacena, "The large-N limit of superconformal field theories and supergravity," https://link.springer.com/article/10.1023[http://arXiv.org/abs/hep-th/9711200`arXiv:hep-th/9711200`].
6. G. F. de Téramond and S. J. Brodsky, " Light-front holography: A first approximation to QCD," http://prl.aps.org/abstract/PRL/v102/i8/e081601 Phys. Rev. Lett. **102**, 081601 (2009) [http://arXiv.org/abs/0809.4899`arXiv:0809.4899 [hep-ph]`].
7. G. F. de Téramond, H. G. Dosch and S. J. Brodsky, " Baryon spectrum from superconformal quantum mechanics and its light-front holographic embedding," https://journals.aps.org/prd/abstract/10.1103/PhysRevD.91.045040Phys. Rev. D **91**, 045040 (2015) [http://arxiv.org/abs/1411.5243`arXiv:1411.5243 [hep-ph]`].
8. H. G. Dosch, G. F. de Téramond and S. J. Brodsky, "Superconformal baryon-meson symmetry and light-front holographic QCD," https://journals.aps.org/prd/abstract/10.1103/PhysRevD.91.085016Phys. Rev. D **91**, 085016 (2015) [http://arxiv.org/abs/1501.00959`arXiv:1501.00959 [hep-th]`].
9. S. J. Brodsky, G. F. de Téramond, H. G. Dosch and J. Erlich, "Light-front holographic QCD and emerging confinement," Phys. Rept. **584**, 1-105 (2015), [https://arxiv.org/abs/1407.8131`arXiv:1407.8131 [hep-ph]`].
10. S. J. Brodsky, G. F. de Téramond and H. G. Dosch, "Light-front holography and supersymmetric conformal algebra: A novel approach to hadron spectroscopy, structure, and dynamics," [https://arxiv.org/abs/2004.07756`arXiv:2004.07756 [hep-ph]`].
11. S. J. Brodsky, P. Hoyer, C. Peterson and N. Sakai, "The Intrinsic Charm of the Proton," Phys. Lett. B **93**, 451-455 (1980) doi:10.1016/0370-2693(80)90364-0
12. S. J. Brodsky, J. C. Collins, S. D. Ellis, J. F. Gunion and A. H. Mueller, "Intrinsic Chevrolets at the SSC," DOE/ER/40048-21 P4.
13. G. F. de Téramond, H. G. Dosch and S. J. Brodsky, "Kinematical and dynamical aspects of higher-spin bound-state equations in holographic QCD," https://journals.aps.org/prd/abstract/10.1103/PhysRevD.87.075005Phys. Rev. D **87**, 075005 (2013) [https://arxiv.org/abs/1301.1651`arXiv:1301.1651 [hep-ph]`].
14. H. G. Dosch, G. F. de Téramond and S. J. Brodsky, "Supersymmetry across the light and heavy-light hadronic spectrum," https://journals.aps.org/prd/abstract/10.1103/PhysRevD.92.074010Phys. Rev. D **92**, 074010 (2015) [https://arxiv.org/abs/1504.05112`arXiv:1504.05112 [hep-ph]`].
15. H. G. Dosch, G. F. de Téramond and S. J. Brodsky, "Supersymmetry across the light and heavy-light hadronic spectrum II," https://journals.aps.org/prd/abstract/10.1103/PhysRevD.95.034016Phys. Rev. D **95**, 034016 (2017) [https://arxiv.org/abs/1612.02370`arXiv:1612.02370 [hep-ph]`].

16. M. Nielsen and S. J. Brodsky, "Hadronic superpartners from a superconformal and supersymmetric algebra," https://journals.aps.org/prd/abstract/10.1103/PhysRevD.97.114001Phys. Rev. D **97**, 114001 (2018) [https://arxiv.org/abs/1802.09652arXiv:1802.09652 [hep-ph]].

17. M. Nielsen, S. J. Brodsky, G. F. de Téramond, H. G. Dosch, F. S. Navarra and L. Zou, "Supersymmetry in the double-heavy hadronic spectrum," https://journals.aps.org/prd/abstract/10.1103/PhysRevD.98.034002Phys. Rev. D **98**, 034002 (2018) [https://arxiv.org/abs/1805.11567arXiv:1805.11567 [hep-ph]].

18. S. J. Brodsky and A. H. Mueller, "Using Nuclei to Probe Hadronization in QCD," Phys. Lett. B **206**, 685-690 (1988) doi:10.1016/0370-2693(88)90719-8

19. S. J. Brodsky and G. F. de Teramond, MDPI Physics **4**, no.2, 633-646 (2022) doi:10.3390/physics4020042 [arXiv:2202.13283 [hep-ph]].

20. H. G. Dosch, G. F. de Téramond and S. J. Brodsky, Nucl. Part. Phys. Proc. **318-323**, 133-137 (2022) doi:10.1016/j.nuclphysbps.2022.09.028

21. R. S. Sufian, G. F. de Téramond, S. J. Brodsky, A. Deur and H. G. Dosch, Analysis of nucleon electromagnetic form factors from light-front holographic QCD: The space-like region, https://journals.aps.org/prd/abstract/10.1103/PhysRevD.95.014011Phys. Rev. D **95**, 014011 (2017) [https://arxiv.org/abs/1609.06688arXiv:1609.06688 [hep-ph]].

22. G. F. de Téramond, T. Liu, R. S. Sufian, H. G. Dosch, S. J. Brodsky and A. Deur, "Universality of generalized parton distributions in light-front holographic QCD," https://journals.aps.org/prl/abstract/10.1103/PhysRevLett.120.182001Phys. Rev. Lett. **120**, 182001 (2018) [https://arxiv.org/abs/1801.09154arXiv:1801.09154 [hep-ph]].

23. T. Liu, R. S. Sufian, G. F. de Téramond, H. G. Dosch, S. J. Brodsky and A. Deur, Unified description of polarized and unpolarized quark distributions in the proton, https://journals.aps.org/prl/abstract/10.1103/PhysRevLett.124.082003Phys. Rev. Lett. **124**, 082003 (2020) [https://arxiv.org/abs/1909.13818arXiv:1909.13818 [hep-ph]].

24. S. J. Brodsky, G. F. de Téramond and A. Deur, "Nonperturbative QCD coupling and its β function from light-front holography," https://journals.aps.org/prd/abstract/10.1103/PhysRevD.81.096010Phys. Rev. D **81**, 096010 (2010) [https://arxiv.org/abs/1002.3948arXiv:1002.3948 [hep-ph]].

25. A. Deur, S. J. Brodsky and G. F. de Teramond, "Connecting the Hadron Mass Scale to the Fundamental Mass Scale of Quantum Chromodynamics," Phys. Lett. B **750**, 528-532 (2015) doi:10.1016/j.physletb.2015.09.063 [arXiv:1409.5488 [hep-ph]].

26. G. Grunberg, "Renormalization Group Improved Perturbative QCD," Phys. Lett. B **95**, 70 (1980) [erratum: Phys. Lett. B **110**, 501 (1982)] doi:10.1016/0370-2693(80)90402-5

27. A. Karch, E. Katz, D. T. Son and M. A. Stephanov, Linear confinement and AdS/QCD, https://journals.aps.org/prd/abstract/10.1103/PhysRevD.74.015005Phys. Rev. D **74**, 015005 (2006) [https://arxiv.org/abs/hep-ph/0602229arXiv:hep-ph/0602229].

28. S. J. Brodsky, G. F. de Téramond, A. Deur and H. G. Dosch, "The Light-Front Schrödinger Equation and the Determination of the Perturbative QCD Scale from Color Confinement: A First Approximation to QCD," Few Body Syst. **56**, no.6-9, 621-632 (2015) doi:10.1007/s00601-015-0964-1 [arXiv:1410.0425 [hep-ph]].

29. G. F. de Téramond *et al.* [HLFHS], Phys. Rev. Lett. **133**, no.18, 181901 (2024) doi:10.1103/PhysRevLett.133.181901 [arXiv:2403.16126 [hep-ph]].

30. S. J. Brodsky, G. F. de Téramond, H. G. Dosch and C. Lorcé, Int. J. Mod. Phys. A **31**, no.19, 1630029 (2016) doi:10.1142/S0217751X16300295 [arXiv:1606.04638 [hep-ph]].

31. R. Haag, J. T. Lopuszanski and M. Sohnius, Nucl. Phys. B **88**, 257 (1975) doi:10.1016/0550-3213(75)90279-5

32. S. J. Brodsky, A. Deur, G. F. de Téramond and H. G. Dosch, Int. J. Mod. Phys. Conf. Ser. **39**, 1560081 (2015) doi:10.1142/S2010194515600812 [arXiv:1510.01011 [hep-ph]].

33. T. Liu and B. Q. Ma, Phys. Rev. D **92**, no.9, 096003 (2015) doi:10.1103/PhysRevD.92.096003 [arXiv:1510.07783 [hep-ph]].

34. S. J. Brodsky and S. D. Drell, "The Anomalous Magnetic Moment and Limits on Fermion Substructure," Phys. Rev. D **22**, 2236 (1980) doi:10.1103/PhysRevD.22.2236

35. S. J. Brodsky, D. S. Hwang and I. Schmidt, "Final state interactions and single spin asymmetries in semi-inclusive deep inelastic scattering," Phys. Lett. B **530**, 99-107 (2002) doi:10.1016/S0370-2693(02)01320-5 [arXiv:hep-ph/0201296 [hep-ph]].

36. S. J. Brodsky, G. P. Lepage and P. B. Mackenzie, Phys. Rev. D **28**, 228 (1983) doi:10.1103/PhysRevD.28.228

37. S. J. Brodsky, M. Mojaza and X. G. Wu, Phys. Rev. D **89**, 014027 (2014) doi:10.1103/PhysRevD.89.014027 [arXiv:1304.4631 [hep-ph]].

38. S. J. Brodsky and H. J. Lu, Phys. Rev. D **51**, 3652-3668 (1995) doi:10.1103/PhysRevD.51.3652 [arXiv:hep-ph/9405218 [hep-ph]].

39. M. Binger and S. J. Brodsky, Phys. Rev. D **69**, 095007 (2004) doi:10.1103/PhysRevD.69.095007 [arXiv:hep-ph/0310322 [hep-ph]].

40. S. J. Brodsky and L. Di Giustino, Phys. Rev. D **86**, 085026 (2012) doi:10.1103/PhysRevD.86.085026 [arXiv:1107.0338 [hep-ph]].

41. S. J. Brodsky and X. G. Wu, 86 054018 2012.

42. A. Deur, S. J. Brodsky and G. F. de Teramond, 757 275 2016.

43. A. Deur, S. J. Brodsky and G. F. de Teramond, 90 1 2016.

44. A. Deur, J. M. Shen, X. G. Wu, S. J. Brodsky and G. F. de Teramond, 773 98 2017.

45. M. Mojaza, S. J. Brodsky and X. G. Wu, 110 192001 2013.

46. S. J. Brodsky, M. Mojaza and X. G. Wu, Phys. Rev. D **89**, 014027 (2014) doi:10.1103/PhysRevD.89.014027 [arXiv:1304.4631 [hep-ph]].

47. H. Y. Bi, X. G. Wu, Y. Ma, H. H. Ma, S. J. Brodsky and M. Mojaza, 748 13 2015.

48. H. J. Lu and C. A. R. Sa de Melo, 273 260 1991.

49. H. J. Lu, 45 1217 1992.

50. M. Binger and S. J. Brodsky, 74 2006 054016.

51. J. M. Shen, Z. J. Zhou, S. Q. Wang, J. Yan, Z. F. Wu, X. G. Wu and S. J. Brodsky, [arXiv:2209.03546 [hep-ph]].

52. G. Kramer and B. Lampe, 39 101 1988.

53. G. Kramer and B. Lampe, 339 189 1991.

54. S. Q. Wang, S. J. Brodsky, X. G. Wu and L. Di Giustino, arXiv:1902.01984 [hep-ph].

55. T. Gehrmann, N. Häfliger and P. F. Monni, 74 2896 2014.

56. A. Heister *et al.* [ALEPH Collaboration], 35 457 2014.

57. L. Di Giustino, S. J. Brodsky, P. G. Ratcliffe, S. Q. Wang and X. G. Wu, [arXiv:2407.08570 [hep-ph]].

58. L. Di Giustino, S. J. Brodsky, P. G. Ratcliffe, X. G. Wu and S. Q. Wang, PoS **RADCOR2023**, 071 (2024) doi:10.22323/1.432.0071 [arXiv:2310.08178 [hep-ph]].

59. A. Deur, S. J. Brodsky and C. D. Roberts, Prog. Part. Nucl. Phys. **134**, 104081 (2024) doi:10.1016/j.ppnp.2023.104081 [arXiv:2303.00723 [hep-ph]].

60. J. M. Shen, X. G. Wu, B. L. Du and S. J. Brodsky, 95 094006 2017.

61. P. A. Baikov, K. G. Chetyrkin and J. H. Kühn, 101 012002 2008.

62. P. A. Baikov, K. G. Chetyrkin and J. H. Kühn, 104 132004 2010.

63. P. A. Baikov, K. G. Chetyrkin, J. H. Kühn and J. Rittinger, 714 62 2012.

64. P. A. Baikov, K. G. Chetyrkin, J. H. Kühn and J. Rittinger, 108 222003 2012.

65. S. Q. Wang, X. G. Wu and S. J. Brodsky, 90 037503 2014.

66. L. Di Giustino, S. J. Brodsky, S. Q. Wang and X. G. Wu, "Infinite-order scale-setting using the principle of maximum conformality: A remarkably efficient method for eliminating renormalization scale ambiguities for perturbative QCD," Phys. Rev. D **102**, no.1, 014015 (2020) doi:10.1103/PhysRevD.102.014015 [arXiv:2002.01789 [hep-ph]].

67. S. J. Brodsky, A. H. Hoang, J. H. Kühn and T. Teubner, 359 355 1995.

68. S. Q. Wang, S. J. Brodsky, X. G. Wu, J. M. Shen and L. Di Giustino, "Novel method for the precise determination of the QCD running coupling from event shape distributions in electron-positron annihilation," Phys. Rev. D **100**, no.9, 094010 (2019) doi:10.1103/PhysRevD.100.094010 [arXiv:1908.00060 [hep-ph]].

5 On SS433 Micro-quasar jet and the TeV resurgence beam

Daniele Fargion[1][2] **

[1] Physics Department, Rome University1,Sapienza, Pl.A.Moro 2,Rome,Italy
[2] INAF, Osservatorio Astronomico di Capodimonte, Naples, Italy

Abstract: The understanding of micro-quasars in our galaxy is one of the frontier of high-energy astrophysics. Their models are based on a growing mass Black Hole (BH) with a nearby spiralling binary companion star. Their main stage is the feeding, by the companion star mass, of the accretion disk around the BH that fuels also an orthogonal precessing X-gamma jets. The spiral precessing tail of such micro-quasars, as the SS433 system, is a jet spraying matter and electrons at relativistic speed. The up-down twin precessing jet is observed clearly along its tails, spread and smeared within a year light distance. Very recently HESS, HAWC and LHAASO surprisingly discovered , at a much far separated distance, the resurgence of a twin trace, as a twin hard beam-gamma tail. It is starting at nearly 75 years light distance from the same SS433 source. The most standard model is based on a shock wave particle re-accelleration along a Fermi process, far from the SS433 system. The un-expected and also surprising re-collimation of this TeV beam jet is difficult to understand, in such a planar Fermi shock process model. We offer here a quite different model , based on known high energy nuclear physics, able to explain at once both the disconnected as well as the aligned hard TeV jet appearence. This model is assuming that SS433 ejected tens Pevatron hadron beam, 75 years ago in an explosive accreation disk stage. The ejecting had been both of a tens Pev protons jet, but also, by photo-pion creation, a collinear secondary tens PeV neutron jet. Its presence explain the collimated, separeted appearence of a tens TeV electron secondary, after the boosted relativistic beta decay of the PeVs neutron.

Povzetek: Raziskave mikrokvazarjev v naši galaksiji so eno izmed mejnih področij visokoenergijske astrofizike. Modeli obravnavajo naraščanje mase črne luknje na račun mase spremljevalke, ki kroži okoli črne luknje in polni akrecijski disk okoli črne luknje in tudi pravokotni precesijski curek v rentgenskem in gama spektru. Spiralno precesijski rep mikrokvazarjev, kot je sistem SS433, je curek, ki z relativistično hitrostjo izmetava snov in elektrone. Razpršen dvojni precesijski curek (zgornji in spodnji), dolg kako svetlobno leto, je dolž repov lepo viden. Zadnje raziskave observatorijev HESS, HAWC in LHAASO so odkrile na veliko večji oddaljenosti ponovni izbruh kot dvojno sled trdega curka gama, ki je približno 75 svetlobnih let oddaljen od vira SS433. Nepričakovano in presenetljivo ponovno fokusiranje tega curka pri energijah TeV je težko razložiti zgolj z ravninskim Fermi-

---

** Daniele.Fargion@uniroma1.it

jevim modelom za te procese, ki so ga uporabljali doslej. Članek ponuja drugačen model, ki temelji na znani visokoenergijski jedrski fiziki in lahko razloži ta pojav: Privzamejo da je SS433 pred približno 75 svetlobnimi leti, v eksplozivni fazi akreci-jskega diska, izstrelil curek hadronov z energijami v območju desetih PeV. Izmet je vseboval curek protonov z energijami desetih PeV in tudi kolinearen sekundarni curek nevtronov z enakimi energijami, ki je nastal s fotopionsko tvorbo. Prisotnost tega nevtronskega curka pojasnjuje kolimiran ločen pojav sekundarnih elektronov z energijami desetih TeV, ki nastanejo po razpadu beta nevtonov energije PeV.

5.1   Introduction: SS433 and its separated TeV beam

The micro-quasars are binary systems where a neutron star (NS), of a few or tens solar masses Black Hole (BH), are bounded by gravity with an orbital star of a comparable (or larger) mass, capturing the star mass by tidal forces. While such a tail of mass is collapsing onto the NS (or the BH), the same mass first feeds an accreting disk around the NS or BH. This disk usually produce asymmetric spinning charged flows and consequent huge currents that are building up , a toroidal power-full magnetic field. Such magnetic field may show fast time variability that induce also huge electric spiral fields that accelerate, rotating, the free charges . They spin along a twin disk-conical ring , above and below the same accretion disk. These ultra-high energy charges are bounded spiraling along the accretion disk. At the end, these relativistic particles are forced to be aligned along the NS or BH poles axis. The best jet accelerator are localized very nearby the NS or BH accretion disks and magnetic fields. The magnetic field line shrinkage and the charge acceleration may finally produce the up-down charge ejection, in a very twin collimated jet. Tidal forces among orbital star companion and accretion disk, may also lead to a conical precession of the same jet. These events in their primordial and in the late mass accretion phase, may shine in a thin persistent, precessing jet ,. Its blazing may be observed rarely on axis, as Gamma Ray Burst (GRB) or Soft Gamma Repeaters. [1]. The magnetic field lines along the jet constrain and collimate the beam. The leptonic component of this jet is able, by synchrotron radiation and by Inverse Compton Scattering (ICS), to shine in radio, X and sometimes into gamma photon energy spectra, at energy edges as hard as MeV, GeV, TeV and ,to PeV ones. These hard signals had been discovered since nearly half a century and very recently in details.

As the micro quasar name suggest they are just a small scale (parsecs) system of a much famous and larger quasar, made by million or billion solar mass BH, hidden in galactic centers, called also Active Galactic Nuclei, (AGN), able to eject much wider, longer and harder jet beam, even in Mega parsec sizes. The SS433 is a quite peculiar binary system containing a supergiant star that is overflowing its Roche lobe with matter accreting on nearby BH. The separeted tens TeV beam appearence was a discovered this year by Hess [2], confirmed also by HAWC and LHAASO , more recently . Its presence and re-collimation at such far distance, is puzzling .

Here we consider the possibility that a rarest explosive flare episode in earliest micro-quasar epochs may shine , at the same time, ultra-violet hot photons and ultra relativistic energy (UHE) proton (on nuclei) jet. Their scattering and interaction was leading to Delta Δ photo-pion creation. This phenomena is in analogy , (in cosmic volumes and by thermal big bang radiation), of a similar phenomena , taking place between UHECR (Ultra High Energy Cosmic Ray) at 10^{20} eV energy and infrared cosmic black body photon. The phenomena is known under the author initial, as the "GZK cut-off" in the CR spectra [3], and [4]. The Delta resonance at ultra-relativistic energy (UHE) decay may produce neutral and charged pion respectively with associated proton or neutron. The presence and the quite dark surviving of such tens PeV neutron beam along SS433 flight is the key of our model. The observed 75 years light distance of the UHE neutron decay, the consequent electron radiiation , by ICS; as TeV gamma resurgence beam, is the main key engine of present model.

5.1.1   Pevatron Neutron jet and its decay distances

The distance of an UHE (about 25 PeV) neutron beta decay in flight is nearly 75 years light . Indeed:

$$L_n = 877(E_n/m_n)s \cdot c.; L_n = 75y \cdot c(E_n/25PeV) \tag{5.1}$$

A main question arises about the observed discontinuity in SS433 separated TeV beam versus an expected continuity of the cosmic-ray spectra of the jet. The observed cosmic ray spectra on Earth , up to GZK cut-off edges, decrease smoothly by a power law, without any sudden peak or cut-off discontinuity. One would imagine a neutron secondary jet spectra ruled by an un-disconnected signature in their decay distances. Our model need and find a natural, tuned , nearly monochromatic neutron energy. See for a SS433 system description. See for a description, the following Figures below.

5.1.2   Delta resonance by proton-photon interaction

The GZK cut-off is defined by a peculiar threshold, so the UHE neutron jet formed by tens PeV protons in SS433 jet, require a tuned scenario. Indeed the threshold for the meson resonance is defined by the center of mass-energy for the Δ formation made by an UHE proton E_p scattering onto a hot thermal bath of photons E_γ is in their ultra-relativistic approximation :

$$\sqrt{2 \cdot E_p \cdot E_\gamma} = m_\Delta \tag{5.2}$$

We remind, that baryon resonant Delta mass, m_Δ, has a value = 1232 MeV. This equation defines the corresponding critical thermal photon energy E_γ , and therefore, the tuned accretion disk temperature and its luminosity needed to take place for such a processes to occur . The Δ decay may lead to a UHE proton with a neutral pion, π^0. This pion is decaying soon in a photon pair secondary. With the same rate the Δ baryon may also decay into a neutron and its pion charged
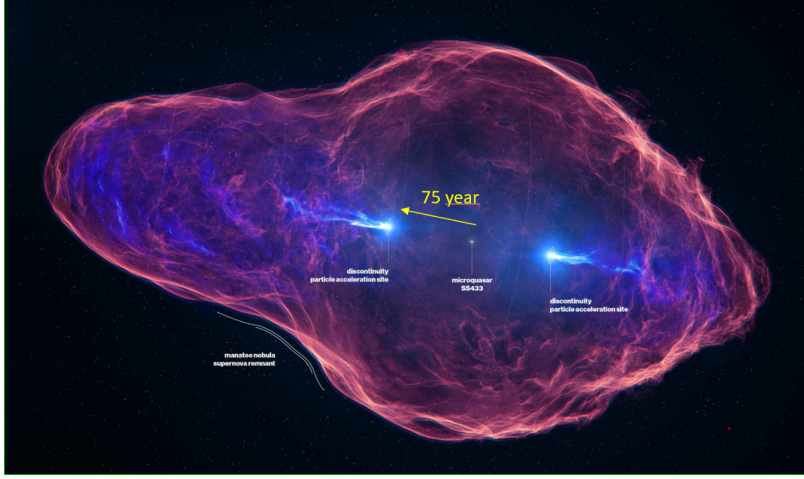
Fig. 5.1: A simplified description of the separated TeV beam observed by Hess, HAWC and LHAASO. The resurgence of the collimated gamma beam at $75y \cdot c$ is very puzzling.

companion, π^+. The charged pion also decay soon into muon and its neutrino and finally also the muon secondary itself will decay into electron and their two needed neutrino flavors. The final electromagnetic secondaries (photon pairs, electron pairs) shine and dissolve within a very near (parsec) distances from the source. They cannot reach far distances and cannot play any role at $75y \cdot c$ distance. However a neutron beam is also created. The proton at Pevatron energy are bent by the galactic magnetic fields. loosing their directionality and also smearing their beam into wider spiral trajectory . The PeVs neutron beam, instead, may escape and fly keeping directionality, with no losses, up to its beta decay.

The correlated photon energy to allow such a proton-pion , Delta resonance with a $E_p = 25\,\text{PeV}$ proton must be:

$$E_\gamma = (m_\Delta)^2/E_p = 30.35 eV/(E_p/(25PeV)) \tag{5.3}$$

One must also take care of a partial loss of energy for the final proton (or neutron) secondary, because the pion secondaries in the Delta decay absorb part of the primary energy. This loss is just at ten percent level. Therefore for a final 25 PeV neutron, we must consider a primary proton at higher energy, nearly of 27.5 PeV. Consequently, the interacting photon energy E_γ would lead to a resonance at

$$E_\gamma = (m_\Delta)^2/E_p = 31.68 eV/(E_p/(27.5PeV)) = 3.676 \cdot 10^5 K^\circ/(E_p/(27.5PeV)) \tag{5.4}$$

This photon is 63.6 times larger than the peak solar one. Let us show in the following figure the possible, present, parameters of the SS433 with their nominal comparable mass of 10 solar masses, in a circular Keplerian orbit of 13 day period (and 162 day precession time). The star companion radius, the BH accretion disk size are shown approximated values , while the orbit distance is tuned for their

assumed 10 solar mass each. This mutual distance D may be slightly re-calibrated , for any different f binary masses , following the Keplerian (cubic root) law:

$$D = 146 \cdot ((M_{BH}/10M_o) + (M_{Star}/10M_o))^{1/3} s \cdot c \qquad (5.5)$$
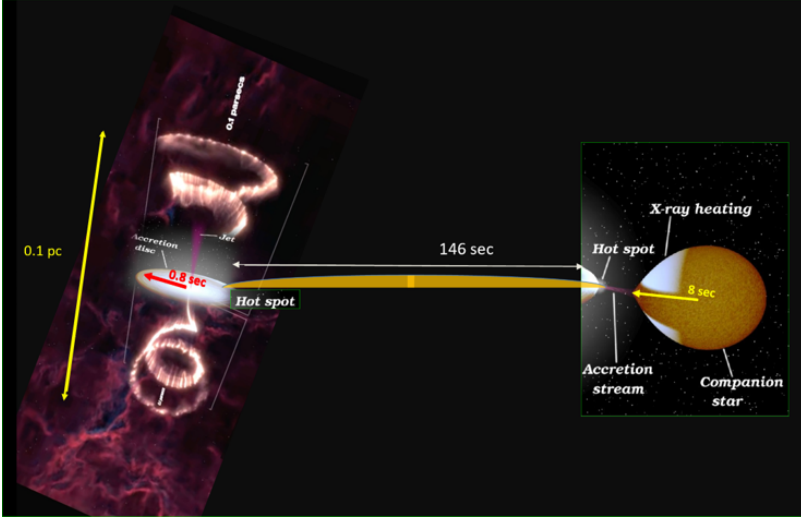
Fig. 5.2: A simplified description of the inner SS433 binary , in approximated size, system: an accretion disk on a BH and a companion star of comparable mass, both of them, with a nominal ten solar mass, in their corresponding Keplerian circular distance. The star radius and in particular, the accretion disk, are approximated just for a comprehensive view, but they may be a little larger.

5.1.3   Temperature, photon density, SS433 flare luminosity

Let us assume for sake of simplicity that the accretion disk , in the figure assumed about 0.8s · c size, extends a lttle more, with a radius comparable to our Sun or better, to its spherical total surface (occuring , for a disk radius $R_{disk} = \sqrt{2} \cdot R_{Sun}$) . Because, as shown above, the disk flare temperature required for the resonance to arise is 63 times the solar one, the corresponding peak flare luminosity L_{Flare} would be (by scale Stephan Botzmann law), $(63)^4$ times larger than our Sun., or

$$L_{Flare} = 6.03 \cdot 10^{40} \cdot erg/s \qquad (5.6)$$

It should also remind here that this flare power (considering the additional outflow energy in mass ejection jet and mass loss inside the BH) require a much larger mass- energy rate falling into the BH. We suggest an energy output (and a corresponding mass collapse from the companion star to the BH) thousand times larger, as : $(dM/dt)_{tot} \cdot c^2 > 6.03 \cdot 10^{43} \cdot erg/s$. This output is not far from

the usual SS433 observed one., but it requires a quite brighter, near a Nova like $(dM/dt)_{Nova} > 10^{44} \cdot erg/s$, explosive event. The total duration of such a huge explosion may hold hours or a few days. For such a brief day duration, the SS433 precessing jet (162 day period) could be considered to be "frozen" pointing in a unique direction, as the observed TeV separated beam.

5.1.4   Delta resonance creation in SS433 by Nova-like event

As above estimate, the total mass in rapid capture may be as large as a part of a thousand a solar mass. Thus such a high brightening might be due to a very nearby tidal encounter of the companion star mass , or, more probably, due to the capture of a large wind or even a planet (Juppiter like) in near orbit along the companion star, suddenly falling onto the BH own gravity. Such a Nova like Burst , 75-80 years ago, might be occurring at the end of War World II, when astronomy could not be carefully and actively observing that sky region. Indeed the same SS433 system nature had been discovered only on 1977. If our hypothesis of a Nova-like flare is correct, a more care-full study of old the past sky photo-plate in that direction , on those epochs, might, be luckly, finding traces of that expected event.

The maximal cross section σ for a photo-pion resonance, has a peak value as the following one:

$$\sigma_{\Delta} = 500\mu b \tag{5.7}$$

Such a cross-section defines an isolated peak, well explaining the consequent, nearly mono-chromatic, neutron beam energy. We verify therefore the self consistence for such a thermal photon bath model able to reach an interaction probability above its threshold. This the hot UV temperature fixed and considered above, contained in a black body volume near the flaring "over-Eddington" accretion disk, defines also the same photon number density $n_{Th=3.676 \cdot 10^5 K^{\circ}}$ where and along the jet ultra-relativistic proton propagation : The main interaction distance the disk, D_j should be comparable with the same accretion disk radius, leading to an approximated probability $P_{Photo-pion}$, for the photo-pion conversion into a Delta (and a consequent neutron beam creation.

$$P_{Photo-pion} = \sigma_{\Delta} \cdot n_{Th} \cdot D_j = 48 >> 1 \tag{5.8}$$

This order of magnitude guarantee a quite complete Delta resonance production and a consequent realistic neutron beam formation, even at a far (hundred sec c distance) from the same accreting SS433 disk. The self-consistent, neutron beam energy, to fit the 75 $y \cdot c$ has a corresponding flare temperature, and the associated thermal photon number density, leading to a large threshold , $P_{Photo-pion} >> 1$, for the Δ resonance production. All the puzzle pieces are all in agreement, offering support to the present model thesis.

5.1.5   Larmor radius for PeV proton and TeV electrons

As we had proposed above, tens PeV neutron decay, 75yc far away, might become source of the observed 25 TeV separated gamma beam. We may inquire to the role

of the twin proton secondaries of the Δ decay at comparable energies. These 25 PeV energetic proton, contrary to neutron ones, are bent. Their Larmor radius R_p is constrained by the minimal galactic disk magnetic fields B_g , at least , of few micro Gauss: .

$$R_p = (E_p/25 PeV) \cdot (B_g/(3 \cdot \mu \cdot Gauss))^{-1} \cdot 26.4 \cdot yc \qquad (5.9)$$

These spiral radius are nearly one third of the 75 TeV beam distance. Therefore these proton components are diffused and smeared: they cannot play a role in the separated TeV jet. Also the secondary electrons at nearly 25 TeV energy , the parasite secondaries traces of the neutron beta decay, are even more confined along the neutron beta trajectory, within a much smaller spirals of radius R_e

$$R_e = (E_e/25 TeV) \cdot (B_g/(3 \cdot \mu \cdot Gauss))^{-1} \cdot 0.026.4 \cdot yc \qquad (5.10)$$

Therefore the electron role is not able to survive hundreds years light, in absence of the suggested primary 25 PeV energetic neutron beam.

5.1.6   Neutrons by photo-nuclear Giant Dipole Resonance

Recent UHECR model imagined lightest nuclei currier being fragmented by photonuclear distruption, via the Giant Dipole Resonance , GDR., in concurrence with "standard model foreseeing the proton or iron UHECR courier. The GDR process, in analogy with the previous photo-pion one, is capable to lead among the fragments,also to UHE neutrons. The lightest nuclei mudel was considered mainly to filter or hide the otherwise Virgo cluster inevitable presence (and unobserved signals) for proton in UHECR model. The GDR processes has a lower energy threshold, but it is not acting on a proton or a neutron, but it regards only nuclei. Here we just mention this additional opportunity windows. We also remind the possibility that such neutron process extend, from few 10^{16} eV also to several 10^{19} eV energy (for wider accretion disk and lower thermal bath). In this extreme scenario, we noted the very rare clustering of 4 UHECR events by AUGER and by TA array detectors in last two decades, all of the overlapping within a narrow spot of events at SS433 direction. Their few degrees collimation and their short time (decades) period of recording, might be well consistent , as discussed elsewhere [5], with such tens EeV energy neutron collimated flight . The GDR processes considered here does not sound as the most probable one for the neutron beam , but it must be taken in consideration.

5.2   Conclusions

A past flare in SS433, could be the source of a 25 PeV neutron jet , possibly explaining the puzzling separated twin, TeV , gamma beam at 75 years far distance. The unobservable PeV neutron flight show its presence and its beam resurgence as soon it decay at far distance and its electron may shine by synchrotron and ICS radiation. its collimation is an advantage respect the standard model of a schock

wave processes . This ultra-relativistic beta decay imply also additional interesting consequences:

An early trigger explosive event, nearly 75/80 years ago, as powerfull as a Nova star burst, for a duration of few hours or few days at SS433 system shine almost in a fixed direction (not along a conical precessing jet volume). This event occurrence is around the War World II end times. Such a Nova event (to-day observed at a rate of a dozen a year), could have been escaped detection, at those post war times . Indeed the same nature of SS433 had been discovered much later, on 1977. It could be possible and worth-full to inspect such luminosity variability, in oldest astronomical photo-plate array in that direction and at those epochs, looking for such a sudden variability signal.

The presence of such neutron PeV separated beam in SS433, may suggest also the search in other micro-quasars system elsewhere, for such disconnected signatures. Their statistics may define a corresponding neutrino spectra rate in PeV and hundred TeV energy range,

The 25 PeV neutron beta decay and its primary 27 PeV proton-pion event, while on axis toward us , may shine both of a brightest prompt $(1-2)$ PeV gamma burst but also of a secondary (electron and muon ones) neutrino at $(0.2-0.5)$ PeV energy . Such a tuned energies are quite interesting , because they may reflect in the TeV PeV apparent energy dis-continuity, in neutrino spectra . Such spectra feature might be already hidden in the highest energy Ice-Cube neutrino data, assuming that their observed origin is really astrophysical and not , as some suggested, a charmed atmospheric noise. .

Acknowledgements and Dedication

References

1. D.Fargion: GRBs and SGRs as precessing gamma jets
2. Hess Collaboration : Acceleration and transport of relativistic electrons in the jets of the microquasar SS 433
3. K. Greisen : https://inspirehep.net/literature/50010End to the cosmic ray spectrum?
4. G.T. Zatsepin,V.A. Kuzmin: Upper limit of the spectrum of cosmic rays *Pisma Zh.Eksp.Teor.Fiz.* **4.**: 114-117 (1966)
5. D.Fargion, P.G.D.S. Lucentini, M.Khlopov: UHECR Clustering: Lightest Nuclei from Local Sheet Galaxies
6. S.Takahiro: Multiwavelength Emission from Galactic Jets: The Case of the Microquasar SS433

.

6 The Elusive Influence of Dark Matter on Ionospheric Observations

A.M. Kharakhashyan[1,2]**

[1] Research Institute of Physics, Southern Federal University, Rostov-on-Don, 344090, Russia
[2] Department of Applied Mathematics, Don State Technical University, Rostov-on-Don, 344000, Russia

Abstract. In recent years, the number of publications devoted to the study of the influence of Dark Matter on the Solar System has increased significantly. Observational evidence indicates the existence of possible focusing effects of Dark Matter in the vicinity of the Earth, which affects the results of measurements of parameters characterizing the state of the ionosphere and stratosphere. Such data can shed light on many processes in the Solar System, since it is accumulated over relatively long periods of time under known conditions, and the volume of this data will only increase. Over the years of research, a number of unexplained anomalies in the behavior of these parameters have been observed, the sources of which have not been identified. In most recent publications, the effects that Dark Matter can have on the ionosphere are associated with the influence of Dark Photons and Axion-like particles, due resonant conversion into electromagnetic waves in the magnetic field in ionized plasma, and due coupling. In this work, we use the galactic reference frame and consider a set of ionospheric parameters and solar wind parameters measured on the Earth's surface or near the Earth, and construct vectors of changes in these parameters at different times and in different directions in order to determine possible inhomogeneities in the behavior of these parameters due to distribution of hidden mass in the Solar System in spacetime. It is shown that for the selected parameters, the difference vectors calculated since 1986 have clearly defined directions that are not determined by the Sun at certain time intervals, and the directional vectors are consistent between the parameters.

Povzetek V zadnjih letih se je znatno povečalo število publikacij, ki preučujejo vpliv temne snovi na Osončje. Merjenja nakazujejo, da zgoščevanje temne snovi v bližini Zemlje vpliva na parametre, ki označujejo stanje ionosfere in stratosfere. Ta merjenja lahko osvetlijo številne procese v Osončju, saj se zbirajo v razmeroma dolgih časovnih obdobjih pod znanimi pogoji. Raziskave kažejo številne nepojasnjene anomalije v izmerjenih parametrih. Zadnje publikacije povezujejo vpliv temne snovi na ionosfero preko temnih fotonov in delcev, podobnih aksionom, ki prožijo elektromagnetne valove v magnetnem polju ioniziranie plazme. V tem prispevku uporablja avtor galaktični sistem. Preučuje ionosferske parametre ter parametre sončnega vetra, izmerjene na površini Zemlje ali v njeni bližini, ter konstruira vektorje sprememb teh parametrov, izmerjenih v različnih časih in smereh, da bi ugotovil ali se parametri spreminjajo zaradi sprememb porazdelitve temne snovi v Osončju. Za določene parametre je ugotovljeno, da imajo razlike vektorjev, ki jih določajo od leta 1986, jasno določene smeri, ki ob določenih časovnih intervalih niso odvisne od Sonca, pri čemer so smerni vektorji enaki za različne parametre.

** aharahashyan@sfedu.ru

6.1   Introduction

The detection and study of Dark Matter has been a hot topic in cosmology, astrophysics and particle physics for many decades. During the observations in each of the research areas, a substantial amount of evidence has been collected that cannot be explained within the framework of traditional approaches [1]. The research area is constantly expanding and has already gone beyond the classical domains, with increasing attention being paid to the search for the effects of Dark Matter in the Solar System. In recent years, interdisciplinary research has revealed a number of new anomalies within the Solar System [2-4], and new explanations have been proposed [2-5] using effects associated with the influence of Dark Matter. The zones of interest that are attracting increased attention include the ionosphere, stratosphere, solar corona, and near-Earth space in general [2-12]. The complexity of studying these regions is related to their proximity to each other and the presence of numerous layers with fundamentally different characteristics. These layers are in constant interaction, particularly the adjacent ones, are interdependent, and subject to external effects caused by solar activity, cosmic rays, interplanetary space radiation, and noise induced by human activity. However, such diversity and complexity provide great opportunities to track the development of these processes at different stages and to conduct cross-analysis. Over a long period of observation of the Earth's ionosphere, significant amounts of data have been accumulated on the processes occurring there and in the neighboring layers. The state of the ionosphere is described by many parameters, some of which are not specific to the ionosphere only, and relate to the adjacent layers or even interplanetary space. While many processes are largely determined by the 11-year solar cycle, a significant number of anomalies have been discovered over time. These include stratospheric temperature December-January variations, lack of correlations between those stratospheric temperature variations and solar UV and EUV emission, total electron content (TEC) planetary correlation and unexpected seasonal differences, that are not related to Earth-Sun distance, correlation between earthquakes and TEC, and unexpected trends in solar cycles[2-6]. Some of these anomalies can be attributed to gravitational Dark Matter focusing [6], and to the influence of Dark Photons and Axion-like particles [7-10], due resonant conversion into electromagnetic waves in the magnetic field in ionized plasma, and due coupling. Since there are many Dark Matter candidates, and they have a strong theoretical background, while their properties vary significantly and each type has its own unique interactions, we will focus on finding more anomalies that can provide the information required to determine the most probable candidate.

6.2   Data and Methods

This paper studies a set of parameters characterizing the state of the ionosphere, solar wind, plasma, interplanetary magnetic field and magnetosphere, as well as solar activity proxies and energetic particle fluxes. The study includes a frequency-time domain analysis of the original signals, as well as a number of derived

parameters calculated using a framework for the analysis of spatio-temporal characteristics.

The collected dataset included data from January 1, 1986 to January 1, 2024, in 1-hour increments. It included data from various satellites as well as data from ground stations. The data was extracted from the OMNIWeb service, developed by SPDF NASA Goddard Space Flight Center. The OMNIWeb service provides aggregated information on solar wind, plasma, ionospheric indices and particle fluxes from various sources, a full list of data sources is presented on the service's web page.

The set of parameters for which calculations and further research were carried out included: F10.7 (sfu = 10-22W m-2 Hz-1) - solar radio flux at 10.7 cm (2800 MHz), AP (nT) - average level for geomagnetic activity, Dst (nT) - Disturbance Storm Time, Scalar B (nT) - Interplanetary Magnetic Field (IMF) B value, SW Plasma Temperature (K), SW Proton Density (N/cm3), SW Plasma Speed (km/s), PCN - Polar Cap index at Northern Pole, Proton fluxes at >1 MeV, >2 MeV, >4 MeV, >10 MeV, >30 MeV, >60 MeV (1/(cm**2-sec-ster)), SSN - sunspot number, Plasma Beta, E_y (mV/m) - y component of the electric field, Flow pressure (nPa).

Since the parameters considered in this study were measured at different periods of time, with different instrument, and under different conditions, some in Earth orbit and some on the surface, time alignment and normalization procedures were applied to them. These procedures were carried out by the data provider OMNIWeb. The full description is provided by the OMNIWeb developers, therefore, we will only highlight the most relevant excerpts here. For the instruments orbiting the Moon, the IMF and plasma observations are usually collected within 15 minutes upstream of the magnetosphere, and for the most instruments this time is within several minutes. In contrast, the ISEE 3, Wind, and ACE spacecraft are often positioned about an hour upstream. Since their data is to be integrated with the data from spacecraft much closer to Earth, such as IMP 8, it is necessary to apply a time shift to the hour-upstream data at a higher resolution considering the expected arrival time at Earth. In this paper hourly-averaged data is used, some instruments provide data with much higher resolution, so time shifts and normalization were applied before averaging. The performed adjustment utilizes the known positions of these spacecraft along with observed solar wind flow speeds from the datasets being modified. The data obtained by spacecraft in geocentric and Lagrange point L1 orbits have been compared and cross-normalized by the data provider.

The coordinates and trajectories of celestial objects were calculated using the NASA Navigation and Ancillary Information Facility (NAIF) SPICE Toolkit implementation for MATLAB (MICE). The following files were used as a kernel: the leap seconds file *naif0012.tls*, the ephemerides file *de440t.bsp*, and the orientations file *pck00011.tpc*.

To carry out the calculations, the Galactic Inertial Reference Frame was used, with an observer point located at the position of the Sun (heliocentric). The galactic north pole is at RA = 12h 51.4m, Dec = +27°07' (2000.0), the galactic center at RA = 17h 45.6m, Dec = -28°56' (2000.0). The inclination of the galactic equator to Earth's equator is 63°. In the chosen coordinate system, we calculate the vectors

that characterize the movement of the Earth relative to the Sun over a year $\overline{PV_A}(t)$, over six months $\overline{PV_{SA}}(t)$, and over an hour $\overline{PV_H}(t)$:

$$\overline{PV_A}(t) = Pos_{Earth}(t + shift_A) - Pos_{Earth}(t), \tag{6.1}$$

$$\overline{PV_{SA}}(t) = Pos_{Earth}(t + shift_{SA}) - Pos_{Earth}(t), \tag{6.2}$$

$$\overline{PV_H}(t) = Pos_{Earth}(t + shift_H) - Pos_{Earth}(t). \tag{6.3}$$

The calculated vectors are normalized $\overline{nPV_A}(t) = \overline{PV_A}(t)/\left|\overline{PV_A}(t)\right|$, $\overline{nPV_{SA}}(t) = \overline{PV_{SA}}(t)/\left|\overline{PV_{SA}}(t)\right|$, $\overline{nPV_H}(t) = \overline{PV_H}(t)/\left|\overline{PV_H}(t)\right|$ and used as basis vectors.

We introduce a set of vectors characterizing changes in the chosen parameter p over a specified period of time $shift_s$, in relation to other moments in time using previously calculated basis vectors and forward finite differences $\Delta_s[p](t) = p(t + shift_s) - p(t)$, where s is the index, defining the period:

$$\overline{DV_A}(p, t) = \Delta_A[p](t) \cdot \overline{nPV_A}(t), \tag{6.4}$$

$$\overline{DV_{SA}}(p, t) = \Delta_{SA}[p](t) \cdot \overline{nPV_{SA}}(t), \tag{6.5}$$

$$\overline{DV_H}(p, t) = \Delta_H[p](t) \cdot \overline{nPV_H}(t). \tag{6.6}$$

We will not apply the orthogonalization procedure to the vectors in order to maintain consistent time reference points for events for all three vectors.

Since the chosen coordinate system is heliocentric and the observer point is identical to the Sun position, the spatial coordinates of the Sun in this coordinate system are equal to $(0, 0, 0)$. However, the Sun also moves in time. If we plot the trajectory of the Sun when its spatial coordinates are zero and its time coordinates are changing, we get the trajectory illustrated in Figure 1 as a thick yellow line. Since the planets of the Solar System objects move relative to the Sun in both space and time, they will have helix orbits. Here, the Earth's trajectory is shown as a helix line.

The resulting vector of changes will be calculated as the sum of three vectors, where each vector characterizes the difference for the corresponding periods, along the axis in 4-dimensional space, similar to the gradient vector:

$$\overline{DV}(p, t) = \overline{DV_A}(p, t) + \overline{DV_{SA}}(p, t) + \overline{DV_H}(p, t). \tag{6.7}$$

To analyze the frequency-time characteristics of the original parameters, as well as the calculated vectors, we will use cross wavelet analysis, and after performing the cross-wavelet transform (XWT), we will analyze the wavelet semblance (WS). A wavelet $\psi(x)$ is a time-dependent function, typically an oscillatory process, localized in both frequency and time. Assuming that we have two time-dependent signals $u(t)$ and $v(t)$, we define the cross-wavelet transform as $XWT_\psi^{uv} = CWT_\psi^u\, CWT_\psi^{v*}$, where * denotes the complex conjugate. Then, we will calculate a wavelet phase correlation:

$$WS = \cos(\theta), \; WS \in [-1, 1], \tag{6.8}$$

where $\theta = \tan^{-1}(\Im(XWT_\psi^{uv})/\Re(XWT_\psi^{uv}))$ is the local relative phase.
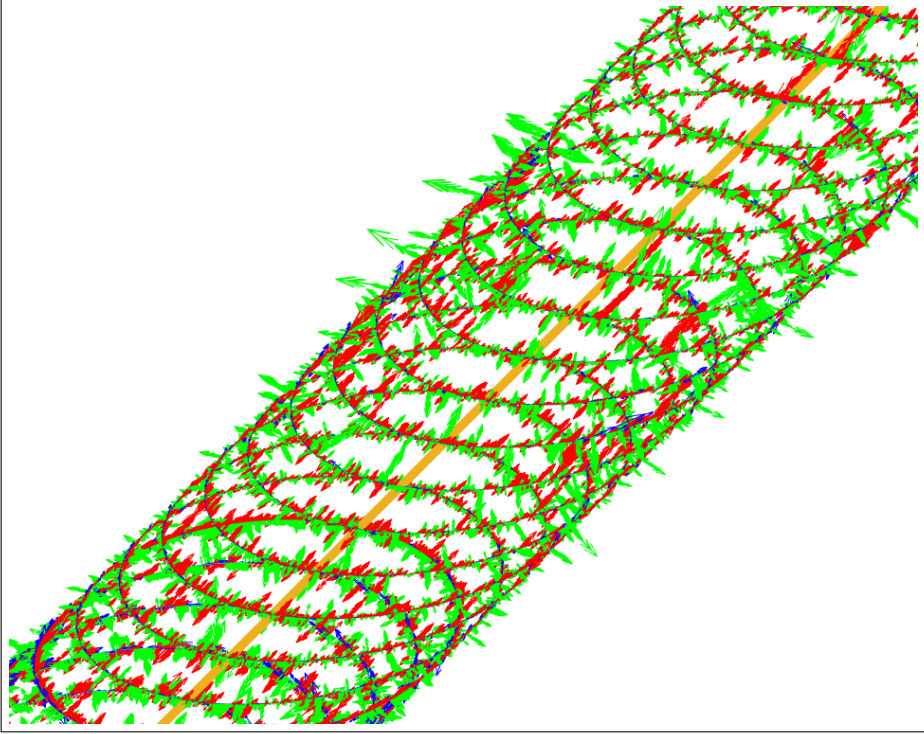
Fig. 6.1: Visualization of vectors $\overline{DV_A}$ (red), $\overline{DV_{SA}}$ (green), $\overline{DV_H}$ (blue), calculated for B parameter, relative to the Earth's orbit.

In this paper, we use the complex Morlet wavelet:

$$\psi(x) = \frac{1}{\sqrt{\pi \cdot fb}} e^{2\pi \cdot i \cdot fc \cdot x} e^{\frac{-x^2}{fb}}. \tag{6.9}$$

Possible phase shifts and periodic dependencies throughout the entire dataset will be considered based on auto-correlation and cross-correlation functions.

6.3   Results and Discussion

A number of selected calculated difference vectors $\overline{DV}$ graphs are presented in the Figure 2. The results are provided in the Galactic coordinate system, with the Sun indicated by a yellow circle. Blue circles, accompanied by numbers, indicate the beginning of each month. The vectors themselves are indicated by colored arrows, a specific parameter is indicated by color within each individual subfigure. Vector lengths are not to scale. For Proton Fluxes, vectors are grouped into distinct clusters, the lengths of vectors outside the clusters being negligibly small compared to vectors within the clusters. The positions of clusters in time between different energy levels are practically identical. The most pronounced clusters are

observed in mid-March, the second half of April - May, mid-July, mid-October - mid-November.

If we compare the vectors for Dst with those for Proton Fluxes, we can see that the vectors with the greatest magnitude for Dst are observed in mid-March, early May, and the period from September to January. The directions of the vectors for these periods are opposite to the directions of the vectors for proton fluxes. Since the Dst index is usually negative, with the lowest values representing the strongest storms, a negative correlation is clearly visible. Similar behavior of vectors, with positive or negative correlation, is observed for most of the parameters considered. It is important to note that although the most pronounced clusters generally coincide, each parameter has unique sets of vectors that are inherent only to it. However, there are a number of exceptions for which most directions are different from those considered earlier, as well as from most other parameters, in particular SW plasma temperature and F10.7.

For the initial parameters, as well as for the obtained difference vectors and their individual projections, auto-correlation functions and cross-correlation functions were calculated. Some of the results are presented in Figures 3, 4. Auto-correlation functions for the initial parameters provided very limited information on the periodicity of the processes, with only annual variations and the 11-year solar cycle clearly visible. While cross-correlation functions revealed a number of phase shifts between different parameters, the dependencies were most clearly visible when calculating the correlation between the projections of the difference vectors, as well as their magnitudes (Figure 4).

The number of phase shift components is very high per plot, and each combination of parameters has its own frequency spectrum, there are most common shifts, not directly related to 11-years solar cycle and annual modulations, that are shared between many parameters. These include approximately: 2 years, 2.55 years, 3 years, 4.5 years, 14 years, 17.15 years, 25 years, most are observed in Figure4a. Although, some pairs produce different patterns: 13.54 years shift in Figure4b; 6.03 years and 6.61 years in Figure4c; 4.89 years, 6.02 years and 17.92 years shifts in Figure 4d, with an approximately 11 years between them (note the sign). Con-

(a)   (b)
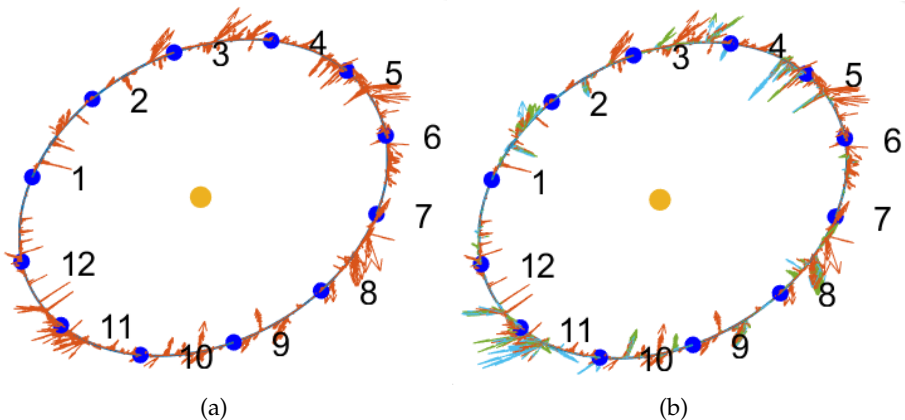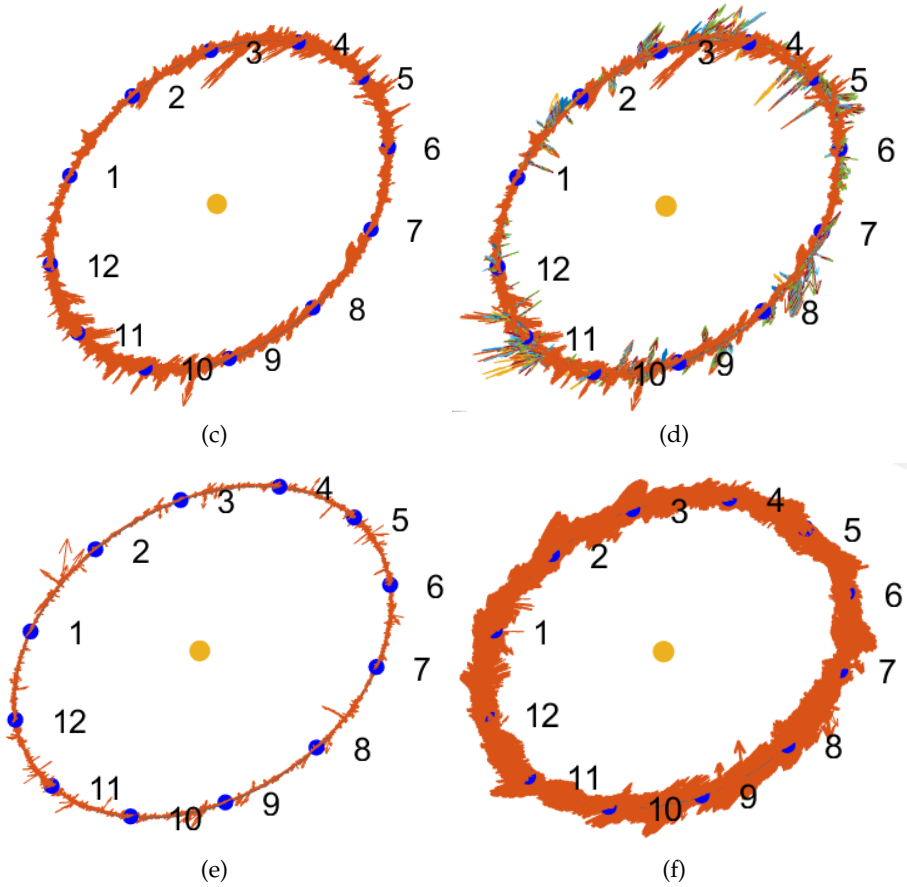
Fig. 6.2: Difference vectors $\overline{DV}$ in relation to the Earth's orbit: Proton Flux >1 MeV (a), Proton Flux >1 MeV [orange], >10 MeV [green], >60 MeV [blue] (b), Dst (c), Dst [orange] and all Proton Fluxes (d), SW Plasma Temperature (e), F10.7 (f).

sidering that all cross-correlations were calculated using zero-padding, the actual correlation is higher.

The dependence of solar radio flux F10.7 on the sunspot number was analyzed using wavelet transform and semblance analysis. This dependence is well studied, and both parameters have an extremely high correlation with each other. At the same time, it is also known about the presence of a phase lag at individual time intervals. The results are provided in Figure 5. Red color represents the semblance close to 1, and blue color represents the semblance close to -1. The figure Figure 5a clearly shows that throughout the entire dataset under consideration, the SSN and F10.7 show an extremely high degree of positive correlation, with the exception of a number of areas shown in blue, where there is a clearly pronounced anti-correlation. There is no obvious periodic pattern, however, the anomalies can be divided into 2 groups by duration. Since there are multiple trends present in the data, we will use the differenced time series and the fact that they are signed, to
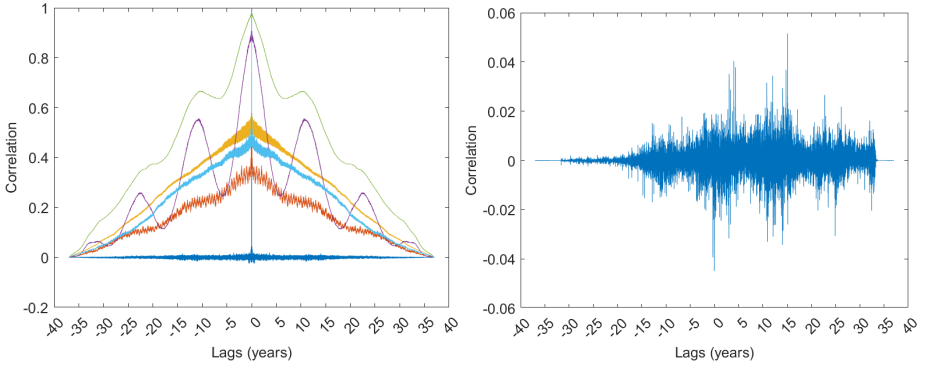
Fig. 6.3: Auto-correlation functions: E_y [blue], Dst [orange], Flow pressure [yellow], SSN [purple], F10.7 [green], SW plasma temperature [light blue] (left); Cross-correlation between E_y and Proton Flux >60 MeV (right).

reduce the effects of possible overlaps and mitigate the random occurrence. By averaging the semblance of the original data with the semblance coefficients of the differenced data, we can improve the resolution and localize the centers of the anomalies with greater accuracy, while simultaneously removing the unstable anomalies, as shown in Figure 5b,c. Figure 5b shows the averaged semblance coefficient when averaging is carried out between the semblance coefficients of the original data and the averaged semblance coefficient of the modulus of the difference vectors without taking into account the sign. Wide areas of medium-low correlation, alternating with wide areas of medium-high correlation, are caused by the ascending and descending trends of solar cycles. When the sign is also taken into account during averaging, we obtain the results shown in Figure 5c. It can be seen that despite the averaging procedures, using differenced time series with varying periods, and eliminating trends, almost all anomalies are still present, their positions have not changed, and the boundaries have become more defined as a result of the above procedures. Although determining the origins of these anomalies is beyond the scope of this study, an interesting observation is that these anomalies are present at frequencies in the expected range for Dark Photon models, within the kinetic mixing parameter limits corresponding to the Earth and Jupiter region [13], and also in the frequency band for certain models of Axion-like particles [10]. However, it is important to note that Figure 5 provides the wavelet frequencies, not the frequencies of the original data.

6.4   Conclusions

In this paper, we investigated parameters characterizing the state of the ionosphere, solar wind, plasma, interplanetary magnetic field and magnetosphere, as well as proxies for solar activity and energetic particle fluxes. The frequency-time analysis was conducted for the original observational data and derived parameters, calcu-lated using a framework for analyzing spatio-temporal characteristics. Calculated
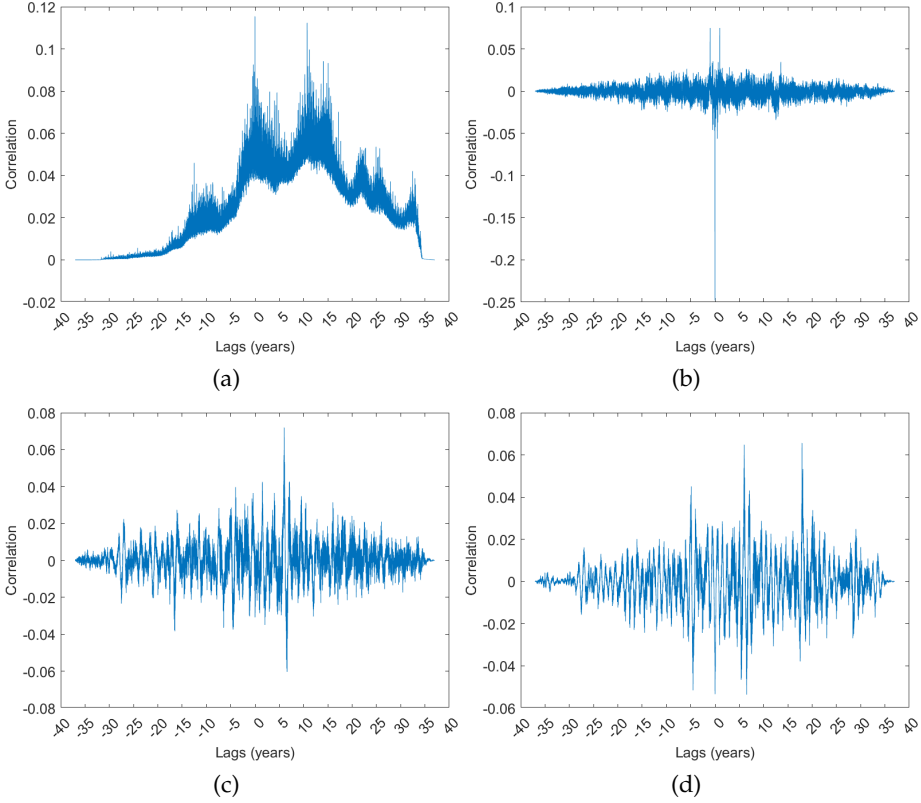
Fig. 6.4: Cross-correlation functions: $\overline{|DV|}_{E_y}$ and $\overline{|DV|}_{Proton\,Flux>60MeV}$ (a), $\overline{DV}_{A,Flow\,Pressure}$ and $\overline{DV}_{A,Dst}$ (b), $\overline{DV}_{A,SW\,Proton\,Density}$ and $\overline{DV}_{A,F10.7}$ (c), $\overline{DV}_{A,Plasma\,Beta}$ and $\overline{DV}_{A,F10.7}$ (d).

difference vectors had clearly defined directions that are not determined by the Sun at certain time intervals, and were consistent between different parameters. Some parameters provide specific vectors that are unique to them while still being consistent to most of the data. Time delay components unrelated to the 11-year solar cycle are observed in the cross-correlation functions for the differenced data, but are absent or difficult to detect in the cross-correlation functions for the original data, and are not present in the auto-correlation functions. A number of localized anomalies were identified in the relationship of F10.7 with SSN, which are observed in the frequency band expected for a Dark Photon and some models of Axion-like particles. It is shown that these anomalies are not due to the solar cycle, as well as annual, semi-annual and hourly variations. It is planned to analyze the identified anomalies with higher resolution and using an extended set of wavelet types.
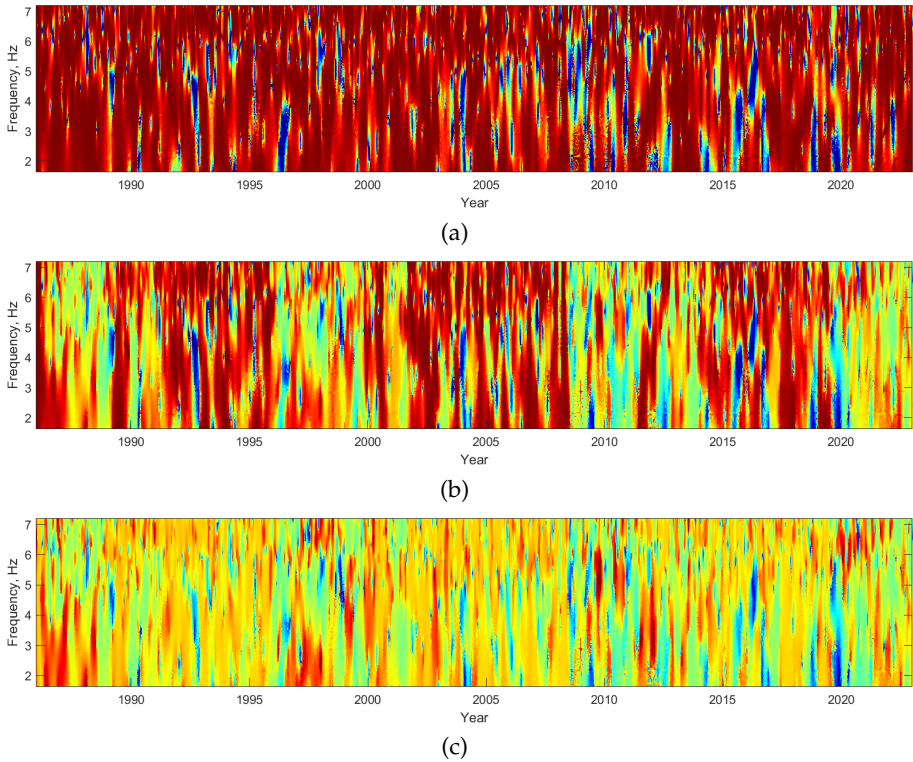
Fig. 6.5: Wavelet semblance for SSN and F10.7: $WS(SSN, F10.7)$ (a), averaged $WS(SSN, F10.7)$ and $WS(SSN, \overline{|DV|}_{F10.7})$, $WS(SSN, \overline{|DV|}_{s,F10.7})$ (b), averaged $WS(SSN, F10.7)$ and $WS(SSN, \overline{|DV|}_{F10.7})$, $WS(SSN, \text{sign} \cdot \overline{|DV|}_{F10.7})$ (c).

Acknowledgements

References

1. M.Khlopov: What comes after the Standard model, Progress in Particle and Nuclear Physics **116** (2021) 103824.
2. K. Zioutas, M. Maroudas, A. Kosovichev: On the origin of the rhythmic Sun's radius variation, Physics, arXiv:2202.04447 [physics.gen-ph] (2022).
3. K. Zioutas et al.: Stratospheric temperature anomalies as imprints from the dark Universe, Phys. Dark Univ. **28**, 100497, arXiv:2004.11006 [astroph. EP] (2020).
4. K. Zioutas et al.: Atmospheric Temperature anomalies as manifestation of the dark Universe, Astrophysics, arXiv:2309.10779 [astro-ph.EP] (2023).

5. A. Zhitnitsky: Mysterious anomalies in Earth's atmosphere and strongly interacting Dark Matter, High Energy Physics - Phenomenology, arXiv:2405.04635 [hep-ph] (2024).

6. A. Kryemadhi et al.: Gravitational focusing effects on streaming dark matter as a new detection concept, Astrophysics, arXiv:2210.07367 [astro-ph.IM] (2023).

7. M. Fedderke et al.: Earth as a transducer for dark-photon dark-matter detection, High Energy Physics - Phenomenology, arXiv:2106.00022 [hep-ph] (2021).

8. C. Beadle, A. Caputo, S. Ellis: Resonant Conversion of Wave Dark Matter in the Ionosphere, High Energy Physics - Phenomenology, arxiv:2405.13882 [hep-ph] (2024).

9. I. Bloch, S. Kalia: Curl up with a good B: Detecting ultralight dark matter with differential magnetometry, High Energy Physics - Phenomenology, arXiv:2308.10931v2 [hep-ph] (2024).

10. I. Sulai et al.: A Hunt for Magnetic Signatures of Hidden-Photon and Axion Dark Matter in the Wilderness, High Energy Physics - Phenomenology, arxiv:2306.11575 [hep-ph] (2023).

11. J. VanDevender et al.: Limits on Magnetized Quark-Nugget Dark Matter from Episodic Natural Events, High Energy Physics - Phenomenology, arXiv:2104.12312 [hep-ph] (2021).

12. Y. Bai, S. Lu, N. Orlofsky: Searching for Magnetic Monopoles with Earth's Magnetic Field, High Energy Physics - Phenomenology, arXiv:2103.06286v1 [hep-ph] (2021).

13. A. Caputo, A. Millar, C. O'Hare, E. Vitagliano: Dark photon limits: a handbook, High Energy Physics - Phenomenology, arXiv:2105.04565 [hep-ph] (2021).

7 Open questions of BSM Cosmology

M.Yu. Khlopov[1,2,3] ⋆⋆

[1] Virtual Institute of Astroparticle Physics, 75018 Paris, France
[2] Center for Cosmoparticle physics "Cosmion" and
National Research Nuclear University MEPhI, 115409 Moscow, Russia
[3] Research Institute of Physics, Southern Federal University,
Stachki 194, Rostov on Don 344090, Russia

Abstract. BSM physics, on which the now standard inflationary cosmology with baryosynthesis and dark matter/energy is based, inevitably leads to cosmological scenarios beyond this standard model, involving specific model dependent choice of models and parameters of BSM physics. Such model dependent cosmological predictions may have already found confirmations in the positive results of direct dark matter searches by DAMA/NaI and DAMA/LIBRA experiments, interpretation of the results of Gravitational Wave experiments in terms of Primordial Black Hole merging, observation of Stochastic Gravitational Wave background by Pulsar Timing Arrays, indications of early galaxy formation in the observations of James Webb Space Telescope and searches for cosmic antihelium in the AMS02 experiment. We discuss the open questions in studies of these signatures of BSM cosmology.

Povzetek Standardni kozmološki model, na katerem temelji zdajšnja standardna inflacijska kozmologija z barionsintezo in temno snovjo ter temno energijo, vodi v nove kozmološke scenarije, ki presegajo ta standardni model. Novi scenariji vključujejo specifične, od modela odvisne parametre, ki pa so morda že naššli potrditve v novih merjenjih; v neposrednih merjenjih temne snovi z eksperimentoma DAMA/NaI in DAMA/LIBRA; v interpretaciji rezultatov merjenj gravitacijskih valov (gre za scenarij združitve primordijalnih črnih lukenj, za opazovanje stohastičnega ozadja gravitacijskih valov z mrežami za merjenje delovanja pulzarjev, za indikacije o zgodnji tvorbi galaksij pri opazovanjih vesoljskega teleskopa James Webb ter pri iskanju kozmičnega antihelija z eksperimentom AMS02). Prispevek razpravlja o odprtih vprašanjih signalov, ki zahtevajo nov model BSM, ki bo pojasnil odprta vprašanja.

7.1 Introduction

The now Standard cosmology involves inflation, baryosynthesis and dark matter/energy [1–3, 3–5, 7–9]. These necessary elements of the modern cosmological paradigm imply physics Beyond the Standard Model (BSM) of fundamental interactions. To probe this physics its model dependent cosmological consequences can be used as cosmological messengers [10–12]. Such messengers lead to deviations from the standard ΛCDM cosmology. Observational evidence for such messengers

---

⋆⋆ khlopov@sfedu.ru

would remove the conspiracy of the deviations from the standard cosmology [13]. Positive hints to such deviations need more detailed analysis of the open questions on physical basis and observable features of the corresponding BSM messengers. Here we discuss the open problems of the analysis of these hints presented at the XXVII Bled Workshop "What comes beyond the Standard models?".

If model dependent messengers of BSM physics are confirmed, it would strongly reduce the set of BSM models and their parameters. Therefore, any approach to the unified description of Nature [14, 15] should inevitably include together with physical basis for inflation, baryosynthesis and dark matter also BSM cosmological signatures, which find observational support.

We consider open questions of the dark atom interpretation of the results of the direct searches of dark matter (Section 7.2.1). We discuss the Axion Like Particle (ALP) models and the footprints of their physics in stochastic gravitational wave background (SGWB) and favored by James Webb Space Telescope (JWST) early galaxy formation. We consider open problems of ALP physics and cosmology in the scenarios of creation and evolution the primordial objects of macroscopic antimatter in our Galaxy, specifying their role as possible sources of antihelium component of cosmic rays (Section 7.3). In the conclusive Section 7.4 we put the signatures and significance of the discussed messengers of BSM physics and cosmology in the context of cosmoparticle physics.

7.2   Open problems of dark matter physics and cosmology

During the last few decades the mainstream of dark matter studies was stimulated by the miracle of Weakly Interacting Massive particles (WIMPs) explaining the cosmological dark matter. Indeed, the frozen out amount of particles with mass in the hundred GeV range with annihilation cross section of the order of ordinary weak interaction could naturally explain the observed dark matter by their predicted contribution into the cosmological density. Theoretical basis for WIMP studies was found in supersymmetry (SUSY), which could naturally predict neutral WIMP-like candidate as stable lightest SUSY particle. It put experimental direct WIMP searches in the correspondence with the search for SUSY particles at the LHC. However, SUSY particles were not detected at the LHC in the hundred GeV range. This lack of positive evidence for SUSY particles can indicate very high energy SUSY scale [16]. Then SUSY cannot be used to solve the internal problems of the Standard model (the divergence of Higgs boson mass and the origin of the energy scale of the electroweak symmetry breaking). It implies a non-SUSY solution of these problems. It inevitably draws attention to non-WIMP candidates for dark matter, originated from non-SUSY physical basis.

7.2.1   Dark atom probe in direct dark matter searches

The results of the underground direct dark matter search look controversial. Positive results of DAMA/NaI and DAMA/LIBRA experiments are presented with increasingly high statistics [17]. It seems to be in sharp contradiction with negative

results of other groups (see [1] for review and references). However, the strategy of most of these groups is aimed to the WIMP search. Though the results of DAMA/NaI and DAMA/LIBRA experiments, taken separately admit their WIMP interpretation [17], confrontation with publications of other groups strongly favors non-WIMP interpretation of these positive results and appeals to consider them as the experimental evidence for dark atom nature of dark matter [1, 12, 18, 19].

The dark atom hypothesis assumes existence of stable particles with negative even electric charge $-2n$. Such particles should be generated in excess over their antiparticles and bind with n primordial helium-4 nuclei, created in Big Bang Nucleosynthesis, in neutral nuclear interacting atom like states.

Multiple charged stable states can be related with the composite nature of Higgs boson. If Higgs boson constituents are charged, their composite multiple charged states can exist. By construction Higgs boson constituents possess electroweak charges. It can not only provide prediction of stable $-2n$ charged particles, but also can give rise to their excess over positively charged antiparticles owing to electroweak sphaleron transitions, which balance this excess with baryon asymmetry. Such balance takes place in Walking Technicolor model (WTC) and the excess of $-2n$ charged particles as the constituents of dark atoms determines the relationship between dark matter density in the form of dark atoms and baryon density. The only parameter of dark atom model is the mass of the stable $-2n$ charged particles. This parameter can be determined under the assumption that dark atoms explain all the observed dark matter density [20–22].

It was shown in [20–22] that the excess of $-2n$ charged particles balanced with baryon excess can be generated in the case of any new particle family, which possess electroweak charges. It makes possible to balance with baryon asymmetry the excess of -2 charged ($\bar{U}\bar{U}\bar{U}$) clusters of stable antiquarks $\bar{U}$ with the charge $-2/3$. Such a new stable generation is predicted as the 5th generation in the approach [15]. The excess generated by the sphaleron balance depends on the mass of multiple charged particles. It can explain the observed dark matter, if the mass of stable multiple charged particles doesn't exceed few TeV. It puts upper limit on the mass of multiple charged particles, at which dark atoms can explain the observed density of dark matter, and challenges their experimental search at the LHC [21].

The problems of dark atom structure and interaction are more close to the nuclear, than to atomic physics. Instead of small nuclear interacting core covered by large leptonic (electronic) shell, multiple charged lepton-like core of dark atom is closely covered by nuclear interacting helium shell of nuclear size.

The structure of dark atom and its properties tend to a nuclearite (Thomson like atom) – to a specific superheavy neutral nuclear matter species.

Bohr-like OHe atom description can be appropriate only for a double charged particle ($n = 1$) bound with primordial helium nucleus. Even in this case radius of the helium Bohr orbit is nearly equal to the size of this nucleus. The $-2n$ charge particle forms at $n > 1$ Thomson-like XHe atom with n helium nuclei. $-2n$ charged lepton is situated in this atom within an n-α-particle nucleus. It makes XHe dark atoms more close to O-nuclearites [23], in which electric charge of nuclear matter is compensated by negative charge of heavy leptons.

Evolution of these species formed in the period of Big Bang Nucleosynthesis is the open problem of dark atom scenario. XHe atoms are formed in the medium enriched by free helium nuclei and their binding with XHe can lead to production of anomalous isotopes, which is now the object of our thorough investigation. The role of the Bose-Einstein nature of α particles is of particular interest in this investigation.

Negative results of direct WIMP searches find natural qualitative explanation by the Dark atom hypothesis. Dark atom nuclear interaction in the terrestrial matter causes their slowing down, which results in negligible nuclear recoil in the dark atom collisions within underground detectors [1, 12, 18].

Local dark atom concentration is determined at each level of terrestrial matter by the balance between the incoming cosmic flux of dark atoms and their diffusion towards the center of Earth. Such concentration is adjusted to the incoming cosmic flux. At the 1 km depth the equilibrium is maintained at the timescale of less than 1 hour. Since the incoming flux possess annual modulations due to the Earth's orbital motion around the Sun, the dark atom concentration experiences annual modulation within the matter of the underground detector. If dark atoms can form low energy (few keV) bound states with nuclei of detector, the energy release in such binding should possess annual modulation. It can explain the signal, detected in DAMA/NaI and DAMA/LIBRA experiments, assuming that the dark atom number density in the detector is adjusted to the incoming flux, that there is a 3 keV bound state of dark atom with sodium nucleus and that the rate of radiative capture to this bound state is determined by the E1 transition with the account for isospin symmetry breaking factor (given by the ratio of the neutron and proton mass difference to the nucleon mass). Under these assumptions the results of DAMA/NaI and DAMA/LIBRA can be explained and it challenges the analysis of these experimental data [17] in the framework of the dark atom hypothesis.

The basic open problem of the dark atom hypothesis is related to the proper quantum-mechanical description of the nuclear interaction of dark atoms. In the lack of small parameters, used in the ordinary atomic physics, the numerical methods of continuous approach to the description of three body problem of dark atom constituents+nucleus were developed [24]. These methods were elaborated for interaction of nuclei with both Bohr-like and Thomson-like dark atoms [25, 26] (see [22] for recent review and references). Development of the proper quantum mechanical description of dark atom interaction with nuclei is necessary for analysis of dark atom formation of anomalous isotopes after BBN, of effects of dark atom capture by stars and effects in stellar nucleosynthesis, as well as for the proof of dark atom interpretation of DAMA/NaI and DAMA/LIBRA results.

7.2.2   Dark Matter in Axion-Like Particle Models

Axion-Like Particle (ALP) models go far beyond the original axion models and their relationship with the Peccei-Quinn solution for the problem of strong CP violation in QCD. ALP can be reduced to a simple model of a complex pseudo-Nambu-Goldstone field

$$\Psi = \psi \exp i\theta$$

with broken global $U(1)$ symmetry [1, 11]. The potential $V = V_0 + \delta V$ leads to spontaneous breaking of the $U(1)$ symmetry by the term

$$V_0 = \frac{\lambda}{2}(\Psi^*\Psi - f^2)^2, \tag{7.1}$$

which retains continuous (phase) degeneracy of the ground state

$$\Psi_{vac} = f\exp(i\theta) \tag{7.2}$$

and to manifest breaking of the residual symmetry by the term

$$\delta V(\theta) = \Lambda^4(1 - \cos\theta) \tag{7.3}$$

with $\Lambda \ll f$, leading to a discrete set of degenerated ground states, corresponding to

$$\theta_{vac} = 0, 2\pi, 4\pi, ...$$

In the result of the symmetry breaking by the term (7.3) an ALP field $\phi = f\theta$ is generated with the mass

$$m_\phi = \Lambda^2/f. \tag{7.4}$$

In the axion models the term (7.3) is generated by instanton transitions. In ALP models, it is present in the theory initially. When Hubble parameter decreases down to the value of the ALP mass, given by the Eq. (7.4), $H = m_\phi = \Lambda^2/f$, coherent oscillations of the ALP field start, The ALP field energy density is proportional to θ_i^2, where θ_i is the amplitude of ALP field oscillations, given by the initial local value of the phase, when the oscillation starts.

The ALP field represents the Bose-Einstein condensate of ALP Bose-gas in its ground state. Therefore. in spite of a very small mass, ALP in the condensate are nonrelativistic and, if they dominate at the matter dominated stage, can play the role Cold Dark matter, reproducing the Standard ΛCDM scenario of Large Scale Structure formation. However, ALP physics can lead to strong deviations of the Standard cosmological paradigm and to creation of strong primordial inhomogeneities of different kinds, discussed in the next section 7.3, .

7.3 BSM cosmology from ALP physics

If the first phase transition takes place after reheating, the correlation radius is small and ALP strings are formed. The string network is converted into unstable walls-surrounded by strings structure after the second phase transition. ALP energy density distribution represents the replica of this structure and preserves large scale correlations in the nonhomogeneity of the ALP energy density [1]. Evolution of this primordial inhomogeneity, its role in structure formation and observational signatures of the corresponding scenario are the open questions of this direction of the ALP studies. The question of the relationship of this large scale structure and formation of axion stars [27] is of special interest.

After the first phase transition, if it takes place at the inflationary stage, the phase has a fixed value within the Hubble radius at each e-folding. Quantum fluctuations

lead to variations in phase between disconnected regions. These fluctuations are given by

$$\delta\theta = \frac{H_{infl}}{2\pi f},\tag{7.5}$$

where H_{infl} is Hubble parameter at the inflationary stage [1]. After the second phase transition the local value of phase determines the amplitude $\theta - \theta_{vac}$ of the ALP field oscillations. If at the e-folding, corresponding to the observed part of the Universe, $\theta < \pi \; \theta_{vac} = 0$. In regions, where the fluctuations (7.5) moved the phase at successive steps of inflation to values greater than π, $\theta_{vac} = 2\pi$. At the border of domains with $\theta_{vac} = 2\pi$ and surrounding regions with $\theta_{vac} = 0$ along the closed surfaces with $\theta = \pi$ closed domain walls are formed in the course of the second phase transition.

If the field Ψ interacts with quarks and leptons with nonconservation of the baryon and lepton numbers, decay of the field $f\theta$ generate baryon asymmetry in its motion to the ground state. If $\theta < \pi$, baryon excess is generated, while the antibaryon excess is generated in domains with $\theta > \pi$ (see Fig. 7.1).
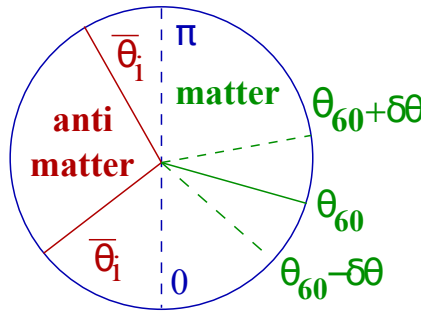
Fig. 7.1: Phase fluctuations at inflationary stage can cross π. It leads to formation of closed domain walls. If the ALP field is unstable relative to decays to quarks and leptons with baryon and lepton number nonconservation, as it is the case in the model of spontaneous baryosynthesis [28], crossing π and 0, results in formation of antibaryon domains in baryon asymmetric Universe [1]

The open question in the scenario with the first phase transition at the inflationary stage is the necessity to suppress large scale fluctuations, excluded by the observed CMB isotropy. One of the possible solution can be a large amplitude ϕ of the complex ALP field (7.2.2) at the stage of inflation, corresponding to the modern horizon, and its decrease down to the broken symmetry value f (see Eq.(7.2)) at successive inflationary stages.

7.3.1   PBH, SGWB and JWST signatures of ALP physics

Inflation provides homogeneous and isotropic initial conditions for evolution of causally disconnected regions within the observed cosmological horizon. However,

such evolution can lead to qualitative difference of conditions in different regions. Formation of closed domain walls, related with the difference in the ground states of the ALP field gives several examples of such kind. Pending on the two fundamental scales of the ALP physics, f and Λ it can lead to three possibilities. The interval of mass M of domain walls, collapsing in primordial black holes (PBH) [16, 29], is given by

$$M_{min} = f \left(\frac{m_{Pl}}{\Lambda} \right)^2 \leq M \leq M_{max} = f \left(\frac{m_{Pl}}{f} \right)^2 \left(\frac{m_{Pl}}{\Lambda} \right)^2. \quad (7.6)$$

Here the minimal mass M_{min} is determined by the condition that the gravitational radius of wall $r_g = 2M/m_{Pl}^2$ exceeds the width of wall $d \sim f/\Lambda^2$. The maximal mass corresponds to the condition that the wall as a whole enters horizon before it starts to dominate within it. Small walls with mass $M < M_{min}$ form oscillons, while large walls with mass $M > M_{max}$ separate the region of their dominance from the other part of the Universe,
At the appropriate value of f and Λ the ALP mechanisms can provide formation of PBHs with stellar mass, and even larger, up to the values corresponding to the seeds for Super Massive Black Holes in Active Galactic nuclei (AGN) [30–32]. Their mass can easily exceed the limit of pair instability and the LIGO/VIRGO detected gravitational wave signal from coalescence of black holes with masses $M > 50M_{\odot}$ naturally puts forward the question on their primordial origin [33, 34]. One can consider recent discovery of Stochastic Gravitational Wave Background (SGWB) by Pulsar Timing Arrays (PTA) [35] as another evidence of ALP physics. Large closed domain walls with mass $M > M_{max}$ separate the region of their dominance from the surrounding Universe. Formation of these walls is accompanied by gravitational wave background radiation, which can reproduce the PTA data [36]. In the ALP model, the contour of the future domain wall is created, when the phase crosses π. The values of phase at the stages of inflation, preceding the this crossing, approach to π. In the result the ALP energy density in the regions surrounding future domain wall is much larger, than the average one for the ALP field. Therefore, when the wall separates from the other part of the Universe the region, where it dominates, the ALP density in the surrounding regions is much higher than the average in the Universe and the galaxy formation in these regions can take place much earlier, than in the rest of the Universe and can happen at the redshifts $z > 10$, as indicated by the data of JWST [37]. In that way ALP physics can simultaneously explain the PTA and JWST data [38]. The open questions in this scenario are generation of GW background from the domain walls and evolution of the regions of the enhanced ALP density. In particular, the question is of special interest whether black hole formation is possible in their central part, or the enhanced ALP density itself plays the role of AGN seeds in the early galaxies. Evolution of wall dominated regions is also of special interest. Their appearance in the Lemaitre-Friedman-Robertson-Walker Universe, supported by inflational scenario, is the effect of fluctuations at the inflationary stage, resulted in the strong deviation of some regions from isotropy and homogeneity. The influence of such regions on the evolution of surrounding regions needs special study.

7.3.2   Antimatter domains in baryon asymmetric Universe

Baryon asymmetry of the Universe reflects the absence in the observed Universe of macroscopic antimatter in the amount comparable with the amount of baryonic matter. In the now standard cosmological paradigm baryon asymmetry is related to baryosynthesis, in which baryon excess is created in very early Universe. If baryosynthesis is inhomogeneous, in the extreme case the sign of the baryon excess can change, giving rise to antimatter domains, produced in the same process, in which the baryon asymmetry is created [28, 39–43]. Such antimatter domains are surrounded by matter. They should be sufficiently large to survive to the present time and to give rise to antimatter objects in the Galaxy. It implies also effect of inflation in addition to nonhomogeneous baryosynthesis. Such combination of inflation and nonhomogeneous baryosynthesis can take place in the ALP model of spontaneous baryosynthesis [28] at the specific choice of its parameters.

This choice determines the properties of antimatter domains, their evolution and the forms of celestial antimatter objects in baryon asymmetrical Universe. The minimal mass of the surviving domain is determined by its annihilation with the surrounding matter. The upper limit on the possible amount of antimatter in our Galaxy follows from the observed gamma background [43, 44]. These limits give the interval of mass M of antimatter in our Galaxy

$$10^3 M_\odot \leq M \leq 10^5 M_\odot, \tag{7.7}$$

which is typical for globular clusters. Symmetry of electromagnetic and nuclear interactions of matter and antimatter would make celestial antimatter objects looking like matter ones. Globular clusters are situated in the halo of our Galaxy, where matter gas density is low. It seemed to favor the hypothesis of antimatter globular cluster in our Galaxy, which may be rather faint gamma source. If antibaryon density is much higher, than the baryonic density, specific ultra-dense antibaryon stars can be formed [45],

Therefore, studies of possible forms of macroscopic antimatter objects in our Galaxy are challenging, involving evolution of antibaryon domains in baryon asymmetrical universe [46, 47] in the context of models of nonhomogeneous baryosynthesis.

The idea of antimatter globular cluster inspired to look for an appropriate galactic Globular cluster as its possible prototype. The observed properties of the M4 globular cluster were used for this purpose [48], but such approach implies strong correction. Indeed, chemical evolution within the isolated antimatter domain cannot be the same as that for the ordinary matter. At rather wide range of antibaryon density one can expect that primordial nucleosynthesis in the domain should lead to production of primordial antihelium. However, products of anti-stellar nucleosynthesis can neither come to the domain from other parts of the Galaxy, nor remain in domain being produced by antimatter stars within it. It makes highly improbable enrichment of antimatter object by metallicity, while all the observed galactic globular clusters don't have metallicity below the Solar one. It demonstrates strong mixture of products of stellar nucleosynthesis over the Galaxy, which is not possible for the chemical evolution of antimatter within the isolated region of antibaryon domain.

Primordial metallicity can be produced in domains with high antibaryon density. In the context of spontaneous baryosynthesis based on ALP physics such high density antibaryon domains can correspond to crossing π. It should be accompanied by massive domain walls at their border. Such walls with the mass

$$M > M_{max} = f\left(\frac{m_{Pl}}{f}\right)^2 \left(\frac{m_{Pl}}{\Lambda}\right)^2 = \left(\frac{m_{Pl}}{f}\right)^2 M_{min}$$

would dominate in the corresponding region, separating it from the rest of the Universe. In such scenario only domains surrounded by walls with $M < M_{max}$ can leave the antibaryon domain observable. It puts an open question, whether such domains are sufficiently large to survive in the matter surrounding and what is the result of the domain wall evolution.

The sensitivity of AMS02 experiment is far below the predicted flux of cosmic antihelium from astrophysical sources [49]. Since 2017 a suspected antihelium-4 event is demonstrated at seminars, but remains unpublished. The unprecedented sensitivity of AMS02 experiment makes the collaboration especially responsible for publication of its results. That is why all the possible background interpretation of such candidates should be checked before the discovery of cosmic antihelium-4 is announced.

In any case to confront AMS02 searches the prediction for composition and spectrum of cosmic antinuclei from antimatter objects in our Galaxy should be made. Such prediction inevitably involves the account for propagation of antinuclei in galactic magnetic fields [50] as well as for the inelastic processes in such propagation.

7.4   Conclusions

The results of DAMA experiments, LIGO-VIRGO-KAGRA, PTA and JWST data, possible existence of antihelium component of cosmic rays increase the hints to new physics phenomena. Their confirmation will manifest deviations from the standard cosmological model. BSM cosmology, involving Warmer-than-Cold dark matter scenario of nuclear interacting dark atoms of dark matter, or primordial strong nonhomogeneities of energy and/or baryon density, can give rise to new scenarios of galaxy formation and evolution. We have outlined here the open questions in the proposed BSM models and scenarios. Answers to these questions need special studies and will deserve discussion at future Bled Workshops.

In the context of cosmoparticle physics, confirmation of the existence of cosmological messengers of new physics would provide a sensitive probe for BSM cosmology and for specific choice of BSM models and their parameters, on which the BSM scenario is based. In this case only such models, which predict the detected deviations from the standard cosmological paradigm can pretend to be realistic. The hints to the cosmological messengers of BSM physics may appeal to reanalysis of the observational constraints and interpretation of the edges of such constraints in the terms of the BSM cosmology. The observed accelerated expansion of the modern Universe may challenge our paradigm of UNIverse, putting us into a baby universe separated from the mother multiverse and appealing to development of special methods to study such cosmology.

Acknowledgements

References

1. M.Khlopov: What comes after the Standard model? Progress in Particle and Nuclear Physics **116** (2021) 103824.
2. A.D. Linde: *Particle Physics and Inflationary Cosmology*, Harwood, Chur, 1990.
3. E.W. Kolb and M.S. Turner: *The Early Universe*, Addison-Wesley, Boston, MA,USA, 1990.
4. D.S. Gorbunov and V.A. Rubakov: *Introduction to the Theory of the Early Universe Hot Big Bang Theory. Cosmological Perturbations and Inflationary Theory*, World Scientific, Singapore, 2011.
5. D.S. Gorbunov and V.A. Rubakov: *Introduction to the Theory of the Early Universe Hot Big Bang Theory*, World Scientific, Singapore, 2011.
6. M.Y. Khlopov: *Cosmoparticle Physics*, World Scientific, Singapore, 1999.
7. M.Y. Khlopov: *Fundamentals of Cosmoparticle Physics*, CISP-Springer, Cambridge, UK: 2012.
8. M. Khlopov: Cosmological Reflection of Particle Symmetry, Symmetry **8** (2016) 81.
9. M. Khlopov: Fundamental particle structure in the cosmological dark matter, Int. J. Mod. Phys. A **28** (2013) 1330042.
10. M.Khlopov: BSM Cosmology from BSM Physics. Bled Workshops in Physics. **22** (2021) 153-160.
11. M.Khlopov: Physics and Cosmology Beyond the Standard Models. Physics of Particles and Nuclei **54** (2023) 896–901.
12. M.Khlopov: Multimessenger Probes for New Physics in Light of A. Sakharov's Legacy in Cosmoparticle Physics. Universe **7** (2021) 222.
13. M.Yu. Khlopov: Removing the conspiracy of BSM physics and BSM cosmology, Int. J. Mod. Phys. D **28** (2019) 1941012.
14. N.S. Mankoc-Borstnik: Unification of spins and charges in Grassmann space? Mod. Phys. Lett.A **10** (1995) 587-596.
15. N.S. Mankoc-Borstnik: Achievements of spin-charge family theory so far. Bled Workshops in Physics. **22** (2021) 202–232.
16. S.V. Ketov, M.Yu. Khlopov: Cosmological Probes of Supersymmetric Field Theory Models at Superhigh Energy Scales, Symmetry **11** (2019) 511.
17. R.Bernabei, et al: Recent efforts in the DAMA project. Bled Workshops in Physics. **24** (2023), This issue.
18. M. Y. Khlopov: Composite dark matter from 4th generation, JETP Letters **83** (2006) 1 –4.
19. V. Beylin, M. Khlopov, V .Kuksa, N. Volchaanskiy: New physics of strong interaction and Dark Universe, Universe **6** (2020) 196.
20. A.Chaudhuri, M.Khlopov: Balancing asymmetric dark matter with baryon asymmetry and dilution of frozen dark matter by sphaleron transition. Universe **7** (2021) 275.
21. V.A.Beylin, M.Yu.Khlopov, D.O. Sopin: Balancing multiple charge particle excesses with baryon asymmetry. International Journal of Modern Physics D (2023) 2340005.
22. V.A. Beylin, T.E. Bikbaev, M.Y. Khlopov, A.G. Mayorov, D.O. Sopin: Dark Atoms of Nuclear Interacting Dark Matter. Universe **10** (2024) 368.
23. V. A. Gani, M.Yu.Khlopov and D. N. Voskresensky: Double charged heavy constituents of dark atoms and superheavy nuclear objects. Phys. Rev. **D99** (2019) 015024.

24. T.E. Bikbaev, M.Yu. Khlopov, A.G. Mayorov: Numerical simulation of dark atom interaction with nuclei, Bled Workshops in Physics **21** (2020) 105–117.

25. T.E.Bikbaev, M.Yu.Khlopov and A.G. Mayorov: Numerical simulation of Bohr-like and Thomson-like dark atoms with nuclei. Bled Workshops in Physics **22** (2021) 65–77.

26. T.E.Bikbaev, M.Yu.Khlopov and A.G. Mayorov: Quantum-mechanical numerical model of interaction between dark atom and nucleus of substance. Bled Workshops in Physics. **25** (2024), This issue.

27. I. I. Tkachev: Coherent scalar-field oscillations forming compact astrophysical objects. Sov. Astron. Lett. **12** (1986) 305–308.

28. A.D. Dolgov: Matter and antimatter in the universe, Nucl. Phys. Proc. Suppl. **113** (2002) 40.

29. M.Yu. Khlopov: Primordial black holes, Res. Astron. Astrophys. **10** (2010) 495.

30. S.G. Rubin, A.S. Sakharov, M.Y. Khlopov: Formation of primordial galactic nuclei at phase transitions in the early Universe, JETP **92** (2001) 921.

31. K.M. Belotsky, V.I. Dokuchaev, Y.N. Eroshenko, E.A. Esipova, M.Y. Khlopov, L.A. Khromykh, A.A. Kirillov, V.V. Nikulin, S.G. Rubin, I.V. Svadkovsky: Clusters of primordial black holes, Eur. Phys. J. C **79** (2019) 246.

32. A.D. Dolgov: Massive primordial black holes in contemporary and young universe (old predictions and new data) Int.J.Mod.Phys. A **33** (2018) 1844029.

33. The LIGO Scientific Collaboration; the Virgo Collaboration; R. Abbott *et al*: GW190521: A Binary Black Hole Merger with a Total Mass of 150 M$_\odot$, Phys. Rev. Lett. **125** (2020) 101102.

34. The LIGO Scientific Collaboration; the Virgo Collaboration; R. Abbott *et al*: Properties and astrophysical implications of the 150 Msun binary black hole merger GW190521, Astrophys J. Lett. **900** (2020) L13

35. NANOGrav Collaboration, G. Agazie et al.; The NANOGrav 15-year Data Set: Evidence for a Gravitational-Wave Background, Astrophys J. Lett. **951** (2023) L8.

36. A.S. Sakharov, Y. N. Eroshenko, S. G. Rubin: Looking at the NANOGrav signal through the anthropic window of axionlike particles, Phys. Rev. D **104** (2021) 043005

37. B.E. Robertson, S. Tacchella, B.D. Johnson, K. Hainline, L. Whitler, D.J. Eisenstein, R. Endsley, M. Rieke, D.P. Stark, S. Alberts, et al: Identification and properties of intense star-forming galaxies at redshifts z ¿ 10, Nat. Astron. **7** (2023) 611–621.

38. Shu-Yuan Guo, Maxim Khlopov, Xuewen Liu, Lei Wu, Yongcheng Wu, Bin Zhu: Footprints of Axion-Like Particle in Pulsar Timing Array Data and JWST Observations. SCIENCE CHINA Physics, Mechanics & Astronomy. **67** (2024) 111011

39. V.M. Chechetkin, M.Yu. Khlopov, M.G. Sapozhnikov, Y.B. Zeldovich: Astrophysical aspects of antiproton interaction with He (Antimatter in the Universe), Phys. Lett. B **118** (1982) 329.

40. A. Dolgov, J. Silk: Baryon isocurvature fluctuations at small scales and baryonic dark matter, Phys. Rev. D **47** (1993) 4244.

41. A.D. Dolgov, M. Kawasaki, N. Kevlishvili: Inhomogeneous baryogenesis, cosmic antimatter, and dark matter, Nucl. Phys. B **807** (2009) 229.

42. M.Y. Khlopov, S.G. Rubin, A.S. Sakharov: Possible origin of antimatter regions in the baryon dominated Universe, Phys. Rev. D **62** (2000) 083505.

43. K.M. Belotsky, Y.A. Golubkov, M.Y. Khlopov, R.V. Konoplich, A.S. Sakharov: Antihelium flux as a signature for antimatter globular cluster in our Galaxy, Phys. Atom. Nucl. **63** (2000) 233.

44. M.Yu. Khlopov: An antimatter globular cluster in our Galaxy - a probe for the origin of the matter, Gravitation and Cosmology, **4** (1998) 69–72.

45. S.I. Blinnikov, A.D. Dolgov, K.A. Postnov: Antimatter and antistars in the universe and in the Galaxy, Phys. Rev. D **92** (2015) 023516.

46. M.Yu.Khlopov, O.M.Lecian: Analyses of Specific Aspects of the Evolution of Antimatter Globular Clusters Domains. Astronomy Reports, **65** (2021) 967—972
47. M.Khlopov, O.M.Lecian: The Formalism of Milky-Way Antimatter-Domains Evolution. Galaxies, **11** (2023) 50
48. M.Yu. Khlopov, A.O. Kirichenko, A.G. Mayorov: Anihelium flux from antimatter globular cluster, Bled Workshops in Physics, **21** (2020) 118-127.
49. V. Poulin, P. Salati, I. Cholis, M. Kamionkowski, J. Silk: Where do the AMS-02 antihelium events come from? Phys. Rev. D **99** (2019) 023016.
50. A.O.Kirichenko, A.V.Kravtsova, M.Yu.Khlopov and A.G. Mayorov Researching of magnetic cutoff for local sources of charged particles in the halo of the Galaxy. Bled Workshops in Physics, **22** (2021) 171–177.

BLED WORKSHOPS
IN PHYSICS
VOL. 25, NO. 1

Proceedings of the 27th Workshop
What Comes Beyond . . . *(p. 87)*
Bled, Slovenia, July 8–17, 2024

8 Quark mass matrices inspired by a numerical relation

A. Kleppe [**]

SACT, Oslo, Norway

Abstract. In 1981, Yoshio Koide noticed that the square root values of the charged lepton masses satisfy the relation

$$Q = \frac{m_e + m_\mu + m_\tau}{(\sqrt{m_e} + \sqrt{m_\mu} + \sqrt{m_\tau})^2} \approx \frac{2}{3}$$

Inspired by this relation, we introduce tentative mass matrices, using numerical values, and find matrices that display an underlying democratic texture.

Povzetek: Leta 1981 je Yoshio Koide opazil, da mase nabitih leptonov ustrezajo relaciji.
$Q = \frac{m_e + m_\mu + m_\tau}{(\sqrt{m_e} + \sqrt{m_\mu} + \sqrt{m_\tau})^2} \approx \frac{2}{3}$
Avtorica uporabi to relacijo pri iskanju simetrij masnih matrik, za katere pričakuje, da bodo skoraj podobne demokratičnim masnim matrikam.

8.1 Introduction

A numerical relation involving the lepton masses have intrigued people ever since it was published by Yoshio Koide [1] in the beginning of the 1980-ies.
Inspired by this relation, in this article we look for mass matrices with a form that agree with the Koide formula. From initial matrices for the square roots of particle masses, we then derive mass matrices for up- and down quarks, and investigate how the two charge sectors are related.

8.2 The Koide relation

In 1981, using the mass values $m_e = 0.510998946\ MeV$, $m_\mu = 105.6583745\ MeV$, $m_\tau = 1776.86\ MeV$, Yoshio Koide noticed that the square root values of the charged lepton masses satisfy the relation

$$Q = \frac{m_e + m_\mu + m_\tau}{(\sqrt{m_e} + \sqrt{m_\mu} + \sqrt{m_\tau})^2} = 0.6666617 \approx \frac{2}{3} \qquad (8.1)$$

This is tantalizing, since it seems to echo the neat rational quantum numbers, like e.g. the electric charges of the elementary particles. Many attempts have been made

---

[**] astri.kleppe@gmail.com

to interpret the relation (8.1), hoping to squeeze some insight out of it. Denoting the square roots of the lepton masses as

$$m_1 = \sqrt{m_e}$$
$$m_2 = \sqrt{m_\mu}$$
$$m_3 = \sqrt{m_\tau},$$

and taking $T = m_1 + m_2 + m_3$ as a fixed number, we can interpret the set (m_1, m_2, m_3) as a *partition* of this number T, which in principle can be expressed as a sum of any three other numbers, where the extreme cases are $T = A + A + A$ and $T = 0 + 0 + T$. The three partitions can also be perceived as the eigenvalues of $3{\times}3$ matrices, and if we compare the quantity $Q = \text{Trace}(M^2)/(\text{Trace}(M))^2$ for these three cases, we see that

$$Q_{(A,A,A)} = \frac{\text{Trace}(A^2)}{(\text{Trace}(A))^2} = \frac{3A^2}{(3A)^2} = \frac{1}{3}$$
$$Q_{lepton} = \frac{2}{3} \tag{8.2}$$
$$Q_{(0,0,T)} = \frac{\text{Trace}(T^2)}{(0 + 0 + T)^2} = 1,$$

so the partition corresonding to the charged lepton sector lies right between the two extremes (A, A, A) and $(0, 0, T)$, which might be interpreted as the lepton mass spectrum having maximal amount of "structure".
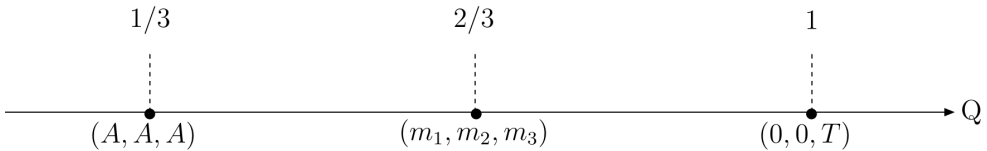
It should be noted that for the square roots of the running charged lepton masses at M_Z around 91 GeV, the results no longer give the exact Koide formula. The relation is however still of interest, because the Koide relation suggests that investigating the square roots of particle masses works as a kind of scale compression. This lessens the overwhelming impact of the largest masses, which tend to make the smallest masses irrelevant.

8.2.1   Matrix invariants

A $3{\times}3$ matrix M has the invariants

$$\text{Trace}(M) = m_1 + m_2 + m_3$$
$$C_2(M) = m_1 m_2 + m_1 m_3 + m_2 m_3 \tag{8.3}$$
$$\text{Det}(M) = m_1 m_2 m_3$$

Now let $\sqrt{M}$ be a matrix whose eigenvalues are the weighted square roots of the lepton masses, $(x_1, x_2, x_3) = (\sqrt{m_e}, \sqrt{m_\mu}, \sqrt{m_\tau})/N$. Defining $N = \text{Trace}(\sqrt{M})/3$, we can express the matrix invariants for the charged leptons as

$$\text{Trace}(\sqrt{M}) = 3N$$
$$C_2(\sqrt{M}) \approx \frac{3}{2}N^2 \qquad (8.4)$$
$$\text{Det}(\sqrt{M}) \approx \frac{N^3}{18}$$

Again comparing the matrix invariants of the observed particle mass spectra, where $m_1 \ll m_2 \ll m_3$, with invariants for the extreme spectra $(0, 0, T)$ and (A, A, A), we get

$$\text{Trace}(0, 0, T) = T, \quad \text{Trace}(A) = 3A$$
$$C_2(0, 0, T) = 0, \qquad C_2(A) = 3A^2$$
$$\text{Det}(0, 0, T) = 0, \qquad \text{Det}(A) = A^3,$$

8.3   Mass states and flavour states

When we talk about mass matrices, it is the form, or texture, of the mass matrices that we are looking for, in the hope to find a clue to the mechanism behind the hierarchical fermion mass spectra.

The mass matrices whose form we want to investigate appear in the mass Lagrangian $\mathcal{L}_{mass} = \bar{\psi}M\psi$. These mass matrices live in the weak basis, meaning that they are not in themselves measurable, but related to the measurable mass eigenstates by unitary rotation matrices U,

$$\mathcal{L}_{mass} = \bar{\psi}M\psi = \bar{\psi}U^\dagger UMU^\dagger U\psi = \bar{\psi}_{phys}D\psi_{phys} \qquad (8.5)$$

where ψ and $\psi_{phys} = U\psi$ denote the flavour states and the physical states, respectively, and $D = \text{diag}(m_1, m_2, m_3)$ is the diagonal mass eigenmatrix containing the masses of the physical particles of a given charge sector.

Our picture that massive up quarks and massive down quarks live in different mass bases, is based on the experimental fact that the Cabbibo-Kobayashi-Maskawa (CKM) mixing matrix V_{CKM} [3] connecting the mass basis of the up-quarks with the mass basis of the down-quarks, deviates from the unit matrix. The mixing matrix appears in the charged current Lagrangian

$$\mathcal{L}_{cc} = -\frac{g}{2\sqrt{2}}\bar{\psi}_L\gamma^\mu V\psi_L' W_\mu + \text{h.c.} \qquad (8.6)$$

where ψ and ψ' are fermion fields with charges Q and $Q - 1$, correspondingly.

It can be argued that flavour states merely exist in our imagination, since they are not directly measurable. This line of thought is however defied by the neutrinos, which as far as we know always appear as flavour states. Neutrino mass states never appear on the scene - in the sense that they never take part in interactions,
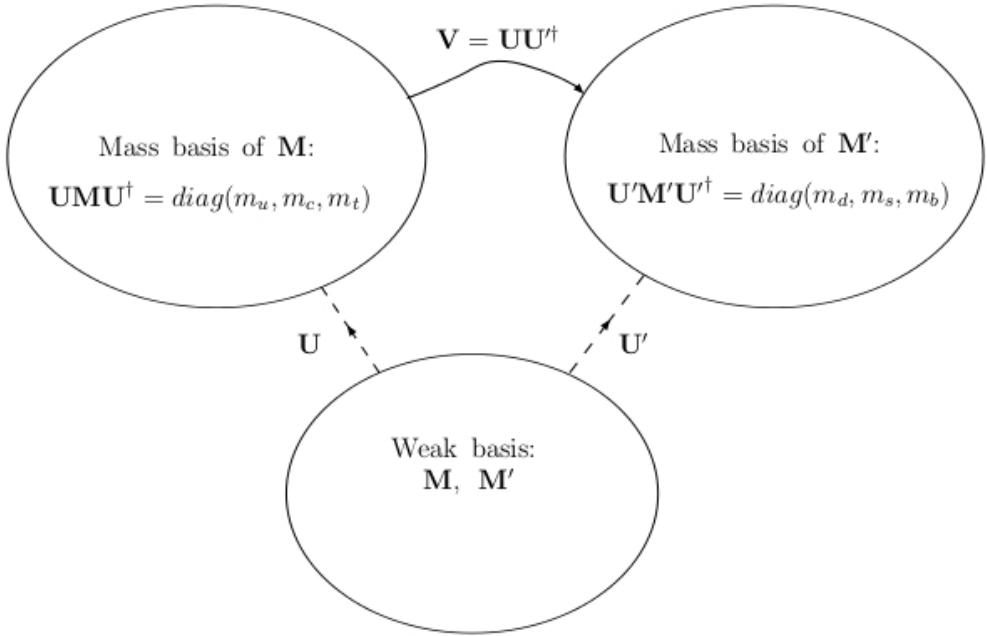
but merely propagate in free space. The observed neutrinos ν_e, ν_μ, ν_τ are flavour states, but we nontheless perceive them as "physical", because they are the only neutrinos that ever appear in interactions, i.e. they are the only neutrinos that we "see".

8.4   Democratic mass matrices

We can perceive (A, A, A) and $(0, 0, T)$ as mass eigenvalues of the unit matrix

$$A \begin{pmatrix} 1 & 0 & 0 \\ 0 & 1 & 0 \\ 0 & 0 & 1 \end{pmatrix}$$

and the democratic matrix

$$\frac{T}{3} \begin{pmatrix} 1 & 1 & 1 \\ 1 & 1 & 1 \\ 1 & 1 & 1 \end{pmatrix},$$

respectively, and the relations (8.2) allow us to guess that a relevant mass matrix for the leptons would be somewhere in between these matrices.

The democratic matrix [4] [5] represents a situation where at a zeroth level, all the particles within a given charge sector have the same Yukawa couplings. The argument for this assumption is that in Standard Model, all fermions get their

masses from the Yukawa couplings by the Higgs mechanism, and since the couplings to the gauge bosons of the strong, weak and electromagnetic interactions are identical for all the fermions in a given charge sector, it seems like a natural assumption that they should also have identical Yukawa couplings.

In the weak basis the democratic matrix M_0 is totally flavour symmetric, in the sense that the (weak) flavours ψ_i of a given charge are indistinguishible ("absolute democracy"). This is contrary to experimental data, but it is reasonable to assume that actual mass matrices that represent physical particles, have some kind of modified democratic texture, since the mass spectrum $(0, 0, 3N)$ of the democratic matrix

$$M_0 = N \begin{pmatrix} 1 & 1 & 1 \\ 1 & 1 & 1 \\ 1 & 1 & 1 \end{pmatrix}$$

reflects the experimental situation with one very heavy and two much lighter fermions. But in order to get correct, non-zero masses, the initial democratic matrix must clearly be modified. A first step towards a more realistic mass spectrum is to introduce an extra parameter while keeping the trace constant, for example like

$$M_1 = N \begin{pmatrix} 1 & 1 & X \\ 1 & 1 & X \\ X & X & 1 \end{pmatrix} \tag{8.7}$$

which has the mass spectrum $N(0, \frac{1}{2}(3 - \sqrt{1 + 8X^2}), \frac{1}{2}(3 + \sqrt{1 + 8X^2}))$. A similar matrix,

$$M_2 = N \begin{pmatrix} 1 & 1 & X \\ 1 & 1 & X \\ X & X & 1 \end{pmatrix} \tag{8.8}$$

has three non-zero eigenvalues, $N(1 - X, 1 - X, 2X + 1)$, but two of them are degenerate.

In order to obtain three physical, non-degenerate, non-zero masses, we introduce yet another parameter, and still keeping the trace constant, we write

$$M_3 = N \begin{pmatrix} 1 & Y & X \\ Y & 1 & X \\ X & X & 1 \end{pmatrix} \tag{8.9}$$

which has the mass spectrum $N(1 - Y, \frac{1}{2}(3 + Y - \sqrt{8X^2 + (Y - 1)^2}), \frac{1}{2}(3 + Y + \sqrt{8X^2 + (Y - 1)^2}))$.

Let us assume that this represents the (square roots of the masses of the) leptons, so $\text{Trace}(\sqrt{M_{\text{lepton}}}) = 3N_{\text{lepton}}$, where $N = 17.716\sqrt{\text{MeV}}$, and X and Y are dimensionless coefficients. The matrix invariants are

$$C_2(\sqrt{M_1}) = N^2(3 - Y^2 - 2X^2) \text{ and } \text{Det}(\sqrt{M_1}) = N^3(1 - Y)(1 + Y - 2X^2),$$

which for $(x_1, x_2, x_3) = (\sqrt{m_e}, \sqrt{m_\mu}, \sqrt{m_\tau})/N$, gives

$$x_1 = (1 - Y)$$
$$x_2 = (2 + Y - \sqrt{Y^2 + 8X^2})/2 \tag{8.10}$$
$$x_3 = (2 + Y + \sqrt{Y^2 + 8X^2})/2,$$

i.e

$$Y = 1 - \sqrt{m_e}/N$$

$$2X^2 = 1 + Y - \frac{\sqrt{m_\mu m_\tau}}{N^2} = 2 - \frac{\sqrt{m_e}}{N} - \frac{\sqrt{m_\mu m_\tau}}{N^2} \tag{8.11}$$

With the lepton mass values $m_e = 0.51099$ MeV, $m_\mu = 105.6584$ MeV, $m_\tau = 1776.86$ MeV, we get the numerical values for the coefficients

$$Y = 0.9597$$

$$X = 0.538$$

Inserting these values into the matrix invariants, we get $C_2(\sqrt{M}) = N^2 \times 1.500027$ and $Det(\sqrt{M_l}) = N^3/17.95$, which is reasonably close to $C_2(\sqrt{M}) = 3N^2/2$ and and $Det(\sqrt{M}) = N^3/18$.

We can add complexity to the matrix, e.g. by multiplication with the matrix

$$\begin{pmatrix} e^{i\alpha} & 0 & 0 \\ 0 & 1 & 0 \\ 0 & 0 & 1 \end{pmatrix}$$

and its conjugate, and obtain the final mass matrix

$$\sqrt{M_l} = N \begin{pmatrix} e^{i\alpha} & 0 & 0 \\ 0 & 1 & 0 \\ 0 & 0 & 1 \end{pmatrix} \begin{pmatrix} 1 & Y & X \\ Y & 1 & X \\ X & X & 1 \end{pmatrix} \begin{pmatrix} e^{-i\alpha} & 0 & 0 \\ 0 & 1 & 0 \\ 0 & 0 & 1 \end{pmatrix} = N \begin{pmatrix} 1 & Ye^{i\alpha} & Xe^{i\alpha} \\ Ye^{-i\alpha} & 1 & X \\ Xe^{-i\alpha} & X & 1 \end{pmatrix} \tag{8.12}$$

8.5   Quarks

The possibility that quarks display a pattern similar to the Koide formula, has of course been examined by many authors [2].

Our approach is to look for relations similar to (8.1) in the quark sector, and use these relations as a basis for new ansätze of the mass matrices of the down- and up-setors, respectively, with the ultimate goal og get a notion of how the mass matrices are related in the weak basis.

Here we use the following mass values for the up- and down sectors [7], [9].

$$m_u(M_z) = 1.24 \text{ MeV}, \ m_c(M_z) = 624 \text{ MeV}, \ m_t(M_z) = 171550 \text{ MeV}$$
$$m_d(M_z) = 2.69 \text{ MeV}, \ m_s(M_z) = 53.8 \text{ MeV}, \ m_b(M_z) = 2850 \text{ MeV} \tag{8.13}$$

and taking the square roots, we get

$$Q_d = \frac{m_d + m_s + m_b}{(\sqrt{m_d} + \sqrt{m_s} + \sqrt{m_b})^2} \approx 3/4$$
$$Q_u = \frac{m_u + m_c + m_t}{(\sqrt{m_u} + \sqrt{m_c} + \sqrt{m_t})^2} \sim 8/9 \tag{8.14}$$

For all the charged fermion sectors, we use the parametrization $Tr(\sqrt{M}) = KN$ where M is a 3×3 matrix, and K is an integer. This gives us

$$Tr(\sqrt{M})_d = 4N$$
$$2C_2(\sqrt{M})_d \approx 4N^2$$
$$Det(\sqrt{M})_d \approx N^3/6 \tag{8.15}$$

and

$$
\begin{aligned}
\text{Tr}(\sqrt{M})_u &= 9N \\
2C_2(\sqrt{M})_u &\sim 9N^2 \\
\text{Det}(\sqrt{M})_u &\sim N^3/10
\end{aligned}
\tag{8.16}
$$

The quark masses are however not as well established as the lepton masses, which in addition are the only ones that satisfy an exact Koide relation.

There are many possible choices for matrices with a given trace. Following the uncertain indications from the mass relations à la Koide, for the square root of the down quark masses we can for example have matrices of the form

$$
\sqrt{M_d} = N_d \begin{pmatrix} 1 & A & B \\ A & 1 & B \\ B & B & 2 \end{pmatrix}, \quad
\sqrt{M_d'} = N_d \begin{pmatrix} 0 & A & B \\ A & 1 & B \\ B & B & 3 \end{pmatrix}, \quad \text{or} \quad
\sqrt{M_d''} = N_d \begin{pmatrix} 0 & A & B \\ A & 0 & B \\ B & B & 4 \end{pmatrix}
$$

where $\text{Trace}(\sqrt{M_d}) = 4N_d$, $N_d = (\sqrt{m_d} + \sqrt{m_s} + \sqrt{m_b})/4 = 15.59\sqrt{\text{MeV}}$, and A and B are dimensionless coefficients. With the democratic form as a guiding line, we choose to study the first matrix. In the case of the up sector, we again follow the indications from the relations for the square root of the up quark masses

$$
\sqrt{M_u} = N_u \begin{pmatrix} 1 & D & E \\ D & 1 & E \\ E & E & 7 \end{pmatrix}, \quad \text{or} \quad
\sqrt{M_u'} = N_u \begin{pmatrix} 2 & D & E \\ D & 2 & E \\ E & E & 5 \end{pmatrix}, \quad \text{or} \quad
\sqrt{M_u''} = N_u \begin{pmatrix} 3 & D & E \\ D & 3 & E \\ E & E & 3 \end{pmatrix}
$$

Our point of departure is a mass matrix for the square roots of the down quark masses, with a nearly democratic texture. Using numerical mass values and a numerical mixing matrix, we derive a matrix for (the square roots of) the up quark masses from our matrix ansatz for the down sector.

With a similar matrix ansatz for the up quarks, we then derive a mass matrix for the down sector. This finally gives us two sets of quark mass matrices, which we study in order to find credible mass matrices for both charge sectors.

8.6   An ansatz for the down quarks

Our initial ansatz is the matrix representing the square roots of the down quark masses,

$$
\sqrt{M_d} = N_d \begin{pmatrix} 1 & A & B \\ A & 1 & B \\ B & B & 2 \end{pmatrix}
\tag{8.17}
$$

where $\text{Trace}(\sqrt{M_d}) = 4N_d$, $N_d = (\sqrt{m_d} + \sqrt{m_s} + \sqrt{m_b})/4 = 15.59\sqrt{\text{MeV}}$, and A and B are dimensionless coefficients. The matrix invariants read

$$
\begin{aligned}
\text{Tr}(\sqrt{M_d}) &= N_d 4 \\
2C_2(\sqrt{M_d}) &= N_d^2(5 - A^2 - 2B^2) \\
\text{Det}(\sqrt{M_d}) &= N_d^3(2 + 2AB^2 - 2A^2 - 2B^2) = 2N_d^3(1 - A)(1 + A - B^2),
\end{aligned}
$$

and the dimensionless eigenvalues read

$$
(x_1, x_2, x_3) = (1 - A, \tfrac{1}{2}(A + 3 - \sqrt{8B^2 + (1 - A)^2}), \tfrac{1}{2}(A + 3 + \sqrt{8B^2 + (1 - A)^2})),
$$

from which we calculate the dimensionless coefficients

$$A = 0.8952$$
$$B = 1.0438$$

The diagonalizing matrix for the matrix (8.17) is

$$U_d = \begin{pmatrix} \frac{1}{\sqrt{2}} & -\frac{1}{\sqrt{2}} & 0 \\ \frac{1}{2}\sqrt{\frac{1-A+S}{S}} & \frac{1}{2}\sqrt{\frac{1-A+S}{S}} & -\frac{2B}{\sqrt{S(1-A+S)}} \\ \frac{1}{2}\sqrt{\frac{A-1+S}{S}} & \frac{1}{2}\sqrt{\frac{A-1+S}{S}} & \frac{2B}{\sqrt{S(A-1+S)}} \end{pmatrix}$$

where $S = \sqrt{8B^2 + (1-A)^2}$.

Using the definition of the weak mixing matrix $V_{CKM} = U_u U_d^\dagger$, together with $U_d^\dagger U_d = 1$, we get

$$U_u = V_{CKM} U_d$$

and using the numerical mixing matrix

$$V_{CKM} = \begin{pmatrix} 0.97373 & 0.2243 & 0.00382 \\ 0.221 & 0.975 & 0.0408 \\ 0.0086 & 0.0415 & 1.014 \end{pmatrix} \tag{8.18}$$

together with the numerical expression of U_d obtained by inserting the numerical values $A = 0.8952$ and $B = 1.0438$, we get a numerical expression for U_u. This allows us to numerically calculate the mass matrix of the up sector.

We are operating at a completely phenomenological level, no theory, just investigating what diagonalization matrix for the up sector that comes together with the diagonalization matrix for the down sector, when we use the ansatz (8.17) for the down sector.

So the diagonal mass matrices for the up quarks and the down quarks, respectively, are tied together by the mixing matrix. The numerical value of the (square root) mass matrix for the up sector is

$$\sqrt{M_u}^{(derived)} = N_u U_u^\dagger \mathrm{diag}(x_1, x_2, x_3) U_u,$$

where $(x_1, x_2, x_3) = (\sqrt{m_u}, \sqrt{m_c}, \sqrt{m_t})/N_u$ and $N_u = (\sqrt{m_u}+\sqrt{m_c}+\sqrt{m_t})/9\sqrt{MeV}$. With the numerical values $(x_1, x_2, x_3) = (0.0299407, 0.508895, 8.46116)\sqrt{MeV}$, the derive the numerical mass matrix for the (square roots) of the up sector,

$$\sqrt{M_u}^{(derived)} = N_u \begin{pmatrix} 2.2142 & 2.0834 & 2.6529 \\ 2.2607 & 2.1377 & 2.4936 \\ 3.0262 & 3.0675 & 4.648 \end{pmatrix},$$

Since $\sqrt{M} = U^\dagger \mathrm{diag}(\sqrt{m_1}, \sqrt{m_2}, \sqrt{m_3})U$, where U and $U^\dagger$ diagonalize $\sqrt{M}$, we get the regular mass matrix $M = (\sqrt{M})^2$:

$$(\sqrt{M})^2 = (U^\dagger \mathrm{diag}(\sqrt{m_1}, \sqrt{m_2}, \sqrt{m_3})U)^2 = U^\dagger \mathrm{diag}(m_1, m_2, m_3)U = M,$$

So the derived mass matrix for the up sector is

$$M_u^{(derived)} = N_u^2 \begin{pmatrix} 17.6407 & 17.204 & 23.3998 \\ 17.3842 & 16.9283 & 22.918 \\ 27.7008 & 27.119 & 37.281 \end{pmatrix} \qquad (8.19)$$

where N_u^2 has dimension MeV.

Inserting numerical values for A and B in the down sector mass matrix (8.17), we get

$$M_d^{(ansatz)} = N_d^2 \begin{pmatrix} 2.8908 & 2.8798 & 4.0657 \\ 2.8798 & 2.8908 & 4.0657 \\ 4.0657 & 4.0657 & 6.179 \end{pmatrix}, \qquad (8.20)$$

and when we rescale $M_u^{(derived)}$, and compare the matrices for both charge sectors,

$$M_u^{(derived)} = 5.97 \times N_u^2 \begin{pmatrix} 2.95 & 2.8798 & 3.92 \\ 2.9 & 2.83 & 3.84 \\ 4.64 & 4.54 & 6.24 \end{pmatrix}, \quad M_d^{(ansatz)} = N_d^2 \begin{pmatrix} 2.8908 & 2.8798 & 4.0657 \\ 2.8798 & 2.8908 & 4.0657 \\ 4.0657 & 4.0657 & 6.179 \end{pmatrix}, \qquad (8.21)$$

we see that they have similar texture.

8.6.1   An alternative ansatz

We now consider another down quark matrix ansatz,

$$\sqrt{M_d} = N_d \begin{pmatrix} 2 & A & B \\ A & 2 & B \\ B & B & 2 \end{pmatrix} \qquad (8.22)$$

where $N_d = (\sqrt{m_d} + \sqrt{m_s} + \sqrt{m_b})/6 = 10.3924\sqrt{MeV}$. From the matrix invariants

$$C_2(\sqrt{M_d}) = N_d^2(12 - A^2 - 2B^2) \quad \text{and} \quad Det(\sqrt{M_d}) = N_d^3 2(2 - A)(2 + A - B^2)$$

we get the dimensionless eigenvalues

$$(x_1, x_2, x_3) = (2 - A, \frac{1}{2}(A + 4 - \sqrt{A^2 + 8B^2}), \frac{1}{2B}(A + 4 + \sqrt{A^2 + 8B^2}))$$

Inserting numerical values from (8.13), we get

$$A = 1.8428$$
$$B = 1.4248$$
$$N_d = 10.39\sqrt{MeV}$$

Inserting the numerical values for A and B in U_d, and using $U_u = V_{CKM}U_d$, we find the numerical expression for $\sqrt{M_u} = U_u^\dagger diag(\sqrt{m_1}, \sqrt{m_2}, \sqrt{m_3})U_u$, which gives the matrices

$$M_u^{(derived)} = N_u^2 \begin{pmatrix} 25.797 & 25.278 & 21.1 \\ 25.469 & 24.93 & 20.72 \\ 25.37 & 24.95 & 21.124 \end{pmatrix} \quad \text{and} \quad M_d^{(ansatz)} = N_d^2 \begin{pmatrix} 9.426 & 9.4 & 8.325 \\ 9.4 & 9.426 & 8.325 \\ 8.325 & 8.325 & 8.06 \end{pmatrix} \qquad (8.23)$$

which have similar, nearly democratic structure.

8.7   An ansatz for the up quarks

We can play the game the other way round, by introducing a matrix ansatz for the square roots of the up-quark masses, from which we derive a matrix for the down sector.

We first consider the matrix

$$\sqrt{M_u} = N_u \begin{pmatrix} 2 & D & E \\ D & 2 & E \\ E & E & 5 \end{pmatrix} \tag{8.24}$$

where $N_u = (\sqrt{m_u} + \sqrt{m_c} + \sqrt{m_t})/9 = 49.09\sqrt{MeV}$, and D and E are dimensionless coefficients. From the matrix invariants

$$\mathrm{Tr}(\sqrt{M_u}) = 9N_u$$
$$2C_2(\sqrt{M_u}) = N_u^2(24 - D^2 - 2E^2)$$
$$\mathrm{Det}(\sqrt{M_u}) = N_u^3(20 + 2DE^2 - 5D^2 - 4E^2) = N_u^3(2 - D)(5(1 + D) - 2E^2)$$

we have that $x_1 = (2 - D)$, and the dimensionless eigenvalues

$$(x_1, x_2, x_3) = (2 - D, \frac{1}{2}(D + 7 - \sqrt{8E^2 + (3 - D)^2}), \frac{1}{2}(D + 7 + \sqrt{8E^2 + (3 - D)^2}))$$

where

$$D = 1.97006$$
$$E = 2.7879$$
$$N_u = 49.09\sqrt{MeV}$$

Following a similar procedure as before, using $U_d = V_{CKM}^\dagger U_u$, using the diagonalization matrix

$$U_u = \begin{pmatrix} \frac{1}{\sqrt{2}} & -\frac{1}{\sqrt{2}} & 0 \\ \frac{1}{2}\sqrt{\frac{S-D+3}{S}} & \frac{1}{2}\sqrt{\frac{S-D+3}{S}} & -\frac{2E}{\sqrt{S(S-D+3)}} \\ \frac{1}{2}\sqrt{\frac{S+D-3}{S}} & \frac{1}{2}\sqrt{\frac{S+D-3}{S}} & \frac{2E}{\sqrt{S(S+D-3)}} \end{pmatrix} \tag{8.25}$$

and again inserting the mass matrix for the square roots of the weighted mass values, $(x_1, x_2, x_3) = (\sqrt{m_d}, \sqrt{m_s}, \sqrt{m_b}/N_d$, with $N_d = (\sqrt{m_d} + \sqrt{m_s} + \sqrt{m_b})/4$, we get the mass matrix for the square roots of the down quarks in the weak basis:

$$\sqrt{M_d}^{(derived)} = N_d U_d^\dagger \begin{pmatrix} 0.10482 & 0 & 0 \\ 0 & 0.47053 & 0 \\ 0 & 0 & 3.42465 \end{pmatrix} U_d = N_d \begin{pmatrix} 0.956 & 0.774 & 0.977 \\ 0.921 & 0.908 & 0.916 \\ 1.072 & 1.168 & 2.136 \end{pmatrix},$$
$$\tag{8.26}$$

which gives

$$M_d^{(derived)} = N_d^2 \begin{pmatrix} 2.674 & 2.583 & 3.729 \\ 2.699 & 2.607 & 3.688 \\ 4.391 & 4.384 & 6.68 \end{pmatrix} \text{ and } M_u^{(ansatz)} = N_u^2 \begin{pmatrix} 15.654 & 15.653 & 25.01 \\ 15.653 & 15.654 & 25.01 \\ 25.01 & 25.01 & 40.545 \end{pmatrix}$$
$$\tag{8.27}$$

which we relate to (8.19) and (8.20).

When we compare the derived mass matrix for the down sector to the downscaled matrix for the up quark masses:

$$M_d^{(derived)} = N_d^2 \begin{pmatrix} 2.674 & 2.583 & 3.729 \\ 2.699 & 2.607 & 3.688 \\ 4.391 & 4.384 & 6.68 \end{pmatrix} \text{ and } M_u^{(ansatz)} = 6 \times N_u^2 \begin{pmatrix} 2.582 & 2.583 & 4.13 \\ 2.583 & 2.582 & 4.13 \\ 4.13 & 4.13 & 6.69 \end{pmatrix},$$

(8.28)

we find that they have similar texture.

8.7.1 An alternative ansatz

We now consider an alternative ansatz for the up sector,

$$\sqrt{M_u} = N_u \begin{pmatrix} 3 & D & E \\ D & 3 & E \\ E & E & 3 \end{pmatrix}$$

(8.29)

where $\text{Trace}(\sqrt{M_u}) = 9N_u$, $N_u = (\sqrt{m_u} + \sqrt{m_c} + \sqrt{m_t})/9 = 49.09\sqrt{MeV}$, and D and E are dimensionless coefficients. The matrix invariants are

$$C_2(\sqrt{M_u}) = N_u^2(27 - D^2 - 2E^2) \text{ and } \text{Det}(\sqrt{M_u}) = N_u^3(3 - D)(9 + 3D - 2E^2)$$

which gives the dimensionless eigenvalues

$$(x_1, x_2, x_3) = (3 - D, \frac{1}{2}(D + 6 - \sqrt{D^2 + 8E^2}), \frac{1}{2}(D + 6 + \sqrt{D^2 + 8E^2}))$$

Inserting numerical values from (8.13), we get

$$D = 2.97$$
$$E = 2.608$$
$$N_u = 49.09\sqrt{MeV}$$

Following the same procedure as above, we get the matrix

$$M_d^{(derived)} = N_d^2 \begin{pmatrix} 4.081 & 4.019 & 3.481 \\ 4.103 & 4.04 & 3.416 \\ 4.113 & 4.137 & 3.84 \end{pmatrix}$$

which we compare to

$$M_u^{(ansatz)} = N_u^2 \begin{pmatrix} 24.623 & 24.622 & 23.394 \\ 24.622 & 24.623 & 23.394 \\ 23.394 & 23.394 & 22.6 \end{pmatrix}$$

(8.30)

The mass matrix from the ansatz and the derived matrix are again of similar texture, which is close to democratic.

If we instead use $N_d = (\sqrt{m_d} + \sqrt{m_s} + \sqrt{m_b})/6$, we get

$$M_u^{(ansatz)} = N_u^2 \begin{pmatrix} 24.623 & 24.622 & 23.394 \\ 24.622 & 24.623 & 23.394 \\ 23.394 & 23.394 & 22.6 \end{pmatrix} \quad \text{and} \quad M(6)_d^{(derived)} = N_d(6)^2 \begin{pmatrix} 9.18 & 9.04 & 7.83 \\ 9.23 & 9.09 & 7.69 \\ 9.25 & 9.31 & 8.64 \end{pmatrix},$$

$$(8.31)$$

a result that consistent with the matrices (8.23).

The above procedures can be repeated with the quark masses $m_q(2GeV)$ [10], leading to similar results.

8.8   Discussion

The ansatz for the square roots of the up quark masses

$$\sqrt{M}_u(3,3,3) = N_u \begin{pmatrix} 3 & D & E \\ D & 3 & E \\ E & E & 3 \end{pmatrix}$$

with $D = 2.97$ and $E = 6.08$, gives the regular up quark matrix

$$M_u^{(ansatz)} = N_u^2 \begin{pmatrix} 24.623 & 24.622 & 23.394 \\ 24.622 & 24.623 & 23.394 \\ 23.394 & 23.394 & 22.6 \end{pmatrix},$$

which is similar to the up quark matrix that we derive from the matrix

$$\sqrt{M}_d(2,2,2) = N_d \begin{pmatrix} 2 & A & B \\ A & 2 & B \\ B & B & 2 \end{pmatrix}$$

which, with $A = 1.8428$ and $B = 1.4248$ inserted, is

$$M_u^{(derived)} = N_u^2 \begin{pmatrix} 25.797 & 25.278 & 21.1 \\ 25.469 & 24.93 & 20.72 \\ 25.37 & 24.95 & 21.124 \end{pmatrix}$$

We therefore perceive that the pair of matrices $\sqrt{M}_u(3,3,3)$ and $\sqrt{M}_d(2,2,2)$ as belonging together, in the sense that from a matrix of the form $\sim \sqrt{M}_u(3,3,3)$ for the up quarks, we derive a matrix for the down quarks of the form $\sim \sqrt{M}_u(2,2,2)$ - and vice versa.

In the same way, from the matrix

$$\sqrt{M}_d(1,1,2) = N_d \begin{pmatrix} 1 & A & B \\ A & 1 & B \\ B & B & 2 \end{pmatrix}$$

we get

$$M_d^{(ansatz)} = N_d^2 \begin{pmatrix} 2.8908 & 2.8798 & 4.0657 \\ 2.8798 & 2.8908 & 4.0657 \\ 4.0657 & 4.0657 & 6.179 \end{pmatrix}$$

which is similar to the down quark matrix derived from the up sector matrix,

$$\sqrt{M}_u(2,2,5) = N_u \begin{pmatrix} 2 & D & E \\ D & 2 & E \\ E & E & 5 \end{pmatrix},$$

namely

$$M_d^{(\mathrm{derived})} = N_d^2 \begin{pmatrix} 2.674 & 2.583 & 3.729 \\ 2.699 & 2.607 & 3.688 \\ 4.391 & 4.384 & 6.68 \end{pmatrix}$$

Therefore we also perceive the matrices $\sqrt{M}_d(1,1,2)$ and $\sqrt{M}_u(2,2,5)$ as belonging together.

Higher powers of this type of matrices, with diagonal (X, X, Y) will asymptotically go towards matrices with the texture

$$\sqrt{M} \sim N \begin{pmatrix} F & F-\epsilon & G \\ F-\epsilon & F & G \\ G & G & H \end{pmatrix}$$

which have a mass spectrum of the type $(\epsilon, \frac{1}{2}(H+2F-\epsilon\pm\sqrt{(H + \epsilon - 2F)^2 + 8G^2)}))$.
Moreover, the (square root) quark mass matrices of the type

$$\sqrt{M} \sim N \begin{pmatrix} H & D & E \\ D & H & E \\ E & E & H \end{pmatrix},$$

with eigenvalues $(H-2, \frac{1}{2}(D+2H\pm\sqrt{D + 8E^2}))$, give rise to matrices with a more democratic texture.

8.9   Appendix

• The diagonalizing matrix for the matrix (8.17)

$$\sqrt{M}_d = N_d \begin{pmatrix} 1 & A & B \\ A & 1 & B \\ B & B & 2 \end{pmatrix}$$

is

$$U_d = \begin{pmatrix} \frac{1}{\sqrt{2}} & -\frac{1}{\sqrt{2}} & 0 \\ \frac{1}{2}\sqrt{\frac{1-A+S}{S}} & \frac{1}{2}\sqrt{\frac{1-A+S}{S}} & -\frac{2B}{\sqrt{S(1-A+S)}} \\ \frac{1}{2}\sqrt{\frac{A-1+S}{S}} & \frac{1}{2}\sqrt{\frac{A-1+S}{S}} & \frac{2B}{\sqrt{S(A-1+S)}} \end{pmatrix}$$

where $S = \sqrt{8B^2 + (1 - A)^2}$.

• The diagonalizing matrix for the matrix (8.22)

$$\sqrt{M}_d = N_d \begin{pmatrix} 2 & A & B \\ A & 2 & B \\ B & B & 2 \end{pmatrix}$$

is

$$U_d = \begin{pmatrix} \frac{1}{\sqrt{2}} & -\frac{1}{\sqrt{2}} & 0 \\ \frac{2B}{\sqrt{2S(S+A)}} & \frac{2B}{\sqrt{2S(S+A)}} & -\sqrt{\frac{S+A}{2S}} \\ \frac{2B}{\sqrt{2S(S-A)}} & \frac{2B}{\sqrt{2S(S-A)}} & \sqrt{\frac{S-A}{2S}} \end{pmatrix}$$

where $S = \sqrt{8B^2 + A^2}$.

• The ansatz (8.24) for the up sector:

$$\sqrt{M_u} = N_u \begin{pmatrix} 2 & D & E \\ D & 2 & E \\ E & E & 5 \end{pmatrix}$$

has the diagonalization matrix

$$U_u = \begin{pmatrix} \frac{1}{\sqrt{2}} & -\frac{1}{\sqrt{2}} & 0 \\ \frac{1}{2}\sqrt{\frac{S-D+3}{S}} & \frac{1}{2}\sqrt{\frac{S-D+3}{S}} & -\frac{2E}{\sqrt{S(S-D+3)}} \\ \frac{1}{2}\sqrt{\frac{S+D-3}{S}} & \frac{1}{2}\sqrt{\frac{S+D-3}{S}} & \frac{2E}{\sqrt{S(S+D-3)}} \end{pmatrix} \qquad (8.32)$$

where $S = \sqrt{3 - D)^2}$.

• The ansatz (8.24) for the up sector

$$\sqrt{M_u} = N_u \begin{pmatrix} 3 & D & E \\ D & 3 & E \\ E & E & 3 \end{pmatrix}$$

has the diagonaization matrix

$$U_u = \begin{pmatrix} \frac{1}{\sqrt{2}} & -\frac{1}{\sqrt{2}} & 0 \\ \frac{1}{2}\sqrt{\frac{S-D}{S}} & \frac{1}{2}\sqrt{\frac{S-D}{S}} & -\frac{2E}{\sqrt{S(S-D)}} \\ \frac{1}{2}\sqrt{\frac{S+D}{S}} & \frac{1}{2}\sqrt{\frac{S+D}{S}} & \frac{2E}{\sqrt{S(S+D)}} \end{pmatrix} \qquad (8.33)$$

where $S = \sqrt{D^2 + 8E^2}$.

8.10   Conclusion

Inspired by the Koide relation, we investigate two types of mass matrices for the square roots of the quark masses, and then derive the regular mass matrices. We evaluate the numerical form for the mass matrices, well aware that one cannot asign exact values to the light quark masses.

The matrices are

$$\sqrt{M} = N \begin{pmatrix} K & A & B \\ A & K & B \\ B & B & P \end{pmatrix} \qquad (8.34)$$

where K, P are integers, and $N = (\sqrt{m_1} + \sqrt{m_2} + \sqrt{m_3})/(2K + P)$, where m_j are quark masses, and

$$\sqrt{M} = N \begin{pmatrix} K & A & B \\ A & K & B \\ B & B & K \end{pmatrix} \qquad (8.35)$$

where K is an integer, and $N = (\sqrt{m_1} + \sqrt{m_2} + \sqrt{m_3})/(3K)$. Starting from a matrix of the form (8.34) for the down sector, the matrix that we numerically derive for the up sector, has a texture similar to (8.34) (and vice versa starting from the up sector). Likewise, starting from a matrix of the form (8.35) for the down sector, we numerically derive a similar matrix for the up sector, and vice versa starting with an ansatz for the up sector.

Both (8.34) and (8.35) display an unbroken flavour symmetry for the first two families, and the mass matrices derived from (8.35) moreover have a nearly democratic structure.

The (unsurprising) conclusion is that the mass matrices for the two sectors tend to have textures that are similar, but different enough to ensure a mixing matrix that is consistent with data.

References

1. Koide, Y. (2019), "What Physics Does The Charged Lepton Mass Relation Tell Us?", https://arxiv.org/abs/1809.00425
2. Koide, Y. (1982), "Fermion-boson two-body model of quarks and leptons and cabibbo mixing". Lettere al Nuovo Cimento. 34 (8): 201–205. doi:10.1007/BF02817096. S2CID 120885232; A. Kartavtsev (2011), "A remark on the Koide relation for quarks", hep-ph/arXiv:1111.0480
3. M. Kobayashi, T. Maskawa; Maskawa (1973), "CP-Violation in the Renormalizable Theory of Weak Interaction", Progress of Theoretical Physics 49 (2): 652–657
4. H. Fritzsch, Phys. Lett. B 70, 436 (1977), Phys. Lett. B 73, 317 (1978)
5. A. Kleppe, "A democratic suggestion", hep-ph/1608.08988 (2016)
6. H. Fritzsch, "Texture Zero Mass Matrices and Flavor Mixing of Quarks and Leptons", hep-ph/1503.07927v1
7. Matthias Jamin, private communication.
8. M. Jamin, J. Antonio Oller and A. Pich, "Light quark masses from scalar sum rules", arXiv:hep-ph/0110194v2
9. FLAG Working Group, "Review of lattice results concerning low energy particle physics" (2014), hep-lat/1310.8555v2
10. Particle Data Group, https://pdg.lbl.gov/2022/tables/rpp2022-sum-quarks.pdf

9   Strong primordial inhomogeneities induced by axion-like scalar field

M.A. Krasnov[1][**], M. Yu. Khlopov[1,2,3], O. Trivedi[4]

[1] National Research Nuclear University "MEPHI", 115409 Moscow, Russia
[2] Research Institute of Physics, Southern Federal University, 344090 Rostov-on-Don, Russia
[3] Virtual Institute of Astroparticle Physics, 75018 Paris, France
[4] International Centre for Space Sciences and Cosmology, Ahmedabad University, Ahmedabad 380009, India

Abstract. Our goal is to consider Axion-like particle (ALP) model to investigate the behaviour of space-time in the vicinity of the domain wall, induced by axion-like field. Here we present first-step approximation in our analysis and discuss the applicability of thin-shell approximation.

Povzetek Avtorji želijo razumeti obnašanje prostora in časa v bližini domenske stene. Uporabijo model delcev, podobnim axionom. V prispevku predstavijo prvo približno analizo modela in razpravljajo o pristopu, ki so ga uporabili.

9.1   Introduction

Axion-like models have become popular candidates for dark matter and present intriguing opportunities for linking particle physics with cosmology. The search for dark matter components has led to investigations into various hypothetical particles beyond the Standard Model (SM). Originally envisioned as an extension of the Peccei-Quinn (PQ) mechanism [1] to address the strong CP problem in Quantum Chromodynamics (QCD), hese pseudo-Nambu-Goldstone bosons have been proposed in different frame- works involving quantum gravity [2–4]. ALPs have garnered significant interest as potential dark matter constituents as despite their inherently feeble masses ($m_a \lesssim 1$ keV), non-thermal production mechanisms in the early universe could have yielded a population of ALPs that persists today, potentially constituting the majority of cold dark matter (CDM). The appeal of ALPs as dark matter candidates lies in their ability to circumvent the limitations of the standard freeze-out mechanism, that affect weakly interacting massive particles (WIMPs) in their dark matter candidature. The low mass of ALPs allows them to remain in thermal equilibrium with the bath of particles in the early universe for an extended period and this period evades the issue of WIMPs becoming too sluggish to interact efficiently after freeze-out, leading to an underabundance of relic WIMPs compared to the observed dark matter density [5–8].

[**] morrowindman1@mail.ru

Exploring the theoretical background and experimental limitations on ALP properties is crucial for understanding their potential role in cosmology. Recent advancements in directly observing gravitational waves (GWs) are driving significant progress [9–11]. Direct GW observations are anticipated to provide important insights into high-energy physics due to their weak interaction with matter, preserving the characteristics of astrophysical or cosmological events [12–16]. Over the past decades, experimental sensitivities for the direct detection of GWs have significantly improved and numerous new GW observatories are planned worldwide and within this framework, it is imperative to explore various potential sources of GWs and determine the extent to which new physics can be inferred from future observations [17–19]. Improved experimental sensitivities for GW detection have led to the planning of numerous new GW observatories worldwide. Among the potential cosmological sources of GWs are topological defects like cosmic strings and domain walls that could have formed in the early universe [20]. Domain walls are sheet-like topological defects that could form in the early universe when a discrete symmetry is spontaneously broken. Given that discrete symmetries are pervasive in high-energy physics beyond the Standard Model (SM), many new physics models predict the formation of domain walls in the early universe. By examining their cosmological evolution, we can derive several constraints on these models, even if their energy scales exceed those probed by laboratory experiments. Many models of ALP fields, for example, have been considered with regards to creation of domain walls in the early universe [21, 22].

Typically the formation of domain walls is considered problematic in cosmology, as their energy density can quickly dominate the total energy density of the universe which one might take as a contradiction to current observational data. While the formation of domain walls is usually considered problematic in cosmology due to their energy density potentially dominating the total energy density of the universe, their instability might prevent this if the discrete symmetry is only approximate and explicitly broken by a small parameter in the theory. In such cases, the collisions and annihilation of domain walls could produce a significant amount of GWs, potentially resulting in a stochastic GW background in the present universe. Observations of relic GWs can offer insights into the early universe and high-energy physics. ALP fields have been shown to contribute to the formation of closed domain walls in scenarios involving an inflationary universe, potentially impacting the nHz stochastic GW background detected by pulsar timing array facilities and early galaxy formation observed by the James Webb Space Telescope [23].

9.2   Thin shell approximation

In this section we will review and discuss the approach of infinitely thin domain wall. For extended analysis, please, see [15] and [24].

Let us denote wall's surface as Σ, which is 3-dimensional spacelike or timelike (this would affect ϵ, it would be $+1$ [spacelike] or -1 [timelike]) hyper-surface embedded in a 4-dimensional spacetime $(\mathcal{M}, g_{\mu\nu})$. We put subscripts $\pm$ to denote

the value on each side of the hypersurface Σ. Following aforementioned papers:

$$[A]^{\pm} A_+ - A_-, \tag{9.1}$$

$$\{A\}^{\pm} A_+ + A_-, \tag{9.2}$$

$$\overline{A} \frac{1}{2} \{A\}^{\pm}. \tag{9.3}$$

Let ξ_μ be the normal unit vector to the Σ, we can define the induced metric $h_{\mu\nu}$ and the extrinsic curvature $K_{\mu\nu}$ as

$$h_{\mu\nu} g_{\mu\nu} - \epsilon \xi_\mu \xi_\nu, \tag{9.4}$$

$$K_{\mu\nu} h_\mu^\alpha \nabla_\alpha \xi_\nu = D_\mu \xi_\nu. \tag{9.5}$$

- First junction condition is:

$$[h_{\mu\nu}]^{\pm} = 0. \tag{9.6}$$

- Second condition is:

$$[K_{\mu\nu}]^{\pm} = 8\pi\epsilon \left(-S_{\mu\nu} + \frac{1}{2} S h_{\mu\nu} \right). \tag{9.7}$$

- Shell equation of motion:

$$S_{\mu\nu} \overline{K}^{\mu\nu} = [T_{\mu\nu} \xi^\mu \xi^\nu]^{\pm}. \tag{9.8}$$

- Shell energy conservation:

$$D_\mu S_\nu^\mu = -[T_{\mu\alpha} \xi^\mu h_\nu^\alpha]^{\pm}. \tag{9.9}$$

$S_{\mu\nu}$ is the energy momentum tensor of matter fields on Σ and $S = h^{\mu\nu} S_{\mu\nu}$. For pure tension surface $S_{\mu\nu} = -\sigma h_{\mu\nu}$. $T_{\mu\nu}$ is the energy momentum tensor in the region $\mathcal{M} - \{\Sigma\}$.

The paper [24] also contains line element in general form:

$$ds^2 = -e^{2\alpha(t,r)} dt^2 + e^{2\beta(t,r)} dr^2 + R^2(t,r) d\Omega^2. \tag{9.10}$$

They consider the motion of a spherical shell in this spacetime described by

$$t = t^\xi(\tau), \chi = \chi^\xi(\tau), \tag{9.11}$$

where τ is proper time associated with the shell trajectory in the radial direction. The coordinate components of the radial tangent vector v^μ is given by

$$v^\mu = \left(\frac{dt^\xi}{d\tau}, \frac{d\chi^\xi}{d\tau}, 0, 0 \right) = (t_{,\tau}, \chi_{,\tau}, 0, 0). \tag{9.12}$$

Further calculations are based on:

$$v_\mu v^\mu = -1, \tag{9.13}$$

$$\xi_\mu \xi^\mu = 1, \tag{9.14}$$

$$\xi^\mu v_\mu = 0. \tag{9.15}$$

Following [24], second junction yields:

$$[\xi^\mu \partial_\mu \ln R]^\pm = -4\pi\sigma, \tag{9.16}$$

$$\left[\xi_\mu(v^\mu_{,\tau} + \Gamma^\mu_{\lambda\sigma}v^\lambda v^\sigma)\right]^\pm = -4\pi\sigma \tag{9.17}$$

We set EMT of cosmological fluids in the form:

$$T^\pm_{\mu\nu} = (\rho_\pm + p_\pm)u^\pm_\mu u^\pm_\nu + p_\pm g^\pm_{\mu\nu}. \tag{9.18}$$

Equation of motion is as follows:

$$\left\{\xi_\mu(v^\mu_{,\tau} + \Gamma^\mu_{\lambda\sigma}v^\lambda v^\sigma) + 2\xi^\mu\partial_\mu \ln R\right\}^\pm = -\frac{2}{\sigma}\left[(p+\rho)(u_\mu\xi^\mu)^2 + p\right]^\pm. \tag{9.19}$$

If we consider the same fluid within and outside the shell, then it is much simpler:

$$\left\{\xi_\mu(v^\mu_{,\tau} + \Gamma^\mu_{\lambda\sigma}v^\lambda v^\sigma) + 2\xi^\mu\partial_\mu \ln R\right\}^\pm = 0, \tag{9.20}$$

if one assume the smooth crossing of the wall by fluid ($[u_\mu\xi^\mu]^\pm = 0$).
Equation of motion of the thin shell could be written as [15]:

$$\frac{ar_{,\tau\tau}}{\sqrt{1+a^2r^2_\tau}} + \frac{4a_{,\tau}r_{,\tau}}{\sqrt{1+a^2r^2_\tau}} + \frac{2\sqrt{1+a^2r^2_\tau}}{ar} = 6\pi\sigma, \tag{9.21}$$

which can also be rewritten in terms of cosmic time as follows:

$$\ddot{r} + (4 - 3a^2\dot{r}^2)H\dot{r} + \frac{2}{a^2r}(1 - a^2\dot{r}^2) = 6\pi\sigma\frac{(1 - a^2\dot{r}^2)^{3/2}}{a}. \tag{9.22}$$

One may notice that equation of motion (9.22) could be utilized in two cases with regards to wall's energy density. The first case is wall's energy density is negligible, i.e. one can put $\sigma = 0$. And the second case is wall's density is considerable, but not arbitrarily big, since there is no corresponding transformation for equation (9.22), i.e. there is no limit of big σ, which makes it inapplicable for consideration of wall-dominated Universe in this framework.

9.3   Axion-like field in Kantowski-Sachs metric

We start by considering a space-time with line element given by

$$ds^2 = A(t,r)^2dt^2 - X(t,r)^2dr^2 - Y(t,r)^2d\Omega^2, \tag{9.23}$$

where $d\Omega^2 = d\theta^2 + \sin^2\theta d\phi^2$. One may notice abuse of symbols in our paper, we denote axion-like scalar field with both θ and ϕ symbols as well as angular coordinates. But there is no explicit utilization of angular coordinates in our analysis, thus, there would be no misunderstanding. Following [15], we set $A(t,r) = 1$, corresponding to gauge symmetry. ALP Lagrangian is set to be

$$\mathcal{L} = \frac{1}{2}g^{\mu\nu}\partial_\mu\phi\partial_\nu\phi - \Lambda^4\left[1 - \cos\left(\frac{\phi}{f}\right)\right]. \tag{9.24}$$

We also take into account anisotropy of the space time via energy-momentum tensor of cosmological fluid:

$$T_\nu^\mu = \text{diag}[1, \omega, -(\omega + \delta), -(\omega + \gamma)]\rho, \tag{9.25}$$

where $\omega = p/\rho$.

As a first step in our analysis we consider limit $r \to \infty$, i.e. what a distant observer could detect. In that case line element (9.23) could be rewritten as

$$ds^2 = dt^2 - X(t)^2 dr^2 - Y(t)^2 d\Omega^2, \tag{9.26}$$

which is Kantowski-Sachs space time [25]. Here we assume that Y is finite as $r \to \infty$. We also set common border condition for the scalar field $\phi_r(t, \infty) = 0$.

Now let us write down system of Einstein's field equations using line element (9.26), Lagrangian (9.24) and cosmological fluid' energy-momentum tensor (9.25):

$$\frac{2\dot{X}\dot{Y}}{XY} + \frac{\dot{Y}^2}{Y^2} + \frac{1}{Y^2} = \frac{1}{2}\dot{\phi}^2 + \Lambda^4 \left[1 - \cos\left(\frac{\phi}{f}\right)\right] + \rho, \tag{9.27}$$

$$\frac{2\ddot{Y}}{Y} + \frac{\dot{Y}^2}{Y^2} + \frac{1}{Y^2} = -\frac{1}{2}\dot{\phi}^2 + \Lambda^4 \left[1 - \cos\left(\frac{\phi}{f}\right)\right] - \omega\rho, \tag{9.28}$$

$$\frac{\ddot{X}}{X} + \frac{\dot{X}\dot{Y}}{XY} + \frac{\ddot{Y}}{Y} = -\frac{1}{2}\dot{\phi}^2 + \Lambda^4 \left[1 - \cos\left(\frac{\phi}{f}\right)\right] - (\omega + \delta)\rho, \tag{9.29}$$

$$\frac{\ddot{X}}{X} + \frac{\dot{X}\dot{Y}}{XY} + \frac{\ddot{Y}}{Y} = -\frac{1}{2}\dot{\phi}^2 + \Lambda^4 \left[1 - \cos\left(\frac{\phi}{f}\right)\right] - (\omega + \gamma)\rho. \tag{9.30}$$

Equation of motion of the scalar field is as follows:

$$\ddot{\phi} + \left(\frac{\dot{X}}{X} + 2\frac{\dot{Y}}{Y}\right)\dot{\phi} + \frac{\Lambda^4}{f}\sin\left(\frac{\phi}{f}\right) = 0. \tag{9.31}$$

Equations (9.29) and (9.30) immediately yield $\gamma = \delta$ and now we are given with four independent equations and six variables. We need to make two assumptions to make system solvable.

To make progress now, we assume the following relation between X and Y:

$$Y = X^n, \tag{9.32}$$

which has been commonly utilized in some previous works by other researchers [26, 27]. Furthermore, it is usually assumed that scalar field is proportional to average scale factor taken in some power [28, 29]

$$\phi \propto a(t)^l = (XY^2)^{1/3}, \tag{9.33}$$

One can then check that relations (9.33) and (9.32) leads to the following relation between the scalar field and metric's potential

$$\frac{\dot{\phi}}{\phi} = \frac{l}{3}(2n+1)\frac{\dot{X}}{X}.$$ (9.34)

We now utilize (9.34) in (9.31), which leads us to arrive at

$$\ddot{\phi} + \frac{3\dot{\phi}^2}{l\phi} + \frac{\Lambda^4}{f}\sin\left(\frac{\phi}{f}\right) = 0.$$ (9.35)

Let us now perform the following variable substitution $\phi = f\theta$ and switch from time derivative to the derivative with respect to $m_\theta t = t\Lambda^2/f$ (represented by prime). We obtain

$$\theta'' + \frac{3}{l}\frac{\theta'^2}{\theta} + \sin\theta = 0.$$ (9.36)

At this point, we could refer to θ as a phase and we could then plot the numerical solution of (9.36) for different values of l. We set initial conditions for θ as follows

$$\theta_{in} = \pi - 0.01, \ \theta'_{in} = 0.$$ (9.37)

This allows us to see the evolution of the scalar field, which we have shown in Figure (3.1).
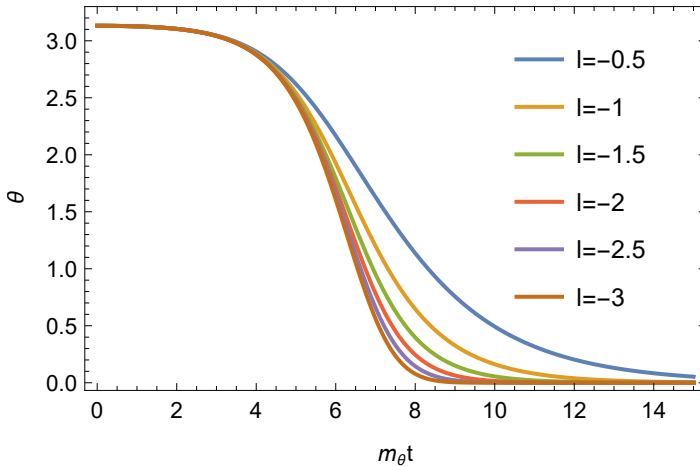
Fig. 9.1: The plot of the solution of (9.36) for different values of of l, where the interesting observation is the impact of l changing slowly for $l < -2$.

The equation of state parameter, given by the usual definition

$$\omega_\theta = \frac{p_\theta}{\rho_\theta}$$

is plotted in Fig.(9.2) [1]
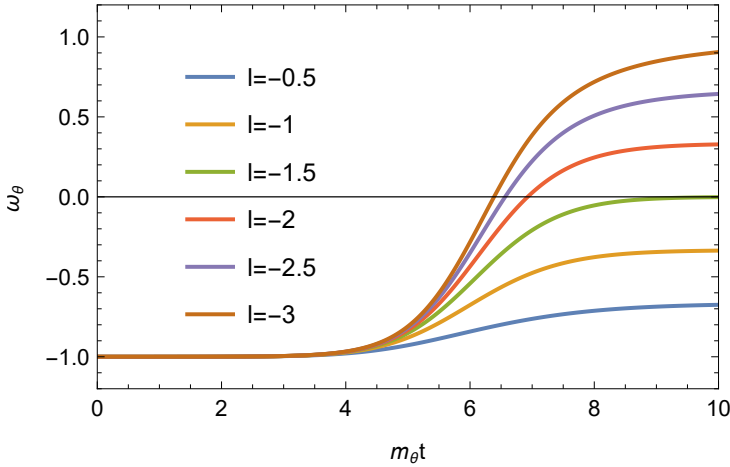
Fig. 9.2: The plot of the equation of state parameter for the scalar field. We see that scalar field could behave differently depending on the value of l and in particular, if $l = -1.5$ then scalar field behaves like non-relativistic matter.

From the Einstein equations (9.27)-(9.30), we find that equation of state parameter for cosmological fluid $\omega \approx const \sim -1$ and skewness parameter $\delta = \gamma \approx 1$ for any value of l.

9.4   Conclusion

In this study, we explored the cosmological behavior of a scalar field with an axion-like potential in a non-standard spacetime background. The metric we examined was generally that of an inhomogeneous and anisotropic spacetime, which, in the limit of a distant observer, resembled a standard Kantowski-Sachs metric. Specifically focusing on this scenario, we analyzed the dynamics of the scalar field in such a setting.

In the model for a distant observer, the parameters of skewness, represented by δ and γ, tended towards minus one, resulting in negligible angular pressures and causing the energy density of the cosmological fluid to align radially. This anisotropic nature suggests that the fluid could support cosmic expansion in specific directions while exhibiting dust-like behavior in angular dimensions.

---

[1] Note that the parameter has also been scaled appropriately with regards to the differential equation with θ variable.

Acknowledgements

References

1. R. D. Peccei, H. R. Quinn: CP conservation in the presence of pseudoparticles, Physical Review Letters **38** (1977) 1440.
2. A. Arvanitaki, S. Dimopoulos, S. Dubovsky, N. Kaloper, J. March-Russell: String axiverse, Physical Review D **81** (2010) 123530.
3. P. Svrcek, E. Witten: Axions in string theory, Journal of High Energy Physics **06** (2006) 051.
4. J. P. Conlon: The qcd axion and moduli stabilisation, Journal of High Energy Physics **05** (2006) 078.
5. M. Buschmann, J. W. Foster, B. R. Safdi: Early- Universe Simulations of the Cosmological Axion. Physical Review Letters **16** (2020) 161103.
6. A. Iwazaki: Spontaneous magnetization of axion domain wall and primordial magnetic field, Physical Review Letters **79** (1997) 2927–2930.
7. M. Gorghetto, E. Hardy: Post-inflationary axions: a min- imal target for axion haloscopes, Journal of High Energy Physics **5** (2023) 1-41.
8. N. Bernal, F. Hajkarim, Y. Xu: Axion Dark Matter in the Time of Primordial Black Holes. Physical Review D **104** (2021) 075007.
9. B. P. Abbott et al: Observation of Gravitational Waves from a Binary Black Hole Merger, Physical Review Letters **6** (2016) 061102.
10. B. P. Abbott et al: Observation of Gravitational Waves from a 22-Solar-Mass Binary Black Hole Coalescence, Physical Review Letters **24** (2016) 241103.
11. M. Maggiore: Gravitational wave experiments and early universe cosmology, Physics Reports **331** (2000) 283–367.
12. S. G. Rubin, M. Yu. Khlopov, A. S. Sakharov: Primordial black holes from nonequilibrium second order phase transition, Gravitation and Cosmology **6** (2000) 51-58.
13. M. Yu. Khlopov, S. G. Rubin, A. S. Sakharov: Primordial structure of massive black hole clusters, Astroparticle Physics **23** (2005) 265.
14. J. Garriga, A. Vilenkin, J. Zhang: Black holes and the multiverse, Journal of Cosmology and Astroparticle Physics **02** (2016) 064.
15. H. Deng, J. Garriga, A. Vilenkin: Primordial black hole and wormhole formation by domain walls, Journal of Cosmology and Astroparticle Physics **04** (2017) 050.
16. B. Liu, V. Bromm: Accelerating Early Massive Galaxy Formation with Primordial Black Holes, Astrophysical Journal Letters **2** (2022) L30.
17. L. P. Grishchuk: Amplification of gravitational waves in an istropic universe, Journal of Experimental and Theoretical Physics **67** (1974) 825-838.
18. A. A. Starobinsky: Spectrum of relict gravitational radiation and the early state of the universe: ournal of Experimental and Theoretical Physics Letters **30** (1979) 682-685.
19. E. Witten: Cosmic Separation of Phases, Physical Review D **30** (1984) 272-285.
20. T. W. B. Kibble: Topology of Cosmic Domains and Strings, Journal of Physics A **9** (1976) 1387-1398.
21. D. I. Dunsky, M. Kongsore: Primordial black holes from axion domain wall collapse, Journal of High Energy Physics **6** (2024).

22. S. Blasi, A. Mariotti, A. Rase, A. Sevrin, K. Turbang: Friction on ALP domain walls and gravitational waves, Journal of Cosmology and Astroparticle Physics **04** (2023) 008.

23. S. Guo, M. Khlopov, X. Liu, L. Wu, Y. Wu,B. Zhu: Footprints of Axion-Like Particle in Pulsar Timing Array Data and JWST Observations, Science China: Physics, Mechanics and Astronomy **67** (2024).

24. N. Tanahashi, C. Yoo: Spherical domain wall collapse in a dust universe, Classical and Quantum Gravity **15** (2015) 155003.

25. R. Kantowski, R. K. Sachs: Some spatially homogeneous anisotropic relativistic cosmological models, Journal of Mathematical Physics **3** (1966) 443–446.

26. C. B. Collins, E. N. Glass, D. A. Wilkinson: Exact spatially homogeneous cosmologies, General Relativity and Gravitation **12** (1980) 805–823.

27. M. V. Santhi, V.U.M. Rao, Y. Aditya: LRS Bianchi type-V universe with variable modified Chaplygin gas in a scalar–tensor theory of gravitation, Canadian Journal of Physics **6** (2016) 578–582.

28. V. B. Johri and K. Desikan: Cosmological models with constant deceleration parameter in Brans-Dicke theory, General Relativity and Gravitation **26** (1994) 1217-1232.

29. V. B. Johri and R. Sudharsan: BD-FRW Cosmology with Bulk Viscosity, Australian Journal of Physics, **42** (1989) 215–222.

10 Do we understand the internal spaces of second quantized fermion and boson fields, with gravity included?

The relation with strings theories

N.S. Mankoč Borštnik

Department of Physics, University of Ljubljana
SI-1000 Ljubljana, Slovenia

Abstract. The article proposes the description of internal spaces of fermion (quarks and leptons and antiquarks and antileptons) and boson (photons, weak bosons, gluons, gravitons and scalars) second quantized fields in an unique way if they all are massless. The internal spaces are described by "basis vectors" which are the superposition of odd (for fermions) and even (for bosons) products of the operators γ^a. For an arbitrarily symmetry $SO(d-1,1)$ of the internal spaces, it is the number of fermion fields (they appear in families and have their Hermitian conjugated partners in a separate group) equal to the number of boson fields (they appear in two orthogonal groups), manifesting a kind of supersymmetry, which differ of the string supersymmetry. On the assumption that fermions and bosons are active (they have momenta different from zero) only in $d = (3 + 1)$ ordinary space-time, bosons present vectors if they carry the space index $\mu = (0, 1, 2, 3)$, and present scalars if they carry the index $\sigma \geq 5$. The author discusses this theory's latest achievements, with a trial to understand whether the extension to strings or to odd-dimensional spaces can lead to new kind of supersymmetry. This model, named *spin-charge-family* theory, manifests in a long series of papers the phenomenological success of the theory in elementary particle physics and cosmology.

Povzetek: Članek predlaga enoten opis notranjih prostorov brezmasnih fermionov (kvarkov in leptonov ter antikvarkov in antileptonov) in bozonov (fotonov, šibkih bozonov, gluonov, gravitonov in skalarjev) v drugi kvantizaciji. Notranji prostori so opisani z "bazičnimi vektorji", ki so superpozicija lihih (za fermione) in sodih (za bozone) produktov operaterjev γ^a. Za izbrano simetrijo $SO(d-1,1)$ notranjih prostorov je število fermionskih "bazičnih vektorjev" (pojavijo se v družinah, njihovi hermitsko konjugirani partnerji pa tvorijo ločeno grupo) enako številu bozonskih "bazičnih vektorjev" (pojavijo se v dveh ortogonalnih grupah), kar manifestira neko vrsto supersimetrije, ki se razlikuje od supersimetrije pri strunah. Ob predpostavki, da so fermioni in bozoni aktivni (imajo od nič različne gibalne količine) samo v $d = (3 + 1)$ prostoru-času, so bozoni vektorji, če nosijo indeks $\mu = (0, 1, 2, 3)$ in so skalarji, če nosijo indeks $\sigma \geq 5$. Avtor predstavi zadnje dosežke te teorije, v katerih poskuša ugotoviti, ali razširitev "bazičnih vektorjev" v strune ali v lihe dimenzionalne prostore lahko vodi do nove vrste supersimetrije. Fenomenološko uspešnost teorije *spina-nabojev-družin* potrjujejo številne objave v uglednih revijah fizike osnovnih delcev in kozmologije.

10.1   Introduction

The proposed article discusses how all the fermion and boson fields can be treated uniquely if they all start as massless fields. One can, namely, describe the internal spaces of fermions and bosons by "basis vectors" which are products of nilpotents and projectors, chosen to be the eigenvectors of the Cartan subalgebra members of the Lorentz algebra in internal spaces of fermions and bosons [1–11].

Nilpotents are the superposition of an odd number of operators γ^a's ($\overset{ab}{(k)}:=$ $\frac{1}{2}(\gamma^a + \frac{\eta^{aa}}{ik}\gamma^b)$, $(\overset{ab}{(k)})^2 = 0$); projectors are the superposition of an even number of operators γ^a's ($\overset{ab}{[k]}:= \frac{1}{2}(1 + \frac{i}{k}\gamma^a\gamma^b)$, $(\overset{ab}{[k]})^2 =\overset{ab}{[k]}$), with the properties : $S^{ab}\overset{ab}{(k)}= \frac{k}{2} \overset{ab}{(k)}$, $S^{ab}\overset{ab}{[k]}= \frac{k}{2} \overset{ab}{[k]}$ with $k^2 = \eta^{aa}\eta^{bb}$.

"Basis vectors" of fermions, chosen to be the algebraic products of an odd number of nilpotents (at least one, the rest are projectors), and of bosons, chosen to be the algebraic products of an even number of nilpotents (or only of projectors) are correspondingly eigenvectors of all $\frac{d(d-1)}{2}$ Cartan subalgebra members.

Fermion "basis vectors" appear in $2^{\frac{d}{2}-1}$ irreducible representations — families — each family having $2^{\frac{d}{2}-1}$ members. All the fermion "basis vectors" are mutually orthogonal, while the "basis vectors" fulfil together with their Hermitian conjugated partners, appearing in a separate group, the Dirac second quantization postulates for fermions, therefore, explaining the Dirac's postulates for fermions. Fermion "basis vectors" and their Hermitian conjugated partners have together 2^{d-1} members.

Boson "basis vectors" appear in two orthogonal groups, each of the two groups with $2^{\frac{d}{2}-1} \times 2^{\frac{d}{2}-1}$ members have their Hermitian conjugated partners within the same group.

Correspondingly, the number of fermion "basis vectors" is equal to the number of boson "basis vectors" manifesting a kind of supersymmetry, which differ from the one offered by string theories [1], requiring the doubling of so far observed fermions and bosons.

Following the Grassmann algebra, the theory proposes two kinds of operators γ^a, namely γ^a's and $\tilde{\gamma}^a$'s [1–4].

Operators γ^a are used to describe the internal spaces of fermions, $\tilde{\gamma}^a$ determine the quantum numbers of families. The operators γ^a describe the internal space of bosons as well [2].

---

[1] The supersymmetry usually requires that to each fermion there exists a superpartner with the same charges but with spin zero; and for each spin 1 boson there exist a superpartner with the same charges but with spin 1/2.

[2] It is not difficult to reproduce the Dirac matrices in any $d = 2n$ dimensional space, but it is no need for this; the "basis vectors" are much more appropriate to work with, what it will be demonstrated in what follows. Let us point out that Dirac matrices were designed for massive fermions; while "basis vectors" describing internal spaces for fermions anti-commute, the Dirac matrices do not [26]. The families do not appear in the Dirac formulations of internal spaces of fermions.

The operators γ^a and $\tilde{\gamma}^a$ fulfil the following commutation relations: $\{\gamma^a, \gamma^b\}_+ = 2\eta^{ab} = \{\tilde{\gamma}^a, \tilde{\gamma}^b\}_+, \{\gamma^a, \tilde{\gamma}^b\}_+ = 0, (a,b) = (0,1,2,3,5,\cdots,d), (\gamma^a)^\dagger = \eta^{aa}\gamma^a, (\tilde{\gamma}^a)^\dagger = \eta^{aa}\tilde{\gamma}^a$, making fermions and bosons second quantized fields since fermion "basis vectors" including odd products of nilpotents correspondingly anti-commute and boson "basis vectors" including even products of nilpotents commute [1–4, 7–10]. Although the multiplication of the fermion "basis vectors" by a γ^a generates the boson "basis vectors", and the multiplication of the boson "basis vectors" by a γ^a generates the fermion "basis vectors", these two kinds of "basis vectors" have completely different properties: Not only that the fermion "basis vectors" anti-commute while the boson "basis vectors" commute; the fermion "basis vectors" appear in $2^{\frac{d}{2}-1}$ families, each family having $2^{\frac{d}{2}-1}$ members, together with their Hermitian conjugated partners, which appear in a separate group, they have $2 \times 2^{\frac{d}{2}-1} \times 2^{\frac{d}{2}-1}$ members; the boson "basis vectors" appear in two orthogonal groups, each of the two groups with $2^{\frac{d}{2}-1} \times 2^{\frac{d}{2}-1}$ members have their Hermitian conjugated partners within the same group; the algebraic multiplication of one of fermion "basis vectors" with one of the Hermitian conjugated partner generates one of the Clifford even "basis vectors"; the algebraic multiplication of one of boson "basis vector" algebraically applying on a fermion "basis vector" generates a fermion "basic vector", demonstrating that since fermion "basis vectors" carry a half-integer value of the Cartan subalgebra members ($S^{ab} = \pm\frac{i}{2}$ or $S^{ab} = \pm\frac{1}{2}$, the same is true for $\tilde{S}^{ab} = \pm\frac{i}{2}$ or $\tilde{S}^{ab} = \pm\frac{1}{2}$), the boson "basis vectors" carry an integer value of the Cartan subalgebra members, determined by $\mathcal{S}^{ab} = S^{ab} + \tilde{S}^{ab}$. These, explained above, are valid in even dimensional spaces. In odd dimensional spaces [9], $d = (2n+1), n \geq 0$, there are two different kinds of "basis vectors": One kind behaves as they do in $2n$ even dimensional spaces; the second kind with the same number of "basis vectors" as the first one behaves completely different — the anti commuting "basis vectors" appear in two orthogonal groups, each with their Hermitian conjugated partners in their group; the commuting "basis vectors" appear $2^{\frac{2n}{2}-1}$ families, each family having $2^{\frac{2n}{2}-1}$ members, while their Hermitian conjugated partners appear in a separate group. The second kind offers the presence of the Fadeev-Popov ghosts [22].

The proposed "basis vectors", describing the internal spaces of fermions and bosons in a tensor product with the basis in ordinary space-time determine creation and annihilation operators, which explain the Dirac's second quantized postulates. Under the assumption that fermions and bosons are active (have non zero momenta) in $d = (3+1)$ while manifesting the internal space in $d = 2(2n+1)$ (the experiments and observations require $n = 3$), the theory offers the explanations of all the assumptions of the Standard model for fermions (quarks and leptons and antiquarks and antileptons), requiring the existence of a right handed neutrinos and left handed anti-neutrinos and of families; the theory explains the existence of photons, weak bosons and gluons, requiring the existence of gravitons.

The theory explains the existence of scalar fields as it is Higgs boson, predicting new scalar fields, which caused the inflation at the Big Bang, explains several cosmological observations.

We briefly discuss the case that the point fermion and boson fields are extended to strings, describing the fermion and boson fields in space-time $d = (3+1)$ as

tensor products of the "basis vectors" and basis in ordinary space-time extended to strings [11]. This article presents shortly also a possibility that the internal space of a string, which has $d = (1+1)$, Sect. 11.2.1, is used. This part is new and yet to be discussed. The longer version will be discussed in a separate article in this proceedings.

Sect. 10.2 presents the properties of "basis vectors" of fermions and bosons. We show how to construct the internal spaces of fermions and bosons, and also demonstrate that the internal spaces of bosons (photons, gravitons, gauge fields, scalar fields) are expressible as algebraic products of the fermion "basis vectors" and their Hermitian conjugated partners, Sect. 10.6, [10], meaning that we do not have to know bosons' internal spaces since they can be presented by algebraic products from fermions' ones.

In Subsect. 10.2.1 "basis vectors" for fermions and bosons in $d = 2(2n+1)$-dimensional internal spaces from the point of view of $d = (3+1)$ are discussed.

Subsect. 10.2.2 presents the relations among the Clifford odd and the Clifford even "basis vectors".

Subsect. 10.2.3 discusses relations among fermions and their vector and scalar gauge fields under the assumptions that all the gauge fields are active (have non zero momentum) only in $d = (3+1)$.

Subsect. 10.2.4 discusses the case with $d = (13+1)$, which offers the explanation of all the assumptions of the *Standard model*, with the families included, requires the existence of right handed neutrinos and the left handed antineutrinos, the dark matter, predicts the fourth family to the observed three, offers the explain for the inflation after Bing Bang and explains also several cosmological observations.

Sect. 10.3 presents creation and annihilation operators for fermion and boson fields in $d = (3+1)$.

Sect. 11.2.1 discusses the possibility to extend ordinary space-time to strings, as well as the offer of the extension of an even dimensional space to one dimension more.

In Sect. 11.3, we shortly overview the whole talk, pointing out the open questions.

10.2   "Basis vectors" describing internal spaces of anticommuting fermion and commuting boson second quantized fields

This section is a short overview of the reference [7] (and the references [1,3]) presenting the "basis vectors" of fermion internal spaces, while the presentation of the "basis vectors" describing the internal spaces of boson internal spaces follows references [1,8,10].

We could start with the Grassmann algebra [1,8] which offers 2×2^d anticommuting operators in d-dimensional space [13], θ^a and $p^{\theta a} = i \frac{\partial}{\partial \theta_a}$ [1], fulfilling the relations $\{\theta^a, \theta^b\}_+ = 0$, $\{\frac{\partial}{\partial \theta_a}, \frac{\partial}{\partial \theta_b}\}_+ = 0$, $\{\theta_a, \frac{\partial}{\partial \theta_b}\}_+ = \delta_{ab}$, $(a,b) = (0,1,2,3,5,\cdots,d)$.

We shall rather use two kinds of the Clifford algebra elements (operators), γ^a and $\tilde{\gamma}^a$, expressible with θ^a's and their Hermitian conjugate momenta $p^{\theta a} = i\frac{\partial}{\partial \theta_a}$ [1],

$$\gamma^a = (\theta^a + \frac{\partial}{\partial \theta_a}), \quad \tilde{\gamma}^a = i(\theta^a - \frac{\partial}{\partial \theta_a}),$$

$$\theta^a = \frac{1}{2}(\gamma^a - i\tilde{\gamma}^a), \quad \frac{\partial}{\partial \theta_a} = \frac{1}{2}(\gamma^a + i\tilde{\gamma}^a),$$

(10.1)

offering together $2 \cdot 2^d$ operators: 2^d are superposition of products of γ^a and 2^d of $\tilde{\gamma}^a$, with the properties

$$\{\gamma^a, \gamma^b\}_+ = 2\eta^{ab} = \{\tilde{\gamma}^a, \tilde{\gamma}^b\}_+,$$
$$\{\gamma^a, \tilde{\gamma}^b\}_+ = 0, \quad (a, b) = (0, 1, 2, 3, 5, \cdots, d),$$
$$(\gamma^a)^\dagger = \eta^{aa}\gamma^a, \quad (\tilde{\gamma}^a)^\dagger = \eta^{aa}\tilde{\gamma}^a.$$

(10.2)

Both kinds offer the description of the internal spaces of fermions with the "basis vectors" which are superpositions of odd products of either γ^a's or $\tilde{\gamma}^a$'s and fulfil correspondingly, the anti-commuting postulates of second quantized fermion fields, as well as the description of the internal spaces of boson fields with the "basis vectors" which are superposition of even products of either γ^a's or $\tilde{\gamma}^a$'s and fulfil correspondingly the commuting postulates of second quantized boson fields. *Since there are not two kinds of anti-commuting fermions, and not two corresponding kinds of their gauge fields, the postulate of Eq. (11.3) gives the possibility that only one of the two kinds of operators are used to describe fermions and their gauge fields, namely γ^a's.*

Postulating how does $\tilde{\gamma}^a$ operate on γ^a, reduces the two Clifford subalgebras, γ^a and $\tilde{\gamma}^a$, to the one described by γ^a [1,3,12]

$$\{\tilde{\gamma}^a B = (-)^B i B\gamma^a\}|\psi_{oc}>,$$

(10.3)

with $(-)^B = -1$, if B is (a function of) odd products of γ^a's, otherwise $(-)^B = 1$ [3], the vacuum state $|\psi_{oc}>$ will be defined in Eq. (10.10).

The operators $\tilde{\gamma}^a$'s can after the postulate, Eq. (11.3), be used to describe the quantum numbers of each of the $2^{\frac{d}{2}-1}$ irreducible representations (with $2^{\frac{d}{2}-1}$ members each, representing "families" of fermions) of the Lorentz group with the infinitesimal generators S^{ab} [3] by $\tilde{S}^{ab}$ [4]. We shall see [8] that the quantum numbers of each irreducible representation of the Lorentz group in the internal space of bosons are equal to $\mathcal{S}^{ab} (= S^{ab} + \tilde{S}^{ab})$ [5].

We shall arrange all the "basis vectors" describing internal spaces of fermion and boson second quantized fields to be the eigenstates of the Cartan subalgebra

---

[3] Lorentz group has in the internal space of fermions the generators $S^{ab} = \frac{i}{4}(\gamma^a\gamma^b - \gamma^b\gamma^a)$
[4] $\tilde{S}^{ab} = \frac{i}{4}(\tilde{\gamma}^a\tilde{\gamma}^b - \tilde{\gamma}^b\tilde{\gamma}^a)$.
[5] One can prove (or read in App. I of Ref. [7]) that the relations of Eq. (11.2) remain valid also after the *postulate*, presented in Eq. (11.3).

members of the Lorentz algebra, chosen to be

$$S^{03}, S^{12}, S^{56}, \cdots, S^{d-1\,d},$$
$$\tilde{S}^{03}, \tilde{S}^{12}, \tilde{S}^{56}, \cdots, \tilde{S}^{d-1\,d},$$
$$\mathcal{S}^{ab} = S^{ab} + \tilde{S}^{ab}. \tag{10.4}$$

In even-dimensional spaces there are $\frac{d}{2}$ members of the Cartan subalgebra, Eq. (11.4) [6].

We define [1,3] in even dimensional spaces $\frac{d}{2}$ nilpotents, $\overset{ab}{(k)}$, each nilpotent is a superposition of an odd number of γ^a's, and projectors, $\overset{ab}{[k]}$, each is a superposition of an even number of γ^a's,

$$\overset{ab}{(k)} := \frac{1}{2}\left(\gamma^a + \frac{\eta^{aa}}{ik}\gamma^b\right), \quad (\overset{ab}{(k)})^2 = 0,$$
$$\overset{ab}{[k]} := \frac{1}{2}\left(1 + \frac{i}{k}\gamma^a\gamma^b\right), \quad (\overset{ab}{[k]})^2 = \overset{ab}{[k]}, \tag{10.5}$$

each nilpotent and projector is chosen to be the eigenvector of one of $\frac{d-1}{2}$ members of the Cartan subalgebra

$$S^{ab}\,\overset{ab}{(k)} = \frac{k}{2}\,\overset{ab}{(k)}, \qquad \tilde{S}^{ab}\,\overset{ab}{(k)} = \frac{k}{2}\,\overset{ab}{(k)},$$
$$S^{ab}\,\overset{ab}{[k]} = \frac{k}{2}\,\overset{ab}{[k]}, \qquad \tilde{S}^{ab}\,\overset{ab}{[k]} = -\frac{k}{2}\,\overset{ab}{[k]}, \tag{10.6}$$

with $k^2 = \eta^{aa}\eta^{bb}$, pointing out that the eigenvalues of S^{ab} on projectors expressed with γ^a differ from the eigenvalues of $\tilde{S}^{ab}$ on projectors expressed with γ^a. Taking into account Eq. (11.2) one finds the relations

$$\gamma^a\,\overset{ab}{(k)} = \eta^{aa}\,\overset{ab}{[-k]}, \quad \gamma^b\,\overset{ab}{(k)} = -ik\,\overset{ab}{[-k]}, \quad \gamma^a\,\overset{ab}{[k]} = \overset{ab}{(-k)}, \quad \gamma^b\,\overset{ab}{[k]} = -ik\eta^{aa}\,\overset{ab}{(-k)},$$
$$\tilde{\gamma}^a\,\overset{ab}{(k)} = -i\eta^{aa}\,\overset{ab}{[k]}, \quad \tilde{\gamma}^b\,\overset{ab}{(k)} = -k\,\overset{ab}{[k]}, \quad \tilde{\gamma}^a\,\overset{ab}{[k]} = i\,\overset{ab}{(k)}, \quad \tilde{\gamma}^b\,\overset{ab}{[k]} = -k\eta^{aa}\,\overset{ab}{(k)},$$
$$\overset{ab}{(k)}\overset{ab}{(-k)} = \eta^{aa}\,\overset{ab}{[k]}, \quad \overset{ab}{(-k)}\overset{ab}{(k)} = \eta^{aa}\,\overset{ab}{[-k]}, \quad \overset{ab}{(k)}\overset{ab}{[k]} = 0, \quad \overset{ab}{(k)}\overset{ab}{[-k]} = \overset{ab}{(k)},$$
$$\overset{ab}{(-k)}\overset{ab}{[k]} = \overset{ab}{(-k)}, \quad \overset{ab}{[k]}\overset{ab}{(k)} = \overset{ab}{(k)}, \quad \overset{ab}{[k]}\overset{ab}{(-k)} = 0, \quad \overset{ab}{[k]}\overset{ab}{[-k]} = 0,$$
$$\overset{ab}{(k)}{}^\dagger = \eta^{aa}\,\overset{ab}{(-k)}, \quad (\overset{ab}{(k)})^2 = 0, \quad \overset{ab}{(k)}\overset{ab}{(-k)} = \eta^{aa}\,\overset{ab}{[k]},$$
$$\overset{ab}{[k]}{}^\dagger = \overset{ab}{[k]}, \quad (\overset{ab}{[k]})^2 = \overset{ab}{[k]}, \quad \overset{ab}{[k]}\overset{ab}{[-k]} = 0. \tag{10.7}$$

More relations are presented in App. A of Ref. [11].

We define [1,3,8] in even dimensional spaces the "basis vectors" of fermion and boson second quantized fields as algebraic, $*_A$, products of nilpotents and projectors so that each product is an eigenvector of all $\frac{d}{2}$ Cartan subalgebra members, Eq. (11.4).

Fermion"basis vectors" must be products of an odd number of nilpotents, at least one, the rest are projectors; boson "basis vectors" must be products of an even

---

[6] In odd-dimensional spaces there are $\frac{d-1}{2}$ members of the Cartan subalgebra.

number of nilpotents, the rest are projectors [7].

We recognize: Half of 2^d different products of γ^a's are odd, and half of them are even. The Clifford odd "basis vectors" appear in $2^{\frac{d}{2}-1}$ irreducible representations, we call them families, each family having $2^{\frac{d}{2}-1}$ members (obtainable from any other member by S^{ab}; the family member of any other family is obtainable by $\tilde{S}^{ab}$).

Since the Hermitian conjugated partner of a nilpotent $\overset{ab}{(k)}^{\dagger}$ is $\eta^{aa}\overset{ab}{(-k)}$, it follows that the Hermitian conjugated partners of the Clifford odd "basis vectors" with an odd number of nilpotents must belong to a different group of $2^{\frac{d}{2}-1}$ members in $2^{\frac{d}{2}-1}$ families.

The Clifford even "basis vectors" with an even number of nilpotents have their Hermitian conjugated partners within the same group; projectors are self adjoint, S^{ac} transforms $\overset{ab}{(k)} *_A \overset{cd}{(k')}$ into $\overset{ab}{[-k]} *_A \overset{cd}{[-k']}$, while $\tilde{S}^{ac}$ transforms $\overset{ab}{(k)} *_A \overset{cd}{(k')}$ into $\overset{ab}{[k]} *_A \overset{cd}{[k']}$, what follows if taking into account Eq. (10.7). Since the number of the Clifford odd products of γ^a's is equal to the number of the Clifford even products of γ^a's, there must be another group of the Clifford even "basis vectors" with $2^{\frac{d}{2}-1} \times 2^{\frac{d}{2}-1}$ members.

We learn [8, 10] that one group of the Clifford even "basis vectors" transforms the family members of the Clifford odd "basis vectors" among themselves, while the second group of the Clifford even "basis vectors" transform any member of a family to the same member of another families.

Let us clear up that the algebraic application, $*_A$, of the Clifford even "basis vectors", we name them either $^I\hat{\mathcal{A}}_f^{m\dagger}$ if they are of the first kind or $^{II}\hat{\mathcal{A}}_f^{m\dagger}$ if they are of the second kind, on the Clifford odd "basis vectors", we name them $\hat{b}_{f^{\cdot}}^{m'\dagger}$, transforms the Clifford odd "basis vectors" into the Clifford odd "basis vectors", meaning that while the Clifford odd "basis vectors" carry the half integer values of the Cartan subalgebra members eigenvalues, $\pm\frac{i}{2}$ or $\pm\frac{1}{2}$, carry the Clifford even "basis vectors" the eigenvalues of the Cartan subalgebra members $(\pm i, 0)$ or $(\pm 1, 0)$, in agreement with $\mathcal{S}^{ab} = (S^{ab} + \tilde{S}^{ab})$ [8, 10].

10.2.1 "Basis vectors" in $d = 2(2n + 1)$-dimensional internal spaces from the point of view of $d = (3 + 1)$

This part overviews several papers with the same topic ([7–10] and references therein).

i. *The Clifford odd "basis vectors"*

---

[7] An odd product of nilpotents anti-commute with another product of an odd number of nilpotents, explaining the anti-commutation postulates for fermions. To the creation operators, which are tensor products of the "basis vectors" and the basis in ordinary space, determine anti-commutativity the "basis vectors". Correspondingly the even products of nilpotents explain the commutation postulates for boson fields.

Let us start in $d = 2(2n + 1)$ with the "basis vector" $\hat{b}_1^{1\dagger}$ which is the product of only nilpotents, all the rest members belonging to the $f = 1$ family follow by the application of S^{ab}, presented on the left-hand side of Eq. (10.8). Their Hermitian conjugated partners, $\hat{b}_f^m = (\hat{b}_f^{m\dagger})^\dagger$, are presented on the right-hand side [8].

$$
\hat{b}_1^{1\dagger} = \overset{03}{(+i)}\overset{12}{(+)}\overset{56}{(+)} \cdots \overset{d-1\,d}{(+)} , \qquad\qquad
\hat{b}_1^1 = \overset{03}{(-i)}\overset{12}{(-)} \cdots \overset{d-1\,d}{(-)} ,
$$
$$
\hat{b}_1^{2\dagger} = \overset{03}{[-i]}\overset{12}{[-]}\overset{56}{(+)} \cdots \overset{d-1\,d}{(+)} , \qquad\qquad
\hat{b}_1^2 = \overset{03}{[-i]}\overset{12}{[-]}\overset{56}{(-)} \cdots \overset{d-1\,d}{(-)} ,
$$
$$
\cdots \qquad\qquad\qquad\qquad\qquad \cdots
$$
$$
\hat{b}_1^{2^{\frac{d}{2}-1}\dagger} = \overset{03}{(+i)}\overset{12}{[-]}\overset{56}{[-]} \cdots \overset{d-3}{[-]}\overset{d-2}{[-]}\overset{d-1\,d}{[-]} , \quad
\hat{b}_1^{2^{\frac{d}{2}-1}} = \overset{03}{(-i)}\overset{12}{[-]}\overset{56}{[-]} \cdots \overset{d-3}{[-]}\overset{d-2}{[-]}\overset{d-1\,d}{[-]} ,
$$
$$
\cdots , \qquad\qquad\qquad\qquad\qquad \cdots . \tag{10.8}
$$

All the members on the left hand side are orthogonal among themselves, and all the members of the right hand side are orthogonal among themselves, due to Eq. (10.7) [9]. The anti-commutation relations among the "basis vectors" and their Hermitian conjugated partners fulfil the anti-commutation relations postulated by Dirac for the second quantized fermion fields, Eq. (10.11).

It is easy to reproduce all the matrices postulated by Dirac for all S^{ab}, although it is not needed; the application of any S^{ab} on any of the members of any of the families is very simple. [10]

The application of $\tilde{S}^{ab}$, they do not appear among the Dirac operators, are equally simple. The application of γ^a's, as well as of $\tilde{\gamma}^a$'s, on these states needs presentation of the Clifford even "basis vectors", since they change the Clifford odd "basis

---

[8] The algebraic product mark, $*_A$, among nilpotents and projectors is skipped.

[9]

$$
\hat{b}_f^{m\dagger} *_A \hat{b}_{f'}^{m'\dagger} = 0, \quad \hat{b}_f^m *_A \hat{b}_{f'}^{m'} = 0, \quad \forall m, m', f, f'. \tag{10.9}
$$

Any member of $2^{\frac{d}{2}-1}$ families follow by the application of $\tilde{S}^{ab}$.

Choosing the vacuum state equal to

$$
|\psi_{oc} >= \sum_{f=1}^{2^{\frac{d}{2}-1}} \hat{b}_f^m *_A \hat{b}_f^{m\dagger} |1 >, \tag{10.10}
$$

for one of the members m, which can be anyone of the odd irreducible representations f it follows that the Clifford odd "basis vectors" obey the relations

$$
\hat{b}_f^m {}_{*_A} |\psi_{oc} > = 0. |\psi_{oc} >,
$$
$$
\hat{b}_f^{m\dagger} {}_{*_A} |\psi_{oc} > = |\psi_f^m >,
$$
$$
\{\hat{b}_f^m, \hat{b}_{f'}^{m'}\}_{*_A +} |\psi_{oc} > = 0. |\psi_{oc} >,
$$
$$
\{\hat{b}_f^{m\dagger}, \hat{b}_{f'}^{m'\dagger}\}_{*_A +} |\psi_{oc} > = 0. |\psi_{oc} >,
$$
$$
\{\hat{b}_f^m, \hat{b}_{f'}^{m'\dagger}\}_{*_A +} |\psi_{oc} > = \delta^{mm'} \delta_{ff'} |\psi_{oc} > . \tag{10.11}
$$

[10] Let be pointed out that the Dirac's matrices were constructed for the massive fermions, correspondingly they do not anticommute [26] .

vectors" into the Clifford even "basis vectors" [8, 10].

ii. *The Clifford even "basis vectors"*

The Clifford even "basis vectors" appear in two orthogonal groups, named $^I\hat{\mathcal{A}}_f^{m\dagger}$ and $^{II}\hat{\mathcal{A}}_f^{m\dagger}$. Each group has $2^{\frac{d}{2}-1} \times 2^{\frac{d}{2}-1}$ members [11].

The generators S^{ab} and $\tilde{S}^{ab}$ generate from the starting "basis vector" of each group all the $2^{\frac{d}{2}-1} \times 2^{\frac{d}{2}-1}$ members. Each group contains the Hermitian conjugated partners within the same group; $2^{\frac{d}{2}-1}$ members of each group are products of only (self-adjoint) projectors, with all the eigenvalues of the Cartan subalgebra members, $\mathcal{S}^{ab} = (S^{ab} + \tilde{S}^{ab})$, presented in Eq. (11.4), equal zero.

$$
\begin{aligned}
^I\hat{\mathcal{A}}_1^{1\dagger} &= \overset{03}{(+i)}\overset{12}{(+)} \cdots \overset{d-1\,d}{[+]}, & ^{II}\hat{\mathcal{A}}_1^{1\dagger} &= \overset{03}{(-i)}\overset{12}{(+)} \cdots \overset{d-1\,d}{[+]}, \\
^I\hat{\mathcal{A}}_1^{2\dagger} &= \overset{03}{[-i]}\overset{12}{[-]}\overset{56}{(+)} \cdots \overset{d-1\,d}{[+]}, & ^{II}\hat{\mathcal{A}}_1^{2\dagger} &= \overset{03}{[+i]}\overset{12}{[-]}\overset{56}{(+)} \cdots \overset{d-1\,d}{[+]}, \\
^I\hat{\mathcal{A}}_1^{3\dagger} &= \overset{03}{(+i)}\overset{12}{(+)}\overset{56}{(+)} \cdots \overset{d-3\,d-2}{[-]}\overset{d-1\,d}{(-)}, & ^{II}\hat{\mathcal{A}}_1^{3\dagger} &= \overset{03}{(-i)}\overset{12}{(+)}\overset{56}{(+)} \cdots \overset{d-3\,d-2}{[-]}\overset{d-1\,d}{(-)}, \\
& \qquad \cdots & & \cdots
\end{aligned}
\tag{10.12}
$$

The Clifford even "basis vectors" belonging to two different groups are orthogonal due to the fact that they differ in the sign of one nilpotent or one projector or the algebraic product of a member of one group with a member of another group gives zero according to the third and fourth lines of Eq. (10.7): $\overset{ab}{(k)}\overset{ab}{[k]} = 0$, $\overset{ab}{[k]}\overset{ab}{(-k)} = 0$, $\overset{ab}{[k]}\overset{ab}{[-k]} = 0$.

$$
^I\hat{\mathcal{A}}_f^{m\dagger} *_A {}^{II}\hat{\mathcal{A}}_f^{m\dagger} = 0 = {}^{II}\hat{\mathcal{A}}^{m\dagger} \cdot_f *_A {}^I\hat{\mathcal{A}}_f^{m\dagger}.
\tag{10.13}
$$

The members of each of these two groups have the property.

$$
^i\hat{\mathcal{A}}_f^{m\dagger} *_A {}^i\hat{\mathcal{A}}_{f'}^{m'\dagger} \rightarrow
\begin{cases}
^i\hat{\mathcal{A}}_{f'}^{m\dagger}, i = (I, II) \\
\qquad \text{or zero}.
\end{cases}
\tag{10.14}
$$

For a chosen (m, f, f') there is only one m' (out of $2^{\frac{d}{2}-1}$) which gives a nonzero contribution.

Two "basis vectors", $^i\hat{\mathcal{A}}_f^{m\dagger}$ and $^i\hat{\mathcal{A}}_{f'}^{m'\dagger}$, the algebraic product, $*_A$, of which gives non zero contribution, "scatter" into the third one $^i\hat{\mathcal{A}}_{f'}^{m\dagger}$, for $i = (I, II)$.

10.2.2   The relations among the Clifford odd and the Clifford even "basis vectors"

The algebraic application, $*_A$, of the Clifford even "basis vectors" $^I\hat{\mathcal{A}}_f^{m\dagger}$ on the Clifford odd "basis vectors" $\hat{b}_{f'}^{m'\dagger}$ and the Clifford odd "basis vectors" $\hat{b}_f^{m\dagger}$ on

---

[11] The members of one group can not be reached by the members of another group by either S^{ab}'s or $\tilde{S}^{ab}$'s or both.

$^{\mathrm{II}}\hat{\mathcal{A}}_{\mathrm{f}}^{\mathrm{m}\dagger}$ gives

$$^{\mathrm{I}}\hat{\mathcal{A}}_{\mathrm{f}}^{\mathrm{m}\dagger} \;*_A\; \hat{\mathfrak{b}}_{\mathrm{f}'}^{\mathrm{m}'\dagger} \to \begin{cases} \hat{\mathfrak{b}}_{\mathrm{f}'}^{\mathrm{m}\dagger}\,, \\ \text{or zero}\,, \end{cases} \tag{10.15}$$

$$\hat{\mathfrak{b}}_{\mathrm{f}}^{\mathrm{m}\dagger} \;*_A\; {}^{\mathrm{II}}\hat{\mathcal{A}}_{\mathrm{f}'}^{\mathrm{m}'\dagger} \to \begin{cases} \hat{\mathfrak{b}}_{\mathrm{f}''}^{\mathrm{m}\dagger}\,, \\ \text{or zero}\,, \end{cases} \tag{10.16}$$

while

$$\hat{\mathfrak{b}}_{\mathrm{f}}^{\mathrm{m}\dagger} \;*_A\; {}^{\mathrm{I}}\hat{\mathcal{A}}_{\mathrm{f}'}^{\mathrm{m}'\dagger} = 0\,, \quad {}^{\mathrm{II}}\hat{\mathcal{A}}_{\mathrm{f}}^{\mathrm{m}\dagger} \;*_A\; \hat{\mathfrak{b}}_{\mathrm{f}'}^{\mathrm{m}'\dagger} = 0\,, \quad \forall(\mathrm{m}, \mathrm{m}', \mathrm{f}, \mathrm{f}')\,. \tag{10.17}$$

Eq. (11.10) demonstrates that $^{\mathrm{I}}\hat{\mathcal{A}}_{\mathrm{f}}^{\mathrm{m}\dagger}$, applying on $\hat{\mathfrak{b}}_{\mathrm{f}'}^{\mathrm{m}'\dagger}$, transforms the Clifford odd "basis vector" into another Clifford odd "basis vector" of the same family, transferring to the Clifford odd "basis vector" integer spins or gives zero.

Scattering of the Clifford odd "basis vector" $\hat{\mathfrak{b}}_{\mathrm{f}}^{\mathrm{m}\dagger}$ on $^{\mathrm{II}}\hat{\mathcal{A}}_{\mathrm{f}'}^{\mathrm{m}'\dagger}$ transforms the Clifford odd "basis vector" into another Clifford odd "basis vector" $\hat{\mathfrak{b}}_{\mathrm{f}''}^{\mathrm{m}\dagger}$ belonging to the same family member m of a different family f''.

Both groups of Clifford even "basis vectors" manifest as the gauge fields of the corresponding fermion fields: One concerning the family members quantum numbers, the other concerning the family quantum numbers.

The Clifford even "basis vectors" can be represented as algebraic products of the Clifford odd "basis vectors" and their Hermitian conjugated partners [10]:
Knowing the Clifford odd "basis vectors" $\hat{\mathfrak{b}}_{\mathrm{f}}^{\mathrm{m}\dagger}$ of one family (any one) we are able to generate all the Clifford even $^{\mathrm{I}}\hat{\mathcal{A}}_{\mathrm{f}'}^{\mathrm{m}'\dagger}$ "basis vectors"

$$^{\mathrm{I}}\hat{\mathcal{A}}_{\mathrm{f}}^{\mathrm{m}\dagger} = \hat{\mathfrak{b}}_{\mathrm{f}'}^{\mathrm{m}'\dagger} \;*_A\; (\hat{\mathfrak{b}}_{\mathrm{f}'}^{\mathrm{m}''\dagger})^{\dagger}\,. \tag{10.18}$$

Knowing the Clifford odd "basis vectors" $\hat{\mathfrak{b}}_{\mathrm{f}}^{\mathrm{m}\dagger}$ of one family member (any one) of all families we are able to generate all the Clifford even $^{\mathrm{II}}\hat{\mathcal{A}}_{\mathrm{f}'}^{\mathrm{m}'\dagger}$ "basis vectors"

$$^{\mathrm{II}}\hat{\mathcal{A}}_{\mathrm{f}}^{\mathrm{m}\dagger} = (\hat{\mathfrak{b}}_{\mathrm{f}'}^{\mathrm{m}'\dagger})^{\dagger} \;*_A\; \hat{\mathfrak{b}}_{\mathrm{f}''}^{\mathrm{m}'\dagger}\,. \tag{10.19}$$

10.2.3 Relations among fermions and their vector and scalar gauge fields under the assumptions that all the gauge fields are active (have non zero momentum) only in $\mathrm{d} = (3 + 1)$

We will learn in Sect. 10.3 that all the Clifford even "basis vectors" have to carry the space index α which is equal to $\mu = (0, 1, 2, 3)$ if they describe the vector component of the "basis vectors", and they are equal to $\sigma = (5, 6, ...)$ if describing the scalar components of the "basis vectors".

Let us start with few examples.

a. The $\mathrm{d} = (1 + 1)$ is very simple. We present it since we shall use it when trying to extend point fermion and boson fields into strings.

We have, in this case, two Clifford odd and two Clifford even eigenvectors of the Cartan subalgebra members

Clifford odd
$$\hat{b}_1^{1\dagger} = \overset{01}{(+i)}, \quad \hat{b}_1^1 = \overset{01}{(-i)},$$

Clifford even
$$^{I}\!\mathcal{A}_1^{1\dagger} = \overset{01}{[+i]}, \quad ^{II}\!\mathcal{A}_1^{1\dagger} = \overset{01}{[-i]}. \tag{10.20}$$

The two Clifford odd "basis vectors" are Hermitian conjugated to each other. The choice is made that $\hat{b}_1^{1\dagger} = \overset{01}{(+i)}$ is the "basis vector", and the second Clifford odd object is its Hermitian conjugated partner. There is only one family ($2^{\frac{d}{2}-1} = 1$) with one member. The vacuum state, Eq.(10.10), is for this choice equal to $|\psi_{oc}> = \overset{01}{[-i]}$. The eigenvalue S^{01} of $\hat{b}_1^{1\dagger}(= \overset{01}{(+i)})$ is $\frac{i}{2}$.

Each of the two Clifford even "basis vectors" is self adjoint (($^{I,II}\!\mathcal{A}_1^{1\dagger})^{\dagger} = {}^{I,II}\!\mathcal{A}_1^{1\dagger}$), with the eigenvalues $\mathcal{S}^{01}$ equal to 0.

We find, according to Eqs. (11.13, 11.14, 10.7), that

$$^{I}\!\mathcal{A}_1^{1\dagger} = \hat{b}_1^{1\dagger} *_A (\hat{b}_1^{1\dagger})^{\dagger}, \qquad ^{II}\!\mathcal{A}_1^{1\dagger} = (\hat{b}_1^{1\dagger})^{\dagger} *_A \hat{b}_1^{1\dagger}.$$

b. The case with $d = 2(2n + 1)$, with $n = 1$, is more illustrative. App. 10.6 presents the Clifford odd and even "basis vectors" in Table 10.1.

We have in this case 16 odd "basis vectors"; 4 families with 4 members each, and 16 their Hermitian conjugated partners.

Each family can represent the internal spaces of "positron" with positive "charge", $S^{56} = \frac{1}{2}$, and of an "electron" with negative "charge", $S^{56} = -\frac{1}{2}$, as can be seen in Table 10.1. The "basis vectors" of the "positron" and "electron" are related by the charge conjugation operator [12], which includes in $d = (5 + 1)$ operators $\gamma^0\gamma^5$, transforming $\hat{b}_f^{1\dagger}$ into $\hat{b}_f^{1\dagger}$, of each family f.

The Clifford even "basis vectors" appear in Table 10.1 in two orthogonal groups, each group has 16 members, their Hermitian conjugated partners appear within the same group. The eigenvalues of the Cartan subalgebra members $\mathcal{S}^{ab} = (S^{ab} + \tilde{S}^{ab})$ are equal to either $(\pm i, 0)$ or $(\pm 1, 0)$.

In Tables (2, 3, 4, 5) of Ref. [10], all the 32 Clifford even "basis vectors" are expressed as the algebraic products of the Clifford odd "basis vectors" and their Hermitian conjugated partners. Two of these tables, Tables (10.2, 10.3), are presented also in App. 10.6 of this contribution.

We will learn in Sect. 10.3 that all the Clifford even "basis vectors" have to carry the space index α which is equal to $\mu = (0, 1, 2, 3)$ if they describe the vector component of the "basis vectors", and they are equal to $\sigma = (5, 6)$ if describing the scalar components of the "basis vectors".

Let us illustrate these two groups of the Clifford even "basis vectors":

---

[12] In Ref. [23], the discrete symmetry operators for fermion fields in $d = 2(2n + 1)$ with the desired properties in $d = (3 + 1)$ are discussed.

Sixteen $^{I}\mathcal{A}_f^{m\dagger}$ transform family members of any of 4 families among themselves. One can check that the Clifford even "basis vectors" can be written as the algebraic products of the Clifford odd "basis vectors" and their Hermitian conjugated partners, Eqs. (11.13, 11.14); $^{I}\hat{\mathcal{A}}_f^{m\dagger} = \hat{b}_{f'}^{m'\dagger} *_A (\hat{b}_{f'}^{m''\dagger})^{\dagger}$.

To describe "photons", the "basis vectors" $^{I}\hat{\mathcal{A}}_f^{m\dagger}$ must not carry any non zero eigenvalues of the Cartan subalgebra members, Eq. (11.4), since the "photons" can give to "fermions" (to "electrons" and "positrons" in our case) only the spin offered by their space index μ. Table 10.2 presents "basis vectors" for four "photons", marked in Table 10.2 with $\bigcirc$. All are selfadjoint operators, offering to "basis vectors" of "electrons" and "positrons" no spin and no charge.

The remaining four Clifford even "basis vectors", appearing in the Hermitian conjugated pairs (marked either by $\triangle$ or by $\bullet$), would be allowed only if "fermions" and "bosons" have the non zero momenta in all six dimensions [13].

To describe "gravitons", the "basis vectors" $^{I}\hat{\mathcal{A}}_f^{m\dagger}$ must be able to offer the internal spin $\mathcal{S}^{12}$, (± 1), (with $\mathcal{S}^{03}$, $(\pm i)$), together with the spin offered by their space index μ, while $\mathcal{S}^{56}$ eigenvalue must be equal to zero (must be described by a projector, not to be able to change the charge of "electrons" and "positrons"). Table 10.3 presents "basis vectors" for four "gravitons", appearing in two Hermitian conjugated pairs, marked in Table 10.3 either by $\ddagger$ or by $\odot\odot$.

The remaining four Clifford even "basis vectors", $^{I}\hat{\mathcal{A}}_f^{m\dagger}$, appearing again in the Hermitian conjugated pairs (marked either by $\star\star$ or by $\otimes$), would be allowed only if "fermions" and "bosons" have the non zero momenta in all six dimensions [14].

Sixteen $^{II}\mathcal{A}_f^{m\dagger}$ transform a family member $\mathfrak{m}$ (any member) of a family f to the same family member $\mathfrak{m}$ of all 4 families. One can check that the Clifford even "basis vectors" can be written as the algebraic products of the Clifford odd "basis vectors" and their Hermitian conjugated partners, Eq. (11.14); $^{II}\hat{\mathcal{A}}_f^{m\dagger} = (\hat{b}_{f'}^{m'\dagger})^{\dagger} *_A \hat{b}_{f'}^{m''\dagger}$.

In Tables (4,5) of Ref. [10] all the sixteen members are presented.

Also $^{II}\mathcal{A}_f^{m\dagger}$ carry the space index α when taking part in creation operators. The space index α must be $\mu = (0, 1, 2, 3)$ when representing vector fields and $\sigma = (5, 6)$ when representing scalars [15].

If fermions and bosons are active (have non zero momenta) only in $d = (3 + 1)$ "gravitons" and "photons" $^{II}\mathcal{A}_f^{m\dagger}$ are only possible.

Let us present here one case among the 32 cases, presented in Table 5 of Ref. [10].

$$^{II}\hat{\mathcal{A}}_1^{4\dagger}(\equiv \overset{03}{[-i]}\,\overset{12}{[-]}\,\overset{56}{[-]}) = (\hat{b}_4^{1\dagger})^{\dagger} *_A \hat{b}_4^{1\dagger}(\equiv \overset{03}{(-i)}\,\overset{12}{(-)}\,\overset{56}{(-)} *_A \overset{03}{(+i)}\,\overset{12}{(+)}\,\overset{56}{(+)}).$$

This can easily be checked if taking into account Eq. (11.2) or Eq. (10.7).

---

[13] The Clifford even "basis vectors" including two nilpotents, $\overset{03}{(\pm i)}\overset{56}{(\pm 1)}$, would transform "electrons" into "positrons" and back, changing spin $\mathcal{S}^{03}$ and charge.

[14] These Clifford even "basis vectors", they include two nilpotents $\overset{12}{(\pm 1)}\overset{56}{(\pm 1)}$, would transform "electrons" into "positrons" and back, changing the spin $\mathcal{S}^{12}$ and charge.

[15] In Ref. ([7], and reference therein) the role of the scalars in the realistic case $d = (13 + 1)$, suggested by experiments while representing Higgs's scalars, is explained.

One can check also that $\hat{b}_4^{1\dagger} *_A {}^{II}\hat{\mathcal{A}}_1^{4\dagger} = \hat{b}_4^{1\dagger}$. The "basis vector" ${}^{II}\hat{\mathcal{A}}_1^{4\dagger}$ with $\mathcal{S}^{03} = \mathcal{S}^{12} = \mathcal{S}^{56} = 0$ can transfer to an "electron" or "positron" only its space momentum while it cannot change their internal properties.

10.2.4   The case with $d = 2(2n + 1)$, with $n = 3$, is what the experiments suggest

We have learned so far that to know all the $2^{\frac{d}{2}-1} \times 2^{\frac{d}{2}-1}$ members of the Clifford even "basis vectors" ${}^{I}\hat{\mathcal{A}}_f^{m\dagger}$ we need to know all the members of one (any one) family (one irreducible representation) of the Clifford odd "basis vectors" $\hat{b}_f^{m\dagger}$, Eq. (11.13) (and their Hermitian conjugated partners).
To know all the $2^{\frac{d}{2}-1} \times 2^{\frac{d}{2}-1}$ members of the Clifford even "basis vectors" ${}^{II}\hat{\mathcal{A}}_f^{m\dagger}$ we need to know one family member (any one) of all the families, Eq. (11.14) (and their Hermitian conjugated partners).
Before generating the Clifford even "basis vectors" as the algebraic products, $*_A$, of members of the Clifford odd "basis vectors", representing quarks and leptons and antiquarks and antileptons, let us shortly overview the properties of one irreducible representation of quarks and leptons appearing together with the antiquark and antileptons in Table 10.4 of App. 10.7.

In the even dimensional space $d = (13 + 1)$ ([14], App. A), one irreducible representation of the Clifford odd "basis vectors" if analysed from the point of view of the subgroups of the group $SO(13, 1)$ (including $SO(7, 1) \times SO(6)$, while $SO(7, 1)$ breaks into $SO(3, 1) \times SO(4)$, and $SO(6)$ breaks into $SU(3) \times U(1)$) contains the Clifford odd "basis vectors" describing internal spaces of quarks and leptons and antiquarks and antileptons, manifesting at low energies the quantum numbers assumed by the *standard model* before the electroweak break. Since $SO(4)$ contains two $SU(2)$ subgroups, $SU(2)_I$ and $SU(2)_{II}$, with the hypercharge of the *standard model* $Y = \tau^{23} + \tau^4$ (with τ^{23} belonging to $SU(2)_{II}$ and τ^4 originating in $SO(6)$, breaking to $SU(3) \times U(1)$), one irreducible representation includes the right-handed neutrinos and the left-handed antineutrinos, which are not in the *standard model* scheme [16].

In Table 10.4, one can read the quantum numbers of the Clifford odd "basis vectors" representing quarks and leptons *and antiquarks and antileptons* if taking into account that all the nilpotents and projectors are eigenvectors of one of the Cartan subalgebra members, $(S^{03}, S^{12}, S^{56}, \ldots, S^{13\,14})$, with the eigenvalues $\pm\frac{i}{2}$ or

---

[16] For an overview of the properties of the vector and scalar gauge fields in the *spin-charge-family* theory, the reader is invited to reed Refs. ([5,7,8,24,25] and the references therein). The reader can find in Table 10.4 that "basis vectors" of quarks have identical content of $SO(7, 1)$ as "basis vectors" of leptons (and antiquarks as antiletons); they differ only in the $SU(3) \times U(1)$.

$\pm\frac{1}{2}$, while for $(\mathcal{S}^{03}, \mathcal{S}^{12}, \mathcal{S}^{56}, \cdots, \mathcal{S}^{13\,14})$ the eigenvalues for $(\overset{ab}{\pm i})$ are $\pm i$, and for $(\overset{ab}{\pm})$ are ± 1, and for $[\overset{ab}{\pm i}]$ and $[\overset{ab}{\pm}]$ the eigenvalues are zero [17].

Taking into account that the third component of the *standard model* weak charge, $\tau^{13} = \frac{1}{2}(S^{56} - S^{78})$, of the third component of the second $SU(2)_{II}$ charge (not appearing in the *standard model*) $\tau^{23} = \frac{1}{2}(S^{56} + S^{78})$, of the colour charge $[\tau^{33} = \frac{1}{2}(S^{9\,10} - S^{11\,12})$ and $\tau^{38} = \frac{1}{2\sqrt{3}}(S^{9\,10} + S^{11\,12} - 2S^{13\,14})]$, of the "fermion charge" $\tau^{4} = -\frac{1}{3}(S^{9\,10} + S^{11\,12} + S^{13\,14})$, of the hyper charge $Y = \tau^{23} + \tau^{4}$, and of the electromagnetic charge $Q = Y + \tau^{13}$, one reproduces all the quantum numbers of quarks, leptons, and antiquarks, and antileptons.

Let us represent internal spaces (that is the "basis vectors") of photons, gravitons, weak bosons and coloured bosons in the way we learned in the cases **iv.b**, that is as algebraic products of the Clifford odd "basis vectors" (represented in Table 10.4 as $u_R^{ci}, d_R^{ci}, u_L^{ci}, d_L^{ci}$ for quarks of colour ci, as $\bar{u}_L^{\bar{c}i}, \bar{d}_L^{\bar{c}i}, \bar{u}_R^{\bar{c}i}, \bar{d}_R^{\bar{c}i}$ for antiquarks of the opposite colour, as ν_R, e_R, ν_L, e_L for leptons, $\bar{\nu}_L, \bar{e}_L, \bar{\nu}_R, \bar{e}_R$ for the corresponding antileptons, their Hermitian conjugated partners will be written as $(\ )^{\dagger}$).

Starting from photons we need to have in mind that photons can give to quarks and leptons only momentum in ordinary space, but cannot change internal spaces of quarks and leptons.

Let us look in Table 10.4 for u_R^{c1}, first line ([10], Eq. (46)). The photon $^{I}\hat{\mathcal{A}}^{\dagger}_{ph\,\bar{u}_R^{\bar{c}1} \to \bar{u}_R^{\bar{c}1}}$ interacts with $\bar{u}_{R\,39th}^{\bar{c}1}$ as follows

$$
^{I}\hat{\mathcal{A}}^{\dagger}_{ph\,\bar{u}_R^{\bar{c}1} \to \bar{u}_R^{\bar{c}1}} (\equiv \overset{03}{[+i]}\overset{12}{[+]}\overset{56}{[-]}\overset{78}{[+]}\overset{9\,10}{[-]}\overset{11\,12}{[+]}\overset{13\,14}{[+]}) \,*_A\, \bar{u}_{R\,39th}^{\bar{c}1} (\equiv \overset{03}{(+i)}\overset{12}{[+]}\overset{56}{(-)}\overset{78}{(+)}\overset{9\,10}{[-]}\overset{11\,12}{(+)}\overset{13\,14}{(+)})
$$
$$
\to \bar{u}_{R\,39th}^{\bar{c}1} (\equiv \overset{03}{(+i)}\overset{12}{[+]}\overset{56}{(-)}\overset{78}{(+)}\overset{9\,10}{[-]}\overset{11\,12}{(+)}\overset{13\,14}{(+)}), \quad ^{I}\hat{\mathcal{A}}^{\dagger}_{ph\,\bar{u}_R^{\bar{c}1} \to \bar{u}_R^{\bar{c}1}} = u_{R\,39th}^{\bar{c}1} \,*_A\, (u_{R\,39th}^{\bar{c}1})^{\dagger}.
$$

$$(10.21)$$

Similarly, one finds photons interacting with the rest of quarks and electrons and antiquarks and positrons [18].

Having in mind that bosons have an even number of nilpotents, and taking u_R^{c1} from the first and the second line of Table 10.4, we find that the "basis vector" of

---

[17] Let us remind the reader the difference between eigenvectors of S^{ab} and $\tilde{S}^{ab}$: Applying on a nilpotent they both give the same eigenvalue, while they give opposite eigenvalue if applying on a projector, Eq. (11.7).

[18] The break of symmetry, discussed in Ref. [7], but not yet really understood in this new way of presenting the internal space of boson fields, prevents neutrinos to interact with photons. Let us add that photons can not directly interact with another photons since the algebraic products of different selfadjoint operators are zero, but can interact with other boson fields, for example, with gravitons [10]. However, algebraic product of the "basis vector" which is a product of projectors by itself is the same "basis vector" back.

the "graviton" $^I\hat{\mathcal{A}}^\dagger_{gr\,u^{c1}_{R\uparrow}\to u^{c1}_{R\downarrow}}$ applies on $u^{c1}_{R\,1st}$ as follows

$$^I\hat{\mathcal{A}}^\dagger_{gr\,u^{c1}_{R\uparrow}\to u^{c1}_{R\downarrow}} (\equiv \overset{03}{(-i)}\overset{12}{(-)}\overset{56}{[+]}\overset{78}{[+]}\overset{9\,10}{[+]}\overset{11\,12}{[-]}\;\overset{13\,14}{[-]}\;) *_A \; u^{c1}_{R\,1st}(\equiv \overset{03}{(+i)}\overset{12}{[+]}\overset{56}{[+]}\overset{78}{(+)}\overset{9\,10}{(+)}\overset{11\,12}{[-]}\;\overset{13\,14}{[-]}\;)$$

$$\to u^{c1}_{R\,2nd}(\equiv \overset{03}{[-i]}\overset{12}{(-)}\overset{56}{[+]}\overset{78}{(+)}\overset{9\,10}{(+)}\overset{11\,12}{[-]}\;\overset{13\,14}{[-]}\;),\; ^I\hat{\mathcal{A}}^\dagger_{gr\,u^{c1}_{R\uparrow}\to u^{c1}_{R\downarrow}} = u^{c1}_{R\,2nd} *_A (u^{c1}_{R\,1st})^\dagger,$$

$$(10.22)$$

Similarly we can find the "basis vectors" of all gravitons transforming the spins S^{03} and S^{12} in internal spaces of quarks and leptons. The gravitons carry in addition the momentum in ordinary space time.

Looking for the weak bosons, which transform $d^{c1}_{L\,5th}$ (presented in Table 10.4 in 5th line) to $u^{c1}_{L\,7th}$ (presented in Table 10.4 in 7th line), we find

$$^I\hat{\mathcal{A}}^\dagger_{w1\,d^{c1}_L\to u^{c1}_L} (\equiv \overset{03}{[-i]}\overset{12}{[+]}\overset{56}{(+)}\overset{78}{(-)}\overset{9\,10}{[+]}\overset{11\,12}{[-]}\;\overset{13\,14}{[-]}\;) *_A \; d^{c1}_{L\,5th}(\equiv \overset{03}{[-i]}\overset{12}{[+]}\overset{56}{(-)}\overset{78}{(+)}\overset{9\,10}{(+)}\overset{11\,12}{[-]}\;\overset{13\,14}{[-]}\;)$$

$$\to u^{c1}_{L\,7th}(\equiv \overset{03}{[-i]}\overset{12}{[+]}\overset{56}{[+]}\overset{78}{[-]}\overset{9\,10}{(+)}\overset{11\,12}{[-]}\;\overset{13\,14}{[-]}\;)(\equiv \overset{03}{[-i]}\overset{12}{[+]}),\; ^I\hat{\mathcal{A}}^\dagger_{w1\,d^{c1}_L\to u^{c1}_L} = u^{c1}_{L\,7th} *_A (d^{c1}_{L\,5th})^\dagger.$$

$$(10.23)$$

We can find equivalently the weak bosons "basis vectors" which cause transformations among other weak pairs.

Let us look for the 'basis vectors' of gluons, transforming colour charges of quarks, for example, of $d^{c1}_{L\,5th}$ (presented in Table 10.4 in 5th line) to $d^{c3}_{L\,21st}$ (presented in Table 10.4 in 21st line)

$$^I\hat{\mathcal{A}}^\dagger_{gl\,d^{c1}_L\to d^{c3}_L} (\equiv \overset{03}{[-i]}\overset{12}{[+]}\overset{56}{[-]}\overset{78}{[+]}\overset{9\,10}{(-)}\;\overset{11\,12}{[-]}\;\overset{13\,14}{(+)}\;) *_A \; d^{c1}_{L\,5th}(\equiv \overset{03}{[-i]}\overset{12}{[+]}\overset{56}{(-)}\overset{78}{(+)}\overset{9\,10}{(+)}\overset{11\,12}{[-]}\;\overset{13\,14}{[-]}\;)$$

$$\to d^{c3}_{L\,21st}(\equiv \overset{03}{[-i]}\overset{12}{[+]}\overset{56}{(-)}\overset{78}{(+)}\overset{9\,10}{[-]}\;\overset{11\,12}{[-]}\;\overset{13\,14}{(+)}\;),\quad ^I\hat{\mathcal{A}}^\dagger_{gl\,d^{c1}_L\to d^{c3}_L} = d^{c3}_{L\,21st} *_A (d^{c1}_{L\,5th})^\dagger.$$

$$(10.24)$$

Let us conclude this section by repeating what we have learned in it: This section presents the internal degrees of freedom as the Clifford odd "basis vectors" for fermion fields and as the Clifford even "basis vectors" for boson fields for internal spaces $d = 2(2n + 1), n = 0, 1$ and for $n = 3$. The creation operators for both fields are tensor products of "basis vectors" and basis in ordinary space-time. The Clifford even "basis vectors" of boson fields carry in addition the space index α, Sect. 10.3.

There is the same number of the "basis vectors" of fermion and boson fields, manifesting a kind of supersymmetry. While fermion fields appear in families and have their Hermitian conjugated partners in a separate groups, appear boson "basis vectors" in two orthogonal groups, with their Hermitian conjugated partners within each group.

There is the break of symmetries which makes the number of observed families of fermions and their observed gauge fields reduced [7]. But the assumption that the

fermion and boson fields have non zero momenta only in $d = (3 + 1)$ breaks the Lorentz symmetry; the rotations $M^{ms} = L^{ms} + S^{ms}$, $m = (0, 1, 2, 3, s = (5, 6, ...)$, ($S^{ms}$ can be replaced by $\tilde{S}^{ms}$ and $\mathcal{S}^{ms}$), for example, can not go.

To extend point fields to strings, we can use the "basis vectors" for the extended part, presented in Eq. (11.18). For the extension of the fermion fields we can have $\hat{b}_1^{1\dagger} = \overset{01}{(+i)}$ and for its Hermitian conjugated partner $\hat{b}_1^1 = (\hat{b}_1^{1\dagger})^\dagger = \overset{01}{(-i)}$. For the two boson fields we have $^I\mathcal{A}_1^{1\dagger} = \overset{01}{[+i]}$ and $^{II}\mathcal{A}_1^{1\dagger} = \overset{01}{[-i]}$ [19].

Sect. 11.2.1 discusses a possible extension of point fields to strings.

10.3 Creation and annihilation operators for fermion and boson fields in $d = (3 + 1)$

To define the creation operators for fermion or boson fields, besides the "basis vectors" defining the internal spaces of fermions and bosons, the basis in ordinary space in momentum or coordinate representation is needed. Let us shortly overview Ref. [10], Sect. 3. (The extended version is presented in Ref. [7] in Subsect. 3.3 and App. J.)
The momentum basis is continuously infinite

$$|\vec{p} > = \hat{b}_{\vec{p}}^\dagger |0_p >, \quad < \vec{p}| = < 0_p |\hat{b}_{\vec{p}},$$

$$< \vec{p}|\vec{p}' > = \delta(\vec{p} - \vec{p}') = < 0_p |\hat{b}_{\vec{p}} \hat{b}_{\vec{p}'}^\dagger |0_p >,$$

pointing out

$$< 0_p |\hat{b}_{\vec{p}'} \hat{b}_{\vec{p}}^\dagger |0_p > = \delta(\vec{p}' - \vec{p}), \tag{10.25}$$

with the normalization $< 0_p |0_p >= 1$. While the quantized operators $\hat{\vec{p}}$ and $\hat{\vec{x}}$ commute $\{\hat{p}^i, \hat{p}^j\}_- = 0$, $\{\hat{x}^k, \hat{x}^l\}_- = 0$, it follows for $\{\hat{p}^i, \hat{x}^j\}_- = i\eta^{ij}$. One correspondingly finds

$$< \vec{p}|\vec{x} > = < 0_{\vec{p}} |\hat{b}_{\vec{p}} \hat{b}_{\vec{x}}^\dagger |0_{\vec{x}} > = (< 0_{\vec{x}} |\hat{b}_{\vec{x}} \hat{b}_{\vec{p}}^\dagger |0_{\vec{p}} >)^\dagger$$

$$< 0_{\vec{p}} |\{\hat{b}_{\vec{p}}^\dagger, \hat{b}_{\vec{p}'}^\dagger\}_- |0_{\vec{p}} > = 0, < 0_{\vec{p}} |\{\hat{b}_{\vec{p}}, \hat{b}_{\vec{p}'}\}_- |0_{\vec{p}} > = 0, < 0_{\vec{p}} |\{\hat{b}_{\vec{p}}, \hat{b}_{\vec{p}'}^\dagger\}_- |0_{\vec{p}} > = 0,$$

$$< 0_{\vec{x}} |\{\hat{b}_{\vec{x}}^\dagger, \hat{b}_{\vec{x}'}^\dagger\}_- |0_{\vec{x}} > = 0, < 0_{\vec{x}} |\{\hat{b}_{\vec{x}}, \hat{b}_{\vec{x}'}\}_- |0_{\vec{x}} > = 0, < 0_{\vec{x}} |\{\hat{b}_{\vec{x}}, \hat{b}_{\vec{x}'}^\dagger\}_- |0_{\vec{x}} > = 0,$$

$$< 0_{\vec{p}} |\{\hat{b}_{\vec{p}}, \hat{b}_{\vec{x}}^\dagger\}_- |0_{\vec{x}} > = e^{i\vec{p}\cdot\vec{x}} \frac{1}{\sqrt{(2\pi)^{d-1}}}, < 0_{\vec{x}} |\{\hat{b}_{\vec{x}}, \hat{b}_{\vec{p}}^\dagger\}_- |0_{\vec{p}} > = e^{-i\vec{p}\cdot\vec{x}} \frac{1}{\sqrt{(2\pi)^{d-1}}}.$$

$$\tag{10.26}$$

 The creation operators for either fermion or boson fields must be tensor products, $*_T$, of both contributions, the "basis vectors" describing the internal space of fermions or bosons and the basis in ordinary momentum or coordinate space.

---

[19] Let us repeat that knowing the fermion "basis vectors" allows us to find both kinds of "boson fields", $^I\mathcal{A}_1^{1\dagger} = \hat{b}_1^{1\dagger} *_A (\hat{b}_1^{1\dagger})^\dagger = \overset{01}{(+i)} *_A \overset{01}{(-i)} = \overset{01}{[+i]}$, and $^{II}\mathcal{A}_1^{1\dagger} = (\hat{b}_1^{1\dagger})^\dagger *_A \hat{b}_1^{1\dagger} = \overset{01}{(-i)} *_A \overset{01}{(+i)} = \overset{01}{[-i]}$.

The creation operators for a free massless fermion field of the energy $p^0 = |\vec{p}|$, belonging to a family f and to a superposition of family members m applying on the extended vacuum state including both spaces, $|\psi_{oc} > *_T |0_{\vec{p}} >$, can be written as

$$\hat{b}_f^{s\dagger}(\vec{p}) = \sum_m c^{sm}{}_f(\vec{p}) \, \hat{b}_{\vec{p}}^\dagger \, *_T \, \hat{b}_f^{m\dagger} . \tag{10.27}$$

The creation operators $\hat{b}_f^{s\dagger}(\vec{p})$ and their Hermitian conjugated partners annihilation operators $\hat{b}_f^s(\vec{p})$, creating and annihilating the single fermion states, respectively, fulfil when applying the vacuum state, $|\psi_{oc} > *_T |0_{\vec{p}} >$, the anti-commutation relations for the second quantized fermions, postulated by Dirac (Ref. [8], Sect.3), explaining the Dirac's second quantization postulates for fermions.

$$< 0_{\vec{p}} | \{\hat{b}_{f'}^{s'}(\vec{p}'), \hat{b}_f^{s\dagger}(\vec{p})\}_+ |\psi_{oc} > |0_{\vec{p}} > = \delta^{ss'} \delta_{ff'} \delta(\vec{p}' - \vec{p}) \cdot |\psi_{oc} >,$$
$$\{\hat{b}_{f'}^{s'}(\vec{p}'), \hat{b}_f^s(\vec{p})\}_+ |\psi_{oc} > |0_{\vec{p}} > = 0 \cdot |\psi_{oc} > |0_{\vec{p}} >,$$
$$\{\hat{b}_{f'}^{s',\dagger}(\vec{p}'), \hat{b}_f^{s\dagger}(\vec{p})\}_+ |\psi_{oc} > |0_{\vec{p}} > = 0 \cdot |\psi_{oc} > |0_{\vec{p}} >,$$
$$\hat{b}_f^{s\dagger}(\vec{p}) |\psi_{oc} > |0_{\vec{p}} > = |\psi_f^s(\vec{p}) >,$$
$$\hat{b}_f^s(\vec{p}) |\psi_{oc} > |0_{\vec{p}} > = 0 \cdot |\psi_{oc} > |0_{\vec{p}} >,$$
$$|p^0| = |\vec{p}| . \tag{10.28}$$

The creation operators for boson gauge fields must carry the space index α, describing the α component of the boson field in the ordinary space [10], Eq. (24)). We, therefore, add the space index α as follows

$$^i \hat{\mathcal{A}}_{f\alpha}^{m\dagger}(\vec{p}) = {}^i \hat{\mathcal{C}}^m{}_{f\alpha}(\vec{p}) \, *_T \, {}^i \hat{\mathcal{A}}_f^{m\dagger} , i = (I, II), \tag{10.29}$$

with $^i \hat{\mathcal{C}}^m{}_{f\alpha}(\vec{p}) = {}^i \mathcal{C}^m{}_{f\alpha} \, \hat{b}_{\vec{p}}^\dagger$, with $\hat{b}_{\vec{p}}^\dagger$ defined in Eqs. (11.15, 10.26). We treat free massless bosons of momentum $\vec{p}$ and energy $p^0 = |\vec{p}|$ and of particular "basis vectors" $^i \hat{\mathcal{A}}_f^{m\dagger}$'s which are eigenvectors of all the Cartan subalgebra members. The creation operators for boson gauge fields commute.

10.4   Points in ordinary space-time extended to strings; representations of fermions and bosons in odd dimensional spaces

One possibility to achieve renormalizability of the proposed theory might be, learning from string theories [18, 19], by extending the points in ordinary space-time to strings. A second possibility might be to find out what can offer the internal odd-dimensional spaces, manifesting two groups of anti-commuting "basis vectors" and two groups of commuting "basis vectors", as mentioned in Sect. 11.1 and explained in Ref. [9, 22]. One of the two groups of either anti-commuting or commuting "basis vectors" manifest a kind of Fadeev-Popov ghost.

Let us start with the first possibility: extending the points in ordinary space-time to strings.

Let us try to extend the fermion and boson fields, expressed as tensor products, $*_T$, of the "basis vectors" describing the internal spaces of fermion and boson fields and the basis in ordinary space-time to strings, in the hope of achieving renormalizability for the theory of free massless fermion and boson fields. As we discussed in Sect. 10.2, the number of "basis vectors" which represent internal spaces of fermions and the number of their Hermitian conjugated partners (both together have $2 \times 2^{\frac{d}{2}-1} \times 2^{\frac{d}{2}-1}$), equals to the number of "basis vectors" representing the internal spaces of bosons, appearing in two orthogonal groups, 2^{d-1} [20], manifesting a kind of supersymmetry. (This is, however, not the usual kind of supersymmetry requiring that each fermion has a partner with the same charge among bosons, and vice versa.

We shall see that a trial to extend point particles in ordinary space-time to strings in a "stringy way" requires to introduce the strings time, besides the ordinary space-time and correspondingly also the corresponding "basis vectors" in $d = (1 + 1)$ in a string.

We assume that fermion and boson fields are active (having non-zero momenta) only in $d = (3 + 1)$ [21], while we choose $d = 2(2n + 1)$ in the internal space. The observations suggest $n = 3$.

Let us first assume a simple starting action, simplifying the action in Ref ([7] and in the references therein) for free massless fermion fields, and the corresponding free massless boson fields in $d = 2(2n + 1)$-dimensional space, having non zero momenta only in $d = (3 + 1)$, while taking into account the creation operators for fermion and boson fields expressed by the corresponding "basic vectors", Eqs. (11.16, 11.17) [22].

$$
\begin{aligned}
\mathcal{A} &= \int d^4x \, \frac{1}{2} \left(\bar{\psi} \gamma^\alpha p_{0\alpha} \psi \right) + \text{h.c.} + \\
&\quad \int d^4x \sum_{i=(I,II)} {}^i \hat{F}^{mf}_{\alpha\beta} \; {}^i \hat{F}^{mf\alpha\beta} , \\
p_{0\alpha} &= p_\alpha - \sum_{mf} {}^I \hat{\mathcal{A}}^{m\dagger}_f \; {}^I \mathcal{C}^m_{f\alpha} - \sum_{mf} {}^{II} \hat{\mathcal{A}}^{m\dagger}_f \; {}^{II} \mathcal{C}^m_{f\alpha} , \\
{}^i \hat{F}^{mf}_{\alpha\beta} &= \partial_\alpha \, {}^i \hat{\mathcal{A}}^{m\dagger}_{f\beta} - \partial_\beta \, {}^i \hat{\mathcal{A}}^{m\dagger}_{f\alpha} + \varepsilon f^{m''f''mfm'f'i} \, {}^i \hat{\mathcal{A}}^{m\dagger}_{f\alpha} \, {}^i \hat{\mathcal{A}}^{m'\dagger}_{f'\beta} , \\
i &= (I, II) .
\end{aligned}
\tag{10.30}
$$

---

[20] One group of boson "basis vectors", while applying to any of members of fermion families, forms a member of the same family. The second group of boson "basis vectors", when applying to a particular member of a family transforms this member into the same member of another family, Subsect. 10.2.4.

[21] This assumption is not needed, but it seems meaningful.

[22] The fermion states ψ are defined by $\hat{b}^{s\dagger}_f(\vec{x}, x^0) = \sum_m \hat{b}^{m\dagger}_f \int_{-\infty}^{+\infty} \frac{d^{d-1}p}{(\sqrt{2\pi})^{d-1}} c^{ms}{}_f \; (\vec{p}) \; \hat{b}^\dagger_{\vec{p}} \; e^{-i(p^0 x^0 - \varepsilon \vec{p} \cdot \vec{x})}$, applying on the vacuum state $|\psi_{oc}> \; *_T |0_{\vec{p}} >$. The boson states are defined by ${}^I \hat{\mathcal{A}}^{m\dagger}_{f\mu}(\vec{x}, x^0) = \int_{-\infty}^{+\infty} \frac{d^{d-1}p}{(\sqrt{2\pi})^{d-1}} \, {}^I \hat{\mathcal{A}}^{m\dagger}_{f\mu}(\vec{p}) \, e^{-i(p^0 x^0 - \varepsilon \vec{p} \cdot \vec{x})}|_{p^0=|\vec{p}|}$, with the vacuum state equal to $| \; 1 >$.

ψ represent $2^{\frac{d}{2}-1}$ members of one family of all the $2^{\frac{d}{2}-1}$ families, and $\bar{\psi} = (\psi)^{\dagger}\gamma^0$ their $2^{\frac{d}{2}-1} \times 2^{\frac{d}{2}-1}$ Hermitian conjugated partners (multiplied by γ^0). $^{i}\hat{\mathcal{A}}_{f}^{m\dagger}\ ^{i}\mathcal{C}_{f\alpha}^{m}, i = (I, II)$, represent two orthogonal groups of "basis vectors" in a tensor product with basis in ordinary space-time, extended by the space index $\alpha = \mu$ for vectors and $\alpha \geq 5$ for scalars in ordinary space-time, each with $2^{\frac{d}{2}-1} \times 2^{\frac{d}{2}-1}$ members [23]. The assumed action, Eq. (10.30), needs further studies, since the studies so far were mainly done by Eqs. (100, 101) of the reference [7].

Let us repeat: The description of the internal spaces of fermion and boson fields with the odd and even Clifford algebra objects, respectively, offers an equal number of fermions and bosons, demonstrating a (kind of) supersymmetry. However, none of the "basis vectors" of the boson fields, obtained by the application of γ^{α} on the fermion "basis vectors" (the application from the left-hand side generates $^{II}\hat{\mathcal{A}}_{f}^{m\dagger}$, the application from the right-hand side generates $^{I}\hat{\mathcal{A}}_{f}^{m\dagger}$) do carry the same internal charges as the fermion "basis vectors" [24].

We represent in Sect. 10.2 the "basis vectors" of fermion and boson fields for any $d = 2(2n + 1)$, in particular also for $d = (13 + 1)$ [25].

We demonstrated the "basis vectors" for the corresponding vector and scalar gauge fields observed so far, Subsect. 10.2.4: Photons, gravitons, weak bosons and gluons. [26]

---

[23] The assumption that all the fermion and boson fields are active (have non zero momentum) only in $d = (3 + 1)$ ordinary space-time mean that the derivative with respect to x_{α} gives zero.

[24] The quantum numbers of u_{L}^{c1}, presented in Table 10.4 in the seventh line $u_{L}^{c1} (\equiv \overset{03}{[-i]} \overset{12}{[+]}$ $\overset{56}{|} \overset{78}{[+]} [-] \overset{9\ 10}{\|} \overset{11\ 12}{(+)} \overset{13\ 14}{[-]} [-]$, are: $S^{12} = \frac{1}{2}, S^{03} = -\frac{i}{2}, \tau^{13} = \frac{1}{2}(S^{56} - S^{78}) = \frac{1}{2}, \tau^{23} = \frac{1}{2}(S^{56} + S^{78}) = 0, \tau^{33} = \frac{1}{2}(S^{9\ 10} - S^{11\ 12}) = \frac{1}{2}, \tau^{38} = \frac{1}{2\sqrt{3}}(S^{9\ 10} + S^{11\ 12} - 2S^{13\ 14}) = \frac{1}{2\sqrt{3}}$.
For the corresponding boson "basic vector" obtained by multiplication of u_{L}^{c1} from the left-hand side by γ^9 one obtains: $\gamma^9\ u_{L}^{c1} \overset{03}{[-i]} \overset{12}{[+]} \overset{56}{|} \overset{78}{[+]} [-] \overset{9\ 10}{\|} \overset{11\ 12}{(+)} \overset{13\ 14}{[-]} [-]$ leading to $\overset{03}{[-i]} \overset{12}{[+]} \overset{56}{|} \overset{78}{[+]} [-] \overset{9\ 10}{\|} \overset{11\ 12}{[-]} \overset{13\ 14}{[-]} [-]$. Having all the quantum numbers equal zero, this boson represents a photon. Having all the members of the algebraic product equal to projectors, and taking into account that for Clifford even "basis vectors" $\mathcal{S}^{ab} = (S^{ab} + \tilde{S}^{ab})$, which gives zero for the projectors, the product of projectors only means that such an object can not change the internal space of Clifford odd "basis vectors", what photons do not. Photons can give to fermions only the momentum in the ordinary space time, Eq. (10.21).

[25] Let us repeat that the choice $d = (13 + 1)$ offers to describe all the quarks and antiquarks and leptons and antileptons observed so far, predicts the existence of the right-handed neutrinos and left-handed antineutrinos and another weak field; requires the existence of families of quarks and leptons and the existence of the dark matter; announces the existence of a fourth family to the observed three; explains the existence of the scalar fields as the Higgs boson; predicts new scalar fields that gave rise to inflation of the universe after the Big Bang, offers the explanation for many a cosmological observation.

[26] There are additional gauge fields which can not be observed since this would break Lorentz invariance if requiring Lorentz transformations of the kind $M^{as}, a = (0, 1, 2, 3)$ and $s \geq 5$ due to the assumption that all the fields have non zero momentum only in $d = (3 + 1)$. Without additional break of symmetry there could exist gauge fields, which change more than only one kind of charge at the same time.

We can obtain gravitino if we extend points in ordinary space-time to strings. Describing strings with "basis vectors" being the eigenvectors of the Cartan subalgebra members $S^{01}, \tilde{S}^{01}, \mathcal{S}^{01} = (S^{01} + \tilde{S}^{01})$, on a string (σ, τ), we have, in this case, two Clifford odd — one "basis vector" and one Hermitian conjugated partner — and two Clifford even objects, Eq. (11.18),

$$\text{Clifford odd}$$
$$\hat{b}_{1s}^{1\dagger} = \overset{01}{(+i)}_s, \quad \hat{b}_{1s}^{1} = \overset{01}{(-i)},$$
$$\text{Clifford even}$$
$${}^{I}\mathcal{A}_{1s}^{1\dagger} = \overset{01}{[+i]}_s, \quad {}^{II}\mathcal{A}_{1s}^{1\dagger} = \overset{01}{[-i]}_s.$$

Index s points out that these "basis vectors" belong to the strings extensions and not to the "basis vectors" representing internal spaces of fermion and boson fields. The two Clifford odd "basis vectors" in the above equation are Hermitian conjugated to each other. Let us make a choice that $\hat{b}_{1s}^{1\dagger} \equiv \overset{01}{(+i)}_s$ is the "basis vector" (applying on the vacuum state, Eq. (10.10), $|\psi_{ocs}> = \overset{01}{[-i]}_s$). There is only one family $(2^{\frac{d}{2}-1} = 1)$ with one member. The eigenvalue S^{01} of $\hat{b}_{1s}^{1\dagger}(=\overset{01}{(+i)}_s)$ is $\frac{i}{2}$. Each of the two Clifford even "basis vectors" is self adjoint $(({}^{I,II}\mathcal{A}_{1s}^{1\dagger})^{\dagger} = {}^{I,II}\mathcal{A}_{1s}^{1\dagger})$, with the eigenvalues $\mathcal{S}^{01}$ equal to 0.

The internal space of photons (like it is ${}^{I}\hat{\mathcal{A}}^{\dagger}_{ph\,\bar{u}_R^{c1} \to \bar{u}_R^{c1}} (\equiv \overset{03}{[+i]}\overset{12}{[+]}\overset{56}{[-]}\overset{78}{[+]}\overset{9\,10}{[-]}\overset{11\,12}{[+]}\overset{13\,14}{[+]})$, Eq.(10.21)), extended by a tensor product, $*_{T'}$, with a string $\hat{b}_{1s}^{1\dagger}(\equiv \overset{01}{(+i)}_s)$, can represent anticommuting gravitinos since the photon carries the space-time index μ.

The extensions of all the other "basis vectors" of space-time — either the Clifford odd ones describing the internal spaces of fermions, or Clifford even ones describing the internal spaces of bosons — by the tensor product, $*_{T'}$ with the two self adjoint "basis vectors" describing the internal space on the string, ${}^{i}\mathcal{A}_{1s}^{1\dagger}, i = (I, II)$, do not change commutation properties. The extended "basis vectors" remain commuting or anti-commuting.

The extensions of "basis vectors" of space-time by the tensor product, $*_{T'}$, with $\hat{b}_{1s}^{1\dagger}$ do change the commutation relations: The commuting ones become anti-commuting, the anti-commuting become commuting.

The meaning of the $2^{\frac{14}{2}-1}$ "basis vectors" in tensor extension by $\hat{b}_{1s}^{1\dagger}$ needs further study.

The extension of point fields in $d = (3+1)$ ordinary space-time (with "basis vectors" determined in $d = (13+1)$) to strings needs the corresponding change of the action, presented in Eq. (10.30), which is under consideration.

In a separate paper of this proceedings the author discusses the content of the "basis vectors" after the "basis vectors" describing the internal spaces of fermions $(\hat{b}_f^{m\dagger})$ and bosons $({}^{I,II}\mathcal{A}_f^{m\dagger})$ in $d = (13+1)$ are extended by a tensor products with the string's "basis vectors" of fermions $(\hat{b}_{1s}^{1\dagger})$ and bosons $({}^{I,II}\mathcal{A}_{1s}^{1\dagger})$ presented in Eq. (11.18).

It follows:

$$\hat{b}_f^{m\dagger} *_{T'} \; ^{I,II}\mathcal{A}_{1s}^{1\dagger}$$

represent the anti-commuting "basis vectors" of fermions in the internal space $SO(d-1,1)$, having the Hermitian conjugated partners in a separate group; the projectors $[\pm i]_s^{\overset{01}{}}$, namely, do not change anti-commutativity of fermion "basis vectors".

$$^{I,II}\mathcal{A}_f^{m\dagger} *_{T'} \; ^{I,II}\mathcal{A}_{1s}^{1\dagger}$$

represent the commuting "basis vectors" of bosons in the internal space $SO(d-1,1)$, appearing in two orthogonal groups; the projectors $[\pm i]_s^{\overset{01}{}}$, namely, do not change commutativity of boson "basis vectors".

$$^{I,II}\mathcal{A}_f^{m\dagger} *_{T'} \; \hat{b}_{1s}^{1\dagger}$$

represent the anticommuting "basis vectors" of new fermions, with the quantum numbers of bosons in the internal space $SO(d-1,1)$; the nilpotents $\hat{b}_{1s}^{1\dagger} \equiv (+i)_s^{\overset{01}{}}$, namely, changes commutativity of boson "basis vectors" keeping their quantum numbers unchanged.

$$\hat{b}_f^{m\dagger} *_{T'} \; \hat{b}_{1s}^{1\dagger}$$

represent the commuting "basis vectors" of new bosons with the quantum numbers of fermions in the internal space $SO(d-1,1)$, $\hat{b}_{1s}^{1\dagger} \equiv (+i)^{\overset{01}{}}$ change the anticommutativity of $\hat{b}_f^{m\dagger}$.

This does not look as the usually desired supersymmetry, requiring that each fermion (in our case one of $2^{\frac{d}{2}-1}$ members appearing in $2^{\frac{d}{2}-1}$ families, having their Hermitian conjugated partner in a separate group) has a supersymmetric partner with the same charges and with the spin 0. It does not look either that any boson field (in our case any one of two groups each with $2^{\frac{d}{2}-1} \times 2^{\frac{d}{2}-1}$ members) has a supersymmetric partner with the same charges and with the spin $\frac{1}{2}$.

There is another possibility to achieve the supersymmetric partners to the "basis vectors" presented fermions and bosons in $2(2n+1)$ dimensional internal spaces of fermions and bosons. It will be discussed in a separate contribution to the Bled Proceeding 2024. One can namely go to an odd dimensional space $d = 2(2n+1) + 1$. As discussed in the article [9] there are two groups of "basis vectors" in odd dimensional spaces;

One group determines the anti-commuting "basis vectors" of $2^{\frac{d-1}{2}-1}$ fermions appearing in $2^{\frac{d-1}{2}-1}$ families with their $2^{\frac{d}{2}-1} \times 2^{\frac{d}{2}-1}$ Hermitian conjugated partners appearing in a separate group, as well as two orthogonal groups each with $2^{\frac{d}{2}-1} \times 2^{\frac{d}{2}-1}$ of "basis vectors", with their Hermitian conjugated partners within the same group.

The second group determines anti-commuting "basis vectors" appearing in two separate orthogonal groups each with $2^{\frac{d}{2}-1} \times 2^{\frac{d}{2}-1}$ of "basis vectors", with their Hermitian conjugated partners within the same group, as well as the commuting "basis vectors" of "fermions" appearing in families with their Hermitian conjugated partners in a separate group.

Also these two groups might demonstrate a kind of supersymmetry.

Let us finish this section by pointing out that the proposed theory offers:

Photons with "basis vectors" including only projectors; gravitons with "basis vectors" having two nilpotents only in $SO(3,1)$ of $SO(13,1)$, all the rest are projectors; weak bosons with "basis vectors" which have two nilpotents only in $SO(4)$ manifesting as $SU(2) \times SU(2)$ of $SO(13,1)$; and gluons "basis vectors" with two nilpotents in $SU(3) \times U(1)$ of $SO(13,1)$, all the rest are projectors.

All the observed gauge fields, either vectors or scalars, are presented by only two nilpotents all the rest are projectors. There are breaks of symmetries [7] which make choices.

The extension of the "basis vectors" to strings in the context of renormalizability, as well as the offer of odd-dimensional spaces needs further studies.

10.5   Conclusions

This contribution presents the "basis vectors" of internal spaces of fermion and boson second quantized fields, Sect. 10.2, manifesting that fermion "basis vectors", written as products of an odd number of nilpotents (at least one, the rest of projectors), anti-commute, while boson "basis vectors", written as products of an even number of nilpotents (or of only projectors), commute, explaining the second quantization postulates of Dirac for fermions and bosons.

Each nilpotent and projector is chosen to be the eigenvector of one of the members of the Cartan subalgebra, Eq. 11.4; correspondingly are the "basis vectors" eigenvectors of all the Cartan subalgebra members; they offer a transparent and elegant way to find the Dirac matrices in any even dimensional space and the corresponding matrices for the boson fields [27]. However, knowing the states and operators, $\mathcal{S}^{ab}, \tilde{\mathcal{S}}^{ab}, \mathcal{S}^{ab} = (\tilde{\mathcal{S}}^{ab} + S^{ab})$, $^{I}\hat{\mathcal{A}}_{f}^{m\dagger}$, $^{II}\hat{\mathcal{A}}_{f}^{m\dagger}$, the matrix representation is not needed.

We demonstrated that the number of fermion "basis vectors" and their Hermitian conjugated partners are equal to the number of "basis vectors" of bosons, appearing in two orthogonal groups, manifesting a (kind of) supersymmetry.

Representing the corresponding creation and annihilation operators for fermion and boson fields as tensor products, $*_T$, of "basis vectors" and basis in ordinary

---

[27] The usual presentation of Dirac matrices in higher dimensional spaces is much more complicated and much less transparent. The same is true for the usual group presentations for either fermions or bosons. The Dirac matrices in $d = (3+1)$ are designed for massive fermions, they do not anticommute. Dirac, having no $\tilde{\gamma}^{a}$, does not include families of fermions; although he could, since he has 2^d products of odd and even possibilities of products of γ^{a}.

space-time, Eqs. (11.16, 11.17) — the boson fields have to obtain the space index — the creation and annihilation operators manifest properties of the second quantized anti-commuting fermion fields and commuting boson fields, Sect. 10.3.

We assumed in this talk that fermions and bosons have non zero momenta only in $d = (3 + 1)$, while the involved internal space needs to be $d = (13 + 1)$ to be able to offer the observed properties of quarks and leptons and antiquarks and antileptons, appearing in families, as well as the corresponding vector (if the space index α is $(0, 1, 2, 3)$) and scalar (if the space index α is ≥ 5) boson fields.

We presented "basis vectors" for fermion and boson fields in any $d = 2(2n + 1)$, Sect. 10.2, in particular in $d = (1 + 1)$ while searching for the "basis vectors" for the strings, for $d = (5 + 1)$ while manifesting how do the "basis vectors" work in a simple case with fermions representing only "positrons" and "electrons" appearing in families and with bosons representing "photons" and "gravitons", and in $d = (13 + 1)$ manifesting "basis vectors" which explain the appearance of the observed quarks and leptons and antiquarks and antileptons appearing in families and of photons, weak bosons, gluons, and a second kind of weak bosons (not yet observed) and gravitons (not yet observed), Subsect. 10.2.1. There are two kinds of boson "basis vectors"; one kind transforms the family members of any family among themselves, the second kind transforms any of the family members into the same family member of all the families.

Does the description of the second quantized fermion and boson fields with the "basis vectors", bringing a new understanding of the second quantized fermion and boson fields, bring also a new understanding of cosmology? It is at least a very promising suggestion. Let us assume that at Big Bang, all the fermion, vector and scalar boson fields were massless, with the "basis vectors" in internal space determined by $SO(13, 1)$; fermion, vector and scalar gauge fields have non zero momenta only in $d = (3 + 1)$ of ordinary space-time; all the scalar gauge fields with the space index $\alpha \geq 5$ (with non-zero momentum only in $d = (3 + 1)$) contribute to inflation. The Lorentz transformations of the kind $M^{ms} = L^{ms} + S^{ms}$ (or $M^{ms} = L^{ms} + \mathcal{S}^{ms}$), $m = (0, 1, 2, 3)$, $s \geq 5$ are not possible (since L^{ms} can not be performed).

As discussed in ([7] and the references therein), the condensate breaks symmetry, so that the second weak $SU(2)_{II}$ bosons, interacting with the condensate, become at low energies massive; all the rest gauge fields ($SU(2)_I$, $SU(3)$, $U(1)$, gravity) [7], do not interact with the condensate, remaining therefore massless up to the electroweak break, which is caused by scalar fields with the space index $\alpha = (5, 6, 7, 8)$. After the electroweak break there are photons, gluons and gravitons which keep their masslessness [10].

We demonstrate that the "basis vectors" for boson second quantized fields can also be expressed as algebraic products of fermion "basis vectors" and their Hermitian conjugated partners; consequently, we need only to know the fermion "basis vectors".

In this contribution, the trial to extend the points in ordinary space-time to strings is presented in Sect. 11.2.1. The internal space of strings, that is their "basis vectors", were added in a tensor product, $*_{T'}$, to the "basis vectors" of fermions and bosons describing the $d = (13 + 1)$ internal space. The tensor products of the fermion and

boson "basis vectors" with the bosons self adjoint "basis vectors" on the string leads to the anti-commuting creation and annihilation operators for fermions and commutation operators for bosons, suggesting that at low energies only the internal spaces of the second quantized fields with the "basis vectors" describing the $d = (13 + 1)$ internal space are important. The tensor product of the "basis vectors" of fermions and bosons describing the $d = (13 + 1)$ internal space with the Clifford odd basis vectors on a string gives to the commuting "basis vectors" in $d = (13 + 1)$ the anti-commuting partners with the same charges, and to the anti-commuting "basis vectors" in $d = (13 + 1)$ the commuting partners with the same charges. This, might be an interesting part, needs further studies.

There is another possibility to achieve the supersymmetric partners to the "basis vectors" presented fermions and bosons in $2(2n + 1)$-dimensional internal spaces of fermions and bosons, Sect. 11.2.1.

In an odd dimensional space $d = 2(2n + 1) + 1$ there are two groups of "basis vectors" [9]: One group determines the anti-commuting "basis vectors" of $2^{\frac{d-1}{2}-1}$ fermions appearing in $2^{\frac{d-1}{2}-1}$ families, with their $2^{\frac{d-1}{2}-1} \times 2^{\frac{d-1}{2}-1}$ Hermitian conjugated partners appearing in a separate group, as well as two orthogonal groups each with $2^{\frac{d-1}{2}-1} \times 2^{\frac{d-1}{2}-1}$ of "basis vectors", with their Hermitian conjugated partners within the same group.

The second group determines anti-commuting "basis vectors" appearing in two separate orthogonal groups each with $2^{\frac{d-1}{2}-1} \times 2^{\frac{d-1}{2}-1}$ of "basis vectors", with their Hermitian conjugated partners within the same group, as well as the commuting "basis vectors" of "fermions" appearing in families with their Hermitian conjugated partners in a separate group.

Also these two groups might demonstrate a kind of supersymmetry, suggesting to be used to achieve renormalizability.

We want to understand whether the elegant and simple description of the internal degrees of freedom of fermions and bosons with the Clifford odd and even "basis vectors" manifesting a kind of supersymmetry — offering explanations for so many observed properties of fermion and boson second quantized fields, explaining as well the second quantization postulates for fermion and boson fields, offering expressions for boson "basis vectors" (their internal spaces) as algebraic products of fermion "basis vectors" and their Hermitian conjugated partners, offering explanations for cosmological observations with inflation included — can be related to strings, or it offers a new way to understand renormalizability on all levels of energy.

10.6   Useful tables

These Tables are mainly taken from Refs. [8, 10] and are meant to illustrate Sects. (10.2,10.2.3 10.2.1,10.2.2).

The case with $d = (5 + 1)$ is meant to learn how Clifford odd and Clifford even "basis vectors" illustrate internal spaces of fermions and bosons, Table 10.1.

Fermions, in this case "electrons" with a negative "charge", $S^{56} = -\frac{1}{2}$, and "positrons" with a positive "charge", $S^{56} = \frac{1}{2}$, appear in 16 odd "basis vectors"

(with one or three nilpotents), in 4 families with 4 members in each family, having 16 Hermitian conjugated partners.

Bosons, in this case "photons" and "gravitons", appear in two orthogonal groups; each group has 16 members, and their Hermitian conjugated partners appear within the same group. The eigenvalues of the Cartan subalgebra members $\mathcal{S}^{ab} = (S^{ab} + \tilde{S}^{ab})$ are equal to either $(\pm i, 0)$ or $(\pm 1, 0)$. "Photons" are products of only projectors, "gravitons" have two nilpotents with $\mathcal{S}^{03}$ equal to $(\pm i)$ and $\mathcal{S}^{12}$ equal to (± 1).

Tables (10.2, 10.3), manifest that the Clifford even "basis vectors" can be expressed as products of the Clifford odd "basis vectors" and their Hermitian conjugated partners. Let us remind the reader that projectors are self adjoint operators, while the Hermitian conjugated partner to $(\overset{ab}{\pm i})$ are $(\overset{ab}{\mp i})$ and to $(\overset{ab}{\pm 1})$ are $(\overset{ab}{\mp 1})$, Eq. (10.7).

10.7   One family representation of Clifford odd "basis vectors" in $d = (13 + 1)$

This appendix, is following App. D of Ref. [10]. In the even dimensional space $d = (13 + 1)$ ([14], App. A), one irreducible representation of the Clifford odd "basis vectors" if analysed from the point of view of the subgroups of the group $SO(13, 1)$ (including $SO(7, 1) \times SO(6)$, while $SO(7, 1)$ breaks into $SO(3, 1) \times SO(4)$, and $SO(6)$ breaks into $SU(3) \times U(1)$) contains the Clifford odd "basis vectors" describing internal spaces of quarks and leptons and antiquarks and antileptons, manifesting at low energies the quantum numbers assumed by the *standard model* before the electroweak break. Since $SO(4)$ contains two $SU(2)$ subgroups, $SU(2)_I$ and $SU(2)_{II}$, with the hypercharge of the *standard model* $Y = \tau^{23} + \tau^4$ (with τ^{23} belonging to $SU(2)_{II}$ and τ^4 originating in $SO(6)$, breaking to $SU(3) \times U(1)$), one irreducible representation includes the right-handed neutrinos and the left-handed antineutrinos, which are not in the *standard model* scheme [28]. An overview of the properties of the vector and scalar gauge fields in the *spin-charge-family* theory can be found in Refs. ([5,7,8,24,25] and the references therein). The reader can find in Table 10.4 that "basis vectors" of quarks have identical content of $SO(7, 1)$ as "basis vectors" of leptons (and antiquarks as antiletons); they differ only in the $SU(3) \times U(1)$ part.

---

[28]   The handedness is defined as follows

$$\Gamma^{(d)} = \prod_a (\sqrt{\eta^{aa}} \gamma^a) \cdot \begin{cases} (i)^{\frac{d}{2}}, & \text{for d even}, \\ (i)^{\frac{d-1}{2}}, & \text{for d odd}. \end{cases} \tag{10.31}$$

Table 10.1: This table, taken from [8], represents $2^d = 64$ "basis vectors", which are the eigenstates of the Cartan subalgebra members, Eq. (11.4). Half of them are the Clifford odd "basis vectors" with the odd number of nilpotents (one or three), the other half are the Clifford even "basis vectors" with the even number of nilpotents (two or none). They are divided into four groups. The first group, odd I, represents $\hat b_f^{m\dagger}$, appearing in $2^{\frac d2 -1} = 4$ families (f = 1, 2, 3, 4), each family having $2^{\frac d2 -1} = 4$ family members (m = 1, 2, 3, 4). The second group, odd II, contains Hermitian conjugated partners of the first group (for each family separately), $\hat b_f^m = (\hat b_f^{m\dagger})^\dagger$. Either odd I or odd II are products of an odd number of nilpotents (one or three) and of projectors (two or none). The family quantum numbers of $\hat b_f^{m\dagger}$ (the eigenvalues of $(\tilde S^{03}, \tilde S^{12}, \tilde S^{56})$) appear for the first *odd I* group above each family, the quantum numbers of the "family" members (S^{03}, S^{12}, S^{56}) are written in the last three columns. For the Hermitian conjugated partners of *odd I*, presented in the group *odd II*, the quantum numbers (S^{03}, S^{12}, S^{56}) are presented above each group of the Hermitian conjugated partners, the last three columns tell eigenvalues of $(\tilde S^{03}, \tilde S^{12}, \tilde S^{56})$. The two groups with the even number of nilpotents (two or none), *even I* and *even II*, have their Hermitian conjugated partners within its groups. The quantum numbers f, that is the eigenvalues of $(\tilde S^{03}, \tilde S^{12}, \tilde S^{56})$, are written above column of four members, the quantum numbers of the members, (S^{03}, S^{12}, S^{56}), are written in the last three columns. The quantum numbers of the even "basi vectors" are $(\mathcal{S}^{03}, \mathcal{S}^{12}, \mathcal{S}^{56})$, determined by $\mathcal{S}^{ab} = S^{ab} + \tilde S^{ab}$.

"basis vectors" $(\tilde S^{03},\tilde S^{12},\tilde S^{56})$	m →	f = 1 $(\frac i2,-\frac12,-\frac12)$ 03 12 56	f = 2 $(-\frac i2,-\frac12,\frac12)$ 03 12 56	f = 3 $(-\frac i2,\frac12,-\frac12)$ 03 12 56	f = 4 $(\frac i2,\frac12,\frac12)$ 03 12 56	S^{03}	S^{12}	S^{56}
odd I $\hat b_f^{m\dagger}$	1	(+i)[+][+]	[+i][+](+)	[+i](+)[+]	(+i)(+)(+)	$\frac i2$	$\frac12$	$\frac12$
	2	[-i](-)[+]	(-i)(-)(+)	(-i)[-][+]	[-i](+)[-]	$-\frac i2$	$-\frac12$	$\frac12$
	3	[-i][+](-)	(-i)[+][-]	(-i)(+)(-)	[-i](+)[-]	$-\frac i2$	$\frac12$	$-\frac12$
	4	(+i)(-)(-)	[+i](-)[-]	[+i][-](-)	(+i)[-][-]	$\frac i2$	$-\frac12$	$-\frac12$
(S^{03},S^{12},S^{56}) →		$(-\frac i2,\frac12,\frac12)$ 03 12 56	$(\frac i2,\frac12,-\frac12)$ 03 12 56	$(\frac i2,-\frac12,\frac12)$ 03 12 56	$(-\frac i2,-\frac12,-\frac12)$ 03 12 56	$\tilde S^{03}$	$\tilde S^{12}$	$\tilde S^{56}$
odd II $\hat b_f^m$	1	(-i)[+][+]	[+i][+](-)	[+i](-)[+]	(-i)(-)(-)	$-\frac i2$	$\frac12$	$-\frac12$
	2	[-i](+)[+]	(+i)(+)(-)	(+i)[-][+]	[-i][-](-)	$\frac i2$	$-\frac12$	$-\frac12$
	3	[-i][+](+)	(+i)[+][-]	(+i)(-)(+)	[-i](-)[-]	$\frac i2$	$-\frac12$	$\frac12$
	4	(-i)(+)(+)	[+i](+)[-]	[+i][-](+)	(-i)[-][-]	$-\frac i2$	$\frac12$	$\frac12$
$(\tilde S^{03},\tilde S^{12},\tilde S^{56})$ →		$(-\frac i2,\frac12,\frac12)$ 03 12 56	$(\frac i2,-\frac12,\frac12)$ 03 12 56	$(-\frac i2,-\frac12,-\frac12)$ 03 12 56	$(\frac i2,\frac12,-\frac12)$ 03 12 56	S^{03}	S^{12}	S^{56}
even I $^{I}\mathcal{A}_f^m$	1	[+i](+)(+)	(+i)[+](+)	[+i][+][+]	(+i)(+)[+]	$\frac i2$	$\frac12$	$\frac12$
	2	(-i)[-](+)	[-i](-)(+)	(-i)(-)[+]	[-i][-][+]	$-\frac i2$	$-\frac12$	$\frac12$
	3	(-i)(+)[-]	[-i][+](-)	(-i)[+](-)	[-i](+)(-)	$-\frac i2$	$\frac12$	$-\frac12$
	4	[+i][-][-]	(+i)(-)[-]	[+i](-)(-)	(+i)[-](-)	$\frac i2$	$-\frac12$	$-\frac12$
$(\tilde S^{03},\tilde S^{12},\tilde S^{56})$ →		$(\frac i2,\frac12,\frac12)$ 03 12 56	$(-\frac i2,-\frac12,\frac12)$ 03 12 56	$(\frac i2,-\frac12,-\frac12)$ 03 12 56	$(-\frac i2,\frac12,-\frac12)$ 03 12 56	S^{03}	S^{12}	S^{56}
even II $^{II}\mathcal{A}_f^m$	1	[-i](+)(+)	(-i)[+](+)	[-i][+][+]	(-i)(+)[+]	$-\frac i2$	$\frac12$	$\frac12$
	2	(+i)[-](+)	[+i](-)(+)	(+i)[+][+]	[+i][-][+]	$\frac i2$	$-\frac12$	$\frac12$
	3	(+i)(+)[-]	[+i][+](-)	(+i)[+](-)	[+i](+)(-)	$\frac i2$	$\frac12$	$-\frac12$
	4	[-i][-][-]	(-i)(-)[-]	[-i](-)(-)	(-i)[-](-)	$-\frac i2$	$-\frac12$	$-\frac12$

Table 10.2: This table is taken from Ref. [10]. The Clifford even "basis vectors", $^{I}\hat{\mathcal{A}}_f^{m\dagger}$, belonging to zero momentum in internal space, $\mathcal{S}^{12} = 0$, for d = (5 + 1), are presented as algebraic products of the f = 1 family "basis vectors" $\hat{b}_1^{m'\dagger}$ and their Hermitian conjugated partners $(\hat{b}_1^{m''\dagger})^\dagger$, presented in Table 10.1: $\hat{b}_1^{m'\dagger} *_A (\hat{b}_1^{m''\dagger})^\dagger$. The two $^{I}\hat{\mathcal{A}}_f^{m\dagger}$ which are Hermitian conjugated partners, are marked with the same symbol (either $\triangle$ or $\bullet$). The symbol $\bigcirc$ presents selfadjoint members. The Clifford even "basis vectors" $^{I}\hat{\mathcal{A}}_f^{m\dagger}$ are products of one projector and two nilpotents or three projectors (they are self-adjoint), the Clifford odd "basis vectors" and their Hermitian conjugated partners are products of one nilpotent and two projectors or of three nilpotents. The Clifford even and Clifford odd objects are eigenvectors of all the corresponding Cartan subalgebra members, Eq. (11.4). There are $\frac{1}{2} \times 2^{\frac{6}{2}-1} \times 2^{\frac{6}{2}-1}$ algebraic products of $\hat{b}_1^{m'\dagger} *_A (\hat{b}_1^{m''\dagger})^\dagger$. The rest 8 of 16 members have $^{I}\hat{\mathcal{A}}_f^{m\dagger}$ with $\mathcal{S}^{12} = +1$ (four) and with $\mathcal{S}^{12} = -1$ (four), presented in Table 10.3. The members $\hat{b}_f^{m'\dagger}$ together with their Hermitian conjugated partners of each of the four families, f = (1, 2, 3, 4), offer the same $^{I}\hat{\mathcal{A}}_f^{m\dagger}$ with $\mathcal{S}^{12} = 0$ as the ones presented in this table. The table is taken from Ref. [10, 11].

$\mathcal{S}^{12}$	symbol	$^{I}\hat{\mathcal{A}}_f^{m\dagger} =$	$\hat{b}_{f'}^{m'\dagger} *_A (\hat{b}_{f'}^{m''\dagger})^\dagger$
0	$\triangle$	$^{I}\hat{\mathcal{A}}_1^{2\dagger} =$	$\hat{b}_1^{2\dagger} *_A (\hat{b}_1^{4\dagger})^\dagger$
		$\overset{03}{(-i)}\overset{12}{[-]}\overset{56}{(+)}$	$\overset{03}{[-i]}\overset{12}{(-)}\overset{56}{[+]} *_A \overset{03}{(-i)}\overset{12}{(+)}\overset{56}{(+)}$
0	$\bigcirc$	$^{I}\hat{\mathcal{A}}_1^{4\dagger} =$	$\hat{b}_1^{4\dagger} *_A (\hat{b}_1^{4\dagger})^\dagger$
		$\overset{03}{[+i]}\overset{12}{[-]}\overset{56}{[-]}$	$\overset{03}{(+i)}\overset{12}{(-)}\overset{56}{(-)} *_A \overset{03}{(-i)}\overset{12}{(+)}\overset{56}{(+)}$
0	$\bullet$	$^{I}\hat{\mathcal{A}}_2^{1\dagger} =$	$\hat{b}_1^{1\dagger} *_A (\hat{b}_1^{3\dagger})^\dagger$
		$\overset{03}{(+i)}\overset{12}{[+]}\overset{56}{(+)}$	$\overset{03}{(+i)}\overset{12}{[+]}\overset{56}{[+]} *_A \overset{03}{[-i]}\overset{12}{[+]}\overset{56}{(+)}$
0	$\bigcirc$	$^{I}\hat{\mathcal{A}}_2^{3\dagger} =$	$\hat{b}_1^{3\dagger} *_A (\hat{b}_1^{3\dagger})^\dagger$
		$\overset{03}{[-i]}\overset{12}{[+]}\overset{56}{[-]}$	$\overset{03}{[-i]}\overset{12}{[+]}\overset{56}{(-)} *_A \overset{03}{[-i]}\overset{12}{[+]}\overset{56}{(+)}$
0	$\bigcirc$	$^{I}\hat{\mathcal{A}}_3^{1\dagger} =$	$\hat{b}_1^{1\dagger} *_A (\hat{b}_1^{1\dagger})^\dagger$
		$\overset{03}{[+i]}\overset{12}{[+]}\overset{56}{[+]}$	$\overset{03}{(+i)}\overset{12}{[+]}\overset{56}{[+]} *_A \overset{03}{(-i)}\overset{12}{[+]}\overset{56}{[+]}$
0	$\bullet$	$^{I}\hat{\mathcal{A}}_3^{3\dagger} =$	$\hat{b}_1^{3\dagger} *_A (\hat{b}_1^{1\dagger})^\dagger$
		$\overset{03}{(-i)}\overset{12}{[+]}\overset{56}{(-)}$	$\overset{03}{[-i]}\overset{12}{[+]}\overset{56}{(-)} *_A \overset{03}{(-i)}\overset{12}{[+]}\overset{56}{[+]}$
0	$\bigcirc$	$^{I}\hat{\mathcal{A}}_4^{2\dagger} =$	$\hat{b}_1^{2\dagger} *_A (\hat{b}_1^{2\dagger})^\dagger$
		$\overset{03}{[-i]}\overset{12}{[-]}\overset{56}{[+]}$	$\overset{03}{[-i]}\overset{12}{(-)}\overset{56}{[+]} *_A \overset{03}{[-i]}\overset{12}{(+)}\overset{56}{[+]}$
0	$\triangle$	$^{I}\hat{\mathcal{A}}_3^{4\dagger} =$	$\hat{b}_1^{4\dagger} *_A (\hat{b}_1^{2\dagger})^\dagger$
		$\overset{03}{(+i)}\overset{12}{[-]}\overset{56}{(-)}$	$\overset{03}{(+i)}\overset{12}{(-)}\overset{56}{(-)} *_A \overset{03}{[-i]}\overset{12}{(+)}\overset{56}{[+]}$

Table 10.3: The Clifford even "basis vectors" $^{I}\hat{\mathcal{A}}_{f}^{m\dagger}$, belonging to transverse momentum in internal space, $\mathcal{S}^{12} = 1$, the first half of $^{I}\hat{\mathcal{A}}_{f}^{m\dagger}$, and $\mathcal{S}^{12} = -1$, the second half of $^{I}\hat{\mathcal{A}}_{f}^{m\dagger}$, for $d = (5+1)$, are presented as algebraic products of the $f = 1$ family "basis vectors" $\hat{b}_{1}^{m'\dagger}$ and their Hermitian conjugated partners $(\hat{b}_{1}^{m''\dagger})^{\dagger}$: $\hat{b}_{1}^{m'\dagger} *_{A} (\hat{b}_{1}^{m''\dagger})^{\dagger}$. Two $^{I}\hat{\mathcal{A}}_{f}^{m\dagger}$ which are the Hermitian conjugated partners are marked with the same symbol ($\star\star$, $\ddagger$, $\otimes$, $\odot\odot$). The Clifford even "basis vectors" $^{I}\hat{\mathcal{A}}_{f}^{m\dagger}$ are products of one projector and two nilpotents, the Clifford odd "basis vectors" and their Hermitian conjugated partners are products of one nilpotent and two projectors or of three nilpotents. The Clifford even and Clifford odd objects are eigenvectors of all the corresponding Cartan subalgebra members, Eq. (11.4). There are $\frac{1}{2} \times 2^{\frac{6}{2}-1} \times 2^{\frac{6}{2}-1}$ algebraic products of $\hat{b}_{1}^{m'\dagger} *_{A} (\hat{b}_{1}^{m''\dagger})^{\dagger}$ with $\mathcal{S}^{12}$ equal to ± 1. The rest 8 of 16 members present $^{I}\hat{\mathcal{A}}_{f}^{m\dagger}$ with $\mathcal{S}^{12} = 0$. The members $\hat{b}_{f}^{m'\dagger}$ together with their Hermitian conjugated partners of each of the four families, $f = (1, 2, 3, 4)$, offer the same $^{I}\hat{\mathcal{A}}_{f}^{m\dagger}$ with $\mathcal{S}^{12} = \pm 1$ as the ones presented in this table. (And equivalently for $\mathcal{S}^{12} = 0$.)

$\mathcal{S}^{12}$	symbol	$^{I}\hat{\mathcal{A}}_{f}^{m\dagger} =$	$\hat{b}_{f'}^{m'\dagger} *_{A} (\hat{b}_{f'}^{m''\dagger})^{\dagger}$
1	$\star\star$	$^{I}\hat{\mathcal{A}}_{1}^{1\dagger} =$	$\hat{b}_{1}^{1\dagger} *_{A} (\hat{b}_{1}^{4\dagger})^{\dagger}$
			$\overset{03}{[+i]} \overset{12}{(+)} \overset{56}{(+)} \quad \overset{03}{(+i)} \overset{12}{[+]} \overset{56}{[+]} *_{A} \overset{03}{(-i)} \overset{12}{(+)} \overset{56}{(+)}$
1	$\ddagger$	$^{I}\hat{\mathcal{A}}_{1}^{3\dagger} =$	$\hat{b}_{1}^{3\dagger} *_{A} (\hat{b}_{1}^{4\dagger})^{\dagger}$
			$\overset{03}{(-i)} \overset{12}{(+)} \overset{56}{[-]} \quad \overset{03}{[-i]} \overset{12}{[+]} \overset{56}{(-)} *_{A} \overset{03}{(-i)} \overset{12}{(+)} \overset{56}{(+)}$
1	$\odot\odot$	$^{I}\hat{\mathcal{A}}_{4}^{1\dagger} =$	$\hat{b}_{1}^{1\dagger} *_{A} (\hat{b}_{1}^{2\dagger})^{\dagger}$
			$\overset{03}{(+i)} \overset{12}{(+)} \overset{56}{[+]} \quad \overset{03}{(+i)} \overset{12}{[+]} \overset{56}{[+]} *_{A} \overset{03}{[-i]} \overset{12}{(+)} \overset{56}{[+]}$
1	$\otimes$	$^{I}\hat{\mathcal{A}}_{4}^{3\dagger} =$	$\hat{b}_{1}^{3\dagger} *_{A} (\hat{b}_{1}^{2\dagger})^{\dagger}$
			$\overset{03}{[-i]} \overset{12}{(+)} \overset{56}{(-)} \quad \overset{03}{[-i]} \overset{12}{[+]} \overset{56}{(-)} *_{A} \overset{03}{[-i]} \overset{12}{(+)} \overset{56}{[+]}$
-1	$\otimes$	$^{I}\hat{\mathcal{A}}_{2}^{2\dagger} =$	$\hat{b}_{1}^{2\dagger} *_{A} (\hat{b}_{1}^{3\dagger})^{\dagger}$
			$\overset{03}{[-i]} \overset{12}{(-)} \overset{56}{(+)} \quad \overset{03}{[-i]} \overset{12}{(-)} \overset{56}{[+]} *_{A} \overset{03}{[-i]} \overset{12}{[+]} \overset{56}{(+)}$
-1	$\ddagger$	$^{I}\hat{\mathcal{A}}_{2}^{4\dagger} =$	$\hat{b}_{1}^{4\dagger} *_{A} (\hat{b}_{1}^{3\dagger})^{\dagger}$
			$\overset{03}{(+i)} \overset{12}{(-)} \overset{56}{[-]} \quad \overset{03}{(+i)} \overset{12}{(-)} \overset{56}{(-)} *_{A} \overset{03}{[-i]} \overset{12}{[+]} \overset{56}{(+)}$
-1	$\odot\odot$	$^{I}\hat{\mathcal{A}}_{3}^{2\dagger} =$	$\hat{b}_{1}^{2\dagger} *_{A} (\hat{b}_{1}^{1\dagger})^{\dagger}$
			$\overset{03}{(-i)} \overset{12}{(-)} \overset{56}{[+]} \quad \overset{03}{[-i]} \overset{12}{(-)} \overset{56}{[+]} *_{A} \overset{03}{(-i)} \overset{12}{[+]} \overset{56}{[+]}$
-1	$\star\star$	$^{I}\hat{\mathcal{A}}_{3}^{4\dagger} =$	$\hat{b}_{1}^{4\dagger} *_{A} (\hat{b}_{1}^{1\dagger})^{\dagger}$
			$\overset{03}{[+i]} \overset{12}{(-)} \overset{56}{(-)} \quad \overset{03}{(+i)} \overset{12}{(-)} \overset{56}{(-)} *_{A} \overset{03}{(-i)} \overset{12}{[+]} \overset{56}{[+]}$

The basis states are written over the oscillator pairs $03\,12\;\|\;56\,78\;\|\;9\,10\;11\,12\;\|\;13\,14$.

(Anti)octet, $\Gamma^{(7,1)}=(-1)\,1$, $\Gamma^{(6)}=(1)\,-1$ of (anti)quarks and (anti)leptons

i		$\lvert {}^{a}\psi_i >$	$\Gamma^{(3,1)}$	S^{12}	τ^{13}	τ^{23}	τ^{33}	τ^{38}	τ^{4}	Y	Q
1	u_R^{c1}	$(+i)[+]\mid[+](+)\;\|\;(+)\,[-]\mid[-]$	1	$\frac12$	0	$\frac12$	$\frac12$	$\frac{1}{2\sqrt3}$	$\frac16$	$\frac23$	$\frac23$
2	u_R^{c1}	$[-i](-)\mid[+](+)\;\|\;(+)\,[-]\mid[-]$	1	$-\frac12$	0	$\frac12$	$\frac12$	$\frac{1}{2\sqrt3}$	$\frac16$	$\frac23$	$\frac23$
3	d_R^{c1}	$(+i)[+]\mid(-)[-]\;\|\;(+)\,[-]\mid[-]$	1	$\frac12$	0	$-\frac12$	$\frac12$	$\frac{1}{2\sqrt3}$	$\frac16$	$-\frac13$	$-\frac13$
4	d_R^{c1}	$[-i](-)\mid(-)[-]\;\|\;(+)\,[-]\mid[-]$	1	$-\frac12$	0	$-\frac12$	$\frac12$	$\frac{1}{2\sqrt3}$	$\frac16$	$-\frac13$	$-\frac13$
5	d_L^{c1}	$[-i][+]\mid(-)(+)\;\|\;(+)\,[-]\mid[-]$	-1	$\frac12$	$-\frac12$	0	$\frac12$	$\frac{1}{2\sqrt3}$	$\frac16$	$\frac16$	$-\frac13$
6	d_L^{c1}	$-(+i)(-)\mid(-)(+)\;\|\;(+)\,[-]\mid[-]$	-1	$-\frac12$	$-\frac12$	0	$\frac12$	$\frac{1}{2\sqrt3}$	$\frac16$	$\frac16$	$-\frac13$
7	u_L^{c1}	$-[-i][+]\mid[+][-]\;\|\;(+)\,[-]\mid[-]$	-1	$\frac12$	$\frac12$	0	$\frac12$	$\frac{1}{2\sqrt3}$	$\frac16$	$\frac16$	$\frac23$
8	u_L^{c1}	$(+i)(-)\mid[+][-]\;\|\;(+)\,[-]\mid[-]$	-1	$-\frac12$	$\frac12$	0	$\frac12$	$\frac{1}{2\sqrt3}$	$\frac16$	$\frac16$	$\frac23$
9	u_R^{c2}	$(+i)[+]\mid[+](+)\;\|\;[-]\,(+)\mid[-]$	1	$\frac12$	0	$\frac12$	$-\frac12$	$\frac{1}{2\sqrt3}$	$\frac16$	$\frac23$	$\frac23$
10	u_R^{c2}	$[-i](-)\mid[+](+)\;\|\;[-]\,(+)\mid[-]$	1	$-\frac12$	0	$\frac12$	$-\frac12$	$\frac{1}{2\sqrt3}$	$\frac16$	$\frac23$	$\frac23$
11	d_R^{c2}	$(+i)[+]\mid(-)[-]\;\|\;[-]\,(+)\mid[-]$	1	$\frac12$	0	$-\frac12$	$-\frac12$	$\frac{1}{2\sqrt3}$	$\frac16$	$-\frac13$	$-\frac13$
12	d_R^{c2}	$[-i](-)\mid(-)[-]\;\|\;[-]\,(+)\mid[-]$	1	$-\frac12$	0	$-\frac12$	$-\frac12$	$\frac{1}{2\sqrt3}$	$\frac16$	$-\frac13$	$-\frac13$
13	d_L^{c2}	$[-i][+]\mid(-)(+)\;\|\;[-]\,(+)\mid[-]$	-1	$\frac12$	$-\frac12$	0	$-\frac12$	$\frac{1}{2\sqrt3}$	$\frac16$	$\frac16$	$-\frac13$
14	d_L^{c2}	$-(+i)(-)\mid(-)(+)\;\|\;[-]\,(+)\mid[-]$	-1	$-\frac12$	$-\frac12$	0	$-\frac12$	$\frac{1}{2\sqrt3}$	$\frac16$	$\frac16$	$-\frac13$
15	u_L^{c2}	$-[-i][+]\mid[+][-]\;\|\;[-]\,(+)\mid[-]$	-1	$\frac12$	$\frac12$	0	$-\frac12$	$\frac{1}{2\sqrt3}$	$\frac16$	$\frac16$	$\frac23$
16	u_L^{c2}	$(+i)(-)\mid[+][-]\;\|\;[-]\,(+)\mid[-]$	-1	$-\frac12$	$\frac12$	0	$-\frac12$	$\frac{1}{2\sqrt3}$	$\frac16$	$\frac16$	$\frac23$
17	u_R^{c3}	$(+i)[+]\mid[+](+)\;\|\;[-]\,[-]\mid(+)$	1	$\frac12$	0	$\frac12$	0	$-\frac{1}{\sqrt3}$	$\frac16$	$\frac23$	$\frac23$
18	u_R^{c3}	$[-i](-)\mid[+](+)\;\|\;[-]\,[-]\mid(+)$	1	$-\frac12$	0	$\frac12$	0	$-\frac{1}{\sqrt3}$	$\frac16$	$\frac23$	$\frac23$
19	d_R^{c3}	$(+i)[+]\mid(-)[-]\;\|\;[-]\,[-]\mid(+)$	1	$\frac12$	0	$-\frac12$	0	$-\frac{1}{\sqrt3}$	$\frac16$	$-\frac13$	$-\frac13$
20	d_R^{c3}	$[-i](-)\mid(-)[-]\;\|\;[-]\,[-]\mid(+)$	1	$-\frac12$	0	$-\frac12$	0	$-\frac{1}{\sqrt3}$	$\frac16$	$-\frac13$	$-\frac13$
21	d_L^{c3}	$[-i][+]\mid(-)(+)\;\|\;[-]\,[-]\mid(+)$	-1	$\frac12$	$-\frac12$	0	0	$-\frac{1}{\sqrt3}$	$\frac16$	$\frac16$	$-\frac13$
22	d_L^{c3}	$-(+i)(-)\mid(-)(+)\;\|\;[-]\,[-]\mid(+)$	-1	$-\frac12$	$-\frac12$	0	0	$-\frac{1}{\sqrt3}$	$\frac16$	$\frac16$	$-\frac13$
23	u_L^{c3}	$-[-i][+]\mid[+][-]\;\|\;[-]\,[-]\mid(+)$	-1	$\frac12$	$\frac12$	0	0	$-\frac{1}{\sqrt3}$	$\frac16$	$\frac16$	$\frac23$
24	u_L^{c3}	$(+i)(-)\mid[+][-]\;\|\;[-]\,[-]\mid(+)$	-1	$-\frac12$	$\frac12$	0	0	$-\frac{1}{\sqrt3}$	$\frac16$	$\frac16$	$\frac23$
25	ν_R	$(+i)[+]\mid[+](+)\;\|\;(+)\,(+)\mid(+)$	1	$\frac12$	0	$\frac12$	0	0	$-\frac12$	0	0
26	ν_R	$[-i](-)\mid[+](+)\;\|\;(+)\,(+)\mid(+)$	1	$-\frac12$	0	$\frac12$	0	0	$-\frac12$	0	0
27	e_R	$(+i)[+]\mid(-)[-]\;\|\;(+)\,(+)\mid(+)$	1	$\frac12$	0	$-\frac12$	0	0	$-\frac12$	-1	-1
28	e_R	$[-i](-)\mid(-)[-]\;\|\;(+)\,(+)\mid(+)$	1	$-\frac12$	0	$-\frac12$	0	0	$-\frac12$	-1	-1
29	e_L	$[-i][+]\mid(-)(+)\;\|\;(+)\,(+)\mid(+)$	-1	$\frac12$	$-\frac12$	0	0	0	$-\frac12$	$-\frac12$	-1
30	e_L	$-(+i)(-)\mid(-)(+)\;\|\;(+)\,(+)\mid(+)$	-1	$-\frac12$	$-\frac12$	0	0	0	$-\frac12$	$-\frac12$	-1
31	ν_L	$-[-i][+]\mid[+][-]\;\|\;(+)\,(+)\mid(+)$	-1	$\frac12$	$\frac12$	0	0	0	$-\frac12$	$-\frac12$	0
32	ν_L	$(+i)(-)\mid[+][-]\;\|\;(+)\,(+)\mid(+)$	-1	$-\frac12$	$\frac12$	0	0	0	$-\frac12$	$-\frac12$	0
33	$\bar d_L^{\bar c1}$	$[-i][+]\mid[+](+)\;\|\;[-]\,(+)\mid(+)$	-1	$\frac12$	0	$\frac12$	$-\frac12$	$-\frac{1}{2\sqrt3}$	$-\frac16$	$\frac13$	$\frac13$
34	$\bar d_L^{\bar c1}$	$(+i)(-)\mid[+](+)\;\|\;[-]\,(+)\mid(+)$	-1	$-\frac12$	0	$\frac12$	$-\frac12$	$-\frac{1}{2\sqrt3}$	$-\frac16$	$\frac13$	$\frac13$
35	$\bar u_L^{\bar c1}$	$-[-i][+]\mid(-)[-]\;\|\;[-]\,(+)\mid(+)$	-1	$\frac12$	0	$-\frac12$	$-\frac12$	$-\frac{1}{2\sqrt3}$	$-\frac16$	$-\frac23$	$-\frac23$
36	$\bar u_L^{\bar c1}$	$-(+i)(-)\mid(-)[-]\;\|\;[-]\,(+)\mid(+)$	-1	$-\frac12$	0	$-\frac12$	$-\frac12$	$-\frac{1}{2\sqrt3}$	$-\frac16$	$-\frac23$	$-\frac23$
37	$\bar d_R^{\bar c1}$	$(+i)[+]\mid[+][-]\;\|\;[-]\,(+)\mid(+)$	1	$\frac12$	$\frac12$	0	$-\frac12$	$-\frac{1}{2\sqrt3}$	$-\frac16$	$-\frac16$	$\frac13$
38	$\bar d_R^{\bar c1}$	$-[-i](-)\mid[+][-]\;\|\;[-]\,(+)\mid(+)$	1	$-\frac12$	$\frac12$	0	$-\frac12$	$-\frac{1}{2\sqrt3}$	$-\frac16$	$-\frac16$	$\frac13$
39	$\bar u_R^{\bar c1}$	$(+i)[+]\mid(-)(+)\;\|\;[-]\,(+)\mid(+)$	1	$\frac12$	$-\frac12$	0	$-\frac12$	$-\frac{1}{2\sqrt3}$	$-\frac16$	$-\frac16$	$-\frac23$
40	$\bar u_R^{\bar c1}$	$[-i](-)\mid(-)(+)\;\|\;[-]\,(+)\mid(+)$	1	$-\frac12$	$-\frac12$	0	$-\frac12$	$-\frac{1}{2\sqrt3}$	$-\frac16$	$-\frac16$	$-\frac23$
41	$\bar d_L^{\bar c2}$	$[-i][+]\mid[+](+)\;\|\;(+)\,[-]\mid(+)$	-1	$\frac12$	0	$\frac12$	$\frac12$	$-\frac{1}{2\sqrt3}$	$-\frac16$	$\frac13$	$\frac13$
42	$\bar d_L^{\bar c2}$	$(+i)(-)\mid[+](+)\;\|\;(+)\,[-]\mid(+)$	-1	$-\frac12$	0	$\frac12$	$\frac12$	$-\frac{1}{2\sqrt3}$	$-\frac16$	$\frac13$	$\frac13$
43	$\bar u_L^{\bar c2}$	$-[-i][+]\mid(-)[-]\;\|\;(+)\,[-]\mid(+)$	-1	$\frac12$	0	$-\frac12$	$\frac12$	$-\frac{1}{2\sqrt3}$	$-\frac16$	$-\frac23$	$-\frac23$

i	$\mid^a \psi_i >$ (Anti)octet, $\Gamma^{(7,1)} = (-1)\,1$, $\Gamma^{(6)} = (1)\,-1$ of (anti)quarks and (anti)leptons	$\Gamma^{(3,1)}$	S^{12}	τ^{13}	τ^{23}	τ^{33}	τ^{38}	τ^4	Y	Q
44	$\bar{u}_L^{\bar{c}2}$ $\;$ 03 12 56 78 9 10 11 12 13 14 $\;$ $-(+i)(-)\mid(-)[-]\parallel(+)\;[-]\;(+)$	-1	$-\frac{1}{2}$	0	$-\frac{1}{2}$	$\frac{1}{2}$	$-\frac{1}{2\sqrt{3}}$	$-\frac{1}{6}$	$-\frac{2}{3}$	$-\frac{2}{3}$
45	$\bar{d}_R^{\bar{c}2}$ $\;$ 03 12 56 78 9 10 11 12 13 14 $\;$ $(+i)[+]\mid[+][-]\parallel(+)\;[-]\;(+)$	1	$\frac{1}{2}$	$\frac{1}{2}$	0	$\frac{1}{2}$	$-\frac{1}{2\sqrt{3}}$	$-\frac{1}{6}$	$-\frac{1}{6}$	$\frac{1}{3}$
46	$\bar{d}_R^{\bar{c}2}$ $\;$ 03 12 56 78 9 10 11 12 13 14 $\;$ $-[-i](-)\mid[+][-]\parallel(+)\;[-]\;(+)$	1	$-\frac{1}{2}$	$\frac{1}{2}$	0	$\frac{1}{2}$	$-\frac{1}{2\sqrt{3}}$	$-\frac{1}{6}$	$-\frac{1}{6}$	$\frac{1}{3}$
47	$\bar{u}_R^{\bar{c}2}$ $\;$ 03 12 56 78 9 10 11 12 13 14 $\;$ $(+i)[+]\mid(-)(+)\parallel(+)\;[-]\;(+)$	1	$\frac{1}{2}$	$-\frac{1}{2}$	0	$\frac{1}{2}$	$-\frac{1}{2\sqrt{3}}$	$-\frac{1}{6}$	$-\frac{1}{6}$	$-\frac{2}{3}$
48	$\bar{u}_R^{\bar{c}2}$ $\;$ 03 12 56 78 9 10 11 12 13 14 $\;$ $[-i](-)\mid(-)(+)\parallel(+)\;[-]\;(+)$	1	$-\frac{1}{2}$	$-\frac{1}{2}$	0	$\frac{1}{2}$	$-\frac{1}{2\sqrt{3}}$	$-\frac{1}{6}$	$-\frac{1}{6}$	$-\frac{2}{3}$
49	$\bar{d}_L^{\bar{c}3}$ $\;$ 03 12 56 78 9 10 11 12 13 14 $\;$ $[-i][+]\mid[+](+)\parallel(+)\;(+)\;[-]$	-1	$\frac{1}{2}$	0	$\frac{1}{2}$	0	$\frac{1}{\sqrt{3}}$	$-\frac{1}{6}$	$\frac{1}{3}$	$\frac{1}{3}$
50	$\bar{d}_L^{\bar{c}3}$ $\;$ 03 12 56 78 9 10 11 12 13 14 $\;$ $(+i)(-)\mid[+](+)\parallel(+)\;(+)\;[-]$	-1	$-\frac{1}{2}$	0	$\frac{1}{2}$	0	$\frac{1}{\sqrt{3}}$	$-\frac{1}{6}$	$\frac{1}{3}$	$\frac{1}{3}$
51	$\bar{u}_L^{\bar{c}3}$ $\;$ 03 12 56 78 9 10 11 12 13 14 $\;$ $-[-i][+]\mid(-)[-]\parallel(+)\;(+)\;[-]$	-1	$\frac{1}{2}$	0	$-\frac{1}{2}$	0	$\frac{1}{\sqrt{3}}$	$-\frac{1}{6}$	$-\frac{2}{3}$	$-\frac{2}{3}$
52	$\bar{u}_L^{\bar{c}3}$ $\;$ 03 12 56 78 9 10 11 12 13 14 $\;$ $-(+i)(-)\mid(-)[-]\parallel(+)\;(+)\;[-]$	-1	$-\frac{1}{2}$	0	$-\frac{1}{2}$	0	$\frac{1}{\sqrt{3}}$	$-\frac{1}{6}$	$-\frac{2}{3}$	$-\frac{2}{3}$
53	$\bar{d}_R^{\bar{c}3}$ $\;$ 03 12 56 78 9 10 11 12 13 14 $\;$ $(+i)[+]\mid[+][-]\parallel(+)\;(+)\;[-]$	1	$\frac{1}{2}$	$\frac{1}{2}$	0	0	$\frac{1}{\sqrt{3}}$	$-\frac{1}{6}$	$-\frac{1}{6}$	$\frac{1}{3}$
54	$\bar{d}_R^{\bar{c}3}$ $\;$ 03 12 56 78 9 10 11 12 13 14 $\;$ $-[-i](-)\mid[+][-]\parallel(+)\;(+)\;[-]$	1	$-\frac{1}{2}$	$\frac{1}{2}$	0	0	$\frac{1}{\sqrt{3}}$	$-\frac{1}{6}$	$-\frac{1}{6}$	$\frac{1}{3}$
55	$\bar{u}_R^{\bar{c}3}$ $\;$ 03 12 56 78 9 10 11 12 13 14 $\;$ $(+i)[+]\mid(-)(+)\parallel(+)\;(+)\;[-]$	1	$\frac{1}{2}$	$-\frac{1}{2}$	0	0	$\frac{1}{\sqrt{3}}$	$-\frac{1}{6}$	$-\frac{1}{6}$	$-\frac{2}{3}$
56	$\bar{u}_R^{\bar{c}3}$ $\;$ 03 12 56 78 9 10 11 12 13 14 $\;$ $[-i](-)\mid(-)(+)\parallel(+)\;(+)\;[-]$	1	$-\frac{1}{2}$	$-\frac{1}{2}$	0	0	$\frac{1}{\sqrt{3}}$	$-\frac{1}{6}$	$-\frac{1}{6}$	$-\frac{2}{3}$
57	$\bar{e}_L$ $\;$ 03 12 56 78 9 10 11 12 13 14 $\;$ $[-i][+]\mid[+](+)\parallel[-]\;[-]\;[-]$	-1	$\frac{1}{2}$	0	$\frac{1}{2}$	0	0	$\frac{1}{2}$	1	1
58	$\bar{e}_L$ $\;$ 03 12 56 78 9 10 11 12 13 14 $\;$ $(+i)(-)\mid[+](+)\parallel[-]\;[-]\;[-]$	-1	$-\frac{1}{2}$	0	$\frac{1}{2}$	0	0	$\frac{1}{2}$	1	1
59	$\bar{\nu}_L$ $\;$ 03 12 56 78 9 10 11 12 13 14 $\;$ $-[-i][+]\mid(-)[-]\parallel[-]\;[-]\;[-]$	-1	$\frac{1}{2}$	0	$-\frac{1}{2}$	0	0	$\frac{1}{2}$	0	0
60	$\bar{\nu}_L$ $\;$ 03 12 56 78 9 10 11 12 13 14 $\;$ $-(+i)(-)\mid(-)[-]\parallel[-]\;[-]\;[-]$	-1	$-\frac{1}{2}$	0	$-\frac{1}{2}$	0	0	$\frac{1}{2}$	0	0
61	$\bar{\nu}_R$ $\;$ 03 12 56 78 9 10 11 12 13 14 $\;$ $(+i)[+]\mid(-)(+)\parallel[-]\;[-]\;[-]$	1	$\frac{1}{2}$	$-\frac{1}{2}$	0	0	0	$\frac{1}{2}$	$\frac{1}{2}$	0
62	$\bar{\nu}_R$ $\;$ 03 12 56 78 9 10 11 12 13 14 $\;$ $-[-i](-)\mid(-)(+)\parallel[-]\;[-]\;[-]$	1	$-\frac{1}{2}$	$-\frac{1}{2}$	0	0	0	$\frac{1}{2}$	$\frac{1}{2}$	0
63	$\bar{e}_R$ $\;$ 03 12 56 78 9 10 11 12 13 14 $\;$ $(+i)[+]\mid[+][-]\parallel[-]\;[-]\;[-]$	1	$\frac{1}{2}$	$\frac{1}{2}$	0	0	0	$\frac{1}{2}$	$\frac{1}{2}$	1
64	$\bar{e}_R$ $\;$ 03 12 56 78 9 10 11 12 13 14 $\;$ $[-i](-)\mid[+][-]\parallel[-]\;[-]\;[-]$	1	$-\frac{1}{2}$	$\frac{1}{2}$	0	0	0	$\frac{1}{2}$	$\frac{1}{2}$	1

Table 10.4: The left-handed ($\Gamma^{(13,1)} = -1$, Eq. (10.31)) irreducible representation of one family of spinors — the product of the odd number of nilpotents and of projectors, which are eigenvectors of the Cartan subalgebra of the $SO(13,1)$ group [3,4], manifesting the subgroup $SO(7,1)$ of the colour charged quarks and antiquarks and the colourless leptons and antileptons — is presented. It contains the left-handed ($\Gamma^{(3,1)} = -1$) weak ($SU(2)_I$) charged ($\tau^{13} = \pm\frac{1}{2}$), and $SU(2)_{II}$ chargeless ($\tau^{23} = 0$) quarks and leptons, and the right-handed ($\Gamma^{(3,1)} = 1$) weak ($SU(2)_I$) chargeless and $SU(2)_{II}$ charged ($\tau^{23} = \pm\frac{1}{2}$) quarks and leptons, both with the spin S^{12} up and down ($\pm\frac{1}{2}$, respectively). Quarks distinguish from leptons only in the $SU(3) \times U(1)$ part: Quarks are triplets of three colours ($c^i = (\tau^{33}, \tau^{38})$ $= [(\frac{1}{2}, \frac{1}{2\sqrt{3}}), (-\frac{1}{2}, \frac{1}{2\sqrt{3}}), (0, -\frac{1}{\sqrt{3}})]$, carrying the "fermion charge" ($\tau^4 = \frac{1}{6}$). The colourless leptons carry the "fermion charge" ($\tau^4 = -\frac{1}{2}$). The same multiplet contains also the left handed weak ($SU(2)_I$) chargeless and $SU(2)_{II}$ charged antiquarks and antileptons and the right handed weak ($SU(2)_I$) charged and $SU(2)_{II}$ chargeless antiquarks and antileptons. Antiquarks distinguish from antileptons again only in the $SU(3) \times U(1)$ part: Antiquarks are anti-triplets carrying the "fermion charge" ($\tau^4 = -\frac{1}{6}$). The anti-colourless antileptons carry the "fermion charge" ($\tau^4 = \frac{1}{2}$). $Y = (\tau^{23} + \tau^4)$ is the hyper charge, the electromagnetic charge is $Q = (\tau^{13} + Y)$.

10.8   Acknowledgement

References

1. N. Mankoč Borštnik, "Spinor and vector representations in four dimensional Grassmann space", *J. of Math. Phys.* **34** (1993) 3731-3745, "Unification of spin and charges in Grassmann space?", hep-th 9408002, IJS.TP.94/22, Mod. Phys. Lett.**A (10)** No.7 (1995) 587-595;

2. A. Borštnik Bračič, N. S. Mankoč Borštnik, "On the origin of families of fermions and their mass matrices", hep-ph/0512062, Phys. Rev. **D 74** 073013-28 (2006).

3. N.S. Mankoč Borštnik, H.B.F. Nielsen, *J. of Math. Phys.* **43**, 5782 (2002) [arXiv:hep-th/0111257]. "How to generate families of spinors", *J. of Math. Phys.* **44** 4817 (2003) [arXiv:hep-th/0303224].

4. N.S. Mankoč Borštnik, "Matter-antimatter asymmetry in the *spin-charge-family* theory", *Phys. Rev.* **D 91** (2015) 065004 [arXiv:1409.7791].

5. N.S. Mankoč Borštnik, D. Lukman, "Vector and scalar gauge fields with respect to d = (3 + 1) in Kaluza-Klein theories and in the *spin-charge-family theory*", *Eur. Phys. J. C* **77** (2017) 231.

6. N.S. Mankoč Borštnik, H.B.F. Nielsen, "Understanding the second quantization of fermions in Clifford and in Grassmann space", *New way of second quantization of fermions — Part I and Part II*, [arXiv:2007.03517, arXiv:2007.03516].

7. N. S. Mankoč Borštnik, H. B. Nielsen, "How does Clifford algebra show the way to the second quantized fermions with unified spins, charges and families, and with vector and scalar gauge fields beyond the *standard model*", Progress in Particle and Nuclear Physics, http://doi.org/10.1016.j.ppnp.2021.103890 .

8. N. S. Mankoč Borštnik, "How Clifford algebra helps understand second quantized quarks and leptons and corresponding vector and scalar boson fields, opening a new step beyond the standard model", Reference: NUPHB 994 (2023) 116326 , [arXiv: 2210.06256, physics.gen-ph V2].

9. N. S. Mankoč Borštnik, "Clifford odd and even objects in even and odd dimensional spaces", Symmetry 2023,15,818-12-V2 94818, https:doi.org/10.3390/sym15040818, [arxiv.org/abs/2301.04466] , https://www.mdpi.com/2073-8994/15/4/818 Manuscript ID: symmetry-2179313.

10. N. S. Mankoč Borštnik, "Can the "basis vectors", describing t he internal spaces of fermion and boson fields with the Clifford odd (for fermion) and Clifford even (for boson) objects, explain interactions among fields, with gravitons included?" [arxiv: 2407.09482].

11. N. S. Mankoč Borštnik, H.B. Nielsen, "Can the "basis vectors", describing the internal space of point fermion and boson fields with the Clifford odd (for fermions) and Clifford even (for bosons) objects, be meaningfully extended to strings?", Proceedings

to the 26$^{\text{rd}}$ Workshop "What comes beyond the standard models", 10 - 19 July, 2023, Ed. N.S. Mankoč Borštnik, H.B. Nielsen, A. Kleppe, Založba Univerze v Ljubljani, DOI: 10.51746/9789612972097, December 23, [arxiv:2312.07548].

12. N.S. Mankoč Borštnik N S, "The spin-charge-family theory is explaining the origin of families, of the Higgs and the Yukawa couplings", *J. of Modern Phys.* **4** (2013) 823[arXiv:1312.1542].

13. N. S. Mankoč Borštnik, "New way of second quantized theory of fermions with either Clifford or Grassmann coordinates and *spin-charge-family* theory " [arXiv:1802.05554v4, arXiv:1902.10628], N. S. Mankoč Borštnik, "How Clifford algebra can help understand second quantization of fermion and boson fields", [arXiv: 2210.06256. physics.gen-ph V1] .

14. N. S. Mankoč Borštnik, "How Clifford algebra can help understand second quantization of fermion and boson fields", [arXiv: 2210.06256. physics.gen-ph V1] ,

15. N. S. Mankoč Borštnik, "Clifford odd and even objects offer description of internal space of fermions and bosons, respectively, opening new insight into the second quantization of fields", The 13$^{\text{th}}$ Bienal Conference on Classical and Quantum Relativistic Dynamics of Particles and Fields IARD 2022, Prague, $6-9$ June, [http://arxiv.org/abs/2210.07004] .

16. M. Blagojević, *Gravitation and gauge symmetries*, IoP Publishing, Bristol 2002.

17. H.B. Nielsen, M. Ninomiya, "Novel String Field Theory and Bound State, Projective Line,and sharply 3-transitive group", [arXiv:2111.05106v1, physics.gen-ph].

18. R. Blumenhagen, D.Lust, S.Theisen, Basic Concepts of String Theory, DOI 10.1007/978-3-642-29497-6, Springer-Verlag Berlin Heidelberg 2013 New York Dordrecht London.

19. K. Wray, "An Introduction to String Theory".

20. E.H.El Kinani, "Between Quantum Virasoro Algebra $\mathcal{L}_\rfloor$ and Generalized Clifford Algebras", [arXiv:math-ph/0310044].

21. Pavšič, M. *The Landscape of Theoretical Physics: Global View*; van der Merwe, A., Ed.; Kluwer Academic Publishers: New York, NY, USA, 2001.

22. Fadeev L.D., Popov V. (1967), "Feynman diagrams for the Young-Mills", *Phys.Lett.* **B** 25 (1) 29.

23. N.S. Mankoč Borštnik, H.B. Nielsen, "Discrete symmetries in the Kaluza-Klein-like theories", doi:10.1007/ *Jour. of High Energy Phys.* **04** (2014) 165 [arXiv:1212.2362].

24. G. Bregar, M. Breskvar, D. Lukman, N.S. Mankoč Borštnik, "Families of Quarks and Leptons and Their Mass Matrices", Proceedings to the 10$^{\text{th}}$ international workshop "What Comes Beyond the Standard Model", 17 -27 of July, 2007, Ed. Norma Mankoč Borštnik, Holger Bech Nielsen, Colin Froggatt, Dragan Lukman, DMFA Založništvo, Ljubljana December 2007, p.53-70 [hep-ph/0711.4681].

25. G. Bregar, N.S. Mankoč Borštnik, "Can we predict the fourth family masses for quarks and leptons?", Proceedings (arxiv:1403.4441) to the 16 th Workshop "What comes beyond the standard models", Bled, 14-21 of July, 2013, Ed. N.S. Mankoč Borštnik, H.B. Nielsen, D. Lukman, DMFA Založništvo, Ljubljana December 2013, p. 31-51 [http://arxiv.org/abs/1212.4055].

26. T. Troha, D. Lukman and N.S. Mankoč Borštnik, "Massless and massive representations in the *spinor technique*", *In. J. Mod. Phys.* **A 29** 1450124 (2014) DOI: 10.1142/S0217751X14501243 [arXiv:1312.1541/v2].

11 A trial to understand the supersymmetry relations through extension of the second quantized fermion and boson fields, either to strings or to odd dimensional spaces

N.S. Mankoč Borštnik[1], H.B. Nielsen[2]

[1]Department of Physics, University of Ljubljana, SI-1000 Ljubljana, Slovenia
[2]Niels Bohr Institute, University of Copenhagen, Blegdamsvej 17, Copenhagen, Denmark

Abstract. The article studies the extension of the internal spaces of fermion and boson second quantized fields, described by the superposition of odd (for fermions) and even (for bosons) products of the operators γ^a, to strings and odd dimensional spaces.
For any symmetry $SO(d-1,1)$ of the internal spaces, it is the number of fermion fields (they appear in families and have their Hermitian conjugated partners in a separate group) equal to the number of boson fields (they appear in two orthogonal groups), manifesting a kind of supersymmetry, which differs from the usual supersymmetry.
The article searches for the supersymmetry arising from extending the "basis vectors" of second quantized fermion and boson fields described in $d = 2(2n+1)$ (in particular $d = (13+1)$) either to strings or to odd-dimensional spaces ($d = 2(2n+1)+1$).

Povzetek: Članek proučuje razširitev notranjih prostorov fermionskih in bozonskih polj v drugi kvantizaciji v strune in v sodo razsežne prostore. Notranji prostori so opisani z "bazičnimi vektorji", ki so superpozicija lihih (za fermione) in sodih (za bozone) produktov operaterjev γ^a. Za vsako simetrijo $SO(d-1,1)$ notranjih prostorov je število fermionskih polj (pojavijo se v družinah in imajo svoje hermitsko konjugirane partnerje v ločeni skupini) enako številu bozonskih polj (pojavijo se v dveh ortogonalnih skupinah), kar kaže neko vrsto supersimetrije, ki pa se razlikuje od običajne supersimetrije. Članek proučuje lastnosti "bazičnih vektorjev" fermionskih in bozonskih polj v dugi kvantizaciji za $d = 2(2n+1)$ (posebej za $d = (13+1)$) po njihovi razširitvi bodisi na strune bodisi na lihe dimenzije ($d = 2(2n+1)+1$).

11.1 Introduction

The contribution, appearing in this proceedings, with the title "Do we understand the internal spaces of second quantized fermion and boson fields, with gravity included?" and in the references therein [1–11], shortly presents the properties of fermion and boson fields treated uniquely if they all start as massless fields.
The *spin-chargge-family* theory, describing the internal spaces of fermion and boson second quantized fields by "basis vectors" which are the superposition of products of an odd number of γ^a (for fermions) and even number of γ^a (for bosons), requires the same number of fermion and boson "basis vectors". Arranging the "basis vectors" to be the eigenvectors of the (chosen) Cartan subalgebra members

(equal to $\frac{d}{2}$ for an even d) of the Lorentz algebra in internal spaces of fermions and bosons, the theory offers an elegant description of the second quantized fermion and boson fields, explaining the second quantization postulates.

The author, with the collaborators [1–11], arrange the "basis vectors" to be the products of nilpotents $(\overset{ab}{(k)}:= \frac{1}{2}(\gamma^a + \frac{\eta^{aa}}{ik}\gamma^b), (\overset{ab}{(k)})^2 = 0)$ and projectors $(\overset{ab}{[k]}:= \frac{1}{2}(1 + \frac{i}{k}\gamma^a\gamma^b), (\overset{ab}{[k]})^2 = \overset{ab}{[k]})$, with the properties $S^{ab}\overset{ab}{(k)} = \frac{k}{2}\overset{ab}{(k)}$, $S^{ab}\overset{ab}{[k]} = \frac{k}{2}\overset{ab}{[k]}$ with $k^2 = \eta^{aa}\eta^{bb}$; $S^{ab} = \frac{i}{2}\gamma^a\gamma^b$.

"Basis vectors" of fermions, chosen to be the algebraic products of an odd number of nilpotents (at least one, the rest are projectors), and "basis vectors" of bosons, chosen to be the algebraic products of an even number of nilpotents (or only of projectors) are correspondingly eigenvectors of all the $\frac{d}{2}$ S^{ab} Cartan subalgebra members of one irreducible representation of fermions.

Fermion "basis vectors" appear in $2^{\frac{d}{2}-1}$ irreducible representations — families — each family having $2^{\frac{d}{2}-1}$ members, including in $d = 2(2n + 1)$ fermions and antifermions. All the fermion "basis vectors" are mutually orthogonal, while the "basis vectors" fulfil together with their Hermitian conjugated partners, appearing in a separate group, the Dirac second quantization postulates for fermions. Fermion "basis vectors" and their Hermitian conjugated partners have together 2^{d-1} members.

Boson "basis vectors" appear in two orthogonal groups, each of the two groups with $2^{\frac{d}{2}-1} \times 2^{\frac{d}{2}-1}$ members have their Hermitian conjugated partners within the same group. There are two kinds of "basis vectors" of boson fields (the ordinary theory does not have two kinds): One kind transforms family members within the family (anyone), and the other transforms any member of a family to the same member of another (or the same) family.

The number of fermion "basis vectors" is equal to the number of boson "basis vectors" manifesting a kind of supersymmetry, which differ from the one offered by string theories [18, 19].

In this contribution, the authors using the *spin-charge-family* theory to represent properties of fermion and boson fields, discuss the extension of the "basis vectors" in $d = 2(2n + 1)$ to strings and to odd-dimensional spaces in order to see which kind of supersymmetry the extension offers.

The vacuum state is constructed from only "basis vectors" of bosons, with spins and charges equal to zero. There are also all fermion and boson "basis vectors" present, all with the momentum equal to zero, if fermions and bosons are not active.

Charges and spins of the vacuum with all the "basis vectors" of fermions and bosons with no momenta present are zero. Any contribution to the vacuum can be written as the algebraic product of a Hermitian conjugated "basis vector" (("basis vector")†) algebraically, $*_A$, multiplied by another "basis vector" ("basis vector"). All the members of one family have the same contribution to the vacuum state and each family has its own contribution to the vacuum state.

Let us shortly repeat the Sect. 2 from the contribution of one of the two authors (N.S.M.B.) in this proceedings (entitled "Do we understand the internal spaces of second quantized fermion and boson fields, with gravity included?").

Starting with the Grassmann algebra [1, 8], offering for the description for the internal degrees of freedom of fermions and bosons 2×2^d anticommuting operators in d-dimensional space [13], θ^a and the derivatives with respect to θ^a, $\frac{\partial}{\partial\theta_a}$ [1], fulfilling the relations $\{\theta^a, \theta^b\}_+ = 0, \{\frac{\partial}{\partial\theta_a}, \frac{\partial}{\partial\theta_b}\}_+ = 0, \{\theta_a, \frac{\partial}{\partial\theta_b}\}_+ = \delta_{ab}$, $(a, b) = (0, 1, 2, 3, 5, \cdots, d)$ we find two kinds of the operators γ^a and $\tilde{\gamma}^a$

$$\gamma^a = (\theta^a + \frac{\partial}{\partial\theta_a}), \quad \tilde{\gamma}^a = i\,(\theta^a - \frac{\partial}{\partial\theta_a}),$$

$$\theta^a = \frac{1}{2}\,(\gamma^a - i\tilde{\gamma}^a), \quad \frac{\partial}{\partial\theta_a} = \frac{1}{2}\,(\gamma^a + i\tilde{\gamma}^a),$$

$$(11.1)$$

offering together $2 \cdot 2^d$ operators: 2^d are superposition of products of γ^a and 2^d of $\tilde{\gamma}^a$, with the properties

$$\{\gamma^a, \gamma^b\}_+ = 2\eta^{ab} = \{\tilde{\gamma}^a, \tilde{\gamma}^b\}_+,$$

$$\{\gamma^a, \tilde{\gamma}^b\}_+ = 0, \quad (a, b) = (0, 1, 2, 3, 5, \cdots, d),$$

$$(\gamma^a)^\dagger = \eta^{aa}\gamma^a, \quad (\tilde{\gamma}^a)^\dagger = \eta^{aa}\tilde{\gamma}^a.$$

$$(11.2)$$

Postulating how does $\tilde{\gamma}^a$ operate on γ^a,

$$\{\tilde{\gamma}^a B = (-)^B\,i\,B\gamma^a\}|\psi_{oc} >,$$

$$(11.3)$$

with $(-)^B = -1$, if B is (a function of) odd products of γ^a's, otherwise $(-)^B = 1$ [3], with the vacuum state $|\psi_{oc} >$, the two Clifford subalgebras, γ^a and $\tilde{\gamma}^a$ reduce to the one described by γ^a [1, 3, 12], while $\tilde{\gamma}^a$ can be used to describe the quantum numbers of the irreducible representations of the superposition of odd products of γ^a. It is useful to arrange all the "basis vectors" describing internal spaces of fermion and boson second quantized fields to be the eigenstates of the Cartan subalgebra members of the Lorentz algebra,

$$S^{03}, S^{12}, S^{56}, \cdots, S^{d-1\,d},$$

$$\tilde{S}^{03}, \tilde{S}^{12}, \tilde{S}^{56}, \cdots, \tilde{S}^{d-1\,d},$$

$$\mathcal{S}^{ab} = S^{ab} + \tilde{S}^{ab},$$

$$(11.4)$$

and write the "basis vectors", describing internal spaces of fermions and boson second quantized fields, to be the products of nilpotents and projectors

$$\overset{ab}{(k)} := \frac{1}{2}(\gamma^a + \frac{\eta^{aa}}{ik}\gamma^b), \quad (\overset{ab}{(k)})^2 = 0,$$

$$\overset{ab}{[k]} := \frac{1}{2}(1 + \frac{i}{k}\gamma^a\gamma^b), \quad (\overset{ab}{[k]})^2 = \overset{ab}{[k]}.$$

$$(11.5)$$

Each nilpotent and projector is chosen to be the eigenvector of one of $\frac{d}{2}$ (for d even) members of the Cartan subalgebra.

The products of an odd number of nilpotents anti-commute, at least one is needed, the rest are projectors. They appear in $2^{\frac{d}{2}-1}$ irreducible representations, representing families; each family has $2^{\frac{d}{2}-1}$ members which are obtainable from any

other member by S^{ab}; the family member of any other family is obtainable by $\tilde{S}^{ab}$ which determine the quantum numbers of a family.

The Hermitian conjugated partners of nilpotents belong to a different group of $2^{\frac{d}{2}-1}$ members in $2^{\frac{d}{2}-1}$ families.

The objects of odd number of nilpotents offers the "basis vectors", $\hat{b}_f^{m\dagger}$, describing the internal space of fermions, which together with the Hermitian conjugated partners, $(\hat{b}_f^{m\dagger})^\dagger = \hat{b}_f^m$ fulfil the postulates of Dirac for the second quantized fermion fields, when applying on the vacuum state, $|\psi_{oc}> = \sum_{f=1}^{2^{\frac{d}{2}-1}} \hat{b}_f^m *_A \hat{b}_f^{m\dagger} |1>$, with m any of the members.

All the odd "basis vectors" are orthogonal among themselves, and all the members of their Hermitian conjugated partners are orthogonal among themselves,

$$\hat{b}_f^{m\dagger} *_A \hat{b}_{f'}^{m'\dagger} = 0, \quad \hat{b}_f^m *_A \hat{b}_{f'}^{m'} = 0, \quad \forall m, m', f, f'. \tag{11.6}$$

The products of an even number of nilpotents commute. They appear in two orthogonal groups, $^I\hat{\mathcal{A}}_f^{m\dagger}$ and $^{II}\hat{\mathcal{A}}_f^{m\dagger}$, each group has $2^{\frac{d}{2}-1} \times 2^{\frac{d}{2}-1}$ members with the Hermitian conjugated partners within the same group. They fulfil the postulates of Dirac for the second quantized boson fields. Their eigenvalues of the Cartan subalgebra members, $\mathcal{S}^{ab} = (\tilde{S}^{ab} + S^{ab})$. Correspondingly, the nilpotents carry the Cartan subalgebra eigenvalue $\pm i$ or ± 1 (since

$$S^{ab} \overset{ab}{(k)} = \frac{k}{2} \overset{ab}{(k)}, \qquad \tilde{S}^{ab} \overset{ab}{(k)} = \frac{k}{2} \overset{ab}{(k)},$$

$$S^{ab} \overset{ab}{[k]} = \frac{k}{2} \overset{ab}{[k]}, \qquad \tilde{S}^{ab} \overset{ab}{[k]} = -\frac{k}{2} \overset{ab}{[k]}, \tag{11.7}$$

with $k^2 = \eta^{aa}\eta^{bb}$), while application of $\mathcal{S}^{ab} = (\tilde{S}^{ab} + S^{ab})$ on any projector gives zero.

The Clifford even "basis vectors" belonging to two different groups are orthogonal.

$$^I\hat{\mathcal{A}}_f^{m\dagger} *_A {}^{II}\hat{\mathcal{A}}_f^{m\dagger} = 0 = {}^{II}\hat{\mathcal{A}}^{m\dagger} \cdot_f *_A {}^I\hat{\mathcal{A}}_f^{m\dagger}. \tag{11.8}$$

The members of each of these two groups have the property.

$$^i\hat{\mathcal{A}}_f^{m\dagger} *_A {}^i\hat{\mathcal{A}}_{f'}^{m'\dagger} \rightarrow \begin{cases} {}^i\hat{\mathcal{A}}_{f'}^{m\dagger}, i = (I, II) \\ \text{or zero}. \end{cases} \tag{11.9}$$

Half of 2^d different products of γ^a's are odd, and half of them are even, manifesting a kind of "supersymmetry", distinguishing from the ordinary supersymmetry.

The algebraic application, $*_A$, of even "basis vectors" $^I\hat{\mathcal{A}}_f^{m\dagger}$ on odd "basis vectors" $\hat{b}_{f'}^{m'\dagger}$ and the odd "basis vectors" $\hat{b}_f^{m\dagger}$ on $^{II}\hat{\mathcal{A}}_f^{m\dagger}$ gives

$$^I\hat{\mathcal{A}}_f^{m\dagger} *_A \hat{b}_{f'}^{m'\dagger} \rightarrow \begin{cases} \hat{b}_{f'}^{m\dagger}, \\ \text{or zero}, \end{cases} \tag{11.10}$$

$$\hat{b}_f^{m\dagger} *_A {}^{II}\hat{\mathcal{A}}_{f'}^{m'\dagger} \rightarrow \begin{cases} \hat{b}_{f''}^{m\dagger}, \\ \text{or zero}, \end{cases} \tag{11.11}$$

while

$$\hat{b}_f^{m\dagger} *_A {}^I\hat{\mathcal{A}}_{f'}^{m'\dagger} = 0, \quad {}^{II}\hat{\mathcal{A}}_f^{m\dagger} *_A \hat{b}_{f'}^{m'\dagger} = 0, \quad \forall (m, m', f, f').$$ (11.12)

If we know the odd "basis vectors" $\hat{b}_f^{m\dagger}$, we are able to generate all the Clifford even ${}^i\hat{\mathcal{A}}_{f'}^{m'\dagger}$, $i = (I, II)$ "basis vectors"

$$ {}^I\hat{\mathcal{A}}_f^{m\dagger} = \hat{b}_{f'}^{m'\dagger} *_A (\hat{b}_{f'}^{m''\dagger})^\dagger. $$ (11.13)

$$ {}^{II}\hat{\mathcal{A}}_f^{m\dagger} = (\hat{b}_{f'}^{m'\dagger})^\dagger *_A \hat{b}_{f''}^{m'\dagger}. $$ (11.14)

We overviewed so far the properties if the internal spaces of fermion and boson second quantized fields. Describing the second quantized fermion and boson fields with nonzero momenta in $d = (3 + 1)$, we represent fermion and boson fields by a tensor product, $*_T$, of the "basis vectors" representing internal spaces and the basis in ordinary space, $\hat{b}_{\vec{p}}^\dagger$,

$$|\vec{p}> = \hat{b}_{\vec{p}}^\dagger |0_p>, \quad <\vec{p}| = <0_p|\hat{b}_{\vec{p}},$$

$$<\vec{p}|\vec{p}'> = \delta(\vec{p} - \vec{p}') = <0_p|\hat{b}_{\vec{p}}\,\hat{b}_{\vec{p}'}^\dagger|0_p>,$$

pointing out

$$<0_p|\hat{b}_{\vec{p}'}\,\hat{b}_{\vec{p}}^\dagger|0_p> = \delta(\vec{p}' - \vec{p}),$$ (11.15)

with the normalization $<0_p|0_p> = 1$.

For the fermion creation operators for a free massless fermion field of the energy $p^0 = |\vec{p}|$, belonging to a family f and to a superposition of family members m applying on the extended vacuum state including both spaces, $|\psi_{oc}> *_T |0_{\vec{p}}>$, we have

$$\hat{b}_f^{s\dagger}(\vec{p}) = \sum_m c^{sm}{}_f(\vec{p})\, \hat{b}_{\vec{p}}^\dagger *_T \hat{b}_f^{m\dagger}.$$ (11.16)

The creation operators $\hat{b}_f^{s\dagger}(\vec{p})$ and their Hermitian conjugated partners annihilation operators $\hat{b}_f^s(\vec{p})$, creating and annihilating the single fermion states, respectively, fulfil when applying the vacuum state, $|\psi_{oc}> *_T |0_{\vec{p}}>$, the anticommutation relations for the second quantized fermions, postulated by Dirac (Ref. [8], Sect.3), explaining the Dirac's second quantization postulates for fermions, Eq. (28) in this proceedings of the author N.S.M.B..

The even "basis vectors" have to carry the space index α which is equal to $\mu = (0, 1, 2, 3)$ if they describe the vector component of the "basis vectors", and they are equal to $\sigma = (5, 6, ...)$ if describing the scalar components of the "basis vectors"

$$ {}^i\hat{\mathcal{A}}_{f\alpha}^{m\dagger}(\vec{p}) = {}^i\hat{\mathcal{C}}^m{}_{f\alpha}(\vec{p}) *_T {}^i\hat{\mathcal{A}}_f^{m\dagger}, i = (I, II), $$ (11.17)

with ${}^i\hat{\mathcal{C}}^m{}_{f\alpha}(\vec{p}) = {}^i\mathcal{C}^m{}_{f\alpha}\,\hat{b}_{\vec{p}}^\dagger$, with $\hat{b}_{\vec{p}}^\dagger$ defined in Eqs. (11.15). We treat free massless bosons of momentum $\vec{p}$ and energy $p^0 = |\vec{p}|$ and of particular "basis vectors"

${}^{i}\hat{\mathcal{A}}_{f}^{m\dagger}$'s which are the eigenvectors of all the Cartan subalgebra members. The creation operators for boson gauge fields commute, explaining the Dirac's second quantization postulates for bosons.

In Table 4 in the contribution of the author N.S.M.B. in this proceedings (NSMB) we can find how do one family of the "basis vectors" of quarks and leptons and anti-quarks and anti-leptons look like. The *spin-charge-family* requires the existence of the right-handed neutrinos and left-handed anti-neutrions. We can read that the $SO(7,1)$ content of $SO(13,1)$ are the same for quarks and leptons, and the same for anti-quarks and anti-leptons. Quarks and leptons differ only in the last product, in the $SU(3) \times U(1)$ content.

The quantum numbers of u_{L}^{c1}, presented in Table 4 (called NSMB from now on in this contribution) in the seventh line $u_{L}^{c1}(\equiv \overset{03}{[-i]} \overset{12}{[+]} | \overset{56}{[+]} \overset{78}{[-]} \| \overset{9\,10}{(+)} \overset{11\,12}{[-]} \overset{13\,14}{[-]}$,
are: $S^{12} = \frac{1}{2}$, $S^{03} = -\frac{i}{2}$, $\tau^{13} = \frac{1}{2}(S^{56} - S^{78}) = \frac{1}{2}$, $\tau^{23} = \frac{1}{2}(S^{56} + S^{78}) = 0$, $\tau^{33} = \frac{1}{2}(S^{9\,10} - S^{11\,12}) = \frac{1}{2}$, $\tau^{38} = \frac{1}{2\sqrt{3}}(S^{9\,10} + S^{11\,12} - 2S^{13\,14}) = \frac{1}{2\sqrt{3}}$.

A photon "basic vector" ${}^{II}\hat{\mathcal{A}}_{phu_{L}^{c1} \to u_{L}^{c1}}^{\dagger}$ can be found by the multiplication of u_{L}^{c1}
from the left-hand side by γ^{9}: $\gamma^{9} u_{L}^{c1} \to \overset{03}{[-i]} \overset{12}{[+]} | \overset{56}{[+]} \overset{78}{[-]} \| \overset{9\,10}{[-]} \overset{11\,12}{[-]} \overset{13\,14}{[-]}$. The
photon "basis vector" ${}^{II}\hat{\mathcal{A}}_{phu_{L}^{c1} \to u_{L}^{c1}}^{\dagger}(\equiv \overset{03}{[-i]} \overset{12}{[+]} | \overset{56}{[+]} \overset{78}{[-]} \| \overset{9\,10}{[-]} \overset{11\,12}{[-]} \overset{13\,14}{[-]}$), having
all the members of the algebraic product equal to projectors, which obey for even "basis vectors" the relation $\mathcal{S}^{ab} = (S^{ab} + \tilde{S}^{ab})$, and has correspondingly all the quantum numbers equal zero, can not change the internal space quantum numbers of an odd "basis vectors", what photons do not. Photons can give to fermions only the momentum in the ordinary space-time.

Let us point out again that knowing all the odd "basis vectors" describing the internal spaces of fermions we are able to write all the even "basis vectors" describing two groups of bosons, Eqs. (11.13, 11.14).

The photon "basis vector" ${}^{II}\hat{\mathcal{A}}_{phu_{L}^{c1} \to u_{L}^{c1}}^{\dagger}(\equiv \overset{03}{[-i]} \overset{12}{[+]} \overset{56}{[+]} \overset{78}{[-]} \| \overset{9\,10}{[-]} \overset{11\,12}{[-]} \overset{13\,14}{[-]}$) can
be written as $(u_{L\,7th}^{c1})^{\dagger} *_{A} u_{L\,7th}^{c1}$ or as $(\bar{u}_{R\,39th}^{c1})^{\dagger} *_{A} \bar{u}_{R\,39th}^{c1}$.

The photon ${}^{I}\hat{\mathcal{A}}_{ph\,\bar{u}_{R}^{c1} \to \bar{u}_{R}^{c1}}^{\dagger}$ can be represented as $\bar{u}_{R\,39th}^{c1} *_{A} (\bar{u}_{R\,39th}^{c1})^{\dagger}$.

One can find in Eqs. (22,23,24) of (NSMB) the "basis vectors" for gravitons $({}^{I}\hat{\mathcal{A}}_{gr\,u_{R\uparrow}^{c1} \to u_{R\downarrow}^{c1}}^{\dagger} = u_{R\,2nd}^{c1} *_{A} (u_{R\,1st}^{c1})^{\dagger})$, weak bosons $({}^{I}\hat{\mathcal{A}}_{w1\,d_{L}^{c1} \to u_{L}^{c1}}^{\dagger} = u_{L\,7th}^{c1} *_{A} (d_{L\,5th}^{c1})^{\dagger})$ and gluons $({}^{I}\hat{\mathcal{A}}_{gl\,d_{L}^{c1} \to d_{L}^{c3}}^{\dagger} = d_{L\,21st}^{c3} *_{A} (d_{L\,5th}^{c1})^{\dagger})$.

In all these case the numbers, $1^{st}, 5^{th}, 7^{th}, 21^{st}$ and 39th tell the lines in Table 4 in (SNMB) where the odd "basis vectors" of quarks, leptons, antiquarks and anti-leptons are presented.

11.2   Extensions of points in ordinary space time to strings, extensions of "basis vectors" to odd-dimensional spaces.

The description of the internal spaces of fermion and boson second quantized fields with the "basis vectors" which are products of an odd and an even number

of nilpotents, the rest are projectors, all are eigenvectors of the Cartan subalgebra members, offers an equal number of fermion and boson "basis vectors", demonstrating a (kind of) supersymmetry. Both, the extension of points in ordinary space-time to strings, and the extension of "basis vectors" to odd-dimensional spaces, might help (following the literature [9, 18, 19, 22]) to achieve renormalizability of the proposed *spin-charge-family* theory.

To extend the points in ordinary space-time to strings we must define the "basis vectors" on a string with coordinates (σ, τ).

We have, in this case, two odd and two even "basis vectors" the eigenvectors of the Cartan subalgebra members $S^{01}, \tilde{S}^{01}, \mathcal{S}^{ab} = (S^{01} + \tilde{S}^{01})$.

$$
\begin{array}{c}
\text{Clifford odd} \\
\hat{b}^{1\dagger}_{1s} = \overset{01}{(+i)}_s, \quad \hat{b}^{1}_{1s} = \overset{01}{(-i)}_s, \\
\text{Clifford even} \\
{}^{I}\mathcal{A}^{1\dagger}_{1s} = \overset{01}{[+i]}_s, \quad {}^{II}\mathcal{A}^{1\dagger}_{1s} = \overset{01}{[-i]}_s.
\end{array} \tag{11.18}
$$

The two nilpotent"basis vectors" are Hermitian conjugated to each other. Making a choice that $\hat{b}^{1\dagger}_1 = \overset{01}{(+i)}_s$ is the "basis vector", the second odd object is then its Hermitian conjugated partner. There is only one family ($2^{\frac{d}{2}-1} = 1$) with one member. The vacuum state is for this choice equal to $|\psi_{oc_s}> = \overset{01}{[-i]}_s |1> = ((\overset{01}{+i})_s)^{\dagger} *_A \overset{01}{(+i)}_s |1>$. There is only one family ($2^{\frac{d}{2}-1} = 1$) with one member ($2^{\frac{d}{2}-1} = 1$). The eigenvalue S^{01} of $\hat{b}^{1\dagger}_{1s}(=\overset{01}{(+i)}_s)$ is $\frac{i}{2}$.

Each of the two Clifford even "basis vectors" is self adjoint $(({}^{I,II}\mathcal{A}^{1\dagger}_{1s})^{\dagger} = {}^{I,II}\mathcal{A}^{1\dagger}_{1s})$, with the eigenvalues $\mathcal{S}^{01} = (S^{01} + \tilde{S}^{01})$ equal to 0, since $S^{01} \overset{01}{[\pm i]}_s = \pm i \overset{01}{[\pm i]}_s$ and $\tilde{S}^{01} \overset{01}{[\pm i]}_s = \mp i \overset{01}{[\pm i]}_s$. It follows that

$$
{}^{I}\mathcal{A}^{1\dagger}_{1s} = \hat{b}^{1\dagger}_{1s} *_A (\hat{b}^{1\dagger}_{1s})^{\dagger}, \qquad {}^{II}\mathcal{A}^{1\dagger}_{1s} = (\hat{b}^{1\dagger}_{1s})^{\dagger} *_A \hat{b}^{1\dagger}_{1s}.
$$

To find the "basis vectors" for second quantized fermion and boson fields extended to strings, we need to make a tensor product '$*_T$', of "basis vectors" of internal space in $d = 2(2n + 1)$ and "basis vectors" on a string.

The extension to strings will be discussed in Subsect. 11.2.1.

We can achieve a kind of a supersymmetric partners to the "basis vectors" presented fermions and bosons in $2(2n + 1)$-dimensional internal spaces of fermions and bosons in an odd dimensional space $d = 2(2n+1)+1$. We can find in this case two groups of "basis vectors" [9]: One group determines the anti-commuting "basis vectors" of $2^{\frac{d-1}{2}-1}$ fermions appearing in $2^{\frac{d-1}{2}-1}$ families, with their $2^{\frac{d-1}{2}-1} \times 2^{\frac{d-1}{2}-1}$ Hermitian conjugated partners appearing in a separate group, as well as two orthogonal groups each with $2^{\frac{d-1}{2}-1} \times 2^{\frac{d-1}{2}-1}$ of "basis vectors", with their Hermitian conjugated partners within the same group.

The second group determines anti-commuting "basis vectors" appearing in two separate orthogonal groups each with $2^{\frac{d-1}{2}-1} \times 2^{\frac{d-1}{2}-1}$ of "basis vectors", with

their Hermitian conjugated partners within the same group, as well as the commuting "basis vectors" of "fermions" appearing in families with their Hermitian conjugated partners in a separate group.

This kind of a supersymmetry will be discussed in Subsect. 11.2.2.

Both kinds of searching for the renormalizability need further discussions, on which we are not yet really prepared.

11.2.1 Extension of "basis vectors" in $d = 2(2n + 1)$ to strings

We might define the "basis vector" of a gravitino as a tensor product, $*_{T^{\cdot}}$, of a photon "basis vector" ${}^{I}\hat{\mathcal{A}}^{\dagger}_{\mathrm{phu}_L^{c1} \to u_L^{c1}}$ $(\equiv \overset{03}{[-i]}\ \overset{12}{[+]}\ |\ \overset{56}{[+]}\ \overset{78}{[-]}\ \|\ \overset{9\,10}{[+]}\ \overset{11\,12}{[-]}\ \overset{13\,14}{[-]}\ )$ (which has spins and charges in internal space equal to zero), for example, with $\hat{b}_{1s}^{1\dagger}(\equiv \overset{01}{(+i)}_s)$ on a string: $\hat{b}_{1\,gravitino}^{1\dagger}(\equiv \overset{03}{[-i]}\ \overset{12}{[+]}\ |\ \overset{56}{[+]}\ \overset{78}{[-]}\ \|\ \overset{9\,10}{[+]}\ \overset{11\,12}{[-]}\ \overset{13\,14}{[-]}\ *_{T^{\cdot}}\ \overset{01}{(+i)}_s)$. This is an anti-commuting object and could manifest gravitino if the photon "basis vector" ${}^{I}\hat{\mathcal{A}}^{\dagger}_{\mathrm{phu}_L^{c1} \to u_L^{c1}}$ is in a tensor product with basis in ordinary space-time, carrying the space index $\mu = (0, 1, 2, 3)$.

The extensions of all the other "basis vectors" — either the ones with an odd number of nilpotents describing the internal spaces of fermions, or with an even number of nilpotents describing the internal spaces of bosons — by the tensor product, $*_{T'}$, with the two commuting self adjoint "basis vectors" describing the internal space on the string, ${}^{i}\mathcal{A}_{1s}^{1\dagger}, i = (I, II)$, do not change commutation properties: The extended "basis vectors" keep commutation properties of the "basis vectors" of fermions and bosons.

The extensions of "basis vectors" describing fermions and bosons by the tensor product, $*_{T'}$, with the nilpotent $\hat{b}_{1s}^{1\dagger}$ do change the commutation relations: The commuting ones become anti-commuting, the anti-commuting become commuting.

Let us try to see general properties of tensor products, $*_{T'}$, of the "basis vectors" with an odd number of nilpotents (describing the internal spaces of the second quantized fermion fields) $\hat{b}_f^{m\dagger}$ and of the "basis vectors" with an even number of nilpotents (describing the internal spaces of the second quantized boson fields) ${}^{I,II}\mathcal{A}_f^{m\dagger}$ with the "basis vectors" of a string.

There are four possibilities:

i.

$$\hat{b}_f^{m\dagger}\ *_{T'}\ {}^{I}\mathcal{A}_{1s}^{1\dagger}$$

represents the anti-commuting "basis vectors" extended with a string offering the description of the internal spaces of fermions in $d = 2(2n + 1)$.

ii.

$$^{I,II}\mathcal{A}_f^{m\dagger}\ *_{T'}\ {}^{I}\mathcal{A}_{1s}^{1\dagger}$$

represents the commuting "basis vectors" extended with a string offering the description of the internal spaces of bosons in d $= 2(2n+1)$. Since $^{II}\mathcal{A}_{1s}^{1\dagger}$ defines the vacuum state $|\psi_{ocs}>=[\overset{01}{-i}]_s|1>$ for $\hat{b}_{1s}^{1\dagger}$, only $^I\mathcal{A}_{1s}^{1\dagger}$ is used in a tensor product $*_{T'}$.

iii.

$$^{I,II}\mathcal{A}_f^{m\dagger} \;*_{T'}\; \hat{b}_{1s}^{1\dagger}$$

represents the anti-commuting "basis vectors" extended with a string offering the description of the internal spaces of anti-commuting objects with the quantum numbers of bosons in d $= 2(2n+1)$.

iv.

$$\hat{b}_f^{m\dagger} \;*_{T'}\; \hat{b}_{1s}^{1\dagger}$$

represents the commuting "basis vectors" extended with a string offering the description of the internal spaces of bosons with the quantum numbers of fermions in d $= 2(2n+1)$.

We recognize the supersymmetry:

Each $^{I,II}\mathcal{A}_f^{m\dagger} \;*_{T'}\; ^I\mathcal{A}_{1s}^{1\dagger}$ and each $\hat{b}_f^{m\dagger} \;*_{T'}\; ^I\mathcal{A}_{1s}^{1\dagger}$ has a supersymmetric partner in either $^{I,II}\mathcal{A}_f^{m\dagger} \;*_{T'}\; \hat{b}_{1s}^{1\dagger}$ or in $\hat{b}_f^{m\dagger} \;*_{T'}\; \hat{b}_{1s}^{1\dagger}$.

The extension of the $2^{\frac{d}{2}-1}$ "basis vectors" with an odd number of nilpotents appearing in $2^{\frac{d}{2}-1}$ families with their Hermitian conjugated partners in a separate group, and of the "basis vectors" of an even number of nilpotents appearing in two orthogonal groups, in a tensor extension by $\hat{b}_{1s}^{1\dagger}$ needs further studies to be understood.

11.2.2 "Supersymmetry" in odd dimensional spaces

Let us come to the second possibility to find out what kind of symmetry the internal odd-dimensional spaces d $= (2(2n+1)+1)$ offer. They namely manifest two groups of anti-commuting "basis vectors" and two groups of commuting "basis vectors", as discussed in the article [9].

"Basis vectors" of the first part of each of the two groups have properties as we presented for $2(2n+1)$-dimensional spaces
— the anti-commuting "basis vectors" with an odd number of nilpotents $\hat{b}_f^{m\dagger}$ appear in families, their Hermitian conjugated partners form a separate group $\hat{b}_f^m$
— the commuting "basis vectors" with an even number of nilpotents appear in two orthogonal groups, $^{I,II}\mathcal{A}_f^{m\dagger}$, each group have the Hermitian conjugated partners within the same group.

"Basis vectors" of the second part of each of the two groups have completely different properties than the first part

— the anti-commuting"basis vectors" appear in two orthogonal groups, with the Hermitian conjugated partners within the same group
— the commuting "basis vectors" appear in families and have their Hermitian conjugated partners in a separate group.

Let us try to understand the properties of the second part of the "basis vectors".

These "basis vectors" and their Hermitian conjugated partners can be obtained from the first part by the application of S^{0d} on the two groups of the first part.

Applying $S^{0d} = \frac{i}{2}\gamma^0\gamma^d$ (having the even number of γ^a) on $\hat{b}^{m\dagger}_f$ does not change the oddness of the new object $\gamma^0\gamma^d\hat{b}^{m\dagger}_f$. However, $\gamma^0\hat{b}^{m\dagger}_f$ represent now $^{II}\mathcal{A}^{m'\dagger}_{f'}$, while γ^d multiplying $^{II}\mathcal{A}^{m'\dagger}_{f'}$, keep the oddness unchanged.

The application of the even operator $S^{0d} = \frac{i}{2}\gamma^0\gamma^d$ on an object with an even number of nilpotents $^{II}\mathcal{A}^{m\dagger}_f$ does not change the evenness of the object $\gamma^0\gamma^d\, ^{II}\mathcal{A}^{m\dagger}_f$. However, $\gamma^0\, ^{II}\mathcal{A}^{m\dagger}_f$ represent indeed $\hat{b}^{m'\dagger}_{f'}$ while γ^d multiplying $\hat{b}^{m'\dagger}_{f'}$, keep the evenness unchanged.

We can conclude that odd dimensional spaces, $d = 2(2n+1)+1$,

i.   offer the anti-commuting $2^{\frac{d-1}{2}-1}$ "basis vectors" $\hat{b}^{m\dagger}_f$ appearing in $2^{\frac{d-1}{2}-1}$ families, with their Hermitian conjugated $2^{\frac{d-1}{2}-1} \times 2^{\frac{d-1}{2}-1}$ partners, $\hat{b}^m_f$, in a separate group, and

ii.   the commuting $2 \times 2^{\frac{d-1}{2}-1} \times 2^{\frac{d-1}{2}-1}$ "basis vectors" $^i\mathcal{A}^{m\dagger}_f, i = (I, II)$, appearing in two orthogonal groups with their Hermitian conjugated partners within the same group.

iii.   They offer as well the anti-commuting $2^{\frac{d-1}{2}-1} \times 2^{\frac{d-1}{2}-1}$ "basis vectors" $^i\mathcal{A}^{m\dagger}_f$ appearing in two orthogonal groups with their Hermitian conjugated partners within the same group, and

iv.   the commuting $2^{\frac{d-1}{2}-1}$ "basis vectors" $\hat{b}^{m\dagger}_f$ appearing in $2^{\frac{d-1}{2}-1}$ families, with their Hermitian conjugated $2^{\frac{d-1}{2}-1} \times 2^{\frac{d-1}{2}-1}$ partners, $\hat{b}^m_f$, in a separate group.

Also this case needs further studies to be understood.

11.3   Conclusions

The description of the internal spaces of fermions and bosons in $d = 2(2n+1)$ with the "basis vectors" with odd and even numbers of nilpotents, respectively, offers a kind of supersymmetry, existing in equal number of anti-commuting fermions and of commuting bosons. This is not the usual supersymmetry.

One way to achieve renormalizability of the proposed *spin-charge-family* theory might be, following the literature [9, 18, 19, 22], to extend the "basis vectors" in $d = 2(2n+1)$ with the tensor product $*_{T'}$ with the "basis vectors" and Hermitian conjugated partners of strings, $\hat{b}^{1\dagger}_{1s}$ and $^I\mathcal{A}^{1\dagger}_{1s}$:

$$\hat{b}^{m\dagger}_f \ *_{T'} \ ^I\mathcal{A}^{1\dagger}_{1s}, \quad ^{I,II}\mathcal{A}^{m\dagger}_f \ *_{T'} \ ^I\mathcal{A}^{1\dagger}_{1s},$$

$$\hat{b}^{m\dagger}_f \ *_{T'} \ \hat{b}^{1\dagger}_{1s}, \quad ^{I,II}\mathcal{A}^{m\dagger}_f \ *_{T'} \ \hat{b}^{1\dagger}_{1s}.$$

The second way is to extend the "basis vectors" in $d = 2(2n+1)$ into "basis vectors" in $d = (2(2n+1) + 1)$. Again we have four possibilities:

$$\text{The anti}-\text{commuting } \hat{b}^{m\dagger}_f, \quad \text{the commuting } ^{I,II}\mathcal{A}^{m\dagger}_f,$$

$$\text{the commuting } \gamma^d \ \hat{b}^{m\dagger}_f, \quad \text{the anti}-\text{commuting } \gamma^d \ ^{I,II}\mathcal{A}^{m\dagger}_f.$$

We can conclude that each of the two possibilities offering a kind of supersymmetry seems meaningful. The extension of the "basis vectors" in $d = 2(2n + 1)$ with the tensor product $*_{T'}$ to strings suggests that at low enough energies only $\hat{b}^{m\dagger}_f$ $*_{T'} \ ^I\mathcal{A}^{1\dagger}_{1s}$ and $^{I,II}\mathcal{A}^{m\dagger}_f \ *_{T'} \ ^I\mathcal{A}^{1\dagger}_{1s}$ can be observable.
The extension of the "basis vectors" in $d = 2(2n+1)$ to the odd-dimensional space only anti-commuting $\hat{b}^{m\dagger}_f$ and commuting $^{I,II}\mathcal{A}^{m\dagger}_f$.
Not all of them, as we realize from the observations.

It might be that nature does not need the supersymmetry "to make the theory renormalizable and anomaly-free.

Acknowledgments

References

1. N. Mankoč Borštnik, "Spinor and vector representations in four dimensional Grassmann space", *J. of Math. Phys.* **34** (1993) 3731-3745, "Unification of spin and charges in Grassmann space?", hep-th 9408002, IJS.TP.94/22, Mod. Phys. Lett.**A (10)** No.7 (1995) 587-595;
2. A. Borštnik Bračič, N. S. Mankoč Borštnik, "On the origin of families of fermions and their mass matrices", hep-ph/0512062, Phys. Rev. **D 74** 073013-28 (2006).
3. N.S. Mankoč Borštnik, H.B.F. Nielsen, *J. of Math. Phys.* **43**, 5782 (2002) [arXiv:hep-th/0111257]. "How to generate families of spinors", *J. of Math. Phys.* **44** 4817 (2003) [arXiv:hep-th/0303224].
4. N.S. Mankoč Borštnik, "Matter-antimatter asymmetry in the *spin-charge-family* theory", *Phys. Rev.* **D 91** (2015) 065004 [arXiv:1409.7791].

5. N.S. Mankoč Borštnik, D. Lukman, "Vector and scalar gauge fields with respect to d $= (3 + 1)$ in Kaluza-Klein theories and in the *spin-charge-family theory*", *Eur. Phys. J. C* **77** (2017) 231.

6. N.S. Mankoč Borštnik, H.B.F. Nielsen, "Understanding the second quantization of fermions in Clifford and in Grassmann space", *New way of second quantization of fermions — Part I and Part II*, [arXiv:2007.03517, arXiv:2007.03516].

7. N. S. Mankoč Borštnik, H. B. Nielsen, "How does Clifford algebra show the way to the second quantized fermions with unified spins, charges and families, and with vector and scalar gauge fields beyond the *standard model*", Progress in Particle and Nuclear Physics, http://doi.org/10.1016.j.ppnp.2021.103890 .

8. N. S. Mankoč Borštnik, "How Clifford algebra helps understand second quantized quarks and leptons and corresponding vector and scalar boson fields, opening a new step beyond the standard model", Reference: NUPHB 994 (2023) 116326 , [arXiv: 2210.06256, physics.gen-ph V2].

9. N. S. Mankoč Borštnik, "Clifford odd and even objects in even and odd dimensional spaces", Symmetry 2023,15,818-12-V2 94818, https:doi.org/10.3390/sym15040818, [arxiv.org/abs/2301.04466]   ,   https://www.mdpi.com/2073-8994/15/4/818 Manuscript ID: symmetry-2179313.

10. N. S. Mankoč Borštnik, "Can the "basis vectors", describing t he internal spaces of fermion and boson fields with the Clifford odd (for fermion) and Clifford even (for boson) objects, explain interactions among fields, with gravitons included?" [arxiv: 2407.09482].

11. N. S. Mankoč Borštnik, H.B. Nielsen, "Can the "basis vectors", describing the internal space of point fermion and boson fields with the Clifford odd (for fermions) and Clifford even (for bosons) objects, be meaningfully extended to strings?", Proceedings to the 26$^{\rm rd}$ Workshop "What comes beyond the standard models", 10 - 19 July, 2023, Ed. N.S. Mankoč Borštnik, H.B. Nielsen, A. Kleppe, Založba Univerze v Ljubljani, DOI: 10.51746/9789612972097, December 23, [arxiv:2312.07548].

12. N.S. Mankoč Borštnik N S, "The spin-charge-family theory is explaining the origin of families, of the Higgs and the Yukawa couplings", *J. of Modern Phys.* **4** (2013) 823[arXiv:1312.1542].

13. N. S. Mankoč Borštnik, "New way of second quantized theory of fermions with either Clifford or Grassmann coordinates and *spin-charge-family* theory " [arXiv:1802.05554v4, arXiv:1902.10628], N. S. Mankoč Borštnik, "How Clifford algebra can help understand second quantization of fermion and boson fields", [arXiv: 2210.06256. physics.gen-ph V1] .

14. N. S. Mankoč Borštnik, "How Clifford algebra can help understand second quantization of fermion and boson fields", [arXiv: 2210.06256. physics.gen-ph V1] ,

15. N. S. Mankoč Borštnik, "Clifford odd and even objects offer description of internal space of fermions and bosons, respectively, opening new insight into the second quantization of fields", The 13$^{\rm th}$ Bienal Conference on Classical and Quantum Relativistic Dynamics of Particles and Fields IARD 2022, Prague, $6-9$ June, [http://arxiv.org/abs/2210.07004] .

16. M. Blagojević, *Gravitation and gauge symmetries*, IoP Publishing, Bristol 2002.

17. H.B. Nielsen, M. Ninomiya, "Novel String Field Theory and Bound State, Projective Line,and sharply 3-transitive group", [arXiv:2111.05106v1, physics.gen-ph].

18. R. Blumenhagen, D.Lust, S.Theisen, Basic Concepts of String Theory, DOI 10.1007/978-3-642-29497-6, Springer-Verlag Berlin Heidelberg 2013 New York Dordrecht London.

19. K. Wray, "An Introduction to String Theory".

20. E.H.El Kinani, "Between Quantum Virasoro Algebra $\mathcal{L}_{\rfloor}$ and Generalized Clifford Algebras", [arXiv:math-ph/0310044].

21. Pavšič, M. *The Landscape of Theoretical Physics: Global View*; van der Merwe, A., Ed.; Kluwer Academic Publishers: New York, NY, USA, 2001.

22. Fadeev L.D., Popov V. (1967), "Feynman diagrams for the Young-Mills", *Phys.Lett.* **B** 25 (1) 29.

23. N.S. Mankoč Borštnik, H.B. Nielsen, "Discrete symmetries in the Kaluza-Klein-like theories", doi:10.1007/ *Jour. of High Energy Phys.* **04** (2014) 165 [arXiv:1212.2362].

24. G. Bregar, M. Breskvar, D. Lukman, N.S. Mankoč Borštnik, "Families of Quarks and Leptons and Their Mass Matrices", Proceedings to the 10th international workshop "What Comes Beyond the Standard Model", 17 -27 of July, 2007, Ed. Norma Mankoč Borštnik, Holger Bech Nielsen, Colin Froggatt, Dragan Lukman, DMFA Založništvo, Ljubljana December 2007, p.53-70 [hep-ph/0711.4681].

25. G. Bregar, N.S. Mankoč Borštnik, "Can we predict the fourth family masses for quarks and leptons?", Proceedings (arxiv:1403.4441) to the 16 th Workshop "What comes beyond the standard models", Bled, 14-21 of July, 2013, Ed. N.S. Mankoč Borštnik, H.B. Nielsen, D. Lukman, DMFA Založništvo, Ljubljana December 2013, p. 31-51 [http://arxiv.org/abs/1212.4055].

26. T. Troha, D. Lukman and N.S. Mankoč Borštnik, "Massless and massive representations in the *spinor technique*", *In. J. Mod. Phys.* **A 29** 1450124 (2014) DOI: 10.1142/S0217751X14501243 [arXiv:1312.1541/v2].

12   Time-Independent Special Theory of Relativity

Euich Miztani[**]

Institute for Fundamental Science (JIFS),5-14, Yoshida-honmachi, Sakyo-ku, Kyoto, Japan 606-8317; Aichi Prefectural Bihoku High School, Kitayamacho-Nishi 4, Konan, Aichi, Japan 483-8157

Abstract. In the process of Albert Einstein establishing the theory of special relativity, the principle of relativity is completely based on a geometrical description. On the other hand, the electro-magnetic theory is purely algebraic and complicated. Minkowski's work extended it for 4-dimensional space-time which is purely algebraic as well.
However, we can understand Einstein's ideas much simpler and more phenomenally in section 1. Such a description of special relativity will facilitate research in spintronics to consider the relativistic effect. Besides, it leads to an unknown special orthogonal group in real space, not the indefinite orthogonal group SO(1,3) in section 2. Furthermore, long-standing controversies of displacement current will be solved in section 3. In this talk we discuss the 'complete' geometric special relativity and its new Lie group in real space. Furthermore, our discussions are based on footnotes [1], [2], [3] and [4].

Povzetek: V tem prispevku razpravlja avtor o "celostni" geometrijski posebni teoriji elativnosti in njeni novi Liejevi grupi v realnem prostoru. Posebna teorija relativnosti Alberta Einsteina temelji na geometrijskem opisu. Elektromagnetna teorija pa je algebrska in zapletena. Minkowskega delo je razširilo opis na tirirazsežni prostor-čas, ki je prav tako popolnoma algebrski. V prvem poglavju prispevka avtor pokaže, kako lahko razumemo Einsteinove ideje enostavneje in bolj fenomenološko. Takšen opis posebne teoije relativnosti olajša raziskave v spintroniki, ko želimo upoštevati relativistični efekt. V drugem poglavju obravnava avtor posebno ortogonalno grupo v realnem prostoru, ki ni ortogonalna grupa SO(1,3). V tretjem poglavju rešuje avtor dolgoletne spore o izpodrivnem toku.

12.1   Another Derivation of Special Relativity Different from Einstein

12.1.1   Relativistic Aberration

Firstly, let us think of an observer when in the static system as shown in Figure 1 and inertia system ′ in Figure 2. A ray of light to the observer leans to the x′ axis by the aberration based on the *principle of the constancy of the speed of light*, as the velocity of the observer v approaches to the velocity of light.

[**] euichi@gmail.com,euichi@gmail.com,Mizutani5567@aichi-c.ac.jp,mizutani5567@aichi-c.ac.jp
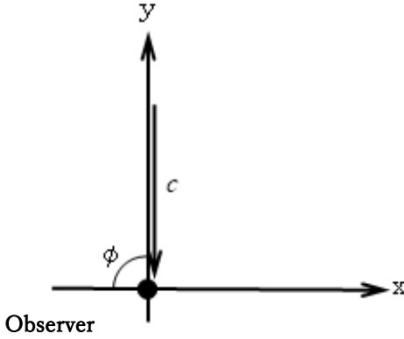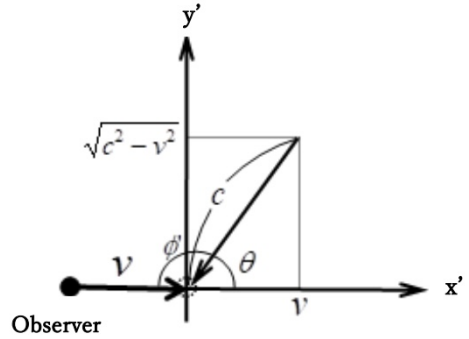
Figure 1   Figure 2

The formula of relativistic aberration is

$$\cos \phi' = \frac{\cos \phi - v/c}{1 - (v/c)\cos \phi}, \tag{1.1}$$

where ϕ and ϕ' are angles between the ray of light and the x axis in and ', and c is the velocity of light. Since $\phi = \pi/2$, in this case as shown in Figure 1, it results in:

$$\cos \phi' = -v/c, \tag{1.2}$$

$$\cos\left(\pi - \phi'\right) = \cos\theta = v/c. \tag{1.3}$$

It corresponds to what Figure 2 shows. Discussing special relativity from a geo-metrical viewpoint, relativistic aberration plays a key role.

12.1.2   Relativistic Coulomb Force

We know that the Coulomb force between an electron and a positron moving with relativistic speed is considerably reduced. It will be explained by the aberration we discussed above. As shown in Figure 3, when the pair of electron and positron travel horizontally at relativistic speed, an observer detects the electric field E by the relativistic aberration.

Since only the vertical component of the electric field is active for the electron, relativistic Coulomb force F' from the observer's viewpoint is

$$F' = qE_\perp, \tag{1.4}$$

where q is a quantity of electric charge, E is a vertical component of E expressed by the static system. Since $E_\perp = E\sin\theta$ from Figure 2, Eq. 1.4 is

$$F' = qE\sin\theta. \tag{1.5}$$
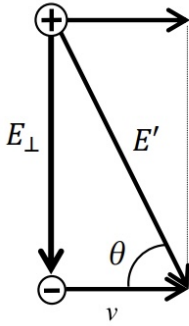
Observer in the static system

Figure 3

From Eq. 1.3, Eq. 1.5 is

$$F' = qE\sqrt{1 - \cos^2\theta} = qE\sqrt{1 - (v/c)^2} \, . \tag{1.6}$$

That corresponds to the original equation by Einstein in [1].

12.1.3   Relativistic Electro-magnetic Field

Relativistic magnetic flux density B'_x, B'_y and B'_z are expressed by

$$B'_x = B_x \, , \tag{1.7}$$

$$B'_y = \beta \left(B_y + \frac{v}{c^2} E_z \right) \, , \tag{1.8}$$

$$B'_z = \beta \left(B_z - \frac{v}{c^2} E_y \right) \, , \tag{1.9}$$

and the electric field E'_x, E'_y and E'_z are expressed by

$$E'_x = E_x \, . \tag{1.10}$$

$$E'_y = \beta(E_y - vB_z) \, , \tag{1.11}$$

$$E'_z = \beta \left(E_z + vB_y \right) \, , \tag{1.12}$$

where $\beta = 1/\sqrt{1 - (v/c)^2}$. Let us discuss those equations from a geometric viewpoint. Firstly, let us think of the magnetic flux:

$$B'_x = B_x \, , \tag{1.7}$$

$$B'_y = \beta \left(B_y + \frac{v}{c^2} E_z \right) \, , \tag{1.8}$$

$$B_z' = \beta \left(B_z - \frac{v}{c^2} E_y \right) .$$
(1.9)

In the original paper by Albert Einstein [1], those equations of 1.7 to 1.12 are derived from very complicated algebraic expansions. However, contrarily, let us derive them by simple geometry. As shown in Figure 4, an observer moves at a speed v along the $+y$-axis and detects the declined magnetic flux B_z of the static system.
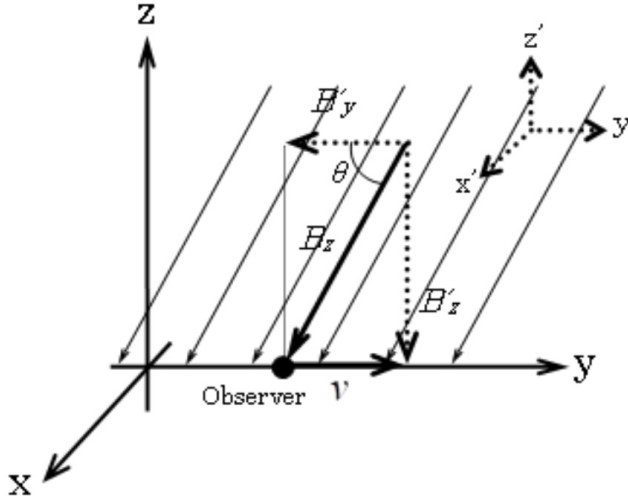
Figure 4

Expressing the magnetic flux by the co-ordinates of the inertia system,

$$B_z = B_y' \sin\theta + B_z' \cos\theta .$$
(1.13)

Since $\sin\theta = \sqrt{1 - (v/c)^2}$ and $\cos\theta = v/c$ from Figure 2 and Eq.1.3, Eq.1.13 is expanded as

$$B_z = \sqrt{1 - (v/c)^2} B_z' + \frac{v}{c} B_y' .$$
(1.14a)

Since $\beta = 1/\sqrt{1 - (v/c)^2}$, Eq. 1.14a is expanded as

$$B_z = \frac{1}{\beta} B_z' + \frac{v}{c} B_y' .$$
(1.14b)

B_z denotes a vector of the declined magnetic flux density of the static system, B_z' the vertical component and B_y' the horizontal by the inertia system. Since B_y' is horizontal to the direction of the observer moving at the speed of v, $B_y = B_y'$ by the 'constancy of the speed of light' claimed by Einstein in [1]. So that Eq. 1.13 is

$$B_z = \frac{1}{\beta} B_z' + \frac{v}{c} B_y \ . \tag{1.15}$$

By the way, since B'_y (or B_y) is perpendicular to B'_z , it seems to the observer as if it is an electric field. Considering B'_y (or B_y) as an electric field, then substituting Maxwell's equation $B = E/c$ to correct the magnitude gap between B and E , Eq. 1.15 is

$$B_z = \frac{1}{\beta} B_z' + \frac{v}{c^2} E_y \ . \tag{1.16}$$

Solving it for B_z',

$$B_z' = \beta \left(B_z - \frac{v}{c^2} E_y \right) \ . \tag{1.17}$$

It corresponds to the original equation 1.9 by Einstein in [1].
Secondly, let us think of B'_y in the same way:
Remark. We discuss them in the left-hand system.
As shown in Figure 5, B_y is

$$B_y = B_y' \sin \theta + B_z' \cos \theta \ . \tag{1.18}$$

From Figure 2 and Eq. 1.3,

$$B_y = \sqrt{1 - (v/c)^2} B_y' + \frac{v}{c} B_z' = \frac{1}{\beta} B_y' + \frac{v}{c} B_z' \ . \tag{1.19}$$

Since B'_z is parallel to the direction of the moving observer, $B_z' = B_z$ by the constancy of the speed of light. So that Eq. 1.19 is

$$B_y = \frac{1}{\beta} B_y' + \frac{v}{c} B_z \ . \tag{1.20}$$

Since B'_z (or B_z) is perpendicular to B'_y , it seems to the observer as if it is an electric field. Substituting Maxwell's equation $B = E/c$ to correct the magnitude gap between B and E , Eq. 1.21 is

$$B_y = \frac{1}{\beta} B_y' + \frac{v}{c^2} E_z \ . \tag{1.21}$$

Solving it for B'_y ,

$$B_y' = \beta \left(B_y - \frac{v}{c^2} E_z \right) \ . \tag{1.22}$$

However, it does not correspond to the original equation 1.8 by Einstein. To solve the problem let us introduce Fleming's left-hand rule or the left-handed system applied to the Lorentz force $F = q(E + v \times B)$. This is assuming that the observer is in the inertia system and then paying attention to each direction of the vectors B_y , B'_y , B'_z for the co-ordinates. Let us set the rule in the co-ordinates as shown in Figure 6. Then, let us see the co-ordinates from the different viewpoint as shown in Figure 7. Although the Lorenz force is negative ($-F'_x$) in the co-ordinates of Figure
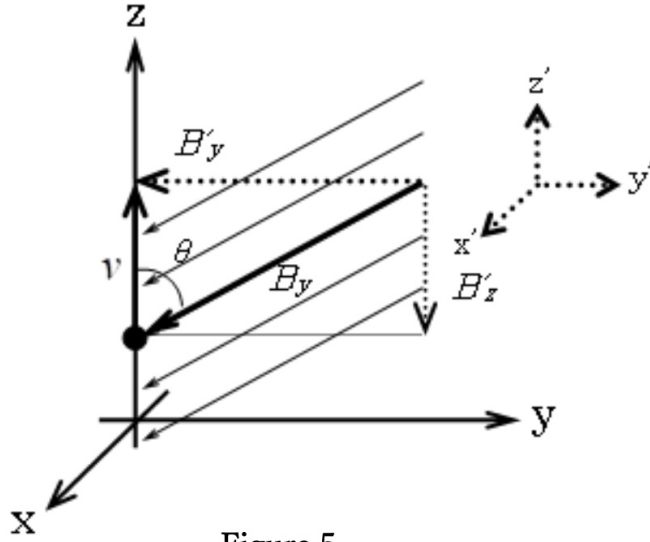
Figure 5

6, it is positive ($+F'_x$) from the different viewpoint in the co-ordinates of Figure 7. However, they are equivalent to each other. So that let us unify all the settings of the co-ordinates by positive direction ($+F'_x$) from now on.
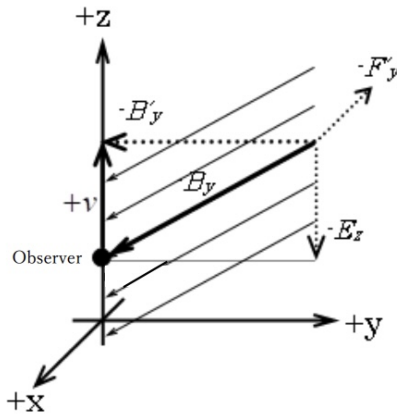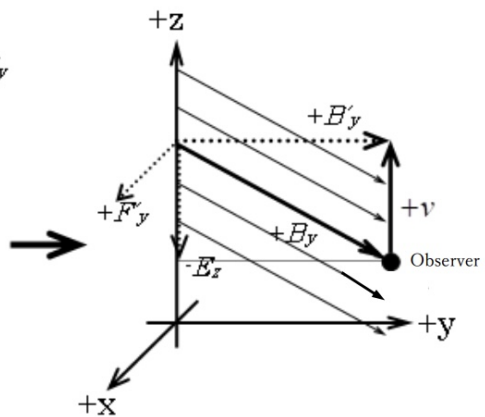
Figure 6   **Figure 7**

Again, let us reconsider equations 1.21 and 1.22 from the latter viewpoint of the co-ordinate settings. The revised equation is

$$B_y = \frac{1}{\beta} B'_y + \frac{v}{c^2}(-E_z) .$$

(1.23)

Solving it by B'_y ,

$$B'_y = \beta \left(B_y + \frac{v}{c^2} E_z \right) . \tag{1.24}$$

It eventually corresponds to the original equation of 1.8 by Einstein.
Now let us similarly reconsider the series of equations 1.13 to 1.17:Since Figure 4
is redrawn as shown in Figure 8, those vectors therefore need to be corrected as
follows: Eq. 1.13 is revised as

$$-B_z = -B'_z \sin \theta + (-B'_y) \cos \theta . \tag{1.25}$$

Multiplying both sides of the equation by -1, it eventually corresponds to Eq. 1.13.
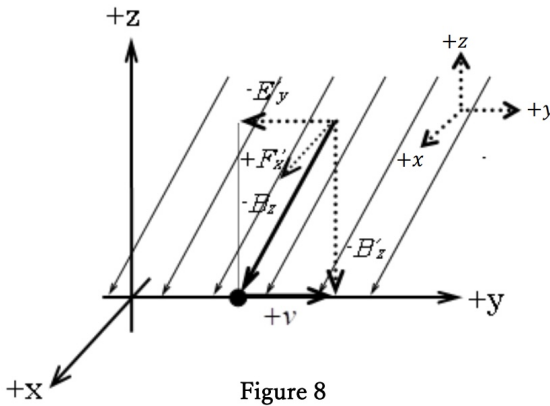
Figure 8

Next, let us think of a relativistic electric field:
As shown in Figure 9, the equation of an electric field of the static system E_y is

$$-E_y = -E'_y \sin \theta + (-E'_z) \cos \theta . \tag{1.26}$$

Multiplying both sides of each equation by -1,

$$E_y = E'_y \sin \theta + E'_z \cos \theta . \tag{1.27}$$

From Eq. 1.3,

$$E_y = \frac{1}{\beta} E'_y + \frac{v}{c} E'_z . \tag{1.28}$$

E'_y denotes the horizontal component and E'_z the vertical one by the inertia
system. Since E'_z is parallel to the direction of the moving observer, $E'_z = E_z$ by
the constancy of the speed of light. So that Eq. 1.28 is

$$E_y = \frac{1}{\beta} E'_y + \frac{v}{c} E_z . \tag{1.29}$$

Since $E'z$ (or Ez) is perpendicular to $E'y$, it seems to the observer as if it is a magnetic flux. Substituting Maxwell's equation $E = cB$ to correct the magnitude gap between B and E , Eq. 1.29 is

$$E_y = \frac{1}{\beta} E_y' + vB_z .$$

(1.30)

Solving it for $E'y$,

$$E_y' = \beta \left(E_y - vB_z \right) .$$

(1.31)

It corresponds to the original equation of 1.11 by Einstein.

Figure 9

As shown in Figure 10, let us think of $E'z$ in the same way: The equation of E_z is

$$E_z = E_z' \sin \theta + (-E_y') \cos \theta .$$

(1.32)

From Eq. 1.3,

$$E_z = \frac{1}{\beta} E_z' - \frac{v}{c} E_y' .$$

(1.33)

Since $E_y' = E_y$ is horizontal to the direction of the moving observer, $E_y' = E_y$, by the constancy of the speed of light. Therefore, Eq. 1.33 is

$$E_z = \frac{1}{\beta} E_z' - \frac{v}{c} E_y .$$

(1.34)

Since E_y' (or E_y) is perpendicular to E_z' , it seems to the observer as if it is a magnetic flux. Substituting Maxwell's equation $E = cB$ to correct the magnitude gap between B and E , Eq. 1.34 is

$$E_z = \frac{1}{\beta} E'_z - v B_y .$$

(1.35)

Solving it for E'_z,

$$E'_z = \beta (E_z + v B_y) .$$

(1.36)

It corresponds to the original equation of 1.12 by Einstein.
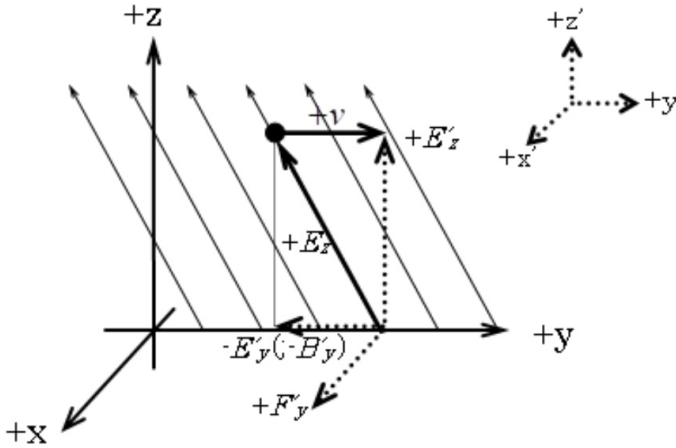
Figure 10

At last, the original equations of 1.7 and 1.10 are easily verified by the constancy of the speed of light as shown in Figure 11:

$$\boldsymbol{B_x = B'_x (= C), E_x = E'_x (= c)}$$

Observer
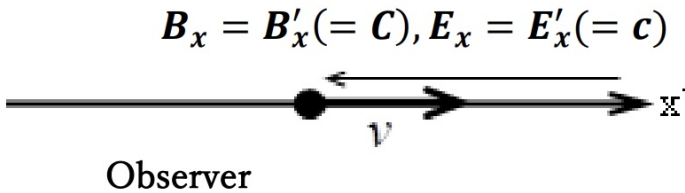
Figure 11

Incidentally, what happens and what does it mean from our viewpoint if $v = c$ (then $\sin \theta = 0$ and $\cos \theta = 1$)? It phenomenally suggests that the magnetic flux totally declines by the relativistic aberration as shown in Figure 12. It then totally corresponds to Maxwell's equations.
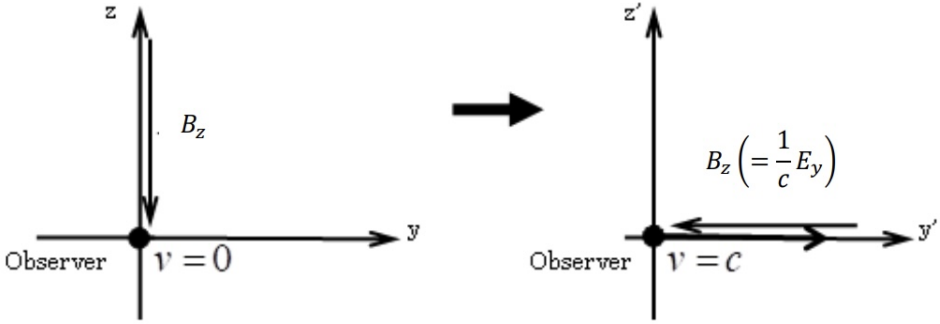
Figure 12

12.2   The Derivation of a New Lorentz Group SO(3) in Real Space

12.2.1   The New Lorentz Group SO(3) in Real Space

From our discussions, it is apparent that there are rotations of electric field E and magnetic field B in the inertia system. It naturally seems to be $SO(3,R)$ in the Euclidean space, not the indefinite orthogonal group $SO(1,3)$ in the Minkowski space. Let us remember that we do not use the Lorentz transformation at all. We can derive the rotation group in the same way as we have discussed in section 1. Let us examine relativistic aberration again. We can denote as follows:

$$\sin \phi (= \cos \theta) = v/c \ , \tag{2.1}$$

$$\cos \phi (= \sin \theta) = \sqrt{1 - (v/c)^2} = 1/\beta \ , \tag{2.2}$$

where ϕ is the angle between the ray of light and the y-axis in ' as shown in Figure 14. Since ϕ is clockwise, it is in the inverse rotation of θ. In this section, we mainly use ϕ for descriptive purposes.

Firstly, let us think of the specific case of Figure 12. Multiplying both sides of Eq.1.9 by $\sqrt{1 - (v/c)^2}$, then $\sqrt{1 - (v/c)^2} B_z' = B_z - \frac{v}{c^2} E_y$. When $v = c$, LHS $= \sqrt{1 - (v/c)^2} B_z' = B_z' \cos \left(\frac{\pi}{2} \right) = 0$ and RHS $= B_y + \frac{c}{C} \left(\frac{1}{C} E_z \right) = B_y + \frac{1}{C} E_z$. $\therefore B_y = -\frac{1}{C} E_z$.

Eq. 1.17 is $E_y = vB_z$ and Eq. 1.18 is $E_z = -vB_y$ when $v = c$ in the same manner. From the results,

$$\begin{pmatrix} B_y \\ B_z \end{pmatrix} = \frac{1}{c} \begin{pmatrix} 0 & 1 \\ 1 & 0 \end{pmatrix} \begin{pmatrix} E_y \\ -E_z \end{pmatrix} \text{ and } \begin{pmatrix} E_y \\ E_z \end{pmatrix} = v \begin{pmatrix} 0 & 1 \\ 1 & 0 \end{pmatrix} \begin{pmatrix} -B_y \\ B_z \end{pmatrix}.$$

They are equivalent to
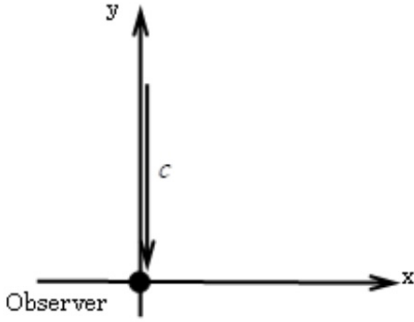
Figure 13
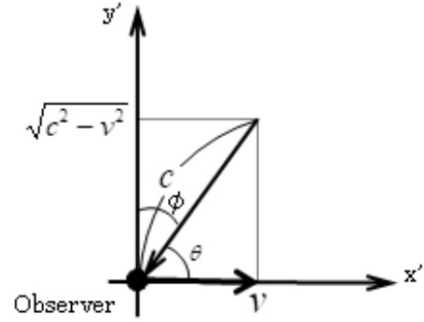
Figure 14

$$\begin{pmatrix} B_y \\ B_z \end{pmatrix} = \frac{1}{c} \begin{pmatrix} 0 & -1 \\ 1 & 0 \end{pmatrix} \begin{pmatrix} E_y \\ E_z \end{pmatrix} \quad \text{and} \quad \begin{pmatrix} E_y \\ E_z \end{pmatrix} = v \begin{pmatrix} 0 & 1 \\ -1 & 0 \end{pmatrix} \begin{pmatrix} B_y \\ B_z \end{pmatrix}.$$

Then, they are naturally related to *SO(2,R)*:

$$\begin{pmatrix} B_y \\ B_z \end{pmatrix} = \frac{1}{c} \begin{pmatrix} \cos\left(\frac{\pi}{2}\right) & -\sin\left(\frac{\pi}{2}\right) \\ \sin\left(\frac{\pi}{2}\right) & \cos\left(\frac{\pi}{2}\right) \end{pmatrix} \begin{pmatrix} E_y \\ E_z \end{pmatrix} \quad \text{and} \quad \begin{pmatrix} E_y \\ E_z \end{pmatrix} = v \begin{pmatrix} \cos\left(\frac{\pi}{2}\right) & \sin\left(\frac{\pi}{2}\right) \\ -\sin\left(\frac{\pi}{2}\right) & \cos\left(\frac{\pi}{2}\right) \end{pmatrix} \begin{pmatrix} B_y \\ B_z \end{pmatrix}.$$

Based on the facts above, let us discuss equations 1.7 to 1.12 in the same way. Initially, let us think of the magnetic flux density. Solving Eq. 1.9 for B_z, the expansion is denoted by equations 2.1 and 2.2 as follows:

$$B_z = \frac{1}{\beta} B_z' + \frac{v}{c^2} E_y = B_z' \cos\phi + \frac{1}{c} E_y \sin\phi .$$

Since $E/c = B = B'$ by the constancy of the speed of light,

$$B_z = \frac{1}{\beta} B_z' + \frac{v}{c^2} E_y = B_z' \cos\phi + B_y' \sin\phi . \tag{2.3}$$

Likewise, solving Eq. 1.8 for B_y, the expansion is

$$B_y = \frac{1}{\beta} B_y' - \frac{v}{c^2} E_z = B_y' \cos\phi - \frac{1}{c} E_z \sin\phi .$$

Since $E/c = B = B'$ by the constancy of the speed of light,

$$B_y = B_y' \cos\phi - B_z' \sin\phi . \tag{2.4}$$

Denoting equations 2.3 and 2.4 by 2-by-2 matrix,

$$\begin{pmatrix} B_z \\ B_y \end{pmatrix} = \begin{pmatrix} \cos\phi & \sin\phi \\ -\sin\phi & \cos\phi \end{pmatrix}\begin{pmatrix} B_z' \\ B_y' \end{pmatrix} = \begin{pmatrix} \cos\phi & \sin\phi \\ -\sin\phi & \cos\phi \end{pmatrix}\begin{pmatrix} 0 & 1 \\ 1 & 0 \end{pmatrix}\begin{pmatrix} B_y' \\ B_z' \end{pmatrix}$$

$$= \begin{pmatrix} \sin\phi & \cos\phi \\ \cos\phi & -\sin\phi \end{pmatrix}\begin{pmatrix} B_y' \\ B_z' \end{pmatrix} . \tag{2.5}$$

Multiplying both sides of Eq. 2.5 by $\begin{pmatrix} 0 & 1 \\ 1 & 0 \end{pmatrix}$,

$$\text{LHS} = \begin{pmatrix} 0 & 1 \\ 1 & 0 \end{pmatrix}\begin{pmatrix} B_z \\ B_y \end{pmatrix} = \begin{pmatrix} B_y \\ B_z \end{pmatrix}, \text{ and}$$

$$\text{RHS} = \begin{pmatrix} 0 & 1 \\ 1 & 0 \end{pmatrix}\begin{pmatrix} \sin\phi & \cos\phi \\ \cos\phi & -\sin\phi \end{pmatrix}\begin{pmatrix} B_y' \\ B_z' \end{pmatrix} = \begin{pmatrix} \cos\phi & -\sin\phi \\ \sin\phi & \cos\phi \end{pmatrix}\begin{pmatrix} B_y' \\ B_z' \end{pmatrix}.$$

$$\therefore \begin{pmatrix} B_y \\ B_z \end{pmatrix} = \begin{pmatrix} \cos\phi & -\sin\phi \\ \sin\phi & \cos\phi \end{pmatrix}\begin{pmatrix} B_y' \\ B_z' \end{pmatrix} . \tag{2.6}$$

Then, multiplying both sides of Eq. 2.6 by $\begin{pmatrix} \cos\phi & -\sin\phi \\ \sin\phi & \cos\phi \end{pmatrix}^{-1}$,

$$\begin{pmatrix} B_y' \\ B_z' \end{pmatrix} = \begin{pmatrix} \cos\phi & -\sin\phi \\ \sin\phi & \cos\phi \end{pmatrix}^{-1}\begin{pmatrix} B_y \\ B_z \end{pmatrix} = \begin{pmatrix} \cos\phi & \sin\phi \\ -\sin\phi & \cos\phi \end{pmatrix}\begin{pmatrix} B_y \\ B_z \end{pmatrix} . \tag{2.7}$$

Secondarily, let us think of the electric field E_y. Solving Eq.1.11 for E_y, the expansion is

$$E_y = \frac{1}{\beta}E_y' + vB_z = E_y'\cos\phi + vB_z .$$

Since $B = B' = E'/c$,

$$E_y'\cos\phi + vB_z = E_y'\cos\phi + \frac{v}{c}E_z' = E_y'\cos\phi + E_z'\sin\phi . \tag{2.8}$$

Likewise, solving Eq. 1.12 for E_y, the expansion is

$$E_z = \frac{1}{\beta}E_z' - vB_y = E_z'\cos\phi - vB_y .$$

Since $B = B'=E'/c$,

$$E_z = E_z'\cos\phi - \frac{v}{c}E_z' = E_z'\cos\phi - E_z'\sin\phi . \tag{2.9}$$

Denoting equations 2.8 and 2.9 by 2-by-2 matrix,

$$\begin{pmatrix} E_y \\ E_z \end{pmatrix} = \begin{pmatrix} \cos\phi & \sin\phi \\ -\sin\phi & \cos\phi \end{pmatrix}\begin{pmatrix} E_y' \\ E_z' \end{pmatrix} . \tag{2.10}$$

Multiplying both sides of Eq. 2.10 by $\begin{pmatrix} \cos\phi & \sin\phi \\ -\sin\phi & \cos\phi \end{pmatrix}^{-1}$,

$$\begin{pmatrix} E_y' \\ E_z' \end{pmatrix} = \begin{pmatrix} \cos\phi & \sin\phi \\ -\sin\phi & \cos\phi \end{pmatrix}^{-1}\begin{pmatrix} E_y \\ E_z \end{pmatrix} = \begin{pmatrix} \cos\phi & -\sin\phi \\ \sin\phi & \cos\phi \end{pmatrix}\begin{pmatrix} E_y \\ E_z \end{pmatrix} . \tag{2.11}$$

The rotation matrices of equations 2.7 and 2.11 can naturally make a special orthogonal group $SO(2,R)$. We could consider it as a new Lorentz group. Furthermore, including the equations 1.7 and 1.10, the matrices of 2.7 and 2.11 are also denoted as $SO(3,R)$, as follows:

$$\begin{pmatrix} B'_y \\ B''_y \\ B'''_y \end{pmatrix} = \begin{pmatrix} 1 & 0 & 0 \\ 0 & \cos\phi & -\sin\phi \\ 0 & \sin\phi & \cos\phi \end{pmatrix}^{-1} \begin{pmatrix} B_x \\ B_y \\ B_z \end{pmatrix},$$ (2.12)

$$\begin{pmatrix} E'_y \\ E''_y \\ E'''_y \end{pmatrix} = \begin{pmatrix} 1 & 0 & 0 \\ 0 & \cos\phi & -\sin\phi \\ 0 & \sin\phi & \cos\phi \end{pmatrix} \begin{pmatrix} E_x \\ E_y \\ E_z \end{pmatrix}.$$ (2.13)

12.2.2 Application for Spintronics —— The spin of electron or magnetic body in the static and inertia system

As shown in Figure 15, the spin in the magnetic field leans as it speeds. The angle between the spin axis (or magnetic body's axis) and the horizon is naturally denoted by $\sin\phi = \cos\theta = v/c$ as we have discussed.
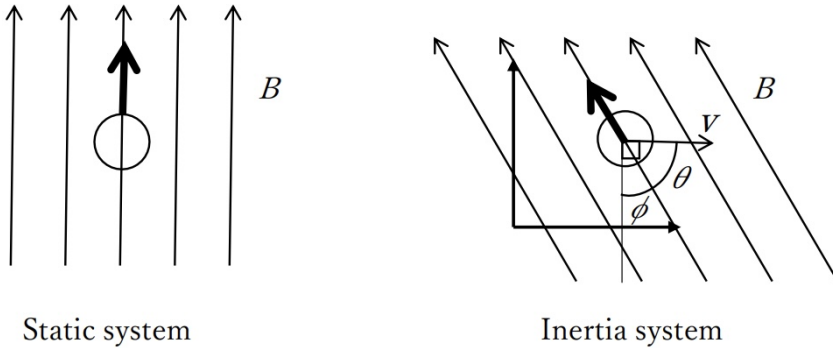
Figure 15

12.3 Discussion of Ampère-Maxwell Equation in the Inertia System (Derivation of Displacement Current from Relativistic Helix)

12.3.1 Magnetic Helix — Relativistic Ampère-Maxwell Law from a Geometric Viewpoint

As shown in Figure 16, a magnetic field in the static system κ is around the observer on the x-axis. However, as shown in Figure 17, it will converge on to the line in the

x-axis drawing a helix in the inertia system κ'. Figure 18 shows when the observer travels at nearly the speed of light. Figure 19 shows when at the speed of light.
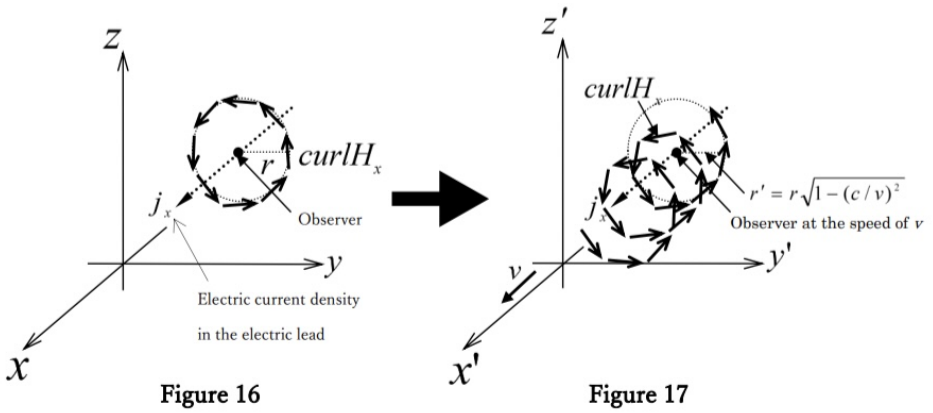
Figure 16

Figure 17

Let us think of the magnetic flux H around the observer in the inertia system κ' as shown in Figures 17 to 19. The original magnetic flux H in the y-z plane converges on to the x-axis as the observer's speed is close to the speed of light. Since the magnetic flux in κ' consists of two components of vector δH_y in the y-z plane and parallel to the x-axis as shown in Figures 20 and 21, $\mathrm{curl}H_x$ in κ' is

$$\mathrm{curl}H_x = \sqrt{1-(v/c)^2}H_x' - (v/c)\mathrm{curl}H_x' . \tag{3.1}$$

Figure 18

Figure 19
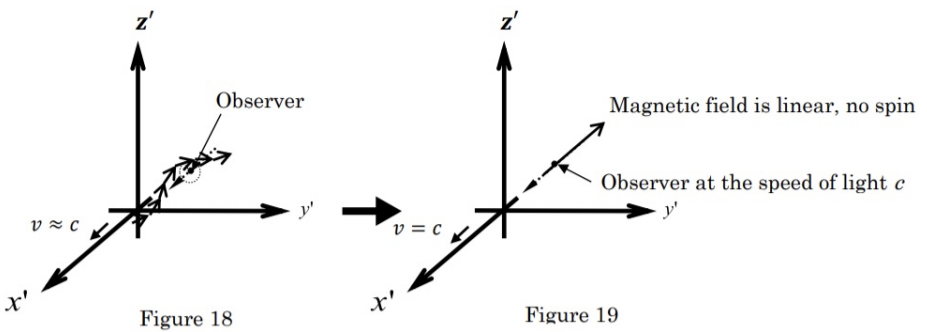
Since $(v/c)\mathrm{curl}H_x'$ is vertical to $\sqrt{1-(v/c)^2}\mathrm{curl}H_x'$, it could be considered as an electric flux density D' in the manner of our discussions in the former sections. Then, from $H = cD$ (from $B = \frac{1}{c}E$, $B = \mu_0 H$, $D = \epsilon_0 E$ and $c = 1/\sqrt{\epsilon_0\mu_0}$, where μ_0 is permeability of vacuum, ϵ_0 permittivity of vacuum),
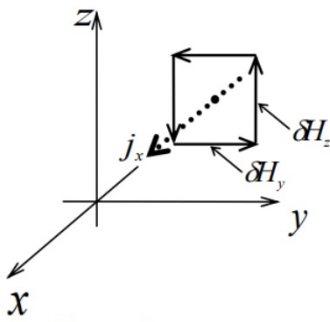
The static system κ
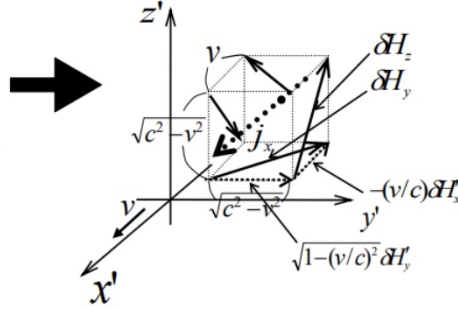
Figure 20

The inertia system κ'

Figure 21

Figures 20 and 21 (intuitive images for Figures 16 to 19)

$$\mathrm{curlH_x} = \sqrt{1-\left(\frac{v}{c}\right)^2}\,\mathrm{curlH_x'} - v\frac{\partial D_x'}{\partial x} = \sqrt{1-\left(\frac{v}{c}\right)^2}\,\mathrm{curlH_x'} - \frac{\partial x}{\partial t}\frac{\partial D_x'}{\partial x}$$

$$= \sqrt{1-\left(\frac{v}{c}\right)^2}\,\mathrm{curlH_x'} - \frac{\partial D_x'}{\partial t}. \tag{3.1}$$

Since D$'$ is equivalent to D by the constancy of the speed of light,

$$\mathrm{curlH_x} = \sqrt{1-\left(\frac{v}{c}\right)^2}\,\mathrm{curlH_x'} - \frac{\partial D_x}{\partial t}. \tag{3.2}$$

Therefore, the relativistic Ampère-Maxwell law is,

$$j_x = \mathrm{curlH_x} = \sqrt{1-\left(\frac{v}{c}\right)^2}\,\mathrm{curlH_x'} - \frac{\partial D_x}{\partial t},$$

$$\therefore j_x + \frac{\partial D_x}{\partial t} = \sqrt{1-\left(\frac{v}{c}\right)^2}\,\mathrm{curlH_x'}, \tag{3.3}$$

where j_x is the electric current density. Likewise, $j_y + \frac{\partial D_y}{\partial t} = \sqrt{1-\left(\frac{v}{c}\right)^2}\,\mathrm{curlH_y'}$, $j_z + \frac{\partial D_z}{\partial t} = \sqrt{1-\left(\frac{v}{c}\right)^2}\,\mathrm{curlH_z'}$ holds. Therefore,

$$j + \frac{\partial D}{\partial t} = \sqrt{1-\left(\frac{v}{c}\right)^2}\,\mathrm{curlH'}. \tag{3.4}$$

As we have seen in the results with Figures 17 and 18, the displacement current cannot generate a magnetic field. From this point of view, since the observer moves, the phenomenon also suggests an electro-magnetic induction.

Furthermore, since the propagation rate of the electro-magnetic wave is always c, the equation of helix from the moving observer in κ' is

$$x = -vt \,, \tag{3.5}$$

$$y = r\sqrt{1 - (v/c)^2} \cos \omega t \,, \tag{3.6}$$

$$z = r\sqrt{1 - (v/c)^2} \sin \omega t \,. \tag{3.7}$$

Now we should decide accurately the value of the angular velocity ω in the equations 3.6 and 3.7. Though it might be $\omega = c/r$ by the formula of the angular speed, it could be greater than the speed of light if the radius is microscopic. It contradicts the principle of the constancy of the speed of light. Therefore, $\omega = c$ also in the inertia system. The replacement of $\omega = c/r$ with $\omega = c$ will be also a 'renormalization'. Therefore, equations 3.6 and 3.7 are

$$y = r\sqrt{1 - (v/c)^2} \cos (c)t \,, \tag{3.8}$$

$$z = r\sqrt{1 - (v/c)^2} \sin(c)t \,. \tag{3.9}$$

From another viewpoint, to simplify this discussion, let us pay attention to the electrons travelling in the electric lead and the magnetic field which the electrons generate as shown in Figures 22 and 23. An observer is always in the static system κ and observes the magnetic helix.

Remark. The directions of the electric current and the electrons in the electric lead are opposite to each other.

Paying attention to the Remark, since the observer is always in the static system κ and the whole helix and electrons move at a speed of v, the relativistic Ampère-Maxwell equation for the observer in κ is

$$\mathrm{curl} H'_x = \sqrt{1 - (v/c)^2} H_x - \left(\frac{v}{c}\right) \mathrm{curl} H_x \,, \tag{3.10}$$

Since $(v/c)\mathrm{curl} H_x$ is vertical to $\sqrt{1 - (v/c)^2}\mathrm{curl} H_x$, it could be considered as D in the manner of our discussions in the former sections. Then, from $H = cD$ (from $B = \frac{1}{c}E$, $B = \mu_0 H$, $D = \epsilon_0 E$ and $c = 1/\sqrt{\epsilon_0 \mu_0}$),

$$\mathrm{curl} H'_x = \sqrt{1 - \left(\frac{v}{c}\right)^2}\mathrm{curl} H_x - v\frac{\partial D_x}{\partial x} = \sqrt{1 - \left(\frac{v}{c}\right)^2}\mathrm{curl} H_x - \frac{\partial x}{\partial t}\frac{\partial D_x}{\partial x}$$
$$= \sqrt{1 - \left(\frac{v}{c}\right)^2}\mathrm{curl} H_x - \frac{\partial D_x}{\partial t} \,. \tag{3.11}$$

Therefore, the relativistic Ampère-Maxwell law is,

$$j_x = \mathrm{curl} H'_x = \sqrt{1 - \left(\frac{v}{c}\right)^2}\mathrm{curl} H_x - \frac{\partial D_x}{\partial t},$$

Figure 22   Figure 23

Remark. Figures 22 and 23 in the box are different from Figures 16 and 17.

$$\therefore j_x + \frac{\partial D_x}{\partial t} = \sqrt{1 - \left(\frac{v}{c}\right)^2} \, \mathrm{curl} H_x \,. \tag{3.12}$$

This derivation will be more faithful to the Ampère-Maxwell equation. The helical equations from the viewpoint of the observer in the static system κ are

$$x' = -vt' \,, \tag{3.13}$$

$$y' = r\sqrt{1 - (v/c)^2} \cos(c)t' \,, \tag{3.14}$$

$$z' = r\sqrt{1 - (v/c)^2} \sin(c)t' \,. \tag{3.15}$$

12.3.2   The Lorentz Covariance in the Minkowski Space

Our discussion in subsection 3.1 eventually gives the time-dependent results from the time-independent discussions The relativistic helical equations are explicitly time-dependent. To scrutinize the results, let us think of the Minkowski metric and check to see if it is Lorentz covariant.

Again, the relativistic helical equations (RHEs) from the viewpoint of the observer in the static system κ are

$$x' = -vt' \,, \tag{3.13}$$

$$y' = r\sqrt{1 - (v/c)^2} \cos(c)t' \,, \tag{3.14}$$

$$z' = r\sqrt{1 - (v/c)^2} \sin(c)t' \,. \tag{3.15}$$

When $v = 0$, equations 3.13, 3.14 and 3.15 are

$$x' = 0 \,, \tag{3.16}$$

$$y' = r\cos{(c)}t\,, \tag{3.17}$$

$$z' = r\sin{(c)}t\,. \tag{3.18}$$

They are RHEs describing a circle of magnetic helix in the static system. See also Figure 24.
To simplify, let $r = 1$ (unit circle). Then, equations 3.16, 3.17 and 3.18 are

$$x = 0\,, \tag{3.19}$$

$$y = \cos{(c)}t\,, \tag{3.20}$$

$$z = \sin{(c)}t\,. \tag{3.21}$$

We can therefore decide the metric s_p in the static system as shown in Figure 24.
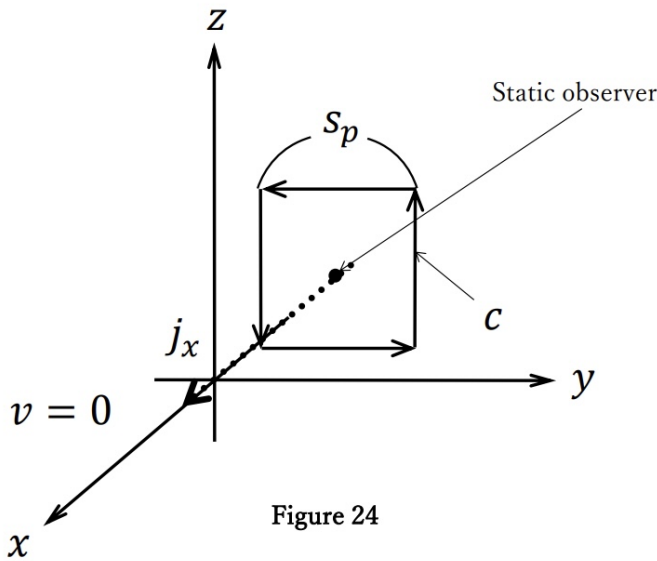
Figure 24

Likewise, we can decide the metric s_p' in the inertia system as shown in Figure 25. Since ds_p is an infinitesimal arc,

$$ds_p = cdt = 1\omega = cdt\,. \tag{3.22}$$

From Eq. 3.22, the Minkowski metric m_s in the static system is

$$m_s^2 = -c^2(dt)^2 + c^2(dt)^2 = 0\,. \tag{3.23}$$

From equations 3.13, 3.14 and 3.15 (see also Figure 25), ds_p' in the inertia system is

Figure 25
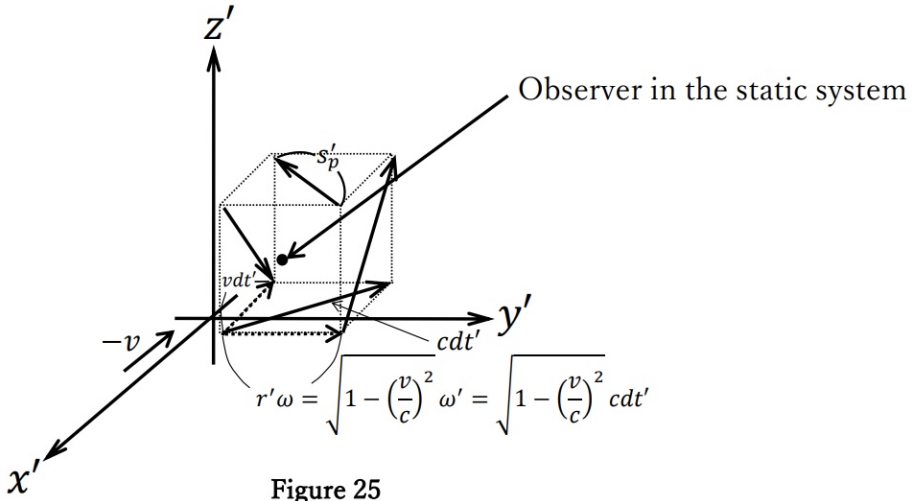
$$ds'_p = cdt' = \sqrt{(vdt')^2 + \left(\sqrt{1 - \left(\frac{v}{c}\right)^2}\,w'\,dt'\right)^2}$$

$$= \sqrt{v^2\,(dt')^2 + \left(\sqrt{1 - \left(\frac{v}{c}\right)^2}\right)^2 (ct')^2}$$

$$= \sqrt{v^2(dt')^2 + \left(1 - \left(\frac{v}{c}\right)^2\right) c^2(dt')^2}\,. \tag{3.24}$$

From Eq. 3.24, m'_s in the inertia system is

$$m'^2_s = -c^2\left(dt'\right)^2 + v^2(dt')^2 + c^2\left(1 - \left(\frac{v}{c}\right)^2\right)(dt')^2$$

$$= -c^2\left(dt'\right)^2 + v^2\left(dt'\right)^2 + c^2\left(dt'\right)^2 - v^2\left(dt'\right)^2$$

$$= 0\,. \tag{3.25}$$

From equations 3.23 and 3.25,

$$m_s^2 = m'^2_s\,. \tag{3.26}$$

Thus, RHEs are Lorentz covariant.

Remark. Any spin in the real space disappears at relativistic speed as we have discussed. However, another spin in the internal space is <u>not</u> influenced at all by the relativistic speed. For example, we know the fact that the non-relativistic Pauli equation is for spin 1/2 particles as well as the relativistic Dirac equation for 1/2

ones. The spin in the internal space is always the same. In other words, it strongly suggests that the internal space is not a subspace of our space.

12.4   Conclusions

As we have discussed, electric and magnetic fields orientated perpendicular to an electron travelling at relativistic speed will be leaned by the relativistic aberration, as shown in Figure 15.

Similarly, the spin angle of an electron or magnetic body will be affected. In spintronics, in the inertia system, the rotation group in the Euclidean space $SO(3,R)$ will be useful.

Additionally, the long-standing controversies of the displacement current originally starting from Maxwell's hypothesis are solved. It is also Lorentz covariant.

Acknowledgments

References

1. Albert Einstein (1905) "Zur Elektrodynamik bewegter Körper", *Annalen der Physik* 17: 891; English translation "On the Electrodynamics of Moving Bodies". See also http://www.fourmilab.ch/etexts/einstein/specrel/specrel.pdf

2. Euich Miztani, Special Relativity from Geometric Viewpoint, *Communications in Applied Geometry*, ISSN 2249-4986, 2011, Vol. 1, No. 1, pp. 17-25.

3. Euich Miztani, Lorentz Group $SO(3,R)$ in non-Minkowski Space, *Communications in Applied Geometry*, ISSN 2249-4986, 2016, Vol. 3, No. 1, pp. 11-16.

4. Euich Miztani, Magnetic Helix Relativistic Ampère-Maxwell Law from Geometric Viewpoint, *Communications in Applied Geometry*, ISSN 2249-4986, 2016, Vol. 3, No. 1, pp. 17-19.

13   Fluctuating Lattice, Several Scales

H.B. Nielsen

Niels Bohr Institute, Copenhagen

Part I: Fluctuating Lattice, Relation between Scales
Part II: Approximate Minimal $SU(5)$, Fine Structure Constants

Abstract. In part I: We find a series physical scales such as 1) Planck scale, 2) Minimal approximate grand unification SU(5), 3) the mass scale of the see saw model right handed or Majorana neutrinos, some invented scale with many scalar bosons, etc., and get the logarithms of these energy scales fitted by a quantity q related to the dimensions of to the scales related dimensionalities of coefficients in Lagrangian densities, or some generalization of this q to something similar in the various cases of the scales. The logarithm of the energies behave as a straight line versus the dimension related number q. This is being explained by an ontologically existing lattice, which fluctuates in lattice constant a from place to place in space time or more precisely, it fluctuates quantum mechanically.
In Part II: We find a fitting of the three fine structure constants in the Standard Model by means of a no-susy and SU(5)-like - but only accurately SU(5) symmetric in the classical approximation - by means of three other parameters for each of which, however, we have speculative predictions: Quantum corrections due to the lattice which are three times as large as naive quantum corrections, because the lattice is supposed to lie in layers, one layer for each fermion-family; criticality of the unified coupling, using the standard model group $S(U(2) \times U(3))$; the unification scale is fitted not the scale-system of part I.

Povzetek: Prvi del: Avtor naniza energijske skale, ki se pojavljajo v modelih za opis osnovnih delcev v fiziki: Planckova skala, skala približne združitve vseh treh interakcij v modelu SU(5), skala, ko je logaritem energije kot funkcija parametra q (ki je povezan z razsežnostjo sistema) premica. Nihanje mreže v prostoru in času avtor razume kot kvantnomehansko nedoločenost.
Drugi del: Kvantno nihanje mreže, ki se pojavi v treh plasteh (za vsako družino predvidi avtor po eno plast), je trikrat večje od naivne kvantne korekcije. Avtor uporabi pri tem grupo $S(U(2) \times U(3))$.

13.1   Overall Introduction

This article is composed of two parts, the first(review of [2]), in section 13.2, of which fits a series of energy scales, or we could say physical phenomena leading to a parameter (with dimension energy after we put $c = \hbar = 1$) and thus potentially a/the "fundamental" energy scale, while the other part(review of [1]) section 13.3 could be considered an attempt to "rescue" grand unification SU(5) by interpreting it by being only an (accidental) classical approximation.

The overall plan will be so that we first discuss the many energy scales, in section 13.2, which we seek to unite by means of the model, which is a really existing lattice fluctuating in size.

Next comes the rescue of the Grand Unification in section 13.3 by allowing it to be only a classical approximation; but then after that we return in section 13.4 to the attempt to unify the energy scales in the light that it is really very much needed because giving up the usually used susy to make SU(5) GOT work points to lower unification energy scale than even the susy SU(5) unification, so that now the distance even in logarithm between the Planck scale and the unification scale has become so large that it is hard to see how to make them compatible. Thus the call for our attempt to unify the scales by our fluctuating lattice has got even more strong, than with usual susy unification.

13.2   Introduction for first part: Energy Scales or Fluctuating lattice

Several seemingly "fundamental" scales like the Planck scale, the see-saw scale, and the unification scale, are not so equal to each other as we would have expected in a philosophy of their being only **one** "fundamental energy scale".

To cure this fact we bring forward the idea of a truly existing lattice, which has **wildly different sizes**, of say the link length, in different places and/or in different components of a superposition. Really we think of the lattice as being superposition of all possible deformations (which could be made by coordinate transformations/reparametrizations), so we can say we have in mind quantum fluctuations in reparametrizations, the gauge group of gravity.

In the tables in which we list the various energy scales we have attached to each scale a number q or $n = 4 - q$, and the meaning is that n should mean the power to which the inverse link size $1/a$ be raised in order to give weighting coming in in the calculation of the energy scale in question. In fact this means that for all the energy scales we have

$$\text{"energy scale"} \approx \sqrt[n]{< (1/a)^n >} \tag{13.1}$$

If the distribution in the fluctuating lattice had been very narrow this n would make no difference, but assume and fit a very broad distribution being a Gaussian distribution in $\ln a$,

$$P(\ln a)\,d\ln a = \frac{1}{2\pi\sigma}\exp(-\frac{1}{2\sigma}(\ln(a) - \ln(a_{0\ counting})^2)\,d\ln(a) \tag{13.2}$$

where the spread $\sigma = 5.5$ turns out, a rather large spread, when we have in mind that it is a spread in the logarithm. In first approximation we might think of a completely flat distribution in the logarithm. If there was scalings symmetry and we got the Haar measure distribution for the group of scalings with different factors, then we would get such a flat distribution in the logarithm $\ln(a)$. Actually you might think of (13.2) as a scaling symmetric distribution only weakly broken. For the purpose of comparing with the $P_{volume}(\ln(a))$ below we might write using that density of hypercubes per unit four volume compared the one per

density per four volume of a hypercube in the lattice is $1/a_{0\,counting}^4$. Using that we can write for the number of hypercubes in an infinitesimal region

$$P(\ln a)d\ln a = \frac{\frac{1}{2\pi\sigma}\exp(-\frac{1}{2\sigma}(\ln(a)-\ln(a_{0\,counting})^2)}{a_{0\,counting}^4}d^4x\,d\ln(a). \quad (13.3)$$

13.2.1   Density definitions etc.

First let us be a bit more specific about how we think of this fluctuating lattice:

- **Lattice in layers** We imagine, that the lattice can lie in several layers compared to a simple Wilson lattice. An idea about having layers is best gotten by imagining, that we take a number , e.g. 3, Wilson lattices and have in nature all of them. Then for each four volume of the size of a hypercube in the lattice in space time we shall not have as in a simple Wilson lattice just one lattice site, but rather 3. We call this, that there are 3 layers. If the lattice fluctuate in size of the links and thus this size also varies of course from place to place in the Minkowski space time, we can in principle ask for such a number of layers in average for each size of link a. That is to say we can define a "numbers of layers for a small a region " = " numbers of sites(or hypercubes) in the four volume of one single hypercube provided we count only hypercubes in a range of sizes a given by say the infinitesimal $d\ln(a)$"

$$P_{layer}(\ln(a))d\ln(a) = \text{" numbers of hyper cubes with link-size}$$
$$a' \in \{a'|a \leq a' \leq a*\exp(d\ln(a))\} \text{ per four}$$
$$\text{volume } a^4 \text{ of the hypercubes for } a" \quad (13.4)$$
$$= \text{"Layer density"}(a)d\ln(a) \quad (13.5)$$

- **Density in Space Time** Usually we consider of course densities per 4-volume of Minkowski (or the curved space time) space and then there is place in every layer for having $1/a^4$ four-cubes. So if the density of say sites per place for a four cube in one of layers say is per interval in the logarithm $d\ln(a)$ is "Layer density"$(a)d\ln(a)$ (and there are $1/a^4$ per $(unit\ length)^4$), then the density of sites per four volume in Minkowski space time is

$$P_{volume}(\ln(a))d^4x\,d\ln(a) = \text{"Layer density"}(a)/a^4 d^4x\,d\ln(a)$$
$$= P_{layer}(\ln(a))/a^4 d^4x\,d\ln(a)$$
$$\text{with ansatz (13.2)}: = \frac{1}{2\pi\sigma}\exp(-\frac{1}{2\sigma}(\ln(a)-\ln(a_{0\,counting})^2)/a^4 d^4x\,d\ln(a)$$
$$= \frac{1}{2\pi\sigma}\exp(-\frac{1}{2\sigma}(\ln(a)-\ln(a_{0\,counting})+4\sigma)^2+$$
$$+4^2/2*\sigma-4\ln(a_{0\,counting}))d^4x\,d\ln(a)$$

Calling

$$\ln(a_0) = \ln(a_{0\ counting}) - 4\sigma$$
$$\text{or } a_0 = a_{(0\ counting)} \exp(-4\sigma)$$
$$\text{then } P_{volume}(\ln(a))d^4xd\ln(a) =$$
$$= \frac{1}{2\pi\sigma}\exp(-\frac{1}{2\sigma}(\ln(a)-\ln(a_0))^2 - 4^2\sigma/2$$
$$-4\ln(a_0))d^4xd\ln(a) =$$
$$= \frac{1}{2\pi\sigma}\exp(-\frac{1}{2\sigma}(\ln(a)-\ln(a_0))^2 - 8\sigma - 4\ln(a_0))d^4xd\ln(a)$$
$$= \frac{1}{2\pi\sigma}\exp(-\frac{1}{2\sigma}(\ln(a)-\ln(a_0))^2)/a_0^4 * \exp(-8\sigma)d^4xd\ln(a)$$
$$= \frac{1}{2\pi\sigma}\exp(-\frac{1}{2\sigma}(\ln(a)-\ln(a_0))^2)/a_{0\ counting}^2/a_0^2 d^4xd\ln(a)$$

But if we should normalize properly this $P_{volume}(\ln(a))$ properly we should have had like in (13.3) that the division with $a_{0\ counting}^2 a_0^2$ should be replaced by $a_{0\ counting}^4$. Thus the normalized $P_{volume}(\ln(a))$ looks rather

$$P_{volume}^{(N)}(\ln(a))d\ln(a)d^4x/a_{0\ counting}^4 = \frac{a_{0\ counting}^2}{a_0^2}P_{volume}(\ln(a))$$

$$d\ln(a)d^4x/a_{0\ counting}^4 \quad (13.6)$$

$$= \exp(8\sigma)P_{volume}(\ln(a))$$

$$d\ln(a)d^4x/a_{0\ counting}^4 \quad (13.7)$$

This means that when we average over the distribution of the link length a or this link length a to some power a^p say the answer is not the same as if we do it just averaging over links or hypercubes by their number. In fact denoting the two different averages $< .. >_{counting}$ and $< ... >_{volume}$ we find

$$< a^p >_{counting} = \int \frac{1}{2\pi\sigma}\exp(-\frac{1}{2\sigma}(\ln(a)-\ln(a_{0\ counting}))^2) * a^p d\ln(a)$$

$$= \int \frac{1}{2\pi\sigma}\exp(-\frac{1}{2\sigma}((\ln(a)-\ln(a_{0\ counting}))^2 - 2p\sigma*\ln(a)))d\ln(a)$$

$$= \int \frac{1}{2\pi\sigma}\exp(-\frac{1}{2\sigma}(\ln(a)-\ln(a_{0\ counting} - \sigma*p)^2 +$$

$$+ p^2\sigma/2 + p*\ln(a_{0\ counting}))d\ln(a)$$

$$= a_{0\ couning}^p \exp(p^2\sigma/2)$$

so that $\sqrt[p]{< a^p >_{counting}} = a_{0\ counting}\exp(p\sigma/2)$

while $< a^p >_{volume} = a_0^p * \exp(p^2\sigma/2)$,

and $\sqrt[p]{< a^p >_{volume}} = a_0\exp(p\sigma/2)$.

Of course

$$< a^p >_{volume} = \frac{< a^p/a^4 >_{counting}}{< a^{-4} >_{counting}}$$

As checked: $= \frac{a_{0\ counting}^{p-4}\exp((p-4)^2\sigma/2)}{a_{0\ counting}^{-4}\exp((-4)^2\sigma/2)}$

$$= a_{0\ counting}^p \exp(p(p-8)\sigma/2)$$

$$= a_0^p \exp(p^2\sigma/2).$$

Also:

$$\frac{\langle a^{p+b}\rangle_{counting}}{\langle a^p\rangle_{counting}} =$$

$$a^b_{0\ counting}\exp((p+b)^2-p^2)\sigma/2)$$

$$=a^b_{0\ counting}\exp(b(2p+b)\sigma/2)$$

so that $\sqrt[b]{\dfrac{<a^{p+b}>_{counting}}{<a^p>_{counting}}}=a_{0\ counting}\exp(2p\sigma/2)*\exp(b\sigma/2)$

$$=a_{0\ p}\exp(b\sigma/2)$$

$$=\sqrt{a_{0\ p}\,a_{0\ p+b}}$$

where $a_{0\ p}=$Peak of $P_{layer}(\ln(a))*a^p$

$$=\text{Peak of }\exp(-\frac{1}{2\sigma}(\ln(a)-\ln(a_{0\ counting})^2+p\ln(a))$$

$$=a_{0\ counting}\exp(p\sigma)$$

so especially $a_0=a_{0\ p=-4}=a_{0\ counting}\exp(-4\sigma)$

(13.8)

Let us especially learn that considering two averages of powers of the link variable in succession you get an increase by a factor

$$\frac{<a^{p+1}>_{counting}}{<a^p>_{counting}}=a_{0\ counting}\exp((p+1/2)\sigma). \qquad (13.9)$$

So the effective energy scale when you work with powers of the link variable of the order of p is about $a_{0\ counting}*\exp(p\sigma)$. So what we have to do to evaluate what the typical power is for the type of physics connected to the energy scale we want.

Basically our procedure is to represent the quantity, which we call the energy scale, as a root of or just the coefficient in the action or a ratio of such action related quantities, and then argue that this combination must - assuming no big (or small) numbers in other coupling or parameters - that it should behave as the average of some power of the link length a, i.e. as say

$$< (1/a)^n >_{counting}=< a^{-n} >_{counting}$$

As just a repetition we used in the tables below also a to the power n of $1/a$ equivalent number $q=4-n$, a notation inspired by considering the scales "see-saw" and "scalars" which are scales at which we postulate/speculate that there are "a lot of" respectively fermion and boson masses. In fact we know that ignoring the interactions for simplicity the fermion and boson actions in field theory are

$$S_{fermion}=\int\mathcal{L}_D(x)d^4x=\int\bar\psi(x)(i\gamma^\mu\partial_\mu-m)\psi(x)d^4x+... \qquad (13.10)$$

$$S_{scalar\ boson}=\int\mathcal{L}(x)d^4x=\int(\frac{1}{2}\eta^{\mu\nu}\partial_\mu\phi\partial_\nu\phi-\frac{1}{2}m^2\phi^2)d^4x+... \qquad (13.11)$$

and that the mass m of the particle occurs in different powers m^q for the two, namely $q=1$ for fermions and $q=2$ for bosons. For dimensional reasons these

mass terms then - including the extra $1/a^4$ factor from number of hyper cubes going as $1/a^4$ in a unit space time - have link a dependensies

$$\text{mass term } a \text{ dependence } \propto (1/a)^{4-q}. \qquad (13.12)$$

and so we have here $n = 4 - q$.

13.2.2   Our tables

Let us first deliver the table of the energy scales I included in the very workshop talk:

When we have to do with the quantities related to the scale being terms in lagrangians in a field theory,we have immediately a factor $1/a^4$ which means a -4 in the power.

It shall turn out from our fitting that the step in the energy scale per unit step in the power is a factor 251, which must then be identified with our step factor $\exp(\sigma)$.

Table of "Fundamental ?" Energy Scales

Name	Energy value	n of $(1/a)^n$	q	Coef. dim.	Fit	Lagrangian d.
Planck scale	$1.22 * 10^{19}$	6	-2	-2	$2.44 * 10^{18}$GeV	$\frac{1}{2\kappa}R$
reduced Planck	$2.43 * 10^{18}$GeV	6	-2	-2	$2.44 * 10^{18}$GeV	$\frac{1}{2\kappa}R$
Min. SU(5) app.	$5.3 * 10^{13}$GeV	4	0	0	$3.91 * 10^{13}$ GeV	$-\frac{1}{16\pi\alpha}F^2_{\mu\nu}$
Susy SU(5)	10^{16} GeV	4	0	0	$3.91 * 10^{13}$ GeV	$-\frac{1}{16\alpha} * F^2_{\mu\nu}$
See-saw	10^{11} GeV	3	1	1	$1.56 * 10^{11}$GeV	$m_R\bar{\psi}\psi$
Fermion extrapolate	10^4GeV	0	4	4	10^4 GeV	"1"

Using $c = \hbar = 1$,

$$\text{"Reduced Planck"} = \frac{1}{\sqrt{G_{Newton} * 8\pi}} = 2.43 * 10^{18} \text{GeV} \quad (13.13)$$

$$\text{"unified (approximate) SU(5)"} = \text{"where lines closest"}$$

$$= (\text{say})5.3 * 10^{13} \text{GeV} \qquad (13.14)$$

$$\text{"see-saw"} \sim \text{"typical right handed neutrino mass"}$$

$$\sim 10^{11} \text{GeV}. \qquad (13.15)$$

The 'scales" **scalars** and **Fermion extrapolate** also called "fermion tip" scale) are my inventions and need explanation later. ($\kappa = 8\pi G = 8\pi G_{Newton}$).

Name coming from status	[Coefficient] Eff. q in m^q term	"Measured" value Our Fitted value	Text ref. Lagangian dens.	n by $1/a^n$
Planck scale Gavitational G wellknown	[mass^2] in kin.t. $q=-2$	$1.22 * 10^{19}$ GeV $2.44 * 10^{18}$ GeV	(??) $\frac{R}{2\kappa}$ $\kappa = 8\pi G$	6
Redused Planck Gravitational $8\pi G$ wellknown	[mass^2] in kin.t. $q=-2$	$2.43 * 10^{18}$ GeV $2.44 * 10^{18}$ GeV	(13.13) $\frac{R}{2\kappa}$ $\kappa = 8\pi G$	6
Minimal SU(5) fine structure const.s α_i only approximate	[1] $q=0$	$5.3 * 10^{13}$ GeV $3.91 * 10^{13}$ GeV	(13.14) $\frac{F^2}{16\pi\alpha}$ $F_{\mu\nu} = \partial_\mu A_\nu - \partial_\nu A_\mu$	4
Susy SU(5) fine structure const.s works	[1] $q=0$	10^{16} GeV $3.91 * 10^{13}$ GeV	(??) $\frac{F^2}{16\pi\alpha}$ $F_{\mu\nu} = \partial_\mu A_\nu - \partial_\nu A_\mu$	4
Inflation H CMB, cosmology "typical" number	[1]? $q=0$?	10^{14} GeV $3.91 * 10^{13}$ GeV	(??) $\lambda\phi^4$ $V = \lambda\phi^4$	4
Inflation $V^{1/4}$ CMB, cosmology "typical"	concistence ? $q=-1$?	10^{16} GeV $9.96 * 10^{15}$ GeV	(??) consistency $V = \lambda\phi^4$?	5
See-saw Neutrino oscillations modeldependent	[mass]in non−kin. $q=1$	10^{11} GeV $1.56 * 10^{11}$ GeV	(13.15) $m_R\bar\psi\psi$ m_R right hand mass	3
Scalars small hierarchy invented by me	[mass^2]in non−kin. $q=2$	$\frac{seesaw}{44 \text{ to } 560}$ $\frac{1.56 GeV}{250}$	(??, ??) $m_{sc}^2|\phi|^2$ breaking $\frac{seesaw}{scalars}$	2
Fermion tip fermion masses extrapolation	"[mass^4]in non−kin." $q=4$	10^4 GeV 10^4 GeV	(??) "1" quadrat fit	0
Monopole dimuon 28 GeV invented	"[mass^5]in non−kin." $q=5$	28 GeV 40 GeV	(??) $m_{monopol} \int ds$ $S \propto a$	-1
String $1/\alpha'$ hadrons intriguing	"[mass^6]in non−kin." $q=6$	1 Gev 0.16 GeV	(??) Nambu Goto $S \propto a^2$	-2
String $T_{hagedorn}$ hadrons intriguing	'[mass^6] in non-kin." $q=6$	0.170 GeV 0.16 GeV	(??) Nambu Goto	-2
Domain wall dark matter far out	"[mass^7] in non-kin." $q=7$	8 MeV 0.64 MeV	(??) twobrane vol.	-3

Next let me deliver the full table (from [2]) with scales which we now have found, including cases of scales judged by very good will:
Important to notice in this table is the very good fitting of our formula

$$\text{“energy scale”} = 10^4\,\text{GeV} * 250^n \tag{13.16}$$

which is compared with the in the third column of the table. The fitted value is the lower one inside each block.

After the Bled I found several new scales that in fact quite remarkably fitted in rather well. In the recent articel arXiv:2411.03552 [hep-ph] [2] I extended the table of scales fitting to by the scales "monopoles" and "strings" for which we what would be with the fluctuating lattice the scales for monopole masses and for the string tension or say the Regge slope in the Veneziano model, when one estimate the actions for a single monopole or for a single string in our scheme. Quite surprisingly the string scale turning out is the one for hadronic strings with which historically string theory were first proposed. The monopole mass scale turns out not so far from the mass of two-muon resonance [55] with 28 GeV mass, which is one of the very few peaks found not belonging to the Standard Model in LHC.
Our fitting of the curve of scales by a linear function as function of the power n may be presented as

$$\text{“energy scale”} = 10^4\,\text{GeV} * 250^n \tag{13.17}$$
$$\text{or } \log_{\text{GeV}}(\text{“energy scale”}) = 4 + 2.40 * n (+\log\text{GeV}) \tag{13.18}$$
$$\text{or } \ln_{\text{GeV}}(\text{“energy scale”}) = 9.21 + 5.53 * n (+\ln\text{GeV}) \tag{13.19}$$

Different "Energy-scales" versus n = 4 -($\pm$)"Coupling dimension"
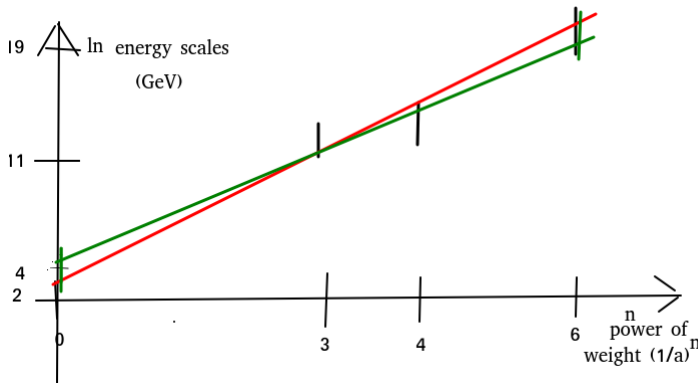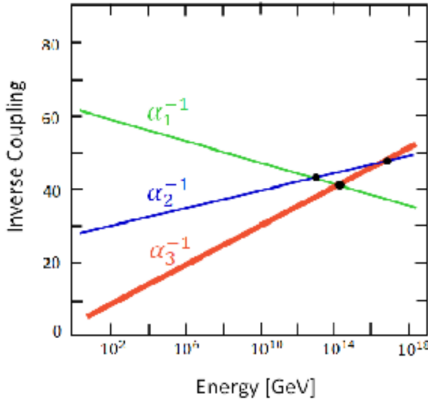
Figure 1: **If I do not believe Susy, just look where lines closest**. This is the usual plot of the running inverse fine structure constants normalized with the usual $3/5$ on the U(1) coupling, so that they should have met in one point all three if exact SU(5) GUT had worked. But now we here refuse to believe in susy and instead assume the SU(5) symmetry only to be an approximate symmetry (see more in Part II) we take the energy (which is on the abscissa) at which the the three inverse fine structure constant curves are the closest to be the approximate unification scale. In our work [1] we found by more accurate lattice model assumptions $5.3 * 10^{13} GeV$ for the approximate unification scale. This approximate unification scale is indicated on the figure by a vertical line.

If we include names for the scales on the figure, it looks:
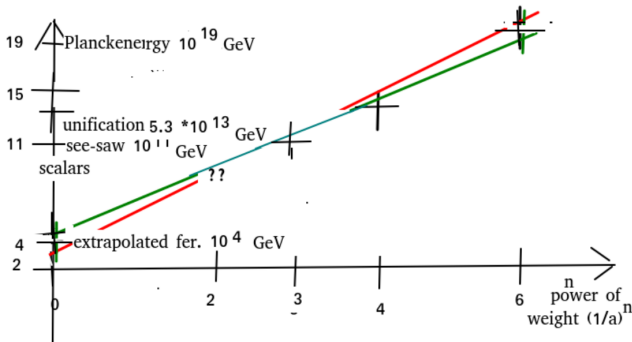
My Speculations on GUT SU(5): Approximate

- There is a physically existing lattice, and the Plaquette action happens **classically** to be SU(5) symmetric.
- Quantum corrections break the classical SU(5) symmetry of the lattice action.

- Because the lattice lies in three layers, the quantum correction SU(5) breaking is just a factor 3 bigger than true quantum correction. The factor 3 is the number of families.

We shall return to this model of an only approximate grand unification SU(5) in the second part 13.3.

Take at First that our Energy Scales (4 of them, when I gave the talk; now ≈ 9) are Observed Phenomenologically on Logarithmic Plot as function of the Coupling Constant Dimension $[\text{GeV}^{\dim}]$ a bit modified to be a power of $1/a$ expected relevant lie on Straight line

Since the power n to which the inverse link length a comes into the action S for the Lagrangian densities for the different sort of physics related to the different (fundamental?) energy scales, $(1/a)^n$, is linearly related to the dimension of the coefficient ["coefficient"]

$$n = 4 - (\pm)\text{Dim}(\text{"Coefficient"}), \tag{13.20}$$

linearity - i.e. straight line - of the logarithm of the energy scales as function of n means also, that we **observed straight line for the relation of Dim("coefficient") to logarithm("energy scale")**

13.2.3   Fluctuating Lattice

"Fluctuating lattice" (in superposition of) being dense somewhere and rough somewhere and often deformed
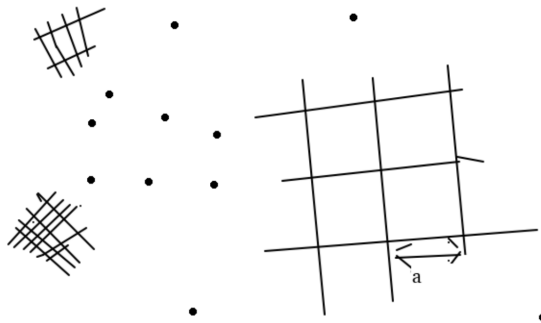
Figure 2: Here we drew for simplicity and easiness a couple of seperate pieces of lattices (two dimensional but of course they should really have been 4 dimensional to be in Minkowski space) of different lattice constant a length and thus density. Meant is, however, that the lattice hangs together and that the link length varies along as one goes fromplace to place, presumably in a continuous way. Raelly it quantum fluctuates.

Densities of, say, Sites in Fluctuating Lattice with several Layers can be defined relative to the hypercube four-volume a^4 or with respect to a four volume unit m^4 say:

For the distribution of different densities of links or of sites in a fluctuating lattice with shall distinguish:

$$\#layers = (say) \#sites \text{ per } a^4 \qquad (13.21)$$

$$density_{/m^4} = \#sites \text{ per } m^4 \qquad (13.22)$$

$$density_{/m^4} = \#layers * a^{-4} \qquad (13.23)$$

$$Ansatz:$$

$$Probability: \qquad (13.24)$$

$$P(\ln(1/a))d\ln(1/a)d^4x \propto$$

$$\propto \exp(-\frac{(\ln(1/a) - \ln(10^4 GeV))^2}{2\sigma}) \quad d\ln(1/a)d^4x \qquad (13.25)$$

where $10^4 GeV$ is our "fitted" value; σ is a spreading to be fitted.

Distribution of Contribution for one of the to Scales associated actions versus
$$\ln(a)$$

One of the actions associated with the candidates for fundamental scales as e.g. the Einstein-Hilbert-action $\frac{1}{2\kappa}R\sqrt{-g}d^4x$ with $(1/a)^n$ proportional contribution get of the form:

$$S = \int \mathcal{L}(x)d^4x \propto$$

$$\propto \int \exp(\frac{-(\ln(1/a)) - \ln(10^4 GeV))^2}{2\sigma})(1/a)^n d\ln(1/a)$$

$$= \exp(\frac{-(\ln(1/a) - \ln(10^4 GeV))^2 + n * 2\sigma * \ln(1/a)}{2\sigma})d\ln(1/a)$$

An Action depends on the spread σ like:

$$S = \int \mathcal{L}(x)d^4x \propto$$

$$\propto \int \exp(-\frac{(\ln(1/a)) - \ln(10^4 GeV) - n * \sigma)^2 + (n * \sigma)^2}{2\sigma})d\ln(1/a)$$

$$= \int \exp(-\frac{(\ln(1/a)) - \ln(10^4 GeV))^2 + (n * \sigma)^2}{2\sigma})d\ln(1/a)$$

$$= \int \exp(-\frac{(\ln(1/a)) - \ln(10^4 GeV))^2}{2\sigma})d\ln(1/a) * \exp(n^2\sigma/2)$$

where only the last factor $\exp(n^2 * \sigma/2)$ depends on n. This was for an action $S \propto (1/a)^n$.

Interpreting the factor $\exp(n^2\sigma/2)$ as correcting the n factors $(1/a)$ we get $(1/a)_{eff} = (1/a)*\exp(n\sigma)$.(because a step in $n^2\sigma/2$ is say $(n+1)^2\sigma/2 - n^2\sigma/2 = (2n+1)\sigma/2 \approx n\sigma$).

The Effect of the in $\ln(1/a)$ **Broadened Distribution is** $1/a \to (1/a)_{eff} = \exp(n\sigma)*$ $(1/a)$

We shall interpret correction to the effective $1/a$ (= the inverse of the link size) as a correction of the "energy scale". So the effect of the spreading with Gauss distribution in the logarithm $\ln(1/a)$ with a width given by σ as

$$\text{Replace "energy scale"} \to \text{"energy scale"} * \exp(n * \sigma) \tag{13.26}$$

$$\text{So } 250 = \exp(\sigma/2)\text{(where 250 from our empirical fit)}$$

$$\text{and thus } \sigma = 5.5. \tag{13.27}$$

13.2.4 Conclusion of Energy Scales and Fluctuating Lattice Part/First Part

- We presented an empirical straight line fit to three wellknown energy scales, valid to crude order of magnitude accuracy,

$$\text{"energy scale"} = 10^4\,\text{GeV} * 250^n \tag{13.28}$$

$$\text{or "energy scale"} = 10^4\,\text{GeV} * 250^{4-(\pm)\texttt{dim(coefficient)}} \tag{13.29}$$

(where $\texttt{dim(coefficient)}$ is the dimension in energy units of the coefficient multiplying in the Lagrangian density the field (product), and $(\pm) = +1$ for the term with the coefficient being a mass term like in the case of the "see-saw"and the "scalars scale", while in the case of "Plack scale" where it is the Einstein Hilbert action, which is a kinetic term carrying a dimension 2 coefficient $(\pm) = -1$)

(13.29)

We explain this empirical fit with a speculated "fluctuating lattice" with a fluctuation distribution being a Gauss distribultion in the logarithm of the statistically fluctuating link length a, i.e. a Gauss distribution in $\ln(1/a)$:

$$P \propto \exp(-\frac{(\ln(1/a) - \ln(10^4\text{GeV})^2}{2*5.5}) \tag{13.30}$$

Last moment development After the talk I found several new ideas for new scales (mainly) of the type that one considers a brane of some dimension D, meaning a space time extension of dimension $D + 1$, and thus having an action, which using dimensionless parameters to make coordinates on the brane-time-track, a coefficient of dimension like a^{D+1} being $[\texttt{energy}^{-D-1}]$, so that $d = -D - 1$. Very interesting it seems that for a string = (D=1)brane the tension of the strings pointed to by our extrapolated fit to $d = -2$ get very close to the tension of the string by which hadrons can crudely be fitted, and which were the historically starting point of string theory.

A plot with the extended system of scales is found in [2] and is reproduced in the figure (3).
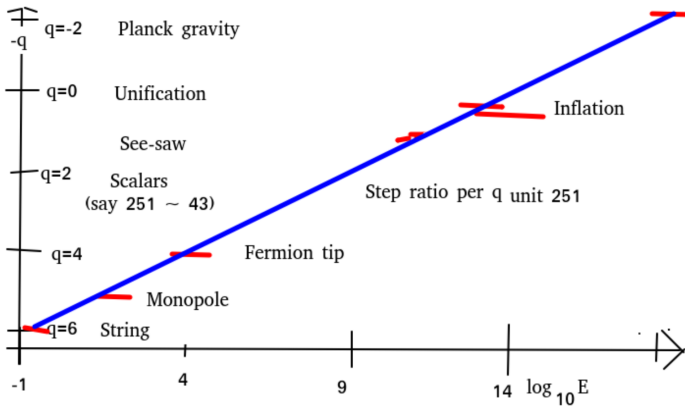
Figure 3: This figure taken from [2] has the logarithm in basis 10 of the energy scales on the abscissa, and the intger $q = 4 - n$, where n is esssentially the power of $1/a$ relevant for the scale. Remark that we have $-q$ as the variable pointing upwards. The names we have given to the scales are attached.

13.3   Approximate GUT SU(5)

part II: Approximate SU(5), Fine Structure Constants

Abstract for Second part: "Approximate $SU(5)$, Fine structure constants"

Abstract. We suggest a model with a physical lattice for the gauge groups in the Standard Model with link variables taking values in the according to O´Raifeartaigh Standard Model**group**, $S(U(2) \times U(3))$, and it is so similar to $SU(5)$, that in what we can call the classical approximation, it gives the same ratios between the three fine structure constants. But including quantum fluctuations we get deviation from the GUT prediction, because there is not true $SU(5)$ and thus the true $SU(5)$ quantum fluctuations are lacking, unless they belong to the Standard Model group. The remarkable thing is, that apart from just a factor 3 the deviations caused by these quantum fluctuations reproduce within uncertainties in the very accurately measured finestructure constants fit the data. The factor 3 we seek to explain by postulating that the truly existing lattice is really lying in three layers (as if we had three copies of the Standard model group, i.e. SMG $\times$ SMg $\times$ SMG).

13.3.1   Introduction to approximate SU(5)

Fit the three Fine Structure Constants in the Standard Model with three Parameters, Derivable in Our Theory.
Shall fit with

- q = "number of families" $* \pi/2$.

- $\alpha_{5\ uncorrected} = \alpha_{5\ critical}$ (unifying coupling (ours)).
- We shall put our replacement for unification energy scale μ_U into aline of four different energy scales, fitting a line in the logarithm of the energy scale versus dimension of related couplings.

Relation to First Part above.: Several "Fundamental" Scales, Their logarithms Fitted on a Line as function of Dimension of the Coefficient in Lagrangian Term Related

Since our replacement for the unification coupling scale is even more deviating from the Planck scale than more popular unifications with susy, we give up that the various " fundamental scales found, see saw, unification (or approximate unification) and Planck scale, should be at the same energy. Rather we allow them to vary in a systematic way with the dimensionality of the related coefficients in the Lagrangian in the quantum field theory.

We interpret this fitting with a model of a truly existing lattice (probably irregular) which is fluctuating both in size and local shape, in a way corresponding to a fluctuation in the reparametrization gauge of general relativity. We though assume that it is somehow cut off so that the distribution of the link length say fluctuate on a logarithmic scale much like a Gaussian distribution in the logarithm.

When one asks for different powers of the link-length for different purposes or different types of interactions, one gets the dominant link length to be somewhat different. This gives different scales for different purposes or lagrange terms: Planck scale, Unification scale, See saw scale,and then a scale related to the fermion masses (to be explained).

Crossing in one point of Minimal $SU(5)$ Running (inverse) Fine structure constants not perfect.
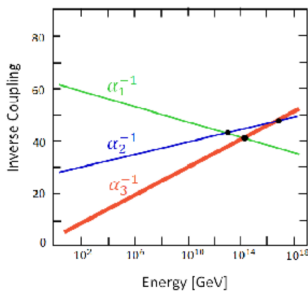
Figure 4: This is the usual graph representing the three Standard Model inverse fine structure constants with the α_1^{-1} being in the notation suitable for $SU(5)$, meaning it is 3/5 times the natural normalization, $\alpha_{1\ SU(5)}^{-1} = 3/5 * \alpha_{1\ SM}^{-1} = 3/5 * \alpha_{EM}^{-1} cos^2 \Theta_W$. The vertical thin line at the energy scale $\mu_U = 5 * 10^{13} GeV$ points out "our unified scale", which is as can be seen not really unifying the couplings, but rather is the scale where the ratio of the two independent differences, $\alpha_2^{-1} - \alpha_{1\ SU(5)}^{-1}$ and $\alpha_{1\ SU(5)}^{-1} - \alpha_3^{-1}$ have just the ratio 2/3 as our model predicts at the " our unification scale". One may note, that this "our unified scale" is actually very close to, where the three inverse couplings are nearest to each other, and in that sense an "approximate" unification scale.

Our prediction of Deviation from $SU(5)$.
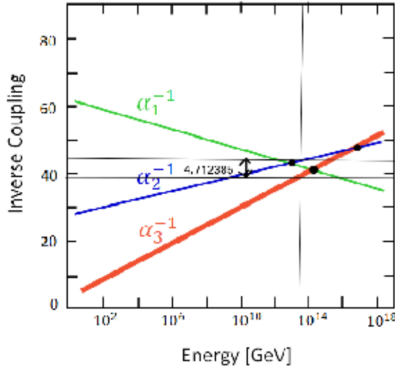
Figure 5: Same as figure 1, but now with our prediction inserted, marked as the number $4.712385 = 3 * \pi/2$, which is predicted to be at the "our unified scale" the difference $1/\alpha_2 - 1/\alpha_3$. Our prediction is, that just at horizontal thin black line, at $5 * 10^{13} GeV$, corresponding to the scale μ_U, given by our fitted to the green line crossing point dividing the region between the blue and the red in the ratio 2 to 3, we shall have the difference in ordinate between the red and the blue crossing points with the vertical black being $3\pi/2$.

Our formulas to be fitted:
The three standard model fine structure constants (inverted):

$$\frac{1}{\alpha_{1\ SU(5)}(\mu_U)} = \frac{1}{\alpha_{5\ uncor.}} - 11/5 * q \qquad (13.31)$$

$$\frac{1}{\alpha_2}(\mu_U) = \frac{1}{\alpha_{5\ uncor.}} - 9/5 * q \qquad (13.32)$$

$$\frac{1}{\alpha_3(\mu_U)} = \frac{1}{\alpha_{5\ uncor.}} - 14/5 * q, \qquad (13.33)$$

where the one parameter $\frac{1}{\alpha_{5\ uncor.}}$, is essentially the unified coupling, although we do not have unification proper.
We work with two related " unified" couplings, $\alpha_{5\ uncor.}$ and $\alpha_{5\ cor.}$

$$\frac{1}{\alpha_{5\ cor.}} = \frac{1}{\alpha_{5\ uncor.}} - 24/5 * q. \qquad (13.34)$$

The other parameter q we believe to have calculated in our model with its 3 families of fermions and in a Wilson lattice in a lowest order approximation:

$$q = \text{``\#families''} * \pi/2 = 3 * \pi/2 = 4.712385.\tag{13.35}$$

Our formulas in "corrected form":
Using this notation we could equally well use the formulation

$$\frac{1}{\alpha_{1\ SU(5)}(\mu_U)} = \frac{1}{\alpha_{5\ cor.}} + 13/5 * q \tag{13.36}$$

$$\frac{1}{\alpha_2(\mu_U)} = \frac{1}{\alpha_{5\ cor.}} + 3 * q \tag{13.37}$$

$$\frac{1}{\alpha_3(\mu_U)} = \frac{1}{\alpha_{5\ cor.}} + 2 * q. \tag{13.38}$$

Table of Fitting the Three parameters

Parameter	Formula	From α's	Theory	Deviation	Section
q	$q = 1/\alpha_2(\mu_U) - 1/\alpha_3(\mu_U)$	4.618	4.712385	-0.094$\pm$0.05	??, ??
$1/\alpha_{5\ uncor.}(\mu_U)$	see above	51.705	45.927	5.778$\pm$ 3.5	??
$\ln(\frac{\mu_U}{M_Z})$	$\ln(\frac{\mu_U}{m_t}) = \frac{2}{3} * \ln(\frac{E_{Pl\ red}}{M_t})$	27.04	24.76	2.28$\pm$ 1 or 0.02	??

In the third line we now replace the top mass m_t with a mass value gotten by extrapolating from the whole spectrum of quarks and leptons, which is about 10TeV and the agreement got very good indeed.

13.3.2   Model

We assume ANTI-GUT: Diagonal subgroup breaking

$$G_{full} = SMG \times SMG \times SMG \tag{13.39}$$

$$\text{where } SMG = S(U(1) \times U(3)) \tag{13.40}$$

$$= (R \times SU(2) \times SU(3))/Z_{app} \tag{13.41}$$

where

$$Z_{app} = \{(r, U_2, U_3)|$$
$$\exists n \in Z[(r, U_2, U_3) = (2\pi, -1, \exp(i2\pi/3)1)^n]\}$$

$$SMG_{as\ observed} = \{(g, g, g)|g \in SMG\} \subset G_{full} \tag{13.42}$$

Action: Trace of in 5×5 embedding of SMG
It is our crucialassumption that we have a lattice theory with plaquette-action given proportional to the trace of the representative of the plaquette group element $U_{Pl}(\square)$ in the/a "smallest" representation - taken here as the representation in the five-plet SU(5) representation 5:

$$\rho(U_{pl}(\square) : 5 \rightarrow 5 \tag{13.43}$$
$$\text{or } \rho(U_{pl}(\square)) \in UnitaryMarix(5 \times 5) \tag{13.44}$$

We have once pointed out that the very standard model group SMG is selected as the one having with appropriate definition the smallest relative to the group faithful representation.

13.3.3   Fitting

We predict two differences between $1/\alpha$s in Absolute number
Taking our $q = 3\pi/2$ as just given in our model, and we predict the differences from a to be fitted "unified" inverted coupling $1/\alpha_{5\ uncor.}$ at a to be fitted "unification scale" μ_U, we really only provide **one predicted parameter at first**. Really we predict the two independent differences, say $1/\alpha_2 - 1/\alpha_3 = q$ and $1/\alpha_2 - 1/\alpha_{1\ SU(5)} = 2/5 * q$ at the "unification scale".
E.g. select the scale by having the ratio of the two differences the predicted one; then the absolute size is a true prediction.
We got $q = 4.6$ by the fine structure constant data and the $3\pi/2 = 4.712$.
Inverse Fine structure constants at the μ_U-scale

Inverse finestructure constants at ``àpproximate unified '" scale:

U(1) in SU(5) notation

5 cont   5 bare

29.35   41.43   51.53   1

SU(3):38.59   SU(2): 43.21

45.93 critical SU(5)
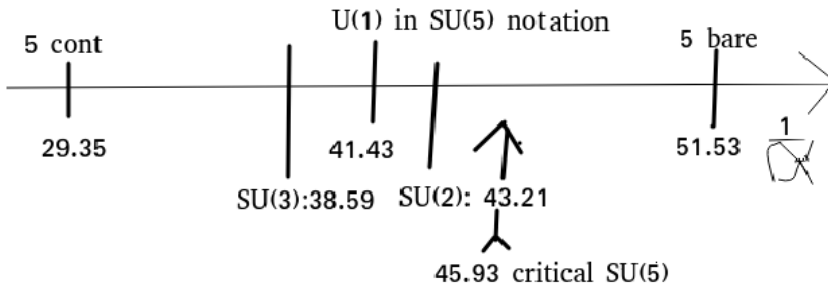
Figure About Critical Coupling

Explaing figure:The axis is the axis of inverse fine structure constants; The group names U(1), SU(2) and Su(3) are the by renormalization group to the replacement of unification scale μ_U extrapolated experimental inverse fine structure constants for these groups respectively. The two SU(5) inverse fine structure constants are respectively with and without the quantum fluctuation contribution.

Helping Approximations to justify Critical Coupling

To justify that the above figure implies that the unified coupling represented by the inverse fine structure constant has indeed the critical value (for a phase transition, presumably between confinement or not) we make use of the following three approximations/assumptions:(see next slide)

The approximations or assumptions

- The critical couplings for a true $SU(5)$ lattice theory and for the Standard Model group deviate only little, because the standard model group can be considered an attenuation of the SU(5) one.
- We can trust a rather simple formula for the critical couplings for the SU(N) groups,

$$\frac{1}{\alpha_N} = \frac{N}{2}\sqrt{\frac{N+1}{N-1}}\alpha^{-1}_{U(1)crit} \tag{13.45}$$

$$\text{where } \alpha^{-1}_{U(1)crit} = 0.2 \pm 0.015 \tag{13.46}$$

found in an article with Laperashvili and others [83].
- The critical coupling for the Standard Model group $S(U(3) \times U(2))$ should be compared to couplings with equally many quantum fluctuation contributions as it has itself.

And then the assumption of the model which is not only an approximation:
We compare the " unified couplings" not to simply the critical one but the by a factor 3 weakened one, so that we have multiplied the critical inverse finestructure constant for the Standard Model group by 3, to compare it with the unified couplings.(the 3 is again the number of families)
A reference to larisa et al.

References

1. Larisa Laperashvili, Dmitri Ryzhikh "[SU(5)]³ SUSY unification" arXiv:hep-th/0112142v1 17 Dec 2001

13.4   Gravity Problem; Return to First Part again

Return to Part I: on the scales in fluctuating lattice model

Really I believe that gauge symmetries could be due to very huge fluctuations in those degrees of freedom which are the gauge-monsters.
If a lattice were connected to a coordinate system in general relativity, but the gauge not fixed but allowed to fluctuate, we should get a lattice fluctuating relative to what we would consider the fixed geometry.

Fluctuating Lattice Imposed by General relativity

stiff lattice   fluctuating, deformed lattice
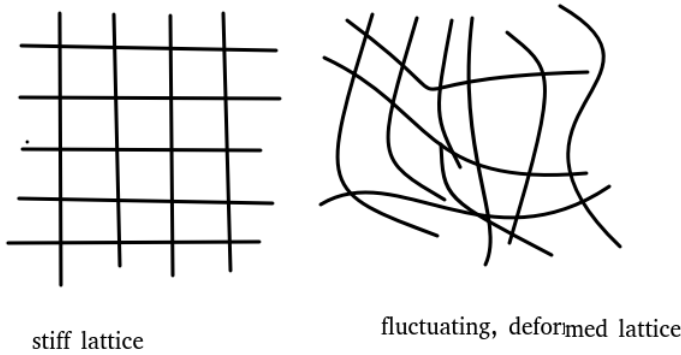
Contributions as function of ln scale in fluctuating lattice:
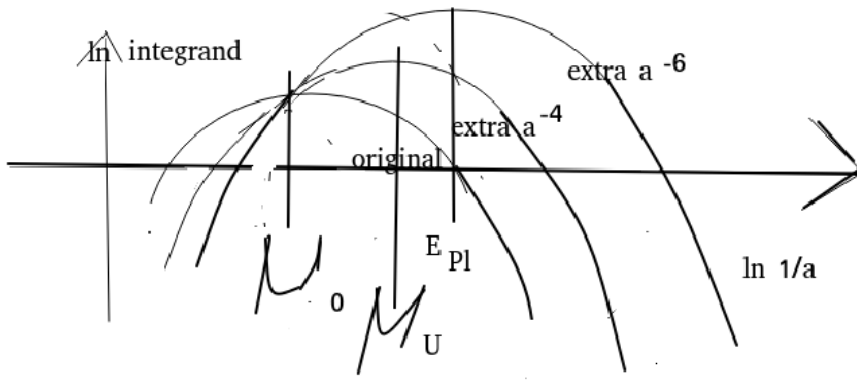
Figure 6: Shifted Scales Depending on Weighting with $(1/a)^n$ weight factor

On the abscissa we have the logarithm $\ln(1/a)$ of energy $1/a$, and for several cases of weighting with powers of the $1/a$ we have on the ordinate the logarithm of the contribution density to the average of these powers of $1/a$. In the Gauss distribution assumption, which we use the logarithm of the distribution density as function of the $\ln(1/a)$ is a parbola (pointing downward) and for the various powers of $1/a$ shown the weighted distribution becomes again a now displaced parabola. It is the displacement component along the abscissa here, which represents the change in effective energy scale, which is the central effect discussed in the first part of this paper.
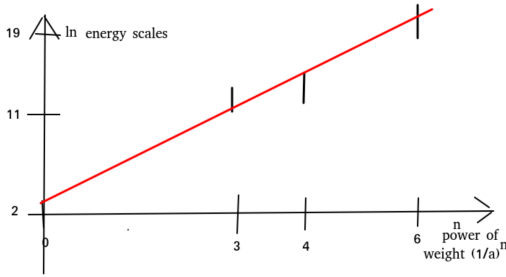
Figure 7: Here we attempted to fit our first four energy scales with the "fermion tip" scale approximated by just the top mass m_t, because of course after all the top quark is the heaviest, so it is approximately the tip scale. On the abscissa we have the energy scale characteristic integer n essentially denoting which power $(1/a)^n$ is relevant for the energy scale in question. The ordinate is the logarithm with basis 10 of the energy scale. We use base 10, because it makes it easier to relate to our ten-power notation for the energy scales.
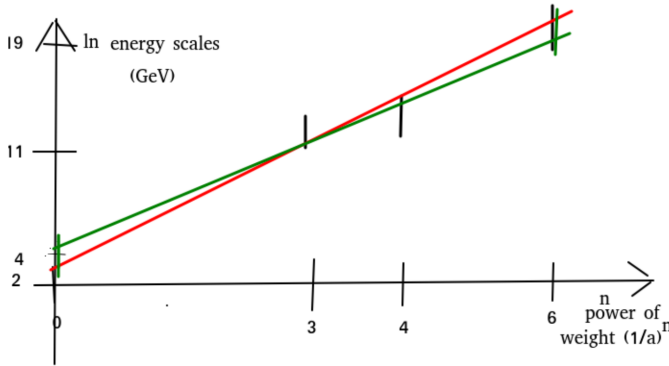
Figure 8: However, taking for the "fermion tip" scale rather than just top mass m_t the value gotten by the extrapolation m_{mnl} as seen in figure 9 and in the tables for respectively quarkmasses and leptonmasses not long below. The fitting is a bit better than for using the top-mass simply.

The plot of scales versus weighting power n

We present 4 energy scales of physical interest together with lattice link size a dependent factor coming into the expression in the action or Lagrangian relevant for the scale in question. It is essentially the dimension of the term in the Lagrangian density without counting the coefficient (so it is rather trivially related to this coefficient). We took:

- **0** $(1/a)^0$ This scale is the scale of maximal number of "active"/effectively massless families. (Needs more explanation below.). Below extrapolation $\sim$ 10TeV.
- **3** $(1/a)^3$ The see-saw neutrino mass scale
- **4** $(1/a)^4$ The our "unification scale",at which the Yang Mills theories are supposed to be given by the truly existing fluctuating lattice.

- **6** $(1/a)^6$ The Planck scale, related to the Einstein-Hilbert-action.
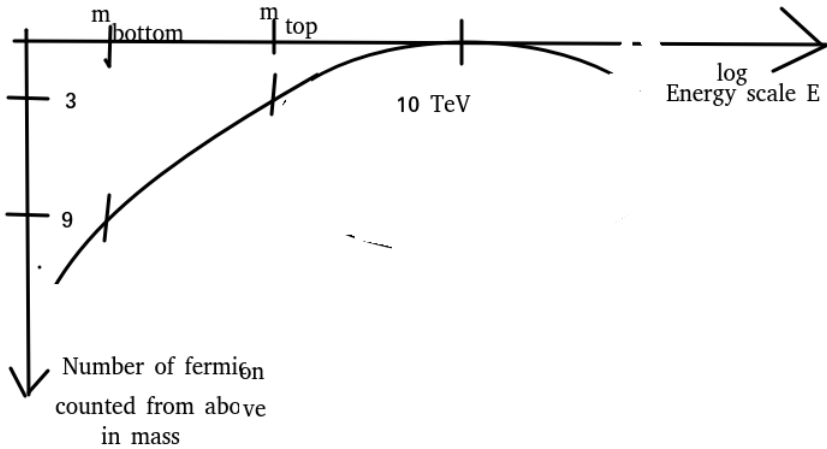
Figure 9: **Fitting Weyl Fermion masses by number after mass by Philosophy of Fluctuating Lattice:** In order to make an as good as possible extrapolation to where the series of masses of the fermions in the Standard Model we should assume how this series of masses is related to some ansatz formula for their density on say the logarithm of mass axis. Inspired by our ideas of a fluctuating lattice with a Gaussian combined with a connection of the number of fermions with relative to that scale negligible mass being proportional to the layer density at the scale, we suggested: The number of a fermion counted from the heaviest, the next heaviest, etc. should be approximately proportional to the square of the distance in logarithm from the "extrapolated tip" of the mass region, which we call m_{mnl} to the mass of the fermion. On this plot we see as function of the logarithm of masses the number in the series counted from the heaviest down according to mass. We have let the axis denoting the number in the series point down. So the curve is to be fitted by a (half) parabola.

$$\textbf{Quark for } m_{mnl} = 10^4 \, GeV$$

m_{mnl} = "maximum number of layers" is the energy scale at which density of the distributuion of inverse lattice sizes $1/a$ is the biggest.
We fit to this density being proportional to the number of Weyl fermions relative to the scale being light/massless. Since the last column diff^2/n fits a constant 1.12 to about 0.1 we have good fit for the 10 TeV.

Name	number n	Mass m	$\log_{10 \, GeV} m$	$\text{diff}=4-\log m$	diff^2	diff^2/n
top	3± 1	172.76 ± 0.3 GeV	2.2374± 0.0008	1.7626	3.1066± 0.003	1.0355 ± 0.001 ±0.4
bottom	9± 0.3	4.18± 0.0079GeV	0.6212±0.001	3.3788	11.416± 0.01	1.268± 0.001±0.03
charm	17 or 15	1.27± 0.02	0.10382± 0.009	3.8962	15.180± 0.07	0.893 ± 0.004 ± 0.06
strange	25 or 23	0.095±0.006 GeV	-1.0223±0.003	5.0223	25.223 ±0.03	1.009±0.001±0.1
down	31	4.79± 0.16 MeV	-2.3197±0.01	6.3197	39.939± 0.06	1.288 ± 0.002
up	37	2.01± 0.14 MeV	-2.6968±0.03	6.6968	44.847± 0.4	1.212± 0.01

$$\textbf{Leptons for } m_{mnl} = 10^4 \, GeV$$

m_{mnl} = "maximum number of layers" is the energy scale at which density of the distribution of inverse lattice sizes $1/a$ is the biggest.

We fit to this density being proportional to the number of Weyl fermions relative to the scale being light/massless. Since the last column diff^2/n fits a constant 1.19 to about 0.1 we have good fit for the 10 TeV.

Name	number n	Mass m	$\log_{10 \text{ GeV}} m$	diff=4 − logm	diff^2	diff^2/n
τ	13 or 19	1.77686 ± 0.00012	0.2496 ± 0.00003	3.7503	14.065 ± 0.0003	$1.082 \pm 0.00002 \pm 0.4$
mu	21 or 27	$105.6583745 \pm 2.4 * 10^{-6}$MeV	$-0.9761... \pm 10^{-8}$	4.9761	24.761 ± 10^{-7}	$1.179 \pm 4 * 10^{-9} \pm 0.3$
electron	41	$0.51099895069 \pm 1.6 * 10^{-10}$	$-3.2915 \pm 4 * 10^{-10}$	7.2916	53.167 ± 10^{-8}	1.297 ± 10^{-11}

Explaining the tables fitting Fermion Masses to Fluctuating Lattice

In the two foregoing tables - one for quarks, the second one for the charged leptons – you have in first column the name of the fermion, then its number in the series of fermions counted as Weyl fermions and after mass, the heaviest first then the lighter and lighter ones. A quark flavour corresponds to two Weyl per particle and it has three colors,so there is under each flavour 6 Weyl and we represent a flavour by the middle one of these 6. So the top quark gets the representative number $n = 3$ (the middle between 0 and 6. We use logarithmic scale and care for the logarithm - we use log of basis 10 for slightly easier calculation - of the ratio of the fermion mass to the scale we test with as m_{mld} = " maximum layer density point on the energy scale".

Because our best fit $m_{mld} = 10^4 GeV = 10TeV$ the log of it is just the 4 in the column $4 - \log_{10} m$ (= diff).Since we want to fit the number of layers as a square function of the logarithm of the masses, we shall square what in the table is called diff and which is just the log of the ratio mentioned.

If the Fermion masses were indeed arranged so as to make the number of (Weyl)fermions with mass under a given scale be proportional to the a quadratic function in the log dropping down from a maximum as we go more and more below m_{mnl} point, then the ratio in the last column diff^2/n should be constant.

If we would have liked to fit with a Gaussian of the logarithm of the masses, we should instead of the number n have used $\log \frac{45-n}{45}$, which for the first small n is approximately proportional to n itself.(45 is the number of Weyl particles in SM).

13.4.1   Seesaw

What to take for the Seesaw neutrino scale?

Name	Seesaw-scale	Comments
Steven King	$3.9 * 10^{10} GeV$	lowest mass;susy
Grimus and Lavoura	$10^{11} GeV$	
Davidson and Ibarra	$\geq 10^9 GeV$	
"statisic" (my own)	$1.4 * 10^9 GeV$	
Mohapatra	10^{14} to 10^{15} GeV	very crude guess
Modernized Takanishi and me(own)	$1.2 * 10^{15} GeV$	
Average of most trustable	$10^{11} GeV$	

13.5   Conclusion

13.5.1   Conclusion for Part I: Fluctuating Lattice, several Energy Scales

We have found for several energy scales, meaning energies constructed from various phenomena, such as gravitation for the Planck scale, See-saw right handed neutrino mass scale from neutrino oscillations, a "unification scale" from extrapolating by renormalization group the measured fine structure constants etc., that they fit very well to the hypothesis that there exist in Nature physically a lattice, that fluctuates with a very broad distribution in size of say the link a. Actually the broadness of the fluctuation of the natural logarithm $\ln(a)$ is given by the width $\sigma = 5.5$, which is so broad that looking powers of the a, i.e. a^{-n} you get a step by a **factor** 251 for each step by 1 in the power in the effective value of a, i.e. $\sqrt[-n]{<a^{-n}>}$.

If this is the right way to look at the energy scales then rather than believing that the fundamental scale of Nature is the Planck scale we should take it to be the one we called "the fermion tip" scale, which is $10^4 \, GeV$. So the fundamental physics would be nearer than we used to think!

13.5.2   Conclusion for Part II on Approximate SU(5) GUT

We had a successful agreement with the values of the fine structure constants in a minimal (i.e. no susy!) approximate GUT SU(5) "unification" at the scale $\mu_U = 5.13 * 10^{13} \, GeV$ (compared susy-models a very low energy scale, but not far at all from the scale needed for see-saw neutrinos to fit the neutrino oscillations). We have three parameters **predicted by our theory**:

- $q = 3 * \pi/2$ is a parameter going into the **deviation** from full GUT-SU(5).
- The replacement for the unification coupling $\alpha_{5 \, uncor.}$ or $\alpha_{5 \, cor.}$, whichever one of them we want to think of, or rather the thirds of one of them, should correspond to the critical value, in the sense that it should be at borderline of two phases of the vacuum.
- The replacement for the unification scale μ_U goes into a series of "fundamental scales" fitted on a line.
- We related four **different** physical/"fundamental" scales by a line relating the energy scale to their dimension of the related Lagrange density term.
  2.5 orders of magnitude per dimension of the Lagrange term coefficient.
  The four scales are:

  - A scale related to the fermion mass distribution of formal dimension of coupling $[GeV^4]$.
  - The See saw scale, coupling dimension $[GeV]$,
  - Approximate Grand unification scale, coupling dimension $[1]$,
  - Planck i.e. gravity scale, coupling dimension $[GeV^{-2}]$

But since the conference virtually in Bled we added:

Added later Scales:

- "scalars" is a scale only in my fantasy at which there should be a lot of scalar boson masses. associated with that presumably also some non-zero expectation values breaking dreamt about symmetries yet to be discovered spontaneously. Such breakings of symmetries by the ratio of this "scalars"scale to the "see saw" scale which is the 1/250 could be the weak breaking responsible for the small hierarchy problem, that the ratio between the fermion masses in the Standard Model typically are large by by factors not so different from 250.
- A "monopole" scale also dreamt up of masses of presumably bound states of some monopoles for the standard model group being confined by their SU(3) part of the monopolic charge. Actually a candidate for having found them is a dimuon-resonance, which is about the only new physics surviving from the LHC [55], also by reanalysis seen in LEP [56].
- A string theory with the energy scale given by our fluctuating lattice turns out to agree surprizingly well with the string theory for hadrons, that were historically the first string theory application.
- The energy scale for "2-branes" with Goto (Nambu) action would get from our fluctuating lattice a scale of tension not violently different from what Coin Froggatt and I get from phenomenological fitting of dark matter as pearls of new vacuum encapsulated by the "2-branes".

Acknowledgement

References

1. Holger Bech Nielsen, " Approximate SU(5), Fine structure constants", arXiv:2403.14034 (hep-ph) (not yet published, but hopefully)
2. H. B. Nielsen "Remarkable Scale relation, Approximate SU(5), Fluctuating Lattice", arXiv:2411.03552v1 [hep-ph] 05 Nov 2024.
3. P. Minkowski, Phys. Lett. B 67, 421 (1977). R. N. Mohapatra and G. Senjanovic, Phys. Rev. Lett. 44, 912 (1980).
4. Georgi, Howard; Glashow, Sheldon (1974). "Unity of All Elementary-Particle Forces". Physical Review Letters. 32 (8): 438. Bibcode:1974PhRvL..32..438G. doi:10.1103/PhysRevLett.32.438. S2CID 9063239.
5. Masiero, A.; Nanopoulos, A.; Tamvakis, K.; Yanagida, T. (1982). "Naturally Massless Higgs Doublets in Supersymmetric SU(5)". Physics Letters B. 115 (5): 380–384. Bibcode:1982PhLB..115..380M. doi:10.1016/0370-2693(82)90522-6.
6. Georgi, Howard; Glashow, Sheldon (1974). "Unity of all elementary-particle forces". Physical Review Letters. 32 (8): 438. Bibcode:1974PhRvL..32..438G. doi:10.1103/PhysRevLett.32.438. S2CID 9063239
7. L. V. Laperashvili (ITEP, Moscow, Russia), H. B. Nielsen, D.A. Ryzhikh "Phase Transition in Gauge Theories and Multiple Point Model" arXiv:hep-th/0109023 Phys.Atom.Nucl.65:353-364,2002; Yad.Fiz.65:377-389,2002

8. Larisa Laperashvili, Dmitri Ryzhikh " [SU(5)]3 SUSY unification" Larisa Laperashvili, Dmitri Ryzhikh arXiv:hep-th/0112142v1 17 Dec 2001 [SU(5)]3 SUSY unification

9. Grigory E. Volovik Introduction: Gut and Anti-Gut
   https://doi.org/10.1093/acprof:oso/9780199564842.003.0001
   Journal: The Universe in a Helium Droplet, 2009, p. 1-8
   Publisher: Oxford University PressOxford
   Author: VOLOVIK GRIGORY E.

10. CRITICAL COUPLINGS AND THREE GENERATIONS IN A RANDOM-DYNAMICS INSPIRED MODEL IVICA PICEK FIZIKA B (1992) 1, 99-110

11. D.L.Bennett, L.V. Laperashvili, H.B. Nielsen, Fine structure Constants at the Planck scale from Multiple Point Prinicple. Bled workshop Vol 8, No. 2 (2007) Proceedings of the Tenth workshop " What comes beyond the standard models Bled Slovenia July 17-27-2007.

12. D. Bennett, H.B. Nielsen, and I Picek. Phys. Lett. B208 275 (1988).

13. H. B. Nielsen, "Random Dynamics and relations between the number of fermion generations and the fine structure constants", Acta Physica Polonica Series B(1), 1989. Crakow School of Theoretical Physics, Zakopane, Poland.

14. H.B. Nielsen and N. Brene, Gauge Glass, Proc. of the XVIII International Symposium on the Theory of Elementary Particles, Ahrenshoop, 1985 (Institut fur Hochenergi- physik, Akad. der Wissenschaften der DDR, Berlin-Zeuthen, 1985); D.L. Bennett, N. Brene, L. Mizrachi

15. H.B. Nielsen, Phys. Lett. B178 (1986) 179.

16. arXiv:hep-ph/9311321v1 19 Nov 1993 November 19, 1993 D.L. Bennett, H.B. Nielsen "Predictions for Nonabelian Fine Structure Constants from Multicriticality" arXiv:hep-ph/9311321v1 19 Nov 1993 November 19, 1993

17. Bennett, D. L. ; Nielsen, H. B. "Gauge Couplings Calculated from Multiple Point Criticality Yield $\alpha^{-1} = 137 \pm 9$: at Last, the Elusive Case of U(1)" arXiv:hep-ph/9607278, Int.J.Mod.Phys. A14 (1999) 3313-3385

18. H.B.Nielsen, Y.Takanishi "Baryogenesis via lepton number violation in Anti-GUT model" arXiv:hep-ph/0101307 Phys.Lett. B507 (2001) 241-251

19. L.V.Laperashvili and C. Das, Corpus ID: 119330911 "[SU(5)]^3 SUSY unification" (2001) arXiv: High Energy Physics - Theory

20. Paolo Cea, Leonardo Cosmai "Deconfinement phase transitions in external fields" XXI-IIrd International Symposium on Lattice Field Theory 25-30 July 2005 Trinity College, Dublin, Ireland

21. L. V. Laperashvili, D. A. Ryzhikh, H. B. Nielsen, "Phase transition couplings in U(1) and SU(N) regularized gauge theories"
    January 2012International Journal of Modern Physics A 16(24)
    DOI:10.1142/S0217751X01005067

22. L.V.Laperashvili, H.B.Nielsen and D.A.Ryzhikh, Int.J.Mod.Phys. A16 , 3989 (2001); L.V.Laperashvili, H.B.Nielsen and D.A.Ryzhikh, Yad.Fiz. 65 (2002).

23. C.R. Das, C.D. Froggatt, L.V. Laperashvili, H.B. Nielsen "Flipped SU(5), see-saw scale physics and degenerate vacua" arXiv:hep-ph/0507182, Mod.Phys.Lett. A21 (2006) 1151-1160

24. Larisa Laperashvili, Dmitri Ryzhikh "[SU(5)]^3 SUSY unification" arXiv:hep-th/0112142v1 17 Dec 2001

25. Holger Bech Nielsen "Random Dynamics and Relations Between the Number of Fermion Generations and the Fine Structure Constants" Jan, 1989, Acta Phys.Polon.B 20 (1989) 427
    Contribution to:
    XXVIII Cracow School of Theoretical Physics

Report number:
NBI-HE-89-01

26. H. B. Nielsen, Astri Kleppe et al., http://bsm.fmf.uni-lj.si/bled2019bsm/talks/HolgerTransparencesconfusion2.pdf Bled Workshop July 2019, "What comes Beyand the Standard Models".

27. D.L. Bennett, , Holger Bech Nielsen, , N. Brene, , L. Mizrachi "THE CONFUSION MECHANISM AND THE HETEROTIC STRING" Jan, 1987, 20th International Symposium on the Theory of Elementary Particles, 361 (exists KEK-scanned version)

28. Holger Bech Nielsen, and Don Bennett, "Seeking a Game in which the standard model Group shall Win" (2011) 33 pages Part of Proceedings, 14th Workshop on What comes beyond the standard models? : Bled, Slovenia, July 11-21, 2011 Published in: Bled Workshops Phys. 12 (2011) 2, 149
Contribution to: Mini-Workshop Bled 2011, 14th Workshop on What Comes Beyond the Standard Models?, 149

29. Holger Bech Nielsen Niels Bohr Institutet, Blegdamsvej 15 -21 DK 2100Copenhagen E-mail: hbech at nbi.dk, hbechnbi at gmail.com "Small Representations Explaining, Why standard model group?" PoS(CORFU2014)045. Proceedings of the Corfu Summer Institute 2014 "School and Workshops on Elementary Particle Physics and Gravity", 3-21 September 2014 Corfu, Greece

30. H. Nielsen Published 22 April 2013 Physics Physical Review D DOI:10.1103/PhysRevD.88.096001Corpus ID: 119245261
"Dimension Four Wins the Same Game as the Standard Model Group"

31. L. O'Raifeartaigh, "The Dawning of Gauge Theory", Princeton University Press (1997)

SEMINAR ZAVODA ZA TEORIJSKU FIZIKU (Zajedniˇcki seminari Zavoda za teorijsku fiziku, Zavoda za eksperimentalnu fiziku i Zavoda za teorijsku fiziku PMF-a) Relations derived from minimizing the Higgs field squared (integrated over space-time) Holger Bech Nielsen The Niels Bohr Institute, Copenhagen, Denmark

32. H.B. Nielsen "Complex Action Support from Coincidences of Couplings" arXiv:1103.3812v2 [hep-ph] 26 Mar 2011

33. H.B. Nielsen,arXiv:1006.2455v2 "Remarkable Relation from Minimal Imaginary Action Model " arXiv:1006.2455v2 [physics.gen-ph] 2 Mar 2011

34.] D. Foerster, H. B. Nielsen and M. Ninomiya, Phys. Lett. B 94, 135 (1980).

35. U.-J. Wiese "Ultracold Quantum Gases and Lattice Systems: Quantum Simulation of Lattice Gauge Theories ", arXiv:1305.1602v1 [quant-ph] 7 May 2013

36. H.B. Nielsen, S.E. Rugh and C. Surlykke, Seeking Inspiration from the Standard Model in Order to Go Beyond It, Proc. of Conference held on Korfu (1992)

37. C.D. Froggatt, H.B. Nielsen and Y. Takanishi, Nucl. Phys. B 631, 285 (2002) [arXiv:hep-ph/0201152];
H.B. Nielsen and Y. Takanishi, Phys. Lett. B 543, 249 (2002) [arXiv:hep-ph/0205180].

38. H.B. Nielsen and C.D. Froggatt, Masses and mixing angles and going be- yond thye Standard Model, Proceedings of the 1st International Workshop on What comes beyond the Standard Model, Bled, July 1998, p. 29, ed. N. Mankoc Borstnik, C.D. Froggatt and H.B. Nielsen DMFA - zaloznistvo, Ljubljana, 1999; hep-ph/9905455
C.D. Froggatt and H.B. Nielsen, Hierarchy of quark masses, Cabibbo angles and CP violation, Nucl. Phys. B147 (1979) 277.
H.B. Nielsen and Y. Takanishi, Neutrino mass matrix in Anti-GUT with see-saw mechanism, Nucl. Phys. B604 (2001) 405.
C.D. Froggatt, M. Gibson and H.B. Nielsen, Neutrino masses and mixing from the AGUT model

39. Ferruccio Feruglio "Fermion masses, critical behavior and universality" JHEP03(2023)236Published for SISSA by Springer Received: March 1, 2023 Accepted: March 13, 2023 Published: March 29, 2023 JHEP03(2023)236

40. H.B. Nielsen* and C.D. Froggatt, "Connecting Insights in Fundamental Physics: Standard Model and Beyond Several degenerate vacua and a model for DarkMatter in the pure Standard Model" Volume 376 - Corfu Summer Institute 2019 "School and Workshops on Elementary Particle Physics and Gravity" (CORFU2019)

41. Keiichi Nagao and Holger Bech Nielsen "Formulation of Complex Action Theory" arXiv:1104.3381v5 [quant-ph] 23 Apr 2012

42. 1) H. B. Nielsen and M. Ninomiya, Int. J. Mod. Phys. A 21 (2006) 5151; arXiv:hep-th/0601048; arXiv:hep-th/0602186; Int. J. Mod. Phys. A 22 (2008) 6227.
    2) D. L. Bennett, C. D. Froggatt and H. B. Nielsen, the proceedings of Wendisch-Rietz 1994 -Theory of elementary particles- , p.394-412; the proceedings of Adriatic Meeting on Particle Physics: Perspectives in Particle Physics '94, p.255-279. Talk given by D. L. Bennett, "Who is Afraid of the Past" (A resume of discussions with H. B. Nielsen) at the meeting of the Cross-disciplinary Initiative at NBI on Sep. 8, 1995. D. L. Bennett, arXiv:hep-ph/9607341.
    3) H. B. Nielsen and M. Ninomiya, the proceedings of Bled 2006 -What Comes Beyond the Standard Models-, p.87-124, arXiv:hep-ph/0612250.
    4) H. B. Nielsen and M. Ninomiya, arXiv:0802.2991 [physics.gen-ph]; Int. J. Mod. Phys. A 23 (2008) 919; Prog. Theor. Phys. 116 (2007) 851.
    5) H. B. Nielsen and M. Ninomiya, the proceedings of Bled 2007 -What Comes Beyond the Standard Models- , p.144-185.
    6) H. B. Nielsen and M. Ninomiya, arXiv:0910.0359 [hep-ph]; the proceedings of Bled 2010 -What Comes Beyond the Standard Models-, p.138-157.
    7) H. B. Nielsen, arXiv:1006.2455 [physic.gen-ph].
    8) H. B. Nielsen and M. Ninomiya, arXiv:hep-th/0701018.
    9) H. B. Nielsen, arXiv:0911.3859 [gr-qc].
    10) H. B. Nielsen, M. S. Mankoc Borstnik, K. Nagao and G. Moultaka, the proceedings of Bled 2010 -What Comes Beyond the Standard Models-, p.211-216.
    11) K. Nagao and H. B. Nielsen, Prog. Theor. Phys. 125 No. 3, 633 (2011)

43. Goran Senjanovic and Michael Zantedeschi, "Minimal SU(5) theory on the edge: the importance of being effective" Goran Senjanovic arXiv:2402.19224v1 [hep-ph] 29 Feb 2024

44. Johan Thoren, Lund University Bachelor Thesis "Grand Unified Theories: SU (5), SO(10) and supersymmetric SU (5)"

45. A.A. Migdal "Phase transitions in gauge and spin-lattice systems" L. D. Landau Theoretical Physics Institute. USSR Academy of Sciences (Submitted June II, 1975) Zh. Eksp. Teor. Fiz. 69, 1457-1465 (October 1975)

46. Stephen F. King "Neutrino mass and mixing in the seesaw playground" Available online at www.sciencedirect.com ScienceDirect Nuclear Physics B 908 (2016) 456–466 www.elsevier.com/locate/nuclphysb

47. Rabindra N. Mohapatra "Physics of Neutrino Mass" SLAC Summer Institute on Particle Physics (SSI04), Aug. 2-13, 2004

48. W. Grimus, L. Lavoura, "A neutrino mass matrix with seesaw mechanism and two-loop mass splitting" arXiv:hep-ph/0007011v1 3 Jul 2000 UWThPh-2000-26

49. Sacha Davidson and Alejandro Ibarra "A lower bound on the right-handed neutrino mass from leptogenesis" arXiv:hep-ph/0202239v2 23 Apr 2002 OUTP-02-10P IPPP/02/16 DCPT/02/32

50. K. Enquist, "Cosmologicaæ Infaltion", arXiv:1201.6164v1 [gr-qc] 30 Jan 2012

51. Andrew Liddle, An Introduction to Cosmological Inflation",arXiv:astro-ph/9901124v1 11 Jan 1999
52. Nicola Bellomo, Nicola Bartolo, Raul Jimenez, Sabino Matarrese,c,d,e,g Licia Verde "Measuring the Energy Scale of Inflation with Large Scale Structures" arXiv:1809.07113v2 [astro-ph.CO] 26 Nov 2018
53. C. D. Froggatt and H. B. Nielsen, Nucl. Phys. B 147, 277-298 (1979)
54. Roberto AUZZI, Stefano BOLOGNESI, Jarah EVSLIN, Kenichi KONISHI, Hitoshi MURAYAMA, "NONABELIAN MONOPOLES" arXiv:hep-th/0405070v3 23 Jun 2004 ULB-TH-04/11, IFUP-TH/2004-5
55. The CMS collaboration EUROPEAN ORGANIZATION FOR NUCLEAR RESEARCH (CERN) CERN-EP-2018-204 2018/12/18 CMS-HIG-16-017 "Search for resonances in the mass spectrum of muon pairs produced in association with b quark jets in proton-proton collisions at $\sqrt{s}$ = 8 and 13 TeV" arXiv:1808.01890v2 [hep-ex] 17 Dec 2018
56. Arno Heister, "Observation of an excess at 30 GeV in the opposite sign di-muon spectra of Z → bb + X events recorded by the ALEPH experiment at LEP" E-mail: Arno.Heister@cern.ch arXiv:1610.06536v1 [hep-ex] 20 Oct 2016 Prepaired for submission to JHEP.
57. D. Foerster, H.B. Nielsen a b, M. Ninomiya, "Dynamical stability of local gauge symmetry Creation of light from chaos" Physics Letters B Volume 94, Issue 2, 28 July 1980, Pages 135-140
58. H.B.Nielsen "Field theories without fundamental gauge symmetries" Published:20 December 1983: https://doi.org/10.1098/rsta.1983.0088, Philosophical Transactions of the Royal Society of London. Series A, Mathematical and Physical Sciences
59. M. Lehto, H.B. Nielsen, Masao Ninomiya "Time translational symmetry" Physics Letters B Volume 219, Issue 1, 9 March 1989, Pages 87-91 Physics Letters B
60. Joan Solà 2013 J. Phys.: Conf. Ser. 453 012015
61. C. D. Froggatt and H.B. Nielsen, "Domain Walls and Hubble Constant Tension" arXiv:2406.07740 [astro-ph.CO] (or arXiv:2406.07740v1 [astro-ph.CO] for this version) https://doi.org/10.48550/arXiv.2406.07740
62. Holger Bech Nielsen, "String Invention, Viable 3-3-1 Model, Dark Matter Black Holes" arXiv 2409.13776 [hep-ph] (to be published in book celebrating Paul Framptons 80 years birthday)
63. Georgi, Howard; Glashow, Sheldon (1974). "Unity of All Elementary-Particle Forces". Physical Review Letters. 32 (8): 438. Bibcode:1974PhRvL..32..438G. doi:10.1103/PhysRevLett.32.438. S2CID 9063239.
64. Masiero, A.; Nanopoulos, A.; Tamvakis, K.; Yanagida, T. (1982). "Naturally Massless Higgs Doublets in Supersymmetric SU(5)". Physics Letters B. 115 (5): 380–384. Bibcode:1982PhLB..115..380M. doi:10.1016/0370-2693(82)90522-6.
65. Georgi, Howard; Glashow, Sheldon (1974). "Unity of all elementary-particle forces". Physical Review Letters. 32 (8): 438. Bibcode:1974PhRvL..32..438G. doi:10.1103/PhysRevLett.32.438. S2CID 9063239
66. L. V. Laperashvili (ITEP, Moscow, Russia), H. B. Nielsen, D.A. Ryzhikh "Phase Transition in Gauge Theories and Multiple Point Model" arXiv:hep-th/0109023 Phys.Atom.Nucl.65:353-364,2002; Yad.Fiz.65:377-389,2002
67. Larisa Laperashvili, Dmitri Ryzhikh " [SU(5)]3 SUSY unification" Larisa Laperashvili, Dmitri Ryzhikh arXiv:hep-th/0112142v1 17 Dec 2001 [SU(5)]3 SUSY unification
68. Grigory E. Volovik Introduction: Gut and Anti-Gut https://doi.org/10.1093/acprof:oso/9780199564842.003.0001 Journal: The Universe in a Helium Droplet, 2009, p. 1-8 Publisher: Oxford University PressOxford Author: VOLOVIK GRIGORY E.

69. CRITICAL COUPLINGS AND THREE GENERATIONS IN A RANDOM-DYNAMICS INSPIRED MODEL IVICA PICEK FIZIKA B (1992) 1, 99-110

70. D.L.Bennett, L.V. Laperashvili, H.B. Nielsen, Fine structure Constants at the Planck scale from Multiple Point Prinicple. Bled workshop Vol 8, No. 2 (2007) Proceedings of the Tenth workshop " What comes beyond the standard models Bled Slovenia July 17-27-2007.

71. D. Bennett, H.B. Nielsen, and I Picek. Phys. Lett. B208 275 (1988).

72. H. B. Nielsen, "Random Dynamics and relations between the number of fermion generations and the fine structure constants", Acta Physica Polonica Series B(1), 1989. Crakow School of Theoretical Physics, Zakopane, Poland.

73. H.B. Nielsen and N. Brene, Gauge Glass, Proc. of the XVIII International Symposium on the Theory of Elementary Particles, Ahrenshoop, 1985 (Institut fur Hochenergi- physik, Akad. der Wissenschaften der DDR, Berlin-Zeuthen, 1985); D.L. Bennett, N. Brene, L. Mizrachi

74. H.B. Nielsen, Phys. Lett. B178 (1986) 179.

75. arXiv:hep-ph/9311321v1 19 Nov 1993 November 19, 1993 D.L. Bennett, H.B. Nielsen "Predictions for Nonabelian Fine Structure Constants from Multicriticality" arXiv:hep-ph/9311321v1 19 Nov 1993 November 19, 1993

76. Bennett, D. L. ; Nielsen, H. B. "Gauge Couplings Calculated from Multiple Point Criticality Yield $\alpha^{-1} = 137 \pm 9$: at Last, the Elusive Case of U(1)" arXiv:hep-ph/9607278, Int.J.Mod.Phys. A14 (1999) 3313-3385

77. H.B.Nielsen, Y.Takanishi "Baryogenesis via lepton number violation in Anti-GUT model" arXiv:hep-ph/0101307 Phys.Lett. B507 (2001) 241-251

78. L.V.Laperashvili and C. Das, Corpus ID: 119330911 "$[SU(5)]^3$ SUSY unification" (2001) arXiv: High Energy Physics - Theory

79. Paolo Cea, Leonardo Cosmai "Deconfinement phase transitions in external fields" XXI-IIrd International Symposium on Lattice Field Theory 25-30 July 2005 Trinity College, Dublin, Ireland

80. L. V. Laperashvili, D. A. Ryzhikh, H. B. Nielsen, "Phase transition couplings in U(1) and SU(N) regularized gauge theories"
January 2012International Journal of Modern Physics A 16(24)
DOI:10.1142/S0217751X01005067

81. L.V.Laperashvili, H.B.Nielsen and D.A.Ryzhikh, Int.J.Mod.Phys. A16 , 3989 (2001); L.V.Laperashvili, H.B.Nielsen and D.A.Ryzhikh, Yad.Fiz. 65 (2002).

82. C.R. Das, C.D. Froggatt, L.V. Laperashvili, H.B. Nielsen "Flipped SU(5), see-saw scale physics and degenerate vacua" arXiv:hep-ph/0507182, Mod.Phys.Lett. A21 (2006) 1151-1160

83. Larisa Laperashvili, Dmitri Ryzhikh "$[SU(5)]^3$ SUSY unification" arXiv:hep-th/0112142v1 17 Dec 2001

84. H. B. Nielsen, "Deriving Locality, Gravity as Spontaneous Breaking of Diffeomor- phism Symmetry" Proceedings to the 26th Workshop What Comes Beyond the Standard Models Bled, July 10–19, 2023 Edited by Norma Susana Mankoc Borstnik Holger Bech Nielsen Maxim Yu. Khlopov Astri Kleppe

85. Holger Bech Nielsen "Random Dynamics and Relations Between the Number of Fermion Generations and the Fine Structure Constants" Jan, 1989, Acta Phys.Polon.B 20 (1989) 427
Contribution to:
XXVIII Cracow School of Theoretical Physics
Report number:
NBI-HE-89-01

86. H. B. Nielsen, Astri Kleppe et al., http://bsm.fmf.uni-lj.si/bled2019bsm/talks/HolgerTransparencesconfusion2.pdf Bled Workshop July 2019, "What comes Beyand the Standard Models".

87. D.L. Bennett, , Holger Bech Nielsen, , N. Brene, , L. Mizrachi "THE CONFUSION MECHANISM AND THE HETEROTIC STRING" Jan, 1987, 20th International Symposium on the Theory of Elementary Particles, 361 (exists KEK-scanned version)

88. Holger Bech Nielsen, and Don Bennett, "Seeking a Game in which the standard model Group shall Win" (2011) 33 pages Part of Proceedings, 14th Workshop on What comes beyond the standard models? : Bled, Slovenia, July 11-21, 2011 Published in: Bled Workshops Phys. 12 (2011) 2, 149

Contribution to: Mini-Workshop Bled 2011, 14th Workshop on What Comes Beyond the Standard Models?, 149

89. Holger Bech Nielsen Niels Bohr Institutet, Blegdamsvej 15 -21 DK 2100Copenhagen E-mail: hbech at nbi.dk, hbechnbi at gmail.com "Small Representations Explaining, Why standard model group?" PoS(CORFU2014)045. Proceedings of the Corfu Summer Institute 2014 "School and Workshops on Elementary Particle Physics and Gravity", 3-21 September 2014 Corfu, Greece

90. H. Nielsen Published 22 April 2013 Physics Physical Review D DOI:10.1103/PhysRevD.88.096001Corpus ID: 119245261

"Dimension Four Wins the Same Game as the Standard Model Group"

91. L. O'Raifeartaigh, "The Dawning of Gauge Theory", Princeton University Press (1997)

92. G. P. Lepage and P. B. Mackenzie, Phys. Rev. D 48, 2250 (1993).

93. Hossein Niyazi, Andrei Alexandru, Frank X. Lee, and Ruairí Brett, "Setting the scale for nHYP fermions with the Lüscher-Weisz gauge action",Physical Review D **102**,094506 (2020)

94. Hans Mathias Mamen Vege Thesis for the degree of Master of Science " Solving SU(3) Yang-Mills theory on the lattice: a calculation of selected gauge observables with gradient flow" Solving SU(3) Yang-Mills theory on the lattice: a calculation of selected gauge observables with gradient flow by Hans Mathias Mamen Vege Thesis for the degree of Master of Science Faculty of Mathematics and Natural Sciences University of Oslo April 2019

95. M. Alford, W. Dimm and G.P. Lepage Floyd R. Newman, G. Hockney and P.B. Mackenzie, Lattice QCD on Small Computers arXiv:hep-lat/9507010v3 18 Sep 1995

96. Holger Bech Nielsen, "Relations derived from minimizing the Higgs field squared (integrated over space-time)" Talk at Rudjer Boskovich Institute: Institut Ruder Boˇskovi´c ZAVOD ZA TEORIJSKU FIZIKU Bijeniˇcka c. 54 Zagreb, Hrvatska

SEMINAR ZAVODA ZA TEORIJSKU FIZIKU (Zajedniˇcki seminari Zavoda za teorijsku fiziku, Zavoda za eksperimentalnu fiziku i Zavoda za teorijsku fiziku PMF-a) Relations derived from minimizing the Higgs field squared (integrated over space-time) Holger Bech Nielsen The Niels Bohr Institute, Copenhagen, Denmark

97. H.B. Nielsen "Complex Action Support from Coincidences of Couplings" arXiv:1103.3812v2 [hep-ph] 26 Mar 2011

98. H.B. Nielsen,arXiv:1006.2455v2 "Remarkable Relation from Minimal Imaginary Action Model " arXiv:1006.2455v2 [physics.gen-ph] 2 Mar 2011

99.] D. Foerster, H. B. Nielsen and M. Ninomiya, Phys. Lett. B 94, 135 (1980).

100. U.-J. Wiese "Ultracold Quantum Gases and Lattice Systems: Quantum Simulation of Lattice Gauge Theories ", arXiv:1305.1602v1 [quant-ph] 7 May 2013

101. H.B. Nielsen, S.E. Rugh and C. Surlykke, Seeking Inspiration from the Standard Model in Order to Go Beyond It, Proc. of Conference held on Korfu (1992)

102. C.D. Froggatt, H.B. Nielsen and Y. Takanishi, Nucl. Phys. B 631, 285 (2002) [arXiv:hep-ph/0201152];
H.B. Nielsen and Y. Takanishi, Phys. Lett. B 543, 249 (2002) [arXiv:hep-ph/0205180].
H.B. Nielsen and C.D. Froggatt, Masses and mixing angles and going be- yond thye Standard Model, Proceedings of the 1st International Workshop on What comes beyond the Standard Model, Bled, July 1998, p. 29, ed. N. Mankoc Borstnik, C.D. Froggatt and H.B. Nielsen DMFA - zaloznistvo, Ljubljana, 1999; hep-ph/9905455
C.D. Froggatt and H.B. Nielsen, Hierarchy of quark masses, Cabibbo angles and CP violation, Nucl. Phys. B147 (1979) 277.
H.B. Nielsen and Y. Takanishi, Neutrino mass matrix in Anti-GUT with see-saw mechanism, Nucl. Phys. B604 (2001) 405.
C.D. Froggatt, M. Gibson and H.B. Nielsen, Neutrino masses and mixing from the AGUT model

103. Ferruccio Feruglio "Fermion masses, critical behavior and universality" JHEP03(2023)236Published for SISSA by Springer Received: March 1, 2023 Accepted: March 13, 2023 Published: March 29, 2023 JHEP03(2023)236

104. H.B. Nielsen* and C.D. Froggatt, "Connecting Insights in Fundamental Physics: Standard Model and Beyond Several degenerate vacua and a model for DarkMatter in the pure Standard Model" Volume 376 - Corfu Summer Institute 2019 "School and Workshops on Elementary Particle Physics and Gravity" (CORFU2019)

105. Keiichi Nagao and Holger Bech Nielsen "Formulation of Complex Action Theory" arXiv:1104.3381v5 [quant-ph] 23 Apr 2012

106. 1) H. B. Nielsen and M. Ninomiya, Int. J. Mod. Phys. A 21 (2006) 5151; arXiv:hep-th/0601048; arXiv:hep-th/0602186; Int. J. Mod. Phys. A 22 (2008) 6227.
2) D. L. Bennett, C. D. Froggatt and H. B. Nielsen, the proceedings of Wendisch-Rietz 1994 -Theory of elementary particles- , p.394-412; the proceedings of Adriatic Meeting on Particle Physics: Perspectives in Particle Physics '94, p.255-279. Talk given by D. L. Bennett, "Who is Afraid of the Past" (A resume of discussions with H. B. Nielsen) at the meeting of the Cross-disciplinary Initiative at NBI on Sep. 8, 1995. D. L. Bennett, arXiv:hep-ph/9607341.
3) H. B. Nielsen and M. Ninomiya, the proceedings of Bled 2006 -What Comes Beyond the Standard Models-, p.87-124, arXiv:hep-ph/0612250.
4) H. B. Nielsen and M. Ninomiya, arXiv:0802.2991 [physics.gen-ph]; Int. J. Mod. Phys. A 23 (2008) 919; Prog. Theor. Phys. 116 (2007) 851.
5) H. B. Nielsen and M. Ninomiya, the proceedings of Bled 2007 -What Comes Beyond the Standard Models- , p.144-185.
6) H. B. Nielsen and M. Ninomiya, arXiv:0910.0359 [hep-ph]; the proceedings of Bled 2010 -What Comes Beyond the Standard Models-, p.138-157.
7) H. B. Nielsen, arXiv:1006.2455 [physic.gen-ph].
8) H. B. Nielsen and M. Ninomiya, arXiv:hep-th/0701018.
9) H. B. Nielsen, arXiv:0911.3859 [gr-qc].
10) H. B. Nielsen, M. S. Mankoc Borstnik, K. Nagao and G. Moultaka, the proceedings of Bled 2010 -What Comes Beyond the Standard Models-, p.211-216.
11) K. Nagao and H. B. Nielsen, Prog. Theor. Phys. 125 No. 3, 633 (2011)

107. Goran Senjanovic and Michael Zantedeschi, "Minimal SU(5) theory on the edge: the importance of being effective" Goran Senjanovic arXiv:2402.19224v1 [hep-ph] 29 Feb 2024

14   Could random dynamics derive quantum mechanics via the weak value?

Holger Bech Nielsen[1][**], Keiichi Nagao[2]

[1] Niels Bohr Institute, University of Copenhagen, Blegdamsvej 17, Copenhagen Ø, Denmark
[2] Faculty of Education, Ibaraki University, Bunkyo 2-1-1, Mito 310-8512 Japan

Abstract. We argue that we could make a scenario of deriving quantum mechanics, as a random dynamics project, in the sense of it being almost unavoidable. The basic idea is based on the weak value formulation.

Povzetek: Avtorja predstavita scenarij, po katerem projekt naključne dinamike neizogibno vodi do kvantne mehanike, če uprabita formulacijo šibke vrednosti.

Keywords: non-Hermitian Hamiltonian, inflation, weak value
PACS: 11.10.Ef, 01.55 +b, 98.80 Qc.

14.1   Introduction

Random dynamics is a projects of calculations in which one or several laws of nature are *not assumed*, but hoped to be *derived*. Indeed it would be very nice if we could realize a theory as fundamental as possible. More fundamental theories should have less conditions supposed at first. For example, we are usually accustomed to using real actions in many kinds of theories, but using real actions by itself means imposing on actions one common restriction that each action has to be real. If we hope for more fundamental theories, we have to be free of such a restriction. Based on such insight, the complex action theory (CAT) was initiated [1]. In the CAT, not only many falsifiable predictions [1–4] but also various topics such as the Higgs mass [5], quantum mechanical philosophy [6–8], some fine-tuning problems [9,10], black holes [11], de Broglie-Bohm particles and a cut-off in loop diagrams [12], the complex coordinate and momentum formalism [13], the momentum relation [14,15], and the harmonic oscillator model [16] were studied. Even if a given action is complex, which means a given Hamiltonian is non-normal[1], we could effectively obtain a Hermitian Hamiltonian after a long time development [22]. This is a very nice property by which the CAT could be viable. Here, to say that more accurately, we note that we need to introduce a modified

---

[**] Speaker at the workshop "What comes beyond the Standard Models" in Bled 2024.
[1] The Hamiltonian H is generically non-normal, so it is not restricted to the class of PT-symmetric non-Hermitian Hamiltonians that were studied in Refs. [17–21].

inner product [22, 23] such that a given non-normal Hamiltonian becomes normal with regard to it. In this article, however, we ignore it for simplicity because we do not need it for the main purpose of this article. We have two types of the CAT. One type is the future-not-included theory, where only a past state $|i(t_i)\rangle$ at the initial time t_i is given. The other type is the future-included theory, where not only a past state $|i(t_i)\rangle$ but also a future state $|f(t_f)\rangle$ at the final time t_f is given. Even though the future-not-included CAT has many intriguing properties [15], it is not favored from a point of view of Feynman path integral [24]. Therefore, we think that the future-included theory is more important than the future-not-included theory.

In the future-included theory[2], we have studied the construction of the so called weak value [26, 27] of an operator O that is the ratio which would look in the Heisenberg representation

$$O_{\text{weak value}}(t) = \frac{\langle f|O(t)|i\rangle}{\langle f|i\rangle}, \tag{14.1}$$

where $|i\rangle$ and $|f\rangle$ are an initial state at the initial time t_i and a final state at the final time t_f, respectively. The weak value has been investigated in the real action theory (RAT). For details, see Ref. [28] and references therein. This is the expression, which we used and suggested as giving an average useful in our complex action theory [1]. Indeed, regarding it as an expectation value leads to obtaining the Heisenberg equation, Ehrenfest's theorem, and a conserved probability current density [29, 30].

Thus the weak value has nice properties, but it has a serious problem: it is generally not real but complex even for Hermitian O, though it has to be real if it is expected to work as an observable. To resolve this problem, in Refs. [31, 32], we proposed a theorem that states that, provided that an operator O is Hermitian, the weak value of O becomes real and time-develops under an effectively obtained Hermitian Hamiltonian for the past and future states selected such that the absolute value of the transition amplitude from the past state to the future state is maximized. We call this way of thinking the maximization principle. We proved this theorem in the case of non-normal Hamiltonians $\hat{H}$ [31] and in the RAT [32]. The maximization principle is reviewed in Refs. [33, 34]. We also found, in the periodic CAT, that a variant type of the maximization principle can select the period [35].

The weak value in the Heisenberg representation (14.1) is expressed better in the Schrödinger representation

$$O_{\text{weak value}}(t) = \frac{\langle f|\exp(-\frac{i}{\hbar}H(t_f - t))O\exp(-\frac{i}{\hbar}H(t - t_i))|i\rangle}{\langle f|\exp(-\frac{i}{\hbar}H(t_f - t_i))|i\rangle}, \tag{14.2}$$

where H is a given non-normal Hamiltonian, and the states $|i(t)\rangle$ and $|f(t)\rangle$ are supposed to time-develop according to the Schrödinger equations $i\hbar\frac{d}{dt}|i(t)\rangle = H|i(t)\rangle$ and $i\hbar\frac{d}{dt}|f(t)\rangle = H^\dagger|f(t)\rangle$, respectively. Rewritten in functional integral

[2] Recently, in the context of quantum gravity, an example of the future-included CAT was derived based on the group field theory coupled to a scalar field, and its possible implication was discussed [25].

formulation, this weak value becomes, say with the understood boundary values at the initial and final states,

$$O_{\text{weak value}}(t) = \frac{\int O(t) \exp(\frac{i}{\hbar}S[\text{hist}])\mathcal{D}\text{hist}}{\int \exp(\frac{i}{\hbar}S[\text{hist}])\mathcal{D}\text{hist}}, \tag{14.3}$$

where hist stands for the history of the fields and $\mathcal{D}$hist is the functional integration measure.

Now the main point of this manuscript is to call attention to that *if we took the action $S[\text{hist}]$ to be purely imaginary, so that $iS[\text{hist}]$ was purely real, then the weak value in the functional integral formulation could be considered an ordinary probability formula for the average of the variable $O(t)$. If we let*

$$\Sigma|O(t) = O'\rangle\langle O(t) = O'| \tag{14.4}$$

be the sum over a set of products of eigenstates with the eigenvalues of $O(t)$ being O', then this operator would be a projection operator on the eigenstates of $O(t)$. For example, in the Heisenberg picture, the "probability" for the eigenvalue of $O(t)$ being O', $P_{O(t)=O'}$, would be

$$P_{O(t)=O'} = \Sigma\langle f|O(t) = O'\rangle\langle O(t) = O'|i\rangle. \tag{14.5}$$

For the weak value being a good replacement for the usual quantum mechanics average of an operator formula, these weights should be positive or zero. We have not yet shown that, but we made some theorems about reality [31,32], which we explained above. To deduce that this distribution should at least be real is not obvious at all to start with. If we took i to be real as our playing assumption which is of course not true, then we could ensure the reality easily for any Hermitian O'. So, in this absurd case, the weak value would look like a probability formula, except that the probabilities could be negative. But the crux of the matter is that *the weak value formally looks like a probability distribution.* So, if we achieved some speculative model providing us some probability distribution - from some graph theory or whatever -, we could claim that now we want to write that as a weak value theory formally, and then we could play in the CAT to describe our world under the wild assumption that S is purely imaginary. We consider some system of dynamical variables such as fields that makes up a complete set of variables, and have some theory for their distribution. Even though our theory has no quantum mechanics, we can just declare the exponentiated purely imaginary action $\exp(\frac{i}{\hbar}S[\text{hist}])$ to give distribution in the quantum mechanics lacking theory we start with. So, *if one could invent a model-speculation that could provide complex numbers to come into the probability, then we might be able to derive the weak value quantum theory.* Of course, it looks too wild to hope to find such a scenario. But, if one could, it would be using the weak value to "derive" quantum mechanics, and one needs strongly some derivation from very little of quantum mechanics in random dynamics.

This manuscript is organized as follows. In section 2, we explain some mild assumptions that we make in a general model based on the random dynamics, and define a specific "action" $S_P[q]$. In section 3 we give a phenomenological example

of the "action" $S_P[q]$ and argue that a favorable path could fit the cosmology. In section 4 we introduce a beating "clock" in a subsystem, and argue that, by the beating "clock", a kind of interference could be caused in the other subsystem. In section 5, after briefly explaining the CAT and the weak value, we argue that the effect of the "clock" could give us the weak value complex path integral. In addition, we discuss how we could add a phase to the logarithm of the action so that our general formalism matches the weak value expression. Section 6 is devoted to discussion.

14.2   Formulation of general model via random dynamics

We start from the formulation of general model via random dynamics. We do not put in say quantum mechanics, but do not exclude it either. Such a formulation is a rather empty framework as described below:

- **Variables and time**
  A lot of dynamical variables are described for short as just one

$$q = (q_1, q_2, ..., q_N),\qquad(14.6)$$

  which is taken as functions of time

$$q(t) = (q_1(t), q_2(t), ..., q_N(t)).\qquad(14.7)$$

  Here N may be infinite or finite or even the q's could be fields. N could be Card($\mathbb{R}$).

- **Probability distribution for paths**
  We assume that details of the theory should give us a functional probability distribution P on the space of all histories $q : \{\text{time}\} \rightarrow \mathbb{R}^N$ thinkable:

$$P[q] = \text{probability distribution on sets of functions } q.\qquad(14.8)$$

$P[q]$ gives probabilities for paths q.

Hoping to obtain quantum mechanics, we make very mild assumptions:

0.) We shall make very mild assumptions, mostly mathematically almost always assumed by physicists. The assumptions are about the "distributional" P such as continuity, differentiability, Taylor expandability, and that sort of things.

1.) In addition we make a little less general assumption: P is exponentially strongly varying, as if of the form

$$P[q] = \exp\left(\frac{1}{\hbar}S_P[q]\right)\qquad(14.9)$$

with $\frac{1}{\hbar} \sim$ very large.
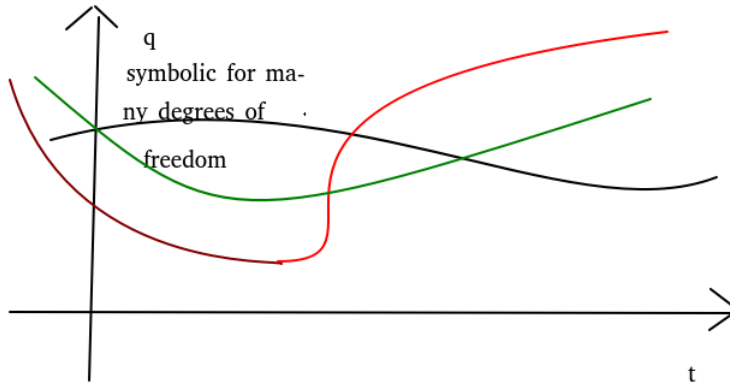
Fig. 14.1: Various paths

2.) Furthermore, we make a mild assumption: There exists weak "interaction" with roughly periodically moving "clock".

Even almost empty assumptions and formulations may have drastic implications. Our formulation is so general that it also would accept a theory in which one has laws for what shall happen at some moment of time. It allows the future to be guiding for what happens or the past, as it seems to be in reality. If we wish, we could impose that every initial conditions would be equally likely; but in reality we have some ideas about the initial state (big bang, inflation, etc.). But making $P[q]$ or $\frac{1}{\hbar}S_P[q] = \ln(P[q])$ some nice smooth function might guide us towards getting such "initial state predictions" not coming from a single moment but being some compromise coming in a bit at all times.

14.3   Phenomenological example of the specific form of S_P

14.3.1   Our formalism determines a favored path

In functional integrals for quantum mechanics we have an action in the exponent

$$\text{"Functional integral"} = \int \exp\left(\frac{i}{\hbar}S[q]\right)\mathcal{D}q. \tag{14.10}$$

The introduction of S_P in Eq.(14.9) tells us that it is not S_P but $-iS_P$ that corresponds to an action $S[q]$. We can put in our own favorite action for $-iS_P[q] = S[q]$ and get our own equations of motion, but let us consider some system of particles

as a typical example of the specific form of S_P:

$$-iS_P[q] = \int L(\dot{q}(t), q(t))dt$$
$$= \int (K(\dot{q}) - V(q(t)))dt, \qquad (14.11)$$

where $K(\dot{q})$ and $V(q(t))$ could be usual kinetic and potential energies respectively, say e.g.,

$$K(\dot{q}) = \sum_i \frac{1}{2}m_i\dot{q}_i^2, \qquad (14.12)$$

$$V(q(t)) = \text{"potential"(that could have peaks and valleys etc.).} \qquad (14.13)$$

When one seeks the path (= history) q_{max} with the highest probability $P[q_{max}]$, one gets that the variation for it there, i.e., the functional derivative of the action, is zero, and derives an equation of motion (classically at least). We note that an overall sign or a constant multiplying the whole action does not change the equation of motion. But the relative weight of different paths (= histories) is violently influenced. Thus, our formalism determines a favored path to be realized.

14.3.2   Does the favorite path fit the cosmology?

For simplicity, we restrict ourselves to the uppermost V-potential favored case. Then the best path stands on the highest mountain. But, if there is a so broad distribution of path around the one with very highest $S_P[q]$ that they cannot all just stand on the peak, then there will be a flow down. Among the flow down paths the most favorable one for getting high S_P would go up to another peak quickly.
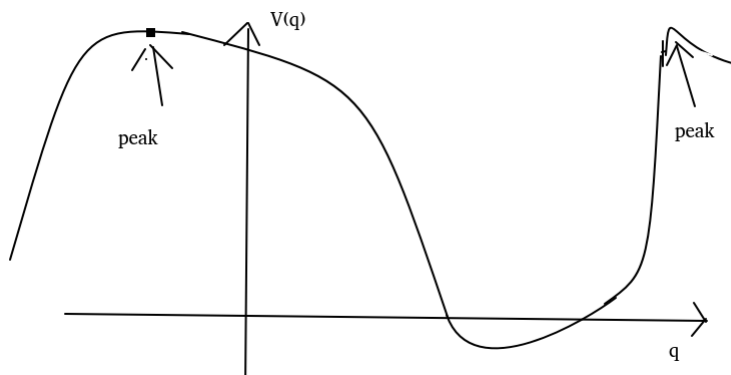
Fig. 14.2: Inflaton potential with two peaks

Let us consider the behavior of the inflaton field in the inflation universe model by supposing a generic potential as drawn in Fig.14.2 for the inflaton potential. We discuss it as follows:

- Waiting on an almost highest peak till it falls down by accident
  The inflaton field is standing on a peak in the potential so long that the physicists consider the famous long-staying problem: "the slow roll problem".
- It seeks quickly to find up to another similar peak to convert kinetic energy to potential energy.
  The Universe did after inflation expand with an enormous Hubble-Lemaitre constant, meaning that it brought quickly massive or massless particles away from each other, so that, in Newtonian gravity say, the gravitational potential energy should begin to raise as quickly as possible.
- It should stay again long on the next peak.
  The Hubble-Lemaitre has slowed down and the time scale of the development is now huge, compared to the one in the beginning (just after inflation stopped).

We speculate that the above picture could be one of solutions to the slow roll problem. See also Ref. [36].

14.4   Introducing a beating "clock"

In this section we discuss mainly how interference, which is one of the important properties of quantum mechanics, could be realized by considering a beating "clock" in our formalism.

14.4.1   A beating "clock" and interference

We begin with considering a couple of important properties of quantum mechanics. They are summarized as follows:

- The system/ the particle can be several places at a time.
  We already have that in our formalism from the point of view of the path integral.
- When it can go two (or more) ways, the probability is not just additive, but depending on each phase, it could be bigger or smaller. This is an interference.
  We obtain a kind of interferece by speculating a "clock" interacting with the system.

In the following we discuss how quantum interference is realized in our formalism. Sometimes there are deviations from determinism, i.e., an optimal path could be separated into two paths as drawn in Fig.14.3. In addition, even if there is a beating "clock" on a path and it is disconnected as drawn in Fig.14.4, it does not matter. But, if the "clock" goes faster on one of the separated tracks than on the other one, as drawn in Fig.14.5, what happens? Really, there could be
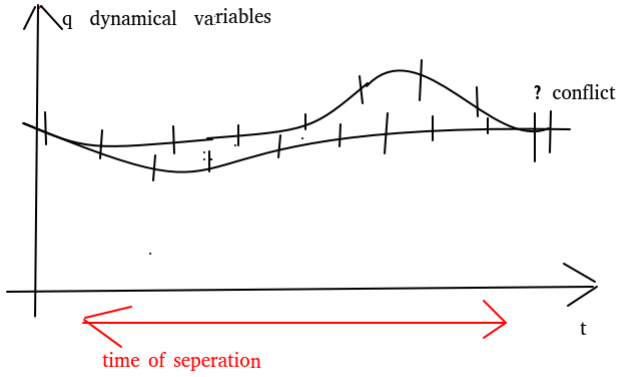
Fig. 14.3: Separated paths
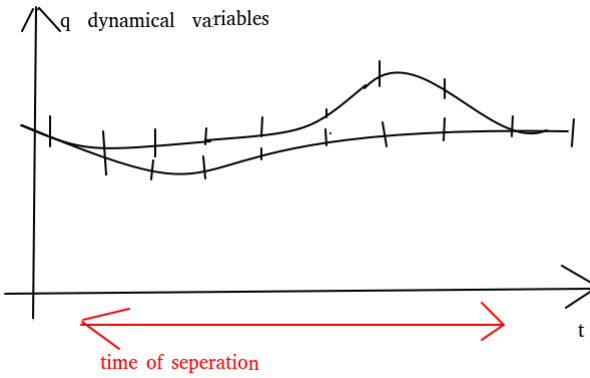
Fig. 14.4: A "clock" beating disconnected
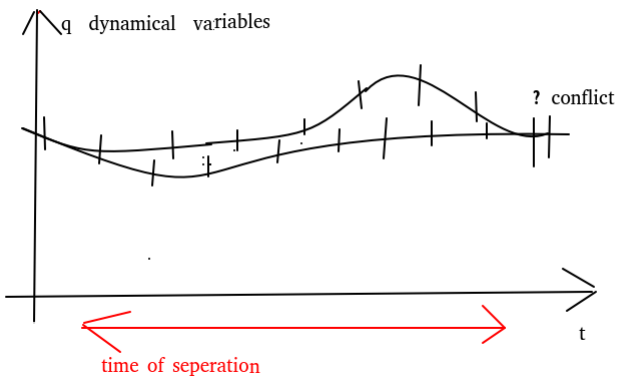
Fig. 14.5: Clocks beat differently on paths

no separation then. Next, what happens in case of different beating rates in the two separate ways? Remembering that the deterministic (classical) tracks really represent narrow bundles of tracks - narrow because the coefficient $\frac{1}{\hbar}$ is very large -, one must imagine that small deviations from the best "classical" path just have a lower probability than the best classical track itself. So, at least small problems of the "clock" not beating consistently would lead to such probability decrease. But, if the difference of the times on the two tracks is just a shift by an integer number times the beating period, there would be no decrease. This sounds like interference. We expect that it gives an imaginary term in the exponent of the functional integral, even though it might look tricky. It would be interesting to calculate the suppression of probabilities from more or less consistent matching of the "clock" beating on various tracks.

14.4.2   Local version of the "clock" and a charged particle

To see that we hopefully are on the right track towards a realistic model, we could make the "clock" be replaced by a separate little clock in each point of space. The model with only *one* of these "clock"s would not be truly local, so having clocks distributed all over space would be better from such a principle of locality. We have had in mind that these "clock"s run so fast that we shall not be able to consider it for us achievable knowledge where they are in their cyclic running. Now let us imagine a pattern of "clock"s all over in space, and for simplicity, a system just with the degrees of freedom of a non-relativistic particle. If we say that we only have access to the difference in progression along different paths in space time between the same two events but not to how far the different clocks have reached at given moments, we have strong similarity to the knowledge of electromagnetic fields, while not knowing the gauge. In other words we propose to look at a system of infinitely many "clocks" (one at every space point) developing a little bit differently here and there, as representing a possibility of different behaviors just in correspondence with electromagnetic fields in space time.
It is not difficult to prove that, if the different phase deviations for the many different loops of curves in Minkowski space shall be consistent in the sense that, when one loop is composable from two, of course the phase deviation for that loop must be the sum of those of the two components, then we can find electromagnetic fields describing the phases for the various loops. The simplest realization of the just mentioned idea would be to simply call the rate of running of the "clock" $\text{clock}(x)$ at position x for $A_0(x)$, meaning identifying it with the electric potential. Then we could look at a gauge transformation in a purely electrostatic theory which is an addition of the same constant to $A_0(x)$ at every point x in space, as a general increase in the running speeds of the small clocks. Well, the idea we seek here to put forward is that there is hope for getting the mysterious i in quantum mechanics connected with clocks that really are connected with the electric properties of the particle. But if so, we might think that, if we had chargeless particles, which would typically be Majorana particles, then we should have real wave function for them. That is indeed true that single particle wave functions for Majorana fermions are real.

14.5   The weak value and our general formalism

Our formalism with $P[q] = \exp(\frac{1}{\hbar} S_P[q])$ was originally inspired from and also is most easy connected to the formalism of quantum mechanics by means of the weak value:

$$O_{\text{weak value}}(t) = \frac{\langle f|O(t)|i\rangle}{\langle f|i\rangle} \quad \text{(Heisenberg representation)} \tag{14.14}$$

where one is so to speak to know or put in some information on the initial state $|i\rangle$ given at the initial time t_i and on the final state $|f\rangle$ given at the final time t_f. O is an operator, say Hermitian. In the Schrödinger representation, the weak value is expressed as

$$O_{\text{weak value}}(t) = \frac{\langle f| \exp(-\frac{i}{\hbar}H(t_f - t))O \exp(-\frac{i}{\hbar}H(t - t_i))|i\rangle}{\langle f| \exp(-\frac{i}{\hbar}H(t_f - t_i))|i\rangle} \tag{14.15}$$

where H is a given Hamiltonian, and the states $|i\rangle$ and $|f\rangle$ are supposed to time-develop according to the Schrödinger equation for a state $|\psi\rangle$: $i\hbar\frac{d}{dt}|\psi\rangle = H|\psi\rangle$. Weak value is the most useful when we have complex action and in principle know even the future. We worked on such complex action theories, and the weak value formalism seemed very natural for the hypothesis we worked on that the action was *complex*. Indeed, in the Wenzel-Dirac-Feynman functional integral expression, the weak value of $q_i(t)$ is symbolically expressed as

$$q_{i \text{ weak value}}(t) = \frac{\int \exp(\frac{i}{\hbar}S[q]) * q_i(t)\mathcal{D}q}{\int \exp(\frac{i}{\hbar}S[q])\mathcal{D}q}, \tag{14.16}$$

which is much simpler than the expression of the usual expectation value of $q_i(t)$. Our great result was that we would get similar equations of motion as for real action, but only in addition to getting some predictions about the "initial conditions". We could say that complex action unites equations of motion with "initial conditions".

14.5.1   Our maximizing overlap assumption and classical interpretation

The choice of the final state $|f\rangle$ and initial state $|i\rangle$ will in most cases with complex action be determined by requiring that the absolute value of the transition amplitude from the initial state to the final state is maximized:

$$|\langle f|i\rangle| \text{ is maximal.} \quad \text{(Heisenberg)} \tag{14.17}$$

$$\left|\langle f| \exp\left(-\frac{i}{\hbar}H(t_f - t_i)\right)|i\rangle\right| \text{ is maximal.} \quad \text{(Schrödinger)} \tag{14.18}$$

In real action case we get from this (14.17) still an undetermined set of states but we get

$$|\langle f|i\rangle|_{max} = 1 \text{ for usual real action case.}$$
$$\text{(Heisenberg)}$$

$$\left|\langle f| \exp\left(-\frac{i}{\hbar}H(t_f - t_i)\right)|i\rangle\right|_{max} = 1 \text{ for usual real action case.}$$
$$\text{(Schrödinger).}$$

One would wonder how we can think classically in complex action and weak value. It is summarized as follows:

- With complex action, typically all that happens in universe at all times gets predestined (because it is a theory also for the "initial conditions").
- In the large $\frac{1}{\hbar}$ approximation only one or very few classical paths are realized, and the one with highest probability wins.
- Paths have a few times where they split up into two or more.
- If we arrange by the "clock" story to make "interference", it can modify the total probability of the path with the splitting that has the "interference" correction.

- Such "interference" corrections may cause an otherwise winning path to get beaten by a slightly less probable competing path. (presumably we shall imagine a sample of near competitors clear to take over if a path gets too much destructive interference.)
- For a dominant path, i.e., in the classical approximation, the weak value for an operator is simply the value of the corresponding dynamical variable at the time t.
- So we can look at the weak value as just a way to extract the classical path, which is determined by our imaginary part of the action.
- Different (bunches of) paths have different probabilities; a path with highest probability is the likeliest to be realized as our history.
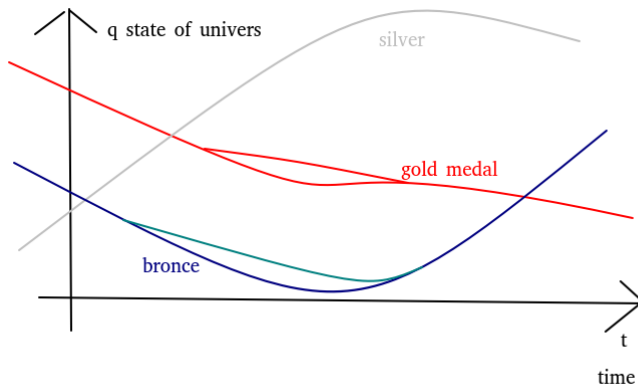
Fig. 14.6: Competing paths

14.5.2 Interpreting the effect of the "clock" as giving us the weak value with complex path integral

Now we want to formulate the result of our general formulation including the "clock" to lead to that expectation value of one of the q variables or a combination

of them being the weak value

$$q_{i \text{ weak value}}(t) = \langle q_i(t) \rangle = \frac{\int \exp(\frac{i}{\hbar} S[q]) * q_i(t) \mathcal{D}q}{\int \exp(\frac{i}{\hbar} S[q]) \mathcal{D}q}. \tag{14.19}$$

If the probability density $P[q]$ contains much information on the initial and final states, it will not be so serious to ignore the boundary conditions, because this information will then be transfered into $S[q]$ used in this formula (14.16).

We compare our general formulation with the weak value in quantum mechanics. An average of one of the q-variables $q_i(t)$ at time t is expressed as

$$q_i(t)_{\text{weak value}} = \langle q_i(t) \rangle = \frac{\int \exp(\frac{i}{\hbar} S[q]) * q_i(t) \mathcal{D}q}{\int \exp(\frac{i}{\hbar} S[q]) \mathcal{D}q}, \tag{14.20}$$

$$\langle q_i(t) \rangle_{\text{our formalism}} = \frac{\int P[q] q_i(t) \mathcal{D}q}{\int P[q] \mathcal{D}q} \tag{14.21}$$

where the denominator $\int P[q] \mathcal{D}q$ is just a normalization. This will not be needed if $P[q]$ is already normalized.

We see an important difference: the weak value consists of *complex* integrals, while in our formalism everything is *real* numbers. The similarity gets even bigger formally when we remember that we want to assume as a helping assumption that $S_P[q]$ is supposed rather smooth, so that the form

$$P[q] = \exp\left(\frac{1}{\hbar} S_P[q]\right) \tag{14.22}$$

is called for. Remember also that q stands for a set of functions, so it really means what we would call a track, a path, or a history of the universe. But, to make the agreement between the two expressions, we would need to provide our expression with an artificially invented phase.

Remembering the q variables are supposed real by themselves, we see that, if only one history or track q dominates, then weak value becomes real for the different q_i which are assumed real/ Hermitian as operators, because, for a single dominating path, there is a reality theorem for the weak value. Even if we have a history with some separation from time to time, but we ask for the weak value for $q_i(t)$ at a time outside the separation period, then the weak value for this $q_i(t)$ will be real. Thus the weak value gives perfect description in classical case, meaning one track or history dominates. If physicists make double slit experiments where a particle goes through two slits simultaneously, the weak value still gives averages, but now the average will usually be *complex*, as we know that asking a stupid question like "Through which slit did the particle go?" in an interference experiment gives a stupid / complex answer. On the other hand, our formalism - before we modify it very artificially - cannot give complex answer, because it is made so, as if it never heard about complex numbers. Therefore, our formalism gives a priori real numbers even for the average while the particle is passing through the double slit experiment.
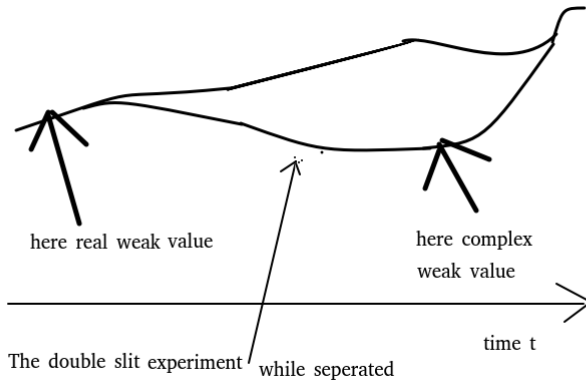
Fig. 14.7: Double slit experiment paths

14.5.3   Adding a phase to $P(q)$ in our formalism

To have our general formalism match the weak value, we have to provide our expression with an artificially invented phase, i.e., we need to add a phase formally to our $P[q]$ to make it look like the integrand in the Feynman-Dirac-Wentzel functional integral. For this purpose, we define a "clock" delay ratio for any path/history q at any moment of time t:

$$\delta[q, t] = \text{"time delay ratio in period"}$$
$$= \frac{c_{\text{standard}}[q, t] - c[q, t]}{\text{period}}, \tag{14.23}$$

where[3]

$$c_{\text{standard}}[q, t] = t, \tag{14.24}$$
$$c[q, t] = \text{the stand of the "clock" on path q at time t.} \tag{14.25}$$

Then we are first suggested to put

$$iS[q] = S_P[q] + i\delta[q, t]. \tag{14.26}$$

Remember that $S_p[q]$ is the logarithm of the probability in our model formulation and thus of course real, while we like the complex action theory (CAT), in which $S[q]$ is complex - while in usual theory real -. By putting in the real $\delta[q, t]$ with an i, we obtain the right hand side of (14.26) being complex with both a real and an imaginary part.

We imagine the "clock" to have very short "period", so the time of the clock is not so important if we use some average period or one about the time t. In fact, we expect the probability for a path with a split time, as represented by a double slit experiment, to be somewhat reduced, because of the interaction of the other degrees of freedom with the "clock" by means of the action $S_P[q]$ that is purely

---

[3] δ and the c's are functionals of q, but functions of t.

imaginary from a usual point of view in our formulation, i.e., because of the not matching of the "clock" and the rest of the system. We hope to have our model give quantum mechanics such that this reduction turns out to be equal to the effect of having the phase addition as we suggested. So, in order not to have it doubled, we improve our suggestion to

$$iS[q] = S_P[q]|_{\text{with "clock" removed}} + i\delta[q, t]. \tag{14.27}$$

Here $S_P[q]_{\text{with "clock" removed}}$ is a modified $S_P[q]$ in our model where we hope that the "clock" is removed, and so only the rest is left.

We hope to calculate that removing "clock" and adding the phase just cancel each other. For two numerically equally high probability paths during the separation seems likely by the probability proportional to $|1 + e^{i\Delta}|^2 \propto \cos^2(\frac{1}{2}\Delta)$, where Δ is an average of $\delta[q, t]$ over separation. We will argue for that, at least being right in the small deviation between the delay in the two separate paths case.

14.6   Discussion

We have put up a very general formalism, in which we may reproduce rather usual classical actions although it comes with the i missing relative to the usual functional integral. But for the action in classical physics an overall sign as e.g. an i does not matter. In the very general model just having probability density $P[q]$ as a functional that we can adjust phenomenologically, describing the probability density for all histories a priori still to be evaluated by the Taylor expansion and the like, we have one property of quantum mechanics already:

- The system/the world can go through different paths, so the state at a moment t is not quite unique.
- Only after assuming the exponent $S_P[q]$, when $P[q] = \exp(\frac{1}{\hbar}S_P[q])$ is very large, we obtain classical physics: only one path is realized with high probability.

The weak value for a quantity (= dynamical variable) and the expectation value in our general formalism with $P[q] = \exp(\frac{1}{\hbar}S_P[q])$ only deviate by an i, as seen by comparing the weak value expression and our expectation value one:

$$\langle O(q(t)) \rangle = \frac{\int \exp(\frac{1}{\hbar}S_P[q])O(q(t))\mathcal{D}q}{\int \exp(\frac{1}{\hbar}S_P[q])\mathcal{D}q} \quad \text{(Our average)}, \tag{14.28}$$

$$\langle O(q(t)) \rangle_{\text{weak value}} = \frac{\int \exp(\frac{i}{\hbar}S[q])O(q(t))\mathcal{D}q}{\int \exp(\frac{i}{\hbar}S[q])\mathcal{D}q} \quad \text{(The weak value)}, \tag{14.29}$$

provided we identify the "actions" as follows:

$$S_P = iS. \tag{14.30}$$

We note that classical equations of motion are not sensitive to this i. The classical approximation or equations of motions for both of them become the same in spite of the i separating them. However, our general formalism has a very strong - and not shared by the weak value with the i - prediction about the *initial state conditions.* The features being favored by our formalism may be matched with the very strongest features of cosmology: slow inflation, huge expansion in the beginning after the "reheating", and much slower expansion in the long run. But we have the problem that our model tends to make a decision about the initial conditions. We proposed a way to - by not quite finished calculations - obtain a relation between our general formulation and the weak value formulation of quantum mechanics, especially in the case of an action being complex, i.e., our complex action theory. In the short run, we could easily arrange by choosing S_P that one would not notice in short terms the tendency of the model to give information on the initial conditions (and possibly also on the future being selected). But the interference needed an extra story: the "clock". We shall hopefully prove that with this"clock" we can obtain the usual quantum mechanics with its mysterious complex numbers. The density operator that we introduced in the future-included CAT [37] would be useful for the study. As a by-product - but may be most interesting - we found that the path favored in probability had some similarities in general properties of escaping as fast as possible not being at the maximal potential energy. This could be interpreted as a model behind slow roll and fast Lemaitre-Hubble expansion in the beginning.

Acknowledgments

References

1. H. B. Nielsen and M. Ninomiya, Proc. Bled 2006: What Comes Beyond the Standard Models, p.87 (2006) [arXiv:hep-ph/0612250].
2. H. B. Nielsen and M. Ninomiya, Int. J. Mod. Phys. A **23**, 919 (2008).
3. H. B. Nielsen and M. Ninomiya, Int. J. Mod. Phys. A **24**, 3945 (2009).
4. H. B. Nielsen and M. Ninomiya, Prog. Theor. Phys. **116**, 851 (2007).
5. H. B. Nielsen and M. Ninomiya, Proc. Bled 2007: What Comes Beyond the Standard Models, p.144 (2007) [arXiv:0711.3080 [hep-ph]].
6. H. B. Nielsen and M. Ninomiya, arXiv:0910.0359 [hep-ph].
7. H. B. Nielsen, Found. Phys. **41**, 608 (2011) [arXiv:0911.4005[quant-ph]].
8. H. B. Nielsen and M. Ninomiya, Proc. Bled 2010: What Comes Beyond the Standard Models, p.138 (2010) [arXiv:1008.0464 [physics.gen-ph]].

9. H. B. Nielsen, arXiv:1006.2455 [physic.gen-ph].
10. H. B. Nielsen and M. Ninomiya, arXiv:hep-th/0701018.
11. H. B. Nielsen, Proc. Black Holes in General Relativity and String Theory, p.25 (2008) [arXiv:0911.3859 [gr-qc]].
12. H. B. Nielsen, M. S. Mankoc Borstnik, K. Nagao, and G. Moultaka, Proc. Bled 2010: What Comes Beyond the Standard Models, p.211 (2010) [arXiv:1012.0224 [hep-ph]].
13. K. Nagao and H. B. Nielsen, Prog. Theor. Phys. **126**, 1021 (2011); **127**, 1131 (2012) [erratum].
14. K. Nagao and H. B. Nielsen, Int. J. Mod. Phys. A**27**, 1250076 (2012); **32**, 1792003 (2017)[erratum].
15. K. Nagao and H. B. Nielsen, Prog. Theor. Exp. Phys. **2013**, 073A03 (2013); **2018**, 029201 (2018)[erratum].
16. K. Nagao and H. B. Nielsen, Prog. Theor. Exp. Phys. **2019**, 073B01 (2019).
17. C. M. Bender and S. Boettcher, Phys. Rev. Lett. **80**, 5243 (1998).
18. C. M. Bender, S. Boettcher, and P. Meisinger, J. Math. Phys. **40**, 2201 (1999).
19. A. Mostafazadeh, J. Math. Phys. **43**, 3944 (2002).
20. A. Mostafazadeh, J. Math. Phys. **44**, 974 (2003).
21. C. M. Bender and P. D. Mannheim, Phys. Rev. D **84**, 105038 (2011).
22. K. Nagao and H. B. Nielsen, Prog. Theor. Phys. **125**, 633 (2011).
23. F. G. Scholtz, H. B. Geyer, and F. J. W. Hahne, Ann. Phys. **213**, 74 (1992).
24. K. Nagao and H. B. Nielsen, Prog. Theor. Exp. Phys. **2017**, 111B01 (2017).
25. J. Liu, S. Alexander, A. Marciano and R. Pasechnik, JHEP **07**, 219 (2024).
26. Y. Aharonov, D. Z. Albert, and L. Vaidman, Phys. Rev. Lett. **60**, 1351 (1988).
27. Y. Aharonov and L. Vaidman J. Phys. A. Math. Gen. **24**, 2315 (1991).
28. Y. Aharonov, S. Popescu, and J. Tollaksen, Phys. Today **63**, 27 (2010).
29. K. Nagao and H. B. Nielsen, Prog. Theor. Exp. Phys. **2013**, 023B04 (2013); **2018**, 039201 (2018)[erratum].
30. K. Nagao and H. B. Nielsen, Proc. Bled 2012: What Comes Beyond the Standard Models, p.86 (2012) [arXiv:1211.7269 [quant-ph]].
31. K. Nagao and H. B. Nielsen, Prog. Theor. Exp. Phys. **2015**, 051B01 (2015).
32. K. Nagao and H. B. Nielsen, Prog. Theor. Exp. Phys. **2017**, 081B01 (2017).
33. K. Nagao and H. B. Nielsen, Fundamentals of Quantum Complex Action Theory (Lambert, Saarbrücken, 2017).
34. K. Nagao and H. B. Nielsen, Proc. Bled 2017: What Comes Beyond the Standard Models, p.121 (2017) [arXiv:1710.02071 [quant-ph]].
35. K. Nagao and H. B. Nielsen, Prog. Theor. Exp. Phys. **2022**, 091B01 (2022).
36. H. B. Nielsen, Entropy **26**, no.10, 830 (2024).
37. K. Nagao and H. B. Nielsen, Prog. Theor. Exp. Phys. **2023**, 031B01 (2023).

15   Exact expressions for the renormalization constants in the MS-like schemes

K.V. Stepanyantz

Moscow State University, 119991, Moscow, Russia

Abstract. We briefly review how it is possible to derive some exact expressions for the renormalization constants for the MS-like renormalization prescriptions using the arguments based on the renormalization group. These expressions are obtained for a version of the dimensional technique in which the dimensionful parameter Λ differs from the renormalization scale μ. They encode the equations relating the coefficients at higher ε-poles, powers of $\ln \Lambda/\mu$, and mixed terms of the structure $\varepsilon^{-q} \ln^p \Lambda/\mu$ to the coefficients of the renormalization group functions (i.e. of the β-function and the anomalous dimension). The general results are verified by some multiloop calculations.

Povzetek: Avtor na kratko predstavi izpeljavo nekaterih natančnih izrazov za konstante renormalizacije, pri katerih lahko uporabi argumente, ki temeljijo na renormalizacijski grupi, kadar se dimenzionalni parameter Λ razlikuje od renormalizacijske skale μ. Izrazi vsebujejo enačbe, ki povezujejo koeficiente višjih polov ε, potence $\ln(\Lambda/\mu)$ in izraze oblike $\varepsilon^{-q}(\ln^p(\Lambda/\mu))$ s koeficienti renormalizacijskih grupnih funkcij (to je funkcij β in anomalne dimenzije). Splošne izraze preverja z izrazi, ki jih dobi s perturbacijskimi metodami višjih redov.

15.1   Introduction

Quantum corrections are very important for understanding nature. For example, a very precise agreement of the electron anomalous magnetic moment value with the theoretical prediction is one of the most convincing arguments in favour of the fact that nature is described by quantum field theory [1]. The unification of running couplings is an indirect evidence in favour of supersymmetry and Grand Unification [2] obtained by combining the experimental values of the coupling constants and theoretical calculations of quantum corrections [3–5].

In most quantum field theory models quantum corrections diverge in the ultraviolet (UV) region, so that a theory for which they are investigated should be properly regularized [6]. The most popular method for this purpose is dimensional regularization [7–10] when a theory is considered in the non-integer dimension $D \equiv 4 - \varepsilon$. In this case divergences appear as ε-poles. These ε-poles should removed by the renormalization of some parameters, e.g., couplings, masses, fields, etc. This is possible in the renormalizable theories.

However, in the supersymmetric case the dimensional regularization is not convenient because supersymmetry is explicitly broken [11]. That is why for supersymmetric theories it is more convenient to use a modification of this technique called

dimensional reduction [12]. Nevertheless, sometimes it is better to use the regulations of the cutoff type, e.g., the higher covariant derivative regularization [13–15]. In this case (logarithmic) divergences are given by powers of $\ln \Lambda/\mu$, where Λ is a dimensionful regularization parameter, and μ is the renormalization point. The superfield formulation of the higher covariant derivative method [16,17] is especially useful for supersymmetric theories, because it does not break supersymmetry and reveals some interesting features of quantum corrections [18]. For instance, the exact Novikov, Shifman, Vainshtein, and Zakharov (NSVZ) β-function [19–22] is naturally obtained with this regularization. According to [23–25], the NSVZ β-function is valid in all loops if a supersymmetric theory is regularized by Higher covariant Derivatives and renormalization is made by Minimal Subtraction of Logarithms (the so-called HD+MSL scheme), see [26] and references therein. In the Abelian case this result was derived earlier in [27,28]. Note that in the $\overline{\text{DR}}$-scheme the NSVZ equation is not valid starting from the approximation where the scheme dependence becomes essential [29–31]. However, in this case the NSVZ relation can be restored in each order of the perturbation theory with the help of a finite renormalization of the coupling constant, because some scheme-independent consequences of the NSVZ equation are satisfied [32,33]. This implies that the NSVZ equation is valid only for a special class of renormalization prescriptions [34], some of them being naturally constructed with the help of the higher covariant derivative regularization.

Note that the ε-poles in the renormalization constants obtained with the help of the dimensional technique are analogs of $\ln \Lambda/\mu$ in the corresponding expressions for the renormalization constants derived using the regularizations of the cutoff type. The relation between the simple poles and the first power of this logarithm has a very simple form, e.g.,

$$\ln Z_\alpha = -\sum_{L=1}^{\infty} \alpha^L \beta_L \left(\frac{1}{L\varepsilon} + \ln \frac{\Lambda}{\mu} \right) + \text{higher poles and logarithms,} \qquad (15.1)$$

where L is a number of loops [35]. However, the coefficients at higher poles and logarithms are related in a rather nontrivial way and no simple relations are seen at the first sight. In this paper the corresponding relations will be constructed in all orders. For this purpose we will use the arguments based on the structure of a group formed by finite renormalizations.

15.2   The group formed by finite renormalizations

In renormalizable quantum field theory models UV divergences can be removed by the renormalization, e.g.,

$$\alpha_0 = \alpha_0(\alpha(\mu), \ln \Lambda/\mu); \qquad \varphi = Z(\alpha, \ln \Lambda/\mu)\varphi_R, \qquad (15.2)$$

where μ is a renormalization point and Λ is the dimensionful parameter introduced by a regularization. However, the way of making the renormalization is not uniquely defined. In general, various renormalization prescriptions are related by the finite renormalizations [36–38] of the form

$$\alpha' = \alpha'(\alpha); \qquad Z'(\alpha', \ln\Lambda/\mu) = z(\alpha)Z(\alpha, \ln\Lambda/\mu). \tag{15.3}$$

Note that the renormalization group functions (RGFs) nontrivially transform under these finite renormalizations [39]. Namely, two first coefficients of the gauge β-function and the first coefficient of the anomalous dimension are scheme independent, while the other coefficients depend on a specific choice of the renormalization prescription.

It is easy to see that finite renormalizations (15.3) form an infinite dimensional Lie group. Following [40], to describe it, we first construct its algebra using the exponential map [41]. For this purpose we recall that if $\mathcal{G}$ is a Lie group, then in a certain vicinity of the identity element 1 it is possible to present the group element $\hat{\omega} \in \mathcal{G}$ as the exponential of the corresponding Lie algebra $\mathcal{A}$ element $\hat{a} \in \mathcal{A}$, $\hat{\omega} = \exp(\hat{a})$. Therefore, it is expedient to consider an infinitesimal finite renormalization of the coupling constant $\alpha \to \alpha'(\alpha)$ and present it as the series

$$\delta\alpha = -\sum_{n=1}^{\infty} a_n \alpha^{n+1} \equiv \sum_{n=1}^{\infty} a_n \hat{L}_n \alpha \equiv \hat{a}\alpha, \tag{15.4}$$

where a_n are arbitrary real parameters. The operators $\hat{L}_n$ with $n \geq 1$ are the generators of the group of finite renormalizations. In the explicit form these generators (acting on an arbitrary function of α) are written as

$$\hat{L}_n = -\alpha^{n+1} \frac{d}{d\alpha} \tag{15.5}$$

and satisfy the commutation relations of the Witt algebra[1]

$$[\hat{L}_n, \hat{L}_m] = (n - m)\hat{L}_{n+m}. \tag{15.6}$$

However, in the Witt algebra n is an arbitrary integer, while in the case under consideration $n \geq 1$ due to the use of the perturbation theory. Therefore, the Lie algebra of the group formed by finite renormalizations (for the renormalization of charge) is a subalgebra of the Witt algebra spanned by $\hat{L}_n$ with $n \geq 1$.

The exponential map allows obtaining the non-infinitesimal transformations,

$$\alpha' = \hat{\omega}\alpha = \exp\Big(\sum_{n=1}^{\infty} a_n \hat{L}_n\Big)\alpha = \exp\Big(-\sum_{n=1}^{\infty} a_n \alpha^{n+1} \frac{d}{d\alpha}\Big)\alpha. \tag{15.7}$$

The explicit form of these transformations in the lowest approximations can be found in [40].

The finite renormalizations that include the renormalization of the matter fields and masses can be considered similarly. According to (15.3), they are determined by the functions $\alpha'(\alpha)$ and $z(\alpha)$. For the infinitesimal finite renormalizations $z(\alpha)$ can be presented in the form

---

[1] The relation between the renormalization group and the Witt algebra was also discussed in [41].

$$z(\alpha) = 1 - \sum_{n=1}^{\infty} z_n \alpha^n + O(\alpha z, z^2). \tag{15.8}$$

This implies that the renormalized fields change as

$$\varphi_R' = z^{-1}(\alpha)\varphi_R = \Big(1 + \sum_{n=1}^{\infty} z_n \alpha^n + O(z^2)\Big)\varphi_R \equiv \varphi_R + \sum_{n=1}^{\infty} z_n \hat{G}_n \varphi_R + O(z^2), \tag{15.9}$$

where we have introduced the operators

$$\hat{G}_n \varphi_R \equiv \alpha^n \varphi_R, \tag{15.10}$$

which satisfy the commutation relations

$$[\hat{L}_n, \hat{L}_m] = (n - m)\hat{L}_{n+m}; \quad [\hat{G}_n, \hat{G}_m] = 0; \quad [\hat{L}_n, \hat{G}_m] = -m\hat{G}_{n+m}, \tag{15.11}$$

where $n, m \geq 1$.

The non-infinitesimal transformations can again be constructed with the help of the exponential map,

$$z(\alpha) = \exp\Big(\sum_{n=1}^{\infty} a_n \hat{L}_n\Big) \exp\Big(-\sum_{n=1}^{\infty} a_n \hat{L}_n - \sum_{n=1}^{\infty} z_n \hat{G}_n\Big). \tag{15.12}$$

15.3 Rescaling subgroup

An important particular case of the finite renormalizations is the transformations changing the renormalization scale.

$$\alpha(\mu) \to \alpha(\mu') \equiv \alpha'(\mu);$$
$$Z\big(\alpha(\mu), \ln\Lambda/\mu\big) \to Z'\big(\alpha(\mu'), \ln\Lambda/\mu'\big) \equiv z\big(\alpha(\mu)\big) Z\big(\alpha(\mu), \ln\Lambda/\mu\big) \tag{15.13}$$

parameterized by $t = \ln\mu'/\mu$. Evidently, these transformations form an Abelian group, which is a subgroup of the group composed of finite renormalizations. For the infinitesimal transformations for which μ' is close to μ (or, equivalently, the parameter t is small)

$$\alpha' - \alpha = \beta(\alpha)t + O(t^2)$$
$$= t\sum_{n=1}^{\infty} \beta_n \alpha^{n+1} + O(t^2) = -t\sum_{n=1}^{\infty} \beta_n \hat{L}_n \alpha + O(t^2);$$
$$\varphi_R' - \varphi_R = -\delta z \varphi_R + O(t^2) = -\gamma(\alpha)t\, \varphi_R + O(t^2)$$
$$= -t\sum_{n=1}^{\infty} \gamma_n \alpha^n \varphi_R + O(t^2) = -t\sum_{n=1}^{\infty} \gamma_n \hat{G}_n \varphi_R + O(t^2), \tag{15.14}$$

so that the generator of the rescaling transformations is the operator

$$\hat{L} = -\sum_{n=1}^{\infty} \left(\beta_n \hat{L}_n + \gamma_n \hat{G}_n \right). \tag{15.15}$$

Applying the exponential map for constructing the non-infinitesimal transformations of the coupling constant we obtain that an arbitrary function of the coupling constant changes as [42, 43].

$$f(\alpha') = \exp\left(\ln \frac{\mu'}{\mu} \beta(\alpha) \frac{\partial}{\partial \alpha} \right) f(\alpha). \tag{15.16}$$

However, it is easy to see that under the rescaling transformations RGFs remains unchanged.

15.4   Exact expresssions for the renormalization constants

As well known, in various renormalization constants the coefficients at higher ε-poles are related to the coefficients of RGFs [44] by the 't Hooft pole equations, see [45] for review. This is also valid for the coefficients at higher powers of logarithms [46]. The argumentation based on the algebraic structure of the rescaling subgroup allows to construct simple and beautiful expressions for renormalization constants that relate them to the renormalization group functions.

It is especially interesting to consider such a regularization when both ε-poles and logarithms are present in the renormalization constants. This structure of divergent contributions can be obtained for a special modification of dimensional regularization. In the dimension $D \neq 4$ the bare gauge coupling constant $\tilde{\alpha}_0$ has the dimension m^ε and can, therefore, be presented as $\tilde{\alpha}_0 = \alpha_0 \Lambda^\varepsilon$, where α_0 is dimensionless and Λ is a parameter with the dimension of mass. Then the coupling constant can be renormalized according to the prescription

$$\alpha_0 = \left(\frac{\mu}{\Lambda} \right)^\varepsilon \alpha \, Z_\alpha^{-1}(\alpha, \varepsilon^{-1}), \tag{15.17}$$

where μ is a renormalization point and α is the renormalized gauge coupling. For the MS scheme the renormalization constants include only ε-poles in the case $\Lambda = \mu$. The $\overline{\text{MS}}$-scheme [47] is obtained by redefining the renormalization point

$$\mu \to \frac{\mu \exp(\gamma/2)}{\sqrt{4\pi}}, \tag{15.18}$$

where $\gamma \equiv -\Gamma'(1) \approx 0.577$. For $\Lambda \neq \mu$ minimal subtraction is obtained if the renormalization constants include only ε-poles and powers of $\ln \Lambda/\mu$. Some multiloop calculations with this regularization can be found in [48–50]

To define a field renormalization constant $Z(\alpha, \varepsilon^{-1})$, we require the finiteness of the corresponding renormalized Green's function G_R in the limit $\varepsilon \to 0$,

$$G_R\left(\alpha, \ln \frac{\mu}{p} \right) = \lim_{\varepsilon \to 0} Z(\alpha, \varepsilon^{-1}) \, G\left[\left(\frac{\mu}{p} \right)^\varepsilon \alpha Z_\alpha^{-1}(\alpha, \varepsilon^{-1}), \varepsilon^{-1} \right]. \tag{15.19}$$

In D-dimensions RGFs are defined according to the prescription

$$\beta(\alpha, \varepsilon) \equiv \frac{d\alpha(\alpha_0(\Lambda/\mu)^\varepsilon, \varepsilon^{-1})}{d\ln\mu}\bigg|_{\alpha_0=\text{const}} ;$$

$$\gamma(\alpha) \equiv \frac{d\ln Z(\alpha, \varepsilon^{-1})}{d\ln\mu}\bigg|_{\alpha_0=\text{const}} . \tag{15.20}$$

(In our notations they are denoted in bold.)

Alternatively, it is possible to perform the renormalization in the four-dimensional form

$$\frac{1}{\alpha_0} = \frac{Z_\alpha(\alpha, \varepsilon^{-1}, \ln\Lambda/\mu)}{\alpha};$$

$$G_R\left(\alpha, \ln\frac{\mu}{P}\right) = \lim_{\varepsilon\to 0} Z(\alpha, \varepsilon^{-1}, \ln\Lambda/\mu)$$

$$\times G\left[\left(\frac{\Lambda}{P}\right)^\varepsilon \alpha Z_\alpha^{-1}(\alpha, \varepsilon^{-1}, \ln\Lambda/\mu), \varepsilon^{-1}\right]. \tag{15.21}$$

In this case the renormalization constants Z_α and Z should not contain positive powers of ε, but include powers of $\ln\Lambda/\mu$. In this case RGFs are defined as

$$\beta(\alpha) \equiv \frac{d\alpha(\alpha_0, \varepsilon^{-1}, \ln\Lambda/\mu)}{d\ln\mu}\bigg|_{\alpha_0=\text{const}} ;$$

$$\gamma(\alpha) \equiv \frac{d\ln Z(\alpha, \varepsilon^{-1}, \ln\Lambda/\mu)}{d\ln\mu}\bigg|_{\alpha_0=\text{const}} \tag{15.22}$$

and are related to the D-dimensional ones by the equations

$$\beta(\alpha, \varepsilon) = -\varepsilon\alpha + \beta(\alpha); \qquad \gamma(\alpha) = \gamma(\alpha). \tag{15.23}$$

It is important that RGFs $\beta(\alpha)$ and $\gamma(\alpha)$ do not depend on both ε and $\ln\Lambda/\mu$. From this requirement it is possible to relate the coefficients at higher ε-poles and higher powers of $\ln\Lambda/\mu$ to the coefficients of the β-function and anomalous dimension. For the regularization considered here the corresponding equations are encoded in the all-order exact formulas [51]

$$\ln\alpha_0 = \exp\left(\ln\frac{\Lambda}{\mu}\beta(\alpha)\frac{\partial}{\partial\alpha}\right)\left\{-\int_0^\alpha \frac{d\alpha}{\alpha}\frac{\beta(\alpha)}{\beta(\alpha)-\varepsilon\alpha} + \ln\alpha\right\}; \tag{15.24}$$

$$\alpha_0^{-S} = \exp\left(\ln\frac{\Lambda}{\mu}\beta(\alpha)\frac{\partial}{\partial\alpha}\right)\alpha^{-S}\exp\left\{S\int_0^\alpha \frac{d\alpha}{\alpha}\frac{\beta(\alpha)}{\beta(\alpha)-\varepsilon\alpha}\right\}; \tag{15.25}$$

$$\ln Z - \int_a^\alpha d\alpha\frac{\gamma(\alpha)}{\beta(\alpha)} = \exp\left(\ln\frac{\Lambda}{\mu}\beta(\alpha)\frac{\partial}{\partial\alpha}\right)$$

$$\times\left[\int_0^\alpha d\alpha\frac{\gamma(\alpha)}{\beta(\alpha)-\varepsilon\alpha} - \int_a^\alpha d\alpha\frac{\gamma(\alpha)}{\beta(\alpha)}\right], \tag{15.26}$$

where the constant a in the last equation can be arbitrary.

This form reveals the renormalization group origin of the considered equations. For this purpose, let us first investigate the case of the cutoff type regularizations (like the regularization by higher covariant derivatives [13, 14]), which is obtained by removing ε-poles in the formal limit $\varepsilon \to \infty$. Then, a renormalization prescription analogous to minimal subtraction is the HD+MSL scheme [28], in which the renormalization constants include only powers of $\ln \Lambda/\mu$. Therefore, choosing $\mu' = \Lambda$ and taking into account that $\alpha'(\mu) = \alpha(\Lambda) = \alpha(\alpha_0, \ln \Lambda/\mu = 0) = \alpha_0$ for an arbitrary function $f(\alpha)$ in the HD+MSL scheme we obtain

$$f(\alpha_0) = \exp\left(\ln \frac{\Lambda}{\mu} \beta(\alpha) \frac{\partial}{\partial \alpha} \right) f(\alpha). \tag{15.27}$$

This equation exactly reproduces the expressions (15.24), (15.25), and (15.26) for $\ln Z_\alpha$, $(Z_\alpha)^S$, and $\ln Z$ if

$$f(\alpha_0) = \ln \alpha_0; \qquad f(\alpha_0) = \alpha_0^{-S}; \qquad f(\alpha_0) = \int\limits_a^{\alpha_0} d\alpha \, \frac{\beta(\alpha)}{\gamma(\alpha)}, \tag{15.28}$$

respectively.

Next, let us consider a more complicated case of the dimensional regularization with $\Lambda \neq \mu$. In this version of dimensional regularization the renormalization constants contain not only ε-poles, but also powers of $\ln \Lambda/\mu$ and various mixed terms. In the standard case $\mu = \Lambda$ from the above equations we see that [44]

$$\alpha \exp\left\{ -\int\limits_0^\alpha \frac{d\alpha}{\alpha} \frac{\beta(\alpha)}{\beta(\alpha) - \varepsilon\alpha} \right\}\Bigg|_{\mu = \Lambda} = \alpha_0 = \alpha Z_\alpha^{-1}(\alpha, \varepsilon^{-1}, 0). \tag{15.29}$$

Using the exponential map, for an arbitrary value of the renormalization point μ we obtain

$$f(\alpha_0) = \exp\left(\ln \frac{\Lambda}{\mu} \beta(\alpha) \frac{\partial}{\partial \alpha} \right) f\left(\alpha \exp\left\{ -\int\limits_0^\alpha \frac{d\alpha}{\alpha} \frac{\beta(\alpha)}{\beta(\alpha) - \varepsilon\alpha} \right\} \right). \tag{15.30}$$

In the particular case $f(\alpha_0) = 1/\alpha_0$ this equation gives

$$Z_\alpha(\alpha, \varepsilon^{-1}, \ln \Lambda/\mu) = \alpha \exp\left(\ln \frac{\Lambda}{\mu} \beta(\alpha) \frac{\partial}{\partial \alpha} \right) \left(\alpha^{-1} Z_\alpha(\alpha, \varepsilon^{-1}, 0) \right), \tag{15.31}$$

where

$$Z_\alpha(\alpha, \varepsilon^{-1}, 0) = \exp\left(\int\limits_0^\alpha \frac{d\alpha}{\alpha} \frac{\beta(\alpha)}{\beta(\alpha) - \varepsilon\alpha} \right). \tag{15.32}$$

After some transformations (see [51] for details) the expression (15.31) can be cast in the form

$$Z_\alpha(\alpha, \varepsilon^{-1}, \ln \Lambda/\mu) = \exp\left\{\ln\frac{\Lambda}{\mu}\left[\beta(\alpha)\frac{\partial}{\partial\alpha} - \frac{\beta(\alpha)}{\alpha}\right]\right\}Z_\alpha(\alpha, \varepsilon^{-1}, 0)$$

$$= \exp\left\{\ln\frac{\Lambda}{\mu}\left[\beta(\alpha)\frac{\partial}{\partial\alpha} - \gamma_\alpha(\alpha)\right]\right\}\exp\left(\int_0^\alpha \frac{d\alpha}{\alpha}\frac{\beta(\alpha)}{\beta(\alpha)-\varepsilon\alpha}\right), \qquad (15.33)$$

where we took into account that $\gamma_\alpha(\alpha) \equiv d\ln Z_\alpha/d\ln\mu = \beta(\alpha)/\alpha$.

This expression is a particular case of the general equation for an arbitrary renormalization constant,

$$Z(\alpha, \varepsilon^{-1}, \ln\Lambda/\mu) = \exp\left\{\ln\frac{\Lambda}{\mu}\left(\beta(\alpha)\frac{\partial}{\partial\alpha} - \gamma(\alpha)\right)\right\}Z(\alpha, \varepsilon^{-1}, 0)$$

$$= \exp\left\{\ln\frac{\Lambda}{\mu}\left(\beta(\alpha)\frac{\partial}{\partial\alpha} - \gamma(\alpha)\right)\right\}\exp\left\{\int_0^\alpha d\alpha\frac{\gamma(\alpha)}{\beta(\alpha)-\varepsilon\alpha}\right\}. \qquad (15.34)$$

As a correctness test, in [51] it was verified that this equation exactly reproduces the five-loop expression for $\ln Z$ presented in [52]. Here write down only the four-loop expression, because it is essentially smaller,

$$\ln Z = -\alpha\gamma_1\left(\frac{1}{\varepsilon} + \ln\frac{\Lambda}{\mu}\right) - \frac{\alpha^2}{2}\left[\gamma_2\left(\frac{1}{\varepsilon} + 2\ln\frac{\Lambda}{\mu}\right) + \gamma_1\beta_1\left(\frac{1}{\varepsilon} + \ln\frac{\Lambda}{\mu}\right)^2\right]$$

$$-\frac{\alpha^3}{3}\left[\gamma_3\left(\frac{1}{\varepsilon} + 3\ln\frac{\Lambda}{\mu}\right) + \gamma_1\beta_2\left(\frac{1}{\varepsilon^2} + \frac{3}{\varepsilon}\ln\frac{\Lambda}{\mu} + \frac{3}{2}\ln^2\frac{\Lambda}{\mu}\right) + \gamma_2\beta_1\left(\frac{1}{\varepsilon^2}\right.\right.$$

$$\left. + \frac{3}{\varepsilon}\ln\frac{\Lambda}{\mu} + 3\ln^2\frac{\Lambda}{\mu}\right) + \gamma_1\beta_1^2\left(\frac{1}{\varepsilon} + \ln\frac{\Lambda}{\mu}\right)^3\right]$$

$$-\frac{\alpha^4}{4}\left[\gamma_4\left(\frac{1}{\varepsilon} + 4\ln\frac{\Lambda}{\mu}\right) + \gamma_1\beta_3\left(\frac{1}{\varepsilon^2} + \frac{4}{\varepsilon}\ln\frac{\Lambda}{\mu} + 2\ln^2\frac{\Lambda}{\mu}\right) + \gamma_2\beta_2\left(\frac{1}{\varepsilon}\right.\right.$$

$$\left. + 2\ln\frac{\Lambda}{\mu}\right)^2 + \gamma_3\beta_1\left(\frac{1}{\varepsilon^2} + \frac{4}{\varepsilon}\ln\frac{\Lambda}{\mu} + 6\ln^2\frac{\Lambda}{\mu}\right) + 2\gamma_1\beta_1\beta_2\left(\frac{1}{\varepsilon^3} + \frac{4}{\varepsilon^2}\ln\frac{\Lambda}{\mu}\right.$$

$$\left. + \frac{5}{\varepsilon}\ln^2\frac{\Lambda}{\mu} + \frac{5}{3}\ln^3\frac{\Lambda}{\mu}\right) + \gamma_2\beta_1^2\left(\frac{1}{\varepsilon^3} + \frac{4}{\varepsilon^2}\ln\frac{\Lambda}{\mu} + \frac{6}{\varepsilon}\ln^2\frac{\Lambda}{\mu} + 4\ln^3\frac{\Lambda}{\mu}\right)$$

$$\left. + \gamma_1\beta_1^3\left(\frac{1}{\varepsilon} + \ln\frac{\Lambda}{\mu}\right)^4\right] + O(\alpha^5). \qquad (15.35)$$

Using Eq. (15.34) it is possible to compare coefficients at higher poles and logarithms. Namely, according to [52–54] the coefficients at higher logarithms for the cutoff type regularizations and at higher ε-poles in the case of using the dimensional technique can be written as

$$\ln Z_\alpha(\alpha, \ln\Lambda/\mu) = -\sum_{q=1}^\infty \sum_{k_1,k_2,\ldots,k_q=1}^\infty \frac{1}{K_q}\cdot\frac{K_q!}{q!}\beta_{k_1}\beta_{k_2}\ldots\beta_{k_q}\alpha^{K_q}\ln^q\frac{\Lambda}{\mu};$$

$$\ln Z_\alpha(\alpha, 1/\varepsilon) = -\sum_{q=1}^\infty \sum_{k_1,k_2,\ldots,k_q=1}^\infty \frac{1}{K_q}\beta_{k_1}\beta_{k_2}\ldots\beta_{k_q}\alpha^{K_q}\varepsilon^{-q}, \qquad (15.36)$$

where $K_m \equiv \sum\limits_{i=1}^{m} k_i;\ \ K_m! \equiv K_1 K_2 \dots K_m;\ \ K_0! \equiv 1.$

Moreover, it is possible to find some other features of the renormalization constant structure. The simplest one is the relation between coefficients at simple ε-poles and at the first power of $\ln \Lambda/\mu$ given by Eq. (15.1). The coefficients at higher poles and logarithms are related in a much more complicated way, but some features can nevertheless be noted [52]. As an example, here we consider the expression for $\ln Z_\alpha$, in which all terms proportional to $1/\varepsilon^2$, $\varepsilon^{-1} \ln \Lambda/\mu$, and $\ln^2 \Lambda/\mu$ are factorized into perfect squares,

$$\ln Z_\alpha = - \sum_{L=1}^{\infty} \alpha^L \beta_L \left(\frac{1}{L\varepsilon} + \ln \frac{\Lambda}{\mu} \right) - \frac{1}{L} \sum_{L=2}^{\infty} \alpha^L \sum_{k=1}^{L-1} \beta_k \beta_{L-k} \left(\frac{1}{\varepsilon} + \frac{L}{2} \ln \frac{\Lambda}{\mu} \right)^2$$

$$+ \text{ higher poles and logarithms.} \tag{15.37}$$

It can also be noted that some terms have a rather simple structure

$$\ln Z_\alpha = - \sum_{m=1}^{\infty} \sum_{k=1}^{\infty} \frac{(\beta_k \alpha^k)^m}{m} k \left(\frac{1}{\varepsilon} + k \ln \frac{\Lambda}{\mu} \right)^m + \text{ the other terms.} \tag{15.38}$$

Some features have also been found for Z_α, $(Z_\alpha)^S$, and $\ln Z$, for instance,

$$\ln Z = - \sum_{L=1}^{\infty} \frac{\alpha^L}{L} \sum_{k=1}^{L} \gamma_{L-k+1} (\beta_1)^{k-1} \varepsilon^{L-k} \left(\frac{1}{\varepsilon} + \ln \frac{\Lambda}{\mu} \right)^L \bigg|_{\varepsilon^s \to 0 \text{ for all } s>0}$$

$$+ \text{ terms containing } \beta_i \text{ with } i \geq 2. \tag{15.39}$$

Thus, it is possible to construct simple all-loop equations for the renormalization constants and, using them, analyse the coefficients at higher poles and logarithms.

15.5 Conclusion

Investigation of various renormalization prescriptions is very important, because some exact relations (e.g., the NSVZ equation) are satisfied only in certain subtraction schemes. Different subtraction schemes can be related by finite renormalizations which form a Lie group. The infinitesimal finite renormalizations of the gauge coupling constant form a certain subalgebra of the Witt algebra (the central extension of which is the Virasoro algebra widely used in string theory). It is also possible to construct the commutation relations for the algebra of the infinitesimal finite renormalizations which involve the matter field renormalizations. The non-infinitesimal finite renormalizations can be obtained in standard way with the help of the exponential map. An important particular case of finite renormalizations is the ones that shift the renormalization point μ. They do not change RGFs and can be used for constructing simple formulas for the renormalization constants. This has been done for a version of dimensional regularization in which the dimensionful regularization parameter Λ is different from the renormalization point μ. The main advantage of this technique is that it has features of both usual dimensional

regularization and the regularizations of the cutoff type. In this case the formulas for the renormalization constants relate the coefficients at ε-poles, powers of ln Λ/μ, and the mixed terms to the coefficients of RGFs, i.e. of the β-function and anomalous dimension. After setting $\Lambda = \mu$ they reproduce the corresponding results for the usual dimensional regularization, and after removing ε-poles give the expressions for the cutoff type regularizations. They also allow establishing the relation between the coefficients at higher poles and at higher logarithms in a simple way, although at the first sight this relation is highly nontrivial. Using the general equations for the renormalization constants we present the corresponding expressions in the lowest approximations and discuss some general features of the results.

References

1. M. E. Peskin, D. V. Schroeder: *An Introduction to quantum field theory*, Addison–Wesley Publishing Company, 1995.
2. R. N. Mohapatra: *Unification and Supersymmetry. The Frontiers of Quark - Lepton Physics: The Frontiers of Quark-Lepton Physics*, Springer, 2002.
3. J. R. Ellis, S. Kelley, D. V. Nanopoulos: Probing the desert using gauge coupling unification, Phys. Lett. B **260** (1991) 131–137.
4. U. Amaldi, W. de Boer, H. Furstenau: Comparison of grand unified theories with electroweak and strong coupling constants measured at LEP, Phys. Lett. B **260** (1991) 447–455.
5. P. Langacker, M. X. Luo: Implications of precision electroweak experiments for M_t, ρ_0, $\sin^2 \theta_W$ and grand unification, Phys. Rev. D **44** (1991) 817–822.
6. C. Gnendiger, A. Signer, D. Stöckinger, A. Broggio, A. L. Cherchiglia, F. Driencourt-Mangin, A. R. Fazio, B. Hiller, P. Mastrolia, T. Peraro, *et al.*: To d, or not to d: recent developments and comparisons of regularization schemes, Eur. Phys. J. C **77** (2017) 471.
7. G. 't Hooft, M. J. G. Veltman: Regularization and Renormalization of Gauge Fields, Nucl. Phys. B **44** (1972) 189–213.
8. C. G. Bollini, J. J. Giambiagi: Dimensional Renormalization: The Number of Dimensions as a Regularizing Parameter, Nuovo Cim. B **12** (1972) 20–26.
9. J. F. Ashmore: A Method of Gauge Invariant Regularization, Lett. Nuovo Cim. **4** (1972) 289–290.
10. G. M. Cicuta, E. Montaldi: Analytic renormalization via continuous space dimension, Lett. Nuovo Cim. **4** (1972) 329–332.
11. I. Jack, D. R. T. Jones: Regularization of supersymmetric theories, Adv. Ser. Direct. High Energy Phys. **21** (2010) 494–513.
12. W. Siegel: Supersymmetric Dimensional Regularization via Dimensional Reduction, Phys. Lett. B **84** (1979) 193–196.
13. A. A. Slavnov: Invariant regularization of nonlinear chiral theories, Nucl. Phys. B **31** (1971) 301–315.
14. A. A. Slavnov: Invariant regularization of gauge theories, Theor. Math. Phys. **13** (1972) 1064–1066.
15. A. A. Slavnov: The Pauli-Villars Regularization for Nonabelian Gauge Theories, Theor. Math. Phys. **33** (1977) 977–981.
16. V. K. Krivoshchekov: Invariant Regularizations for Supersymmetric Gauge Theories, Theor. Math. Phys. **36** (1978) 745–752.

17. P. C. West: Higher Derivative Regulation Of Supersymmetric Theories, Nucl. Phys. B **268** (1986) 113–124.
18. K. Stepanyantz: The higher covariant derivative regularization as a tool for revealing the structure of quantum corrections in supersymmetric gauge theories, Proceedings of the Steklov Institute of Mathematics **309** (2020) 284–298.
19. V. A. Novikov, M. A. Shifman, A. I. Vainshtein, V. I. Zakharov, Exact Gell-Mann-Low Function of Supersymmetric Yang-Mills Theories from Instanton Calculus, Nucl. Phys. B **229** (1983) 381–393.
20. D. R. T. Jones: More on the Axial Anomaly in Supersymmetric Yang-Mills Theory, Phys. Lett. **123B** (1983) 45–46.
21. V. A. Novikov, M. A. Shifman, A. I. Vainshtein, V. I. Zakharov: Beta Function in Supersymmetric Gauge Theories: Instantons Versus Traditional Approach, Phys. Lett. **166B**(1986), 329–333.
22. M. A. Shifman, A. I. Vainshtein: Solution of the Anomaly Puzzle in SUSY Gauge Theories and the Wilson Operator Expansion, Nucl. Phys. B **277** (1986) 456–486.
23. K. V. Stepanyantz: Non-renormalization of the $V\bar{c}c$-vertices in $\mathcal{N} = 1$ supersymmetric theories, Nucl. Phys. B **909** (2016) 316–335.
24. K. V. Stepanyantz: The β-function of $\mathcal{N} = 1$ supersymmetric gauge theories regularized by higher covariant derivatives as an integral of double total derivatives, JHEP **1910** (2019) 011.
25. K. Stepanyantz: The all-loop perturbative derivation of the NSVZ β-function and the NSVZ scheme in the non-Abelian case by summing singular contributions, Eur. Phys. J. C **80** (2020) 911.
26. K. Stepanyantz: Structure of Quantum Corrections in $\mathcal{N} = 1$ Supersymmetric Gauge Theories, Bled Workshops Phys. **18** (2017) 197–213.
27. K. V. Stepanyantz: Derivation of the exact NSVZ β-function in N=1 SQED, regularized by higher derivatives, by direct summation of Feynman diagrams, Nucl. Phys. B **852** (2011) 71-107.
28. A. L. Kataev, K. V. Stepanyantz: NSVZ scheme with the higher derivative regularization for $\mathcal{N} = 1$ SQED, Nucl. Phys. B **875** (2013) 459–482.
29. I. Jack, D. R. T. Jones,d C. G. North: N=1 supersymmetry and the three loop gauge Beta function, Phys. Lett. B **386** (1996) 138–140.
30. I. Jack, D. R. T. Jones, C. G. North: Scheme dependence and the NSVZ Beta function, Nucl. Phys. B **486** (1997) 479–499.
31. I. Jack, D. R. T. Jones, A. Pickering: The Connection between DRED and NSVZ, Phys. Lett. B **435** (1998) 61–66.
32. A. L. Kataev, K. V. Stepanyantz: Scheme independent consequence of the NSVZ relation for $\mathcal{N} = 1$ SQED with N_f flavors, Phys. Lett. B **730** (2014) 184–189.
33. A. L. Kataev, K. V. Stepanyantz: The NSVZ beta-function in supersymmetric theories with different regularizations and renormalization prescriptions, Theor. Math. Phys. **181** (2014) 1531–1540.
34. I. O. Goriachuk, A. L. Kataev, K. V. Stepanyantz: A class of the NSVZ renormalization schemes for $\mathcal{N} = 1$ SQED, Phys. Lett. B **785** (2018) 561–566.
35. K. G. Chetyrkin, A. L. Kataev, F. V. Tkachov: Computation of the α_s^2 Correction Sigma-t ($e^+e^- \to$ Hadrons) in QCD, IYaI-P-0170.
36. G. Källén: The coupling constant in field theory, Nuovo Cim. **12** (1954) 217–225.
37. A. A. Vladimirov: Renormalization Group Equations in Different Approaches, Teor. Mat. Fiz. **25** (1975) 335–343.
38. A. A. Vladimirov, D. V. Shirkov: The renormalization group and ultraviolet asymptotics, Sov. Phys. Usp. **22** (1979) 860–878.

39. A. A. Vladimirov: Unambiguity of Renormalization Group Calculations in QCD, Sov. J. Nucl. Phys. **31** (1980) 558.

40. A. Kataev, K. Stepanyantz: Algebraic structure of the renormalization group in the renormalizable QFT theories, arXiv:2404.15856 [hep-th].

41. A. Isaev, V. Rubakov: *Theory of Groups and Symmetries*, WSP, 2018.

42. S. Groote, J. G. Korner, A. A. Pivovarov: Spectral moments of two point correlators in perturbation theory and beyond, Phys. Rev. D **65** (2002) 036001.

43. S. V. Mikhailov: Generalization of BLM procedure and its scales in any order of pQCD: A Practical approach, JHEP **06** (2007) 009.

44. G. 't Hooft: Dimensional regularization and the renormalization group, Nucl. Phys. B **61** (1973) 455–468.

45. D. I. Kazakov: Radiative Corrections, Divergences, Regularization, Renormalization, Renormalization Group and All That in Examples in Quantum Field Theory, arXiv:0901.2208 [hep-ph].

46. J. C. Collins: *Renormalization: An Introduction to Renormalization, The Renormalization Group, and the Operator Product Expansion*, Cambridge University Press, 1986.

47. W. A. Bardeen, A. J. Buras, D. W. Duke, T. Muta: Deep Inelastic Scattering Beyond the Leading Order in Asymptotically Free Gauge Theories, Phys. Rev. D **18** (1978) 3998.

48. S. S. Aleshin, A. L. Kataev, K. V. Stepanyantz: Structure of three-loop contributions to the β-function of $\mathcal{N} = 1$ supersymmetric QED with N_f flavors regularized by the dimensional reduction, JETP Lett. **103** (2016) 77–81.

49. S. S. Aleshin, I. O. Goriachuk, A. L. Kataev, K. V. Stepanyantz: The NSVZ scheme for $\mathcal{N} = 1$ SQED with N_f flavors, regularized by the dimensional reduction, in the three-loop approximation, Phys. Lett. B **764** (2017) 222–227.

50. S. S. Aleshin, A. L. Kataev, K. V. Stepanyantz: The three-loop Adler D-function for $\mathcal{N} = 1$ SQCD regularized by dimensional reduction, JHEP **03** (2019) 196.

51. N. Meshcheriakov, V. Shatalova, K. Stepanyantz: Higher ε-poles and logarithms in the MS-like schemes from the algebraic structure of the renormalization group, arXiv:2405.11557 [hep-th].

52. N. Meshcheriakov, V. Shatalova, K. Stepanyantz: Higher logarithms and ε-poles for the MS-like renormalization prescriptions, JHEP **12** (2023) 097.

53. C. E. Derkachev, A. V. Ivanov, L. D. Faddeev: Renormalization scenario for the quantum Yang–Mills theory in four-dimensional space–time, Theor. Math. Phys. **192** (2017) 1134–1140.

54. N. Meshcheriakov, V. Shatalova, K. Stepanyantz: Coefficients at powers of logarithms in the higher-derivatives and minimal-subtractions-of-logarithms renormalization scheme, Phys. Rev. D **106** (2022) 105011.

16   A curious example of dimensionality reduction in the E_8 lattice

Elia Dmitrieff

No Institute Given

Abstract: We investigated influence of the Elser-Sloane rotation matrix on the infinite E_8 root lattice and found out that we got three orthogonal spaces - a 3D fractal quasi-crystal, a 2D square lattice and a 3D space in which nodes are concentrated in a finite three-dimensional polyhedral base. The size of base specifies the degree of 3D fractal's detail, so it can be taken small using self-similarity. We interpret this effect as a 8D to (3+2)D dimensional reduction. Further, one can get down to (3+1)D by choosing a path along the nodes of square lattice.

Povzetek: Avtor raziskuje vpliv Elser-Sloanove rotacijske matrike na neskončno korensko mrežo E_8 in ugotovi, da se pojavijo trije ortogonalni prostori: fraktalni trirazsežni kvazikristal, kvadratna dvorazsežna mreža in trirazsežni prostor, v katerem so vozlišča zgoščena v končno trirazsežno poliedrsko strukturo. Podrobnosti na fraktalu določajo velikost baze. Če je fraktal videti majhen, avtor interpretira kot zmanjšanje osem razsežne na (3+2) razsežno, ali celo na (3+1) tedaj, kadar izbere poti vzdolž vozlišč kvadratne mreže.

17   Techniques that allow the implementation of a 4D borderless lattice model in the form of a 3D hardware device

Elia Dmitrieff

No Institute Given

Abstract: We propose a practical way to construct a computing environment in the form of a cellular automaton on a four-dimensional lattice. Specific folding allows us to obtain a logical seamless and borderless 4D network as a 3D hardware device. We believe that the use of such a framework, together with a special reversible computational rule, will make it possible to realistically simulate the behavior of fundamental particles.

Povzetek: Avtor predlaga vzpostavitev računalniškega okolja v obliki celičnega avtomata na štirirazsežni mreži, na kateri vspostavi logično brezšivne in brezrobne štiri razsežne povezave kot tri razsežne hardverske naprave. Avtor meni, da bo uporaba tega okolja omogočila drugačno razumevanje osnovnih gradnikov snovi.

BLED WORKSHOPS
IN PHYSICS
VOL. 25, NO. 1

Proceedings of the 27th Workshop
What Comes Beyond . . . *(p. 237)*
Bled, Slovenia, July 8–17, 2024

18 Fermion masses, mixing and FCNC's within a gauged SU(3) family symmetry

Albino Hernandez-Galeana [**]

Departamento de Física, ESFM - Instituto Politécnico Nacional. U. P. "Adolfo López Mateos". C. P. 07738, Ciudad de México, México

Abstract: Within a gauged SU(3) family symmetry model, we address the problem of mass generation for ordinary fermions. In this framework right handed neutrinos are needed in order to cancel anomalies. We also introduce a set of SU(2)L weak singlet vector-like fermions U,D,E,N, with N a neutral lepton. These vector- like fermions allow the implementation of See-saw mechanisms at tree level to generate the masses of the top and bottom quarks and the tau lepton. Light fermions obtain masses from loop corrections mediated by the massive SU(3) gauge bosons. We show a parameter space region for simultaneous solutions of quark and lepton masses and FCNC's suppression, trying to keep as low as possible the SU(3) gauge boson masses.

Povzetek: Avtor uporabi model SU(3) za določanje lastnosti treh družin kvarkov in leptonov. Vključi desnoročne nevtrine in doda levoročni šibki singlet U,D,E,N, kjer je N lepton brez naboja. Ti šibki singleti določajo mase kvarkov top in bottom ter leptona tau že na drevesnem nivoju z mehanizmom "Sea-saw". Maso lahkih kvarkov določa interakcija kvarkov z družinskimi bozoni v popravkih višjih redov. Avtor predstavi tudi parametrični prostor, znotraj katerega so mase kvarkov in leptonov skladne z izmerjenimi in v soglasju z mejami, ki preprečujejo direktne prehode iste vrste fermionov med družinami. Poskrbi, da so mase družinskih bozonov čim nižje.

[**] ahernandez@ipn.mx

19   Virtual Institute of Astroparticle physics as the online support for studies of BSM physics and cosmology

Maxim Khlopov[1,2,3]
e-mail khlopov@apc.univ-paris7.fr

[1] Centre for Cosmoparticle Physics "Cosmion"
National Research Nuclear University MEPHI", 115409 Moscow, Russia
[2] Virtual Institute of Astroparticle physics, 75018, Paris, France
[3] Institute of Physics, Southern Federal University
Stachki 194, Rostov on Don 344090, Russia

Abstract. We review the experience of the unique complex of Virtual Institute of Astroparticle Physics (VIA) in presentation online for the most interesting theoretical and experimental results, participation online in conferences and meetings, various forms of collaborative scientific work as well as programs of education at distance, combining online videoconferences with extensive library of records of previous meetings and Discussions on Forum. Since 2014 VIA online lectures combined with individual work on Forum acquired the form of Open Online Courses. Aimed to individual work with students the Course is not Massive, but the account for the number of visits to VIA site can convert VIA in a supplementary tool for MOOC activity. VIA sessions, being a traditional part of Bled Workshops' program, became the platform of the XXVII Bled Workshop "What comes beyond the Standard models?" Their interactive format preserved the traditional creative nonformal atmosphere of Bled Workshop meetings. We openly discuss the state of art of VIA platform.

Keywords: astroparticle physics, physics beyond the Standard model, e-learning, e-science, MOOC

19.1   Introduction

Studies in astroparticle physics link astrophysics, cosmology, particle and nuclear physics and involve hundreds of scientific groups linked by regional networks (like ASPERA/ApPEC [1,2]) and national centers. The exciting progress in these studies will have impact on the knowledge on the structure of microworld and Universe in their fundamental relationship and on the basic, still unknown, physical laws of Nature (see e.g. [3,4] for review). The progress of precision cosmology and experimental probes of the new physics at the LHC and in nonaccelerator experiments, as well as the extension of various indirect studies of physics beyond the Standard model involve with necessity their nontrivial links. Virtual Institute of Astroparticle Physics (VIA) [5] was organized with the aim to play the role of an unifying and coordinating platform for such studies.

Starting from the January of 2008 the activity of the Institute took place on its website [6] in a form of regular weekly videoconferences with VIA lectures, covering all the theoretical and experimental activities in astroparticle physics and related topics. The library of records of these lectures, talks and their presentations was accomplished by multi-lingual Forum. Since 2008 there were **220 VIA online lectures**, VIA has supported distant presentations of **192 speakers at 32 Conferences** and provided transmission of talks at **78 APC Colloquiums**.

In 2008 VIA complex was effectively used for the first time for participation at distance in XI Bled Workshop [7]. Since then VIA videoconferences became a natural part of Bled Workshops' programs, opening the virtual room of discussions to the world-wide audience. Its progress was presented in [8–22].

Here the current state-of-art of VIA complex is presented in order to clarify the way in which discussion of open questions beyond the standard models of both particle physics and cosmology were supported by the platform of VIA facility at the XXVII Bled Workshop. Even without pandemia, there appear other obstacles, preventing participants to attend offline meeting and in this situation VIA videoconferencing supported in 2024 traditions of open discussions at Bled meetings at distant talks, involving distant participants in these discussions.

19.2   VIA structure and activity

19.2.1   The problem of VIA site

The structure of the VIA site was initially based on Flash and is virtually ruined now in the lack of Flash support. The original structure is illustrated by the Fig. 19.1. The home page, presented on this figure, contained the information on the coming and records of the latest VIA events. The upper line of menu included links to directories (from left to right): with general information on VIA (About VIA); entrance to VIA virtual rooms (Rooms); the library of records and presentations (Previous), which contained records of VIA Lectures (Previous → Lectures), records of online transmissions of Conferences (Previous → Conferences), APC Colloquiums (Previous → APC Colloquiums), APC Seminars (Previous → APC Seminars) and Events (Previous → Events); Calendar of the past and future VIA events (All events) and VIA Forum (Forum). In the upper right angle there were links to Google search engine (Search in site) and to contact information (Contacts). The announcement of the next VIA lecture and VIA online transmission of APC Colloquium occupied the main part of the homepage with the record of the most recent VIA events below. In the announced time of the event (VIA lecture or transmitted APC Colloquium) it was sufficient to click on "to participate" on the announcement and to Enter as Guest (printing your name) in the corresponding Virtual room. The Calendar showed the program of future VIA lectures and events. The right column on the VIA homepage listed the announcements of the regularly up-dated hot news of Astroparticle physics and related areas.

In the lack of Flash support this system of links is ruined, but fortunately, they continue to operate separately and it makes possible to use VIA Forum, by direct link to it, as well as direct inks to virtual Zoom room for regular Laboratory and
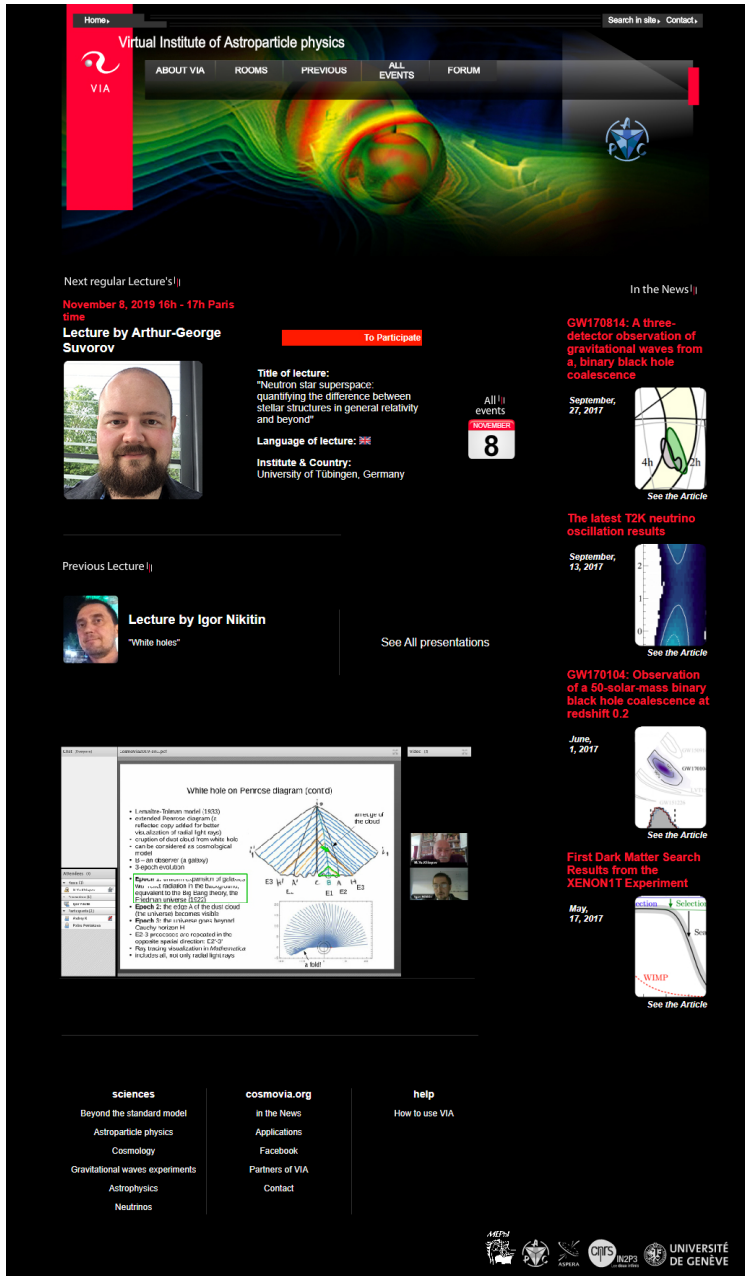
Fig. 19.1: The original home page of VIA site

Seminar meetings (see Fig 19.2). The necessity to restore all the links within VIA complex is a very important task to revive the full scale of VIA activity.

19.2.2   VIA activity

In 2010 special COSMOVIA tours were undertaken in Switzerland (Geneva), Belgium (Brussels, Liege) and Italy (Turin, Pisa, Bari, Lecce) in order to test stability of VIA online transmissions from different parts of Europe. Positive results of these tests have proved the stability of VIA system and stimulated this practice at XIII Bled Workshop. The records of the videoconferences at the XIII Bled Workshop were put on VIA site [23].

Since 2011 VIA facility was used for the tasks of the Paris Center of Cosmological Physics (PCCP), chaired by G. Smoot, for the public program "The two infinities" conveyed by J.L.Robert and for effective support a participation at distance at meetings of the Double Chooz collaboration. In the latter case, the experimentalists, being at shift, took part in the collaboration meeting in such a virtual way.

The simplicity of VIA facility for ordinary users was demonstrated at XIV Bled Workshop in 2011. Videoconferences at this Workshop had no special technical support except for WiFi Internet connection and ordinary laptops with their internal webcams and microphones. This test has proved the ability to use VIA facility at any place with at least decent Internet connection. Of course the quality of records is not as good in this case as with the use of special equipment, but still it is sufficient to support fruitful scientific discussion as can be illustrated by the record of VIA presentation "New physics and its experimental probes" given by John Ellis from his office in CERN (see the records in [24]).

In 2012 VIA facility, regularly used for programs of VIA lectures and transmission of APC Colloquiums, has extended its applications to support M.Khlopov's talk at distance at Astrophysics seminar in Moscow, videoconference in PCCP, participation at distance in APC-Hamburg-Oxford network meeting as well as to provide online transmissions from the lectures at Science Festival 2012 in University Paris7. VIA communication has effectively resolved the problem of referee's attendance at the defence of PhD thesis by Mariana Vargas in APC. The referees made their reports and participated in discussion in the regime of VIA videoconference. In 2012 VIA facility was first used for online transmissions from the Science Festival in the University Paris 7. This tradition was continued in 2013, when the transmissions of meetings at Journées nationales du Développement Logiciel (JDEV2013) at Ecole Politechnique (Paris) were organized [26].

In 2013 VIA lecture by Prof. Martin Pohl was one of the first places at which the first hand information on the first results of AMS02 experiment was presented [25]. In 2014 the 100th anniversary of one of the foundators of Cosmoparticle physics, Ya. B. Zeldovich, was celebrated. With the use of VIA M.Khlopov could contribute the programme of the "Subatomic particles, Nucleons, Atoms, Universe: Processes and Structure International conference in honor of Ya. B. Zeldovich 100th Anniversary" (Minsk, Belarus) by his talk "Cosmoparticle physics: the Universe as a laboratory of elementary particles" [27] and the programme of "Conference YaB-100, dedicated to 100 Anniversary of Yakov Borisovich Zeldovich" (Moscow, Russia) by his talk "Cosmology and particle physics".
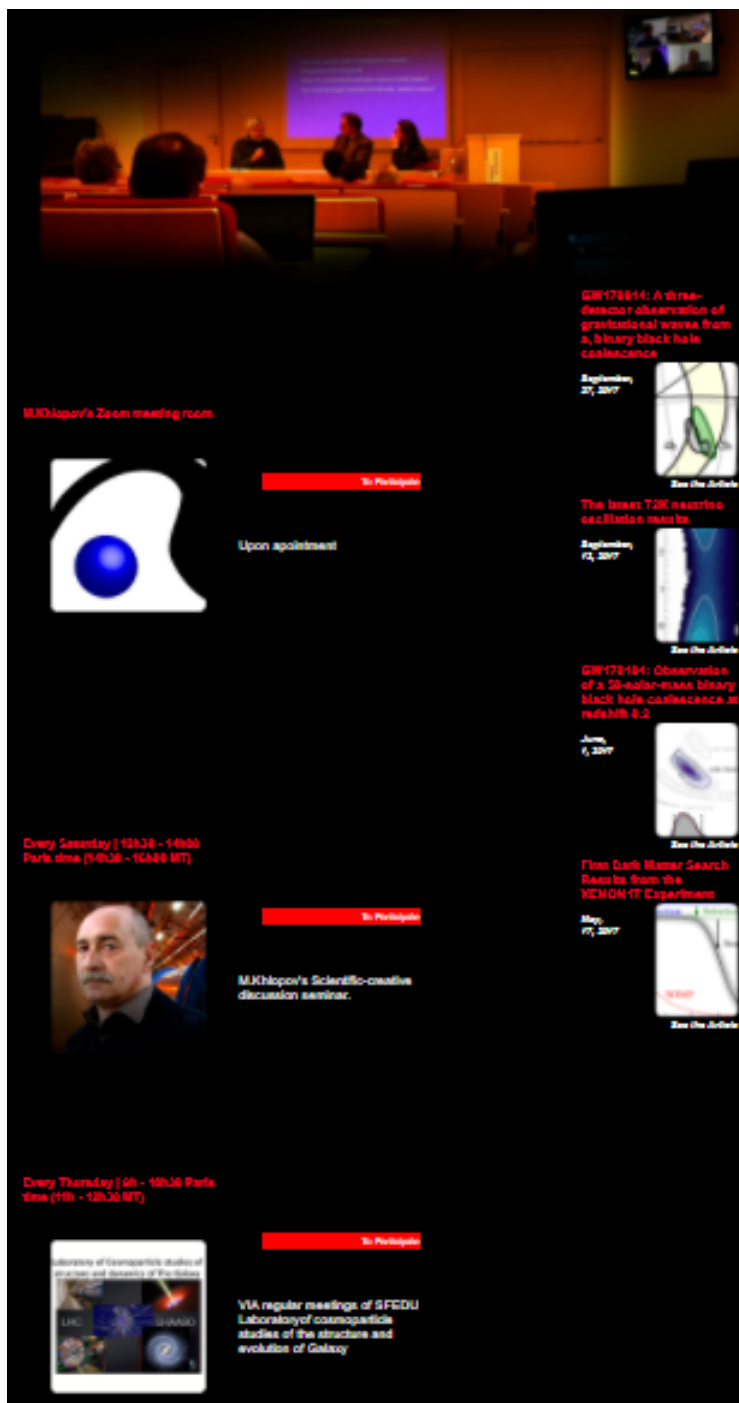
Fig. 19.2: The current home page of VIA site

In 2015 VIA facility supported the talk at distance at All Moscow Astrophysical seminar "Cosmoparticle physics of dark matter and structures in the Universe" by Maxim Yu. Khlopov and the work of the Section "Dark matter" of the International Conference on Particle Physics and Astrophysics (Moscow, 5-10 October 2015). Though the conference room was situated in Milan Hotel in Moscow all the presentations at this Section were given at distance (by Rita Bernabei from Rome, Italy; by Juan Jose Gomez-Cadenas, Paterna, University of Valencia, Spain and by Dmitri Semikoz, Martin Bucher and Maxim Khlopov from Paris) and its proceeding was chaired by M.Khlopov from Paris. In the end of 2015 M. Khlopov gave his distant talk "Dark atoms of dark matter" at the Conference "Progress of Russian Astronomy in 2015", held in Sternberg Astronomical Institute of Moscow State University.

In 2016 distant online talks at St. Petersburg Workshop "Dark Ages and White Nights (Spectroscopy of the CMB)" by Khatri Rishi (TIFR, India) "The information hidden in the CMB spectral distortions in Planck data and beyond", E. Kholupenko (Ioffe Institute, Russia) "On recombination dynamics of hydrogen and helium", Jens Chluba (Jodrell Bank Centre for Astrophysics, UK) "Primordial recombination lines of hydrogen and helium", M. Yu. Khlopov (APC and MEPHI, France and Russia)"Nonstandard cosmological scenarios" and P. de Bernardis (La Sapiensa University, Italy) "Balloon techniques for CMB spectrum research" were given with the use of VIA system. At the defense of PhD thesis by F. Gregis VIA facility made possible for his referee in California not only to attend at distance at the presentation of the thesis but also to take part in its successive jury evaluation.

Since 2018 VIA facility is used for collaborative work on studies of various forms of dark matter in the framework of the project of Russian Science Foundation based on Southern Federal University (Rostov on Don). In September 2018 VIA supported online transmission of **17 presentations** at the Commemoration day for Patrick Fleury, held in APC.

The discussion of questions that were put forward in the interactive VIA events is continued and extended on VIA Forum. Presently activated in English,French and Russian with trivial extension to other languages, the Forum represents a first step on the way to multi-lingual character of VIA complex and its activity. Discussions in English on Forum are arranged along the following directions: beyond the standard model, astroparticle physics, cosmology, gravitational wave experiments, astrophysics, neutrinos. After each VIA lecture its pdf presentation together with link to its record and information on the discussion during it are put in the corresponding post, which offers a platform to continue discussion in replies to this post.

19.2.3   VIA e-learning, OOC and MOOC

One of the interesting forms of VIA activity is the educational work at distance. For the last eleven years M.Khlopov's course "Introduction to cosmoparticle physics" is given in the form of VIA videoconferences and the records of these lectures and their ppt presentations are put in the corresponding directory of the Forum [28]. Having attended the VIA course of lectures in order to be admitted to exam

students should put on Forum a post with their small thesis. In this thesis students are proposed to chose some BSM model and to study the cosmological scenario based on this chosen model. The list of possible topics for such thesis is proposed to students, but they are also invited to chose themselves any topic of their own on possible links between cosmology and particle physics. Professor's comments and proposed corrections are put in a Post reply so that students should continuously present on Forum improved versions of work until it is accepted as admission for student to pass exam. The record of videoconference with the oral exam is also put in the corresponding directory of Forum. Such procedure provides completely transparent way of evaluation of students' knowledge at distance.

In 2018 the test has started for possible application of VIA facility to remote supervision of student's scientific practice. The formulation of task and discussion of progress on work are recorded and put in the corresponding directory on Forum together with the versions of student's report on the work progress.

Since 2014 the second semester of the course on Cosmoparticle physics is given in English and converted in an Open Online Course. It was aimed to develop VIA system as a possible accomplishment for Massive Online Open Courses (MOOC) activity [29]. In 2016 not only students from Moscow, but also from France and Sri Lanka attended this course. In 2017 students from Moscow were accompanied by participants from France, Italy, Sri Lanka and India [30]. The students pretending to evaluation of their knowledge must write their small thesis, present it and, being admitted to exam, pass it in English. The restricted number of online connections to videoconferences with VIA lectures is compensated by the wide-world access to their records on VIA Forum and in the context of MOOC VIA Forum and videoconferencing system can be used for individual online work with advanced participants. Indeed Google Analytics shows that since 2008 VIA site was visited by more than **250 thousand** visitors from **155** countries, covering all the continents by its geography (Fig. 19.3). According to this statistics more than half of these visitors continued to enter VIA site after the first visit. Still the form of individual

Fig. 19.3: Geography of VIA site visits according to Google Analytics

educational work makes VIA facility most appropriate for PhD courses and it

could be involved in the International PhD program on Fundamental Physics, which was planned to be started on the basis of Russian-French collaborative agreement. In 2017 the test for the ability of VIA to support fully distant education and evaluation of students (as well as for work on PhD thesis and its distant defense) was undertaken. Steve Branchu from France, who attended the Open Online Course and presented on Forum his small thesis has passed exam at distance. The whole procedure, starting from a stochastic choice of number of examination ticket, answers to ticket questions, discussion by professors in the absence of student and announcement of result of exam to him was recorded and put on VIA Forum [31].

In 2019 in addition to individual supervisory work with students the regular scientific and creative VIA seminar is in operation aimed to discuss the progress and strategy of students scientific work in the field of cosmoparticle physics.

In 2020 the regular course now for M2 students continued, but the problems of adobe Connect, related with the lack of its support for Flash in 2021 made necessary to use the platform of Zoom, This platform is rather easy to use and provides records, as well as whiteboard tools for discussions online can be solved by accomplishments of laptops by graphic tabloids. In 2022 the Open Online Course for M2 students was accompanied by special course "Cosmoparticle physics", given in English for English speaking M1 students. In 2023 the practice of Open Online Course for M2 students was continued.

19.2.4   Organisation of VIA events and meetings

First tests of VIA system, described in [5, 7–9], involved various systems of video-conferencing. They included skype, VRVS, EVO, WEBEX, marratech and adobe Connect. In the result of these tests the adobe Connect system was chosen and properly acquired. Its advantages were: relatively easy use for participants, a possibility to make presentation in a video contact between presenter and audience, a possibility to make high quality records, to use a whiteboard tools for discussions, the option to open desktop and to work online with texts in any format. The lack of support for Flash, on which VIA site was originally based, made necessary to use Zoom, which shares all the above mentioned advantages.

Regular activity of VIA as a part of APC included online transmissions of all the APC Colloquiums and of some topical APC Seminars, which may be of interest for a wide audience. Online transmissions were arranged in the manner, most convenient for presenters, prepared to give their talk in the conference room in a normal way, projecting slides from their laptop on the screen. Having uploaded in advance these slides in the VIA system, VIA operator, sitting in the conference room, changed them following presenter, directing simultaneously webcam on the presenter and the audience. If the advanced uploading was not possible, VIA streaming was used - external webcam and microphone are directed to presenter and screen and support online streaming. This experience has found proper place in the current weakening of the pandemic conditions and regular meetings in real can be streamed. Moreover, such streaming can be made without involvement of VIA operator, by direction of webcam towards the conference screen and speaker.

19.2.5   VIA activity in the conditions of pandemia and after

The lack of usual offline connections and meetings in the conditions of pandemia made the use of VIA facility especially timely and important. This facility supports regular weekly meetings of the Laboratory of cosmoparticle studies of the structure and dynamics of Galaxy in Institute of Physics of Southern Federal University (Rostov on Don, Russia) and M.Khlopov's scientific - creative seminar and their announcements occupied their permanent position on VIA homepage (Fig. 19.2), while their records were put in respective place of VIA forum, like [33] for Laboratory meetings.

The platform of VIA facility was used for regular Khlopov's course "Introduction to Cosmoparticle physics" for M2 students of MEPHI (in Russian) and in 2020 supported regular seminars of Theory group of APC.

The programme of VIA lectures continued to present hot news of astroparticle physics and cosmology, like talk by Zhen Cao from China on the progress of LHAASO experiment or lecture by Sunny Vagnozzi from UK on the problem of consistency of different measurements of the Hubble constant.

The results of this activity inspired the decision to hold in 2020 XXIII Bled Workshop online on the platform of VIA [19].

The conditions of pandemia continued in 2021 and VIA facility was successfully used to provide the platform for various online meetings. 2021 was announced by UNESCO as A.D.Sakharov year in the occasion of his 100th anniversary VIA offered its platform for various events commemorating A.D.Sakharov's legacy in cosmoparticle physics. In the framework of 1 Electronic Conference on Universe ECU2021), organized by the MDPI journal "Universe" VIA provided the platform for online satellite Workshop "Developing A.D.Sakharov legacy in cosmoparticle physics" [34].

19.3   VIA platform at the XXVII Bled Workshop

VIA sessions at Bled Workshops continued the tradition coming back to the first experience at XI Bled Workshop [7] and developed at XII, XIII, XIV, XV, XVI, XVII, XVIII, XIX, XX, XXI and XXII Bled Workshops [8–18]. They became a regular but supplementary part of the Bled Workshop's program. In the conditions of pandemia it became the only form of Workshop activity in 2020 [19] and in 2021 [20], as well as substantial part of the hybrid Memorial XXV Bled Workshop in 2022 [21] and XXVI Bled Workshop in 2023 [22].

During the XXVII Bled Workshop the announcement of VIA sessions was put on VIA home page, giving an open access to the videoconferences at the Workshop sessions. The preliminary program as well as the corrected program for each day were continuously put on Forum with the slides and records of all the talks and discussions [35].

Starting from its official opening (Figs. 19.5 and 19.6) VIA facility tried to preserve the creative atmosphere of Bled discussions in the format videoconferences as at the talk "How far can we understand nature with the spin-charge-family theory, describing the internal spaces of fermions and bosons with the Clifford algebra" by

Fig. 19.4: M.Khlopov's talk "Multimessenger probes for new physics in the light of A.D.Sakharov legacy in cosmoparticle physics" at the satellite Workshop "Developing A.D.Sakharov legacy in cosmoparticle physics" of ECU2021.
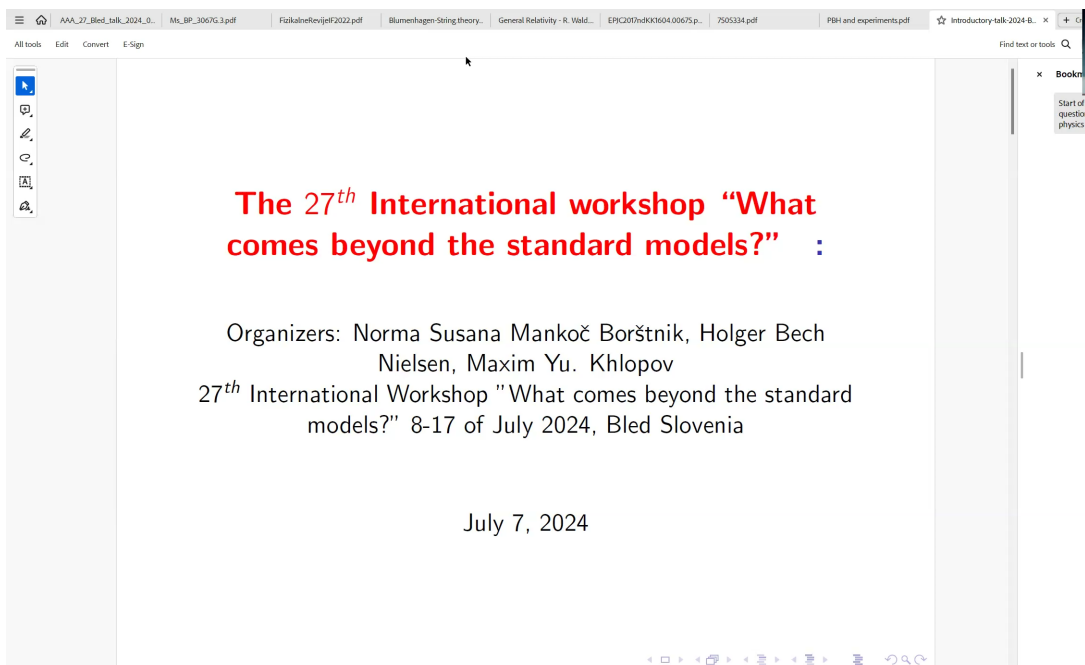
Fig. 19.5: Opening the XXVII Bled Workshop by Norma Mankoc-Borstnik
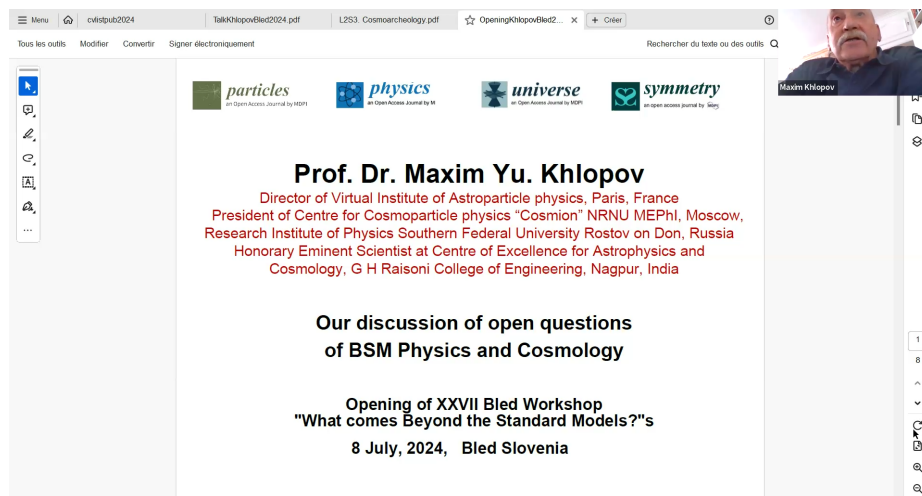
Fig. 19.6: Opening the XXVII Bled Workshop by Maxim Yu. Khlopov

Norma Mankoc-Borstnik (Fig. 19.7) or talks "Status of the DAMA project" given by R.Bernabei, (Fig. 19.8), from Rome University, Italy (see records in [35]).
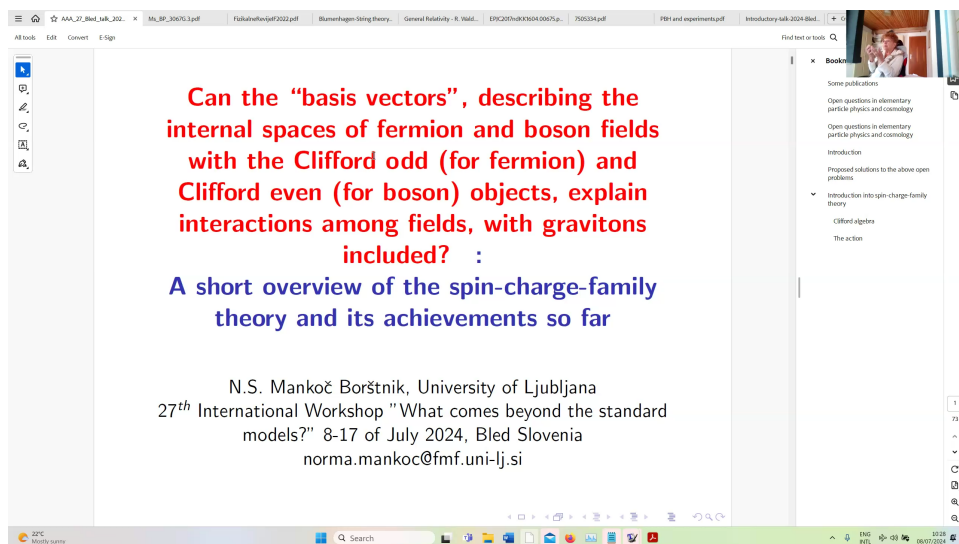
Fig. 19.7: VIA talk "Can the "basis vectors", describing the internal spaces of fermion and boson fields with the Clifford odd (for fermion) and Clifford even (for boson) objects, explain interactions among fields, with gravitons included? A short overview of the spin-charge-family theory and its achievements so far" by Norma Mankoc-Borstnik at XXVII Bled Workshop
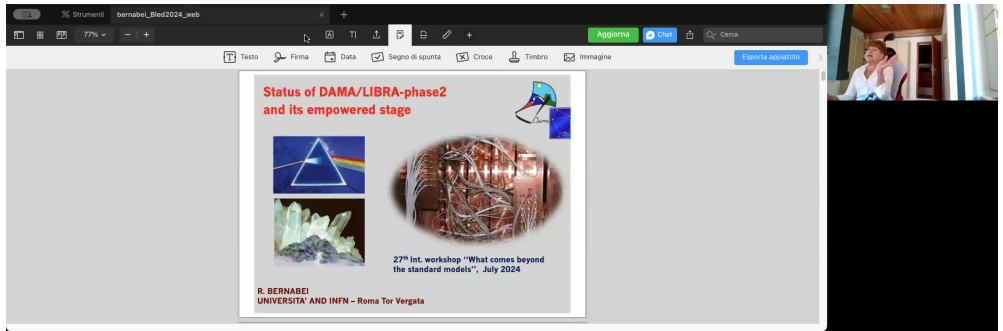
Fig. 19.8: VIA talk "Status of the DAMA project" by R.Bernabei from Rome at XXVII Bled Workshop

During the Workshop the VIA virtual room was open, inviting distant participants to join the discussion and extending the creative atmosphere of these discussions to the world-wide audience. The participants joined these discussions from different parts of world. The talk "Cosmological inflation and High-scale SUSY as the Origin of Dark Matter" was given by Sergey Ketov from Japan (Fig. 19.9), by A. Hernandez-Galeana from Mexico (Fig. 19.11), by S. Roy Chowdhury - from India, by Stan Brodsky "New Perspectives for Hadron Spectroscopy and Dynamics and the QCD Running Coupling from Color-Confining Holographic Light-Front QCD" - from USA, by D.Fargion from Italy. M.Y. Khlopov gave his talk "Open questions of Beyond the Standard model cosmology" from France, while H.B. Nielsen gave his talks "Approximate SU(5), Several Fundamental Scales, Fine Structure Constants", "Random Dynamics, Deriving ? Quantum Mechanics" and "Dark matter from Domain walls" from Croatia (Fig. 19.10) .

VIA talks highly enriched the Workshop program and involved distant participants in fruitful discussions. The use of VIA facility has provided remote presentation of students' scientific debuts in BSM physics and cosmology. The records of all the talks and discussions can be found on VIA Forum [35].

VIA facility has managed to join scientists from Mexico, USA, France, Italy, Russia, Slovenia, India, China and many other countries in discussion of open problems of physics and cosmology beyond the Standard models. In the current situation, hindering visits of Russian scientists, to Europe it made possible Russian students to present their results and participate in these discussions

19.4 Conclusions

The Scientific-Educational complex of Virtual Institute of Astroparticle physics provides regular communication between different groups and scientists, working in different scientific fields and parts of the world, the first-hand information on the newest scientific results, as well as support for various educational programs at distance. This activity would easily allow finding mutual interest and organizing task forces for different scientific topics of cosmology, particle physics,
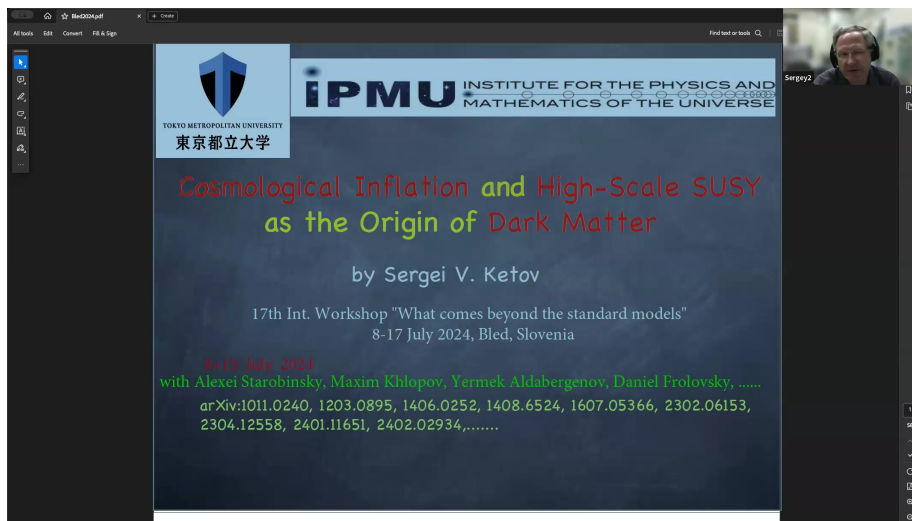
Fig. 19.9: VIA talk "Cosmological inflation and High-scale SUSY as the Origin of Dark Matter" by Sergey Ketov at XXVII Bled Workshop
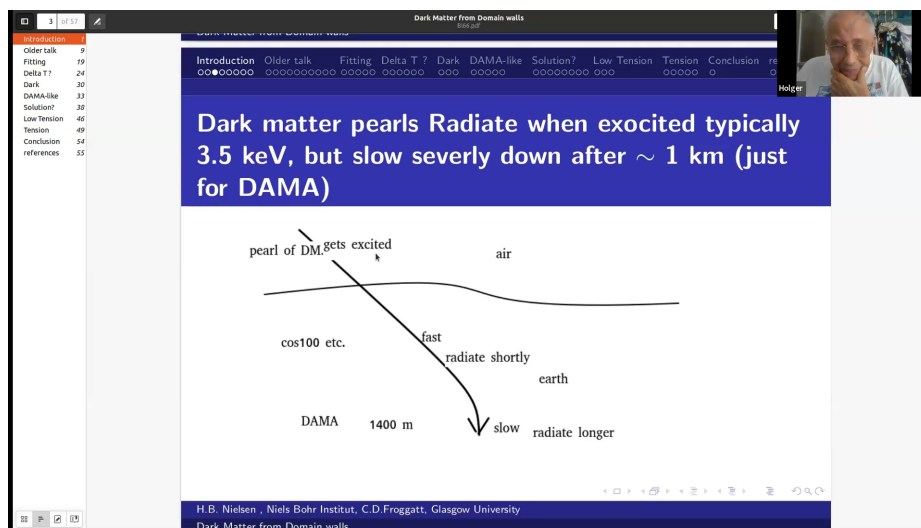
Fig. 19.10: VIA talk "Dark matter from Domain walls" by Holger Bech Nielsen at XXVII Bled Workshop
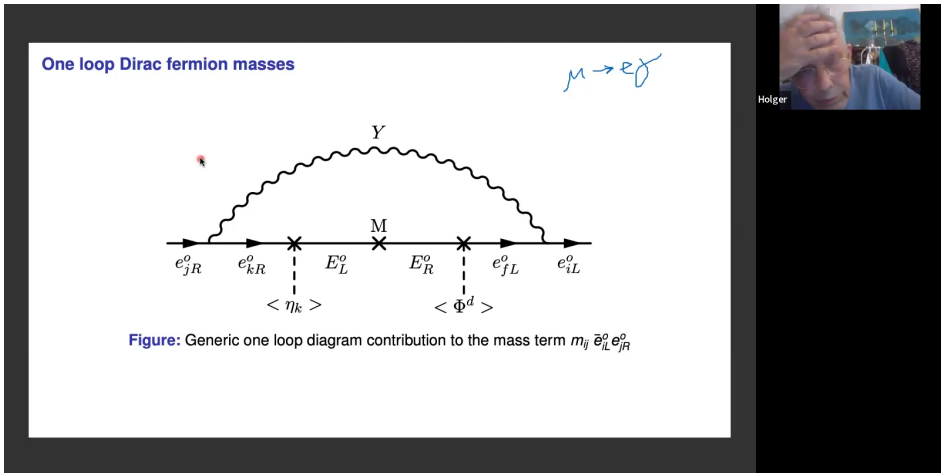
Fig. 19.11: VIA Discussion at the talk "Fermion masses, mixing and FCNC's within a gauged SU(3) family symmetry" by Albino Hernandez-Galeana at XXVII Bled Workshop

astroparticle physics and related topics. It can help in the elaboration of strategy of experimental particle, nuclear, astrophysical and cosmological studies as well as in proper analysis of experimental data. It can provide young talented people from all over the world to get the highest level education, come in direct interactive contact with the world known scientists and to find their place in the fundamental research. These educational aspects of VIA activity can evolve in a specific tool for International PhD program for Fundamental physics. Involvement of young scientists in creative discussions was an important aspect of VIA activity at XXVII Bled Workshop. VIA applications can go far beyond the particular tasks of astroparticle physics and give rise to an interactive system of mass media communications.

VIA sessions, which became a natural part of a program of Bled Workshops, maintained in 2024 the platform for online discussions of physics beyond the Standard Model involving distant participants from all the world in the fruitful atmosphere of Bled offline meeting. This discussion can continue in posts and post replies on VIA Forum. The experience of VIA applications at Bled Workshops plays important role in the development of VIA facility as an effective tool of e-science and e-learning.

One can summarize the advantages and flaws of online format of Bled Workshop. It makes possible to involve in the discussions scientists from all the world (young scientists, especially) free of the expenses related with meetings in real (voyage, accommodation, ...), but loses the advantage of nonformal discussions at walks along the beautiful surrounding of the Bled lake and other places of interest. The improvement of VIA technical support by involvement of Zoom provided better platform for nonformal online discussions, but in no case can be the substitute for offline Bled meetings and its creative atmosphere in real, which as we hope will be revived at the future Bled Workshops. One can summarize that VIA facility

provides the online platform of Bled Workshop, involving world-wide participants in its creative and open discussions of BSM physics and cosmology.

Acknowledgements

References

1. http://www.aspera-eu.org/
2. http://www.appec.org/
3. M.Yu. Khlopov: *Cosmoparticle physics*, World Scientific, New York -London-Hong Kong - Singapore, 1999.
4. M.Yu. Khlopov: *Fundamentals of Cosmic Particle Physics*, CISP-Springer, Cambridge, 2012.
5. M. Y. Khlopov, Project of Virtual Institute of Astroparticle Physics, arXiv:0801.0376 [astro-ph].
6. http://viavca.in2p3.fr/site.html
7. M. Y. Khlopov, Scientific-educational complex - virtual institute of astroparticle physics, 981–862008.
8. M. Y. Khlopov, Virtual Institute of Astroparticle Physics at Bled Workshop, 10177–1812009.
9. M. Y. Khlopov, VIA Presentation, 11225–2322010.
10. M. Y. Khlopov, VIA Discussions at XIV Bled Workshop, 12233–2392011.
11. M. Y. .Khlopov, Virtual Institute of astroparticle physics: Science and education online, 13183–1892012.
12. M. Y. .Khlopov, Virtual Institute of Astroparticle physics in online discussion of physics beyond the Standard model, 14223–2312013.
13. M. Y. .Khlopov, Virtual Institute of Astroparticle physics and "What comes beyond the Standard model?" in Bled, 15285-2932014.
14. M. Y. .Khlopov, Virtual Institute of Astroparticle physics and discussions at XVIII Bled Workshop, 16177-1882015.

15. M. Y. .Khlopov, Virtual Institute of Astroparticle Physics — Scientific-Educational Platform for Physics Beyond the Standard Model, 17221-2312016.
16. M. Y. .Khlopov: Scientific-Educational Platform of Virtual Institute of Astroparticle Physics and Studies of Physics Beyond the Standard Model, 18273-2832017.
17. M. Y. .Khlopov: The platform of Virtual Institute of Astroparticle physics in studies of physics beyond the Standard model, 19383-3942018.
18. M. Y. .Khlopov: The Platform of Virtual Institute of Astroparticle Physics for Studies of BSM Physics and Cosmology, 20249-2612019.
19. M. Y. .Khlopov: Virtual Institute of Astroparticle Physics as the Online Platform for Studies of BSM Physics and Cosmology, 21249-2632020.
20. M. Y. .Khlopov: Challenging BSM physics and cosmology on the online platform of Virtual Institute of Astroparticle physics, 22160-1752021.
21. M. Y. .Khlopov: Virtual Institute of Astroparticle physics as the online platform for studies of BSM physics and cosmology, 23334-3472022.
22. M. Y. .Khlopov: Virtual Institute of Astroparticle physics as the online support for studies of BSM physics and cosmology. 24279-2932023.
23. $http : //viavca.in2p3.fr/what_comes_beyond_the_standard_models_xiii.html$
24. $http : //viavca.in2p3.fr/what_comes_beyond_the_standard_models_xiv.html$
25. $http : //viavca.in2p3.fr/pohl_martin.html$
26. In http://viavca.in2p3.fr/ Previous - Events - JDEV 2013
27. $http : //viavca.in2p3.fr/zeldovich_100_meeting.html$
28. In http://bsm.fmf.uni-lj.si/bled2023bsm/ Cosmovia - Forum- Discussion in Russian - Courses on Cosmoparticle physics
29. In http://bsm.fmf.uni-lj.si/bled2023bsm/ Cosmovia - Forum - Education - From VIA to MOOC
30. In http://bsm.fmf.uni-lj.si/bled2023bsm/ Cosmovia - Forum - Education - Lectures of Open Online VIA Course 2017
31. In http://bsm.fmf.uni-lj.si/bled2023bsm/ Cosmovia - Forum - Education - Small thesis and exam of Steve Branchu
32. $http : //viavca.in2p3.fr/john_ellis.html$
33. In http://bsm.fmf.uni-lj.si/bled2023bsm/ Cosmovia - Forum - LABORATORY OF COSMOPARTICLE STUDIES OF STRUCTURE AND EVOLUTION OF GALAXY
34. In http://bsm.fmf.uni-lj.si/bled2023bsm/ Cosmovia - Forum - CONFERENCES - CONFERENCES ASTROPARTICLE PHYSICS - The Universe of A.D. Sakharov at ECU2021
35. In http://bsm.fmf.uni-lj.si/bled2024bsm/ Cosmovia - Forum - CONFERENCES BEYOND THE STANDARD MODEL - XXVII Bled Workshop "What comes beyond the Standard models?"

20   Code

A. Kleppe

(... a poem)

There is a code here,
only visible at night
and only now and then, by chance
But sometimes you wake up
and see it all, revealing
every second, every speck of dust
That tiny moment
when the veil is lifted
Everything is true